Dark Matter

Jing Shu

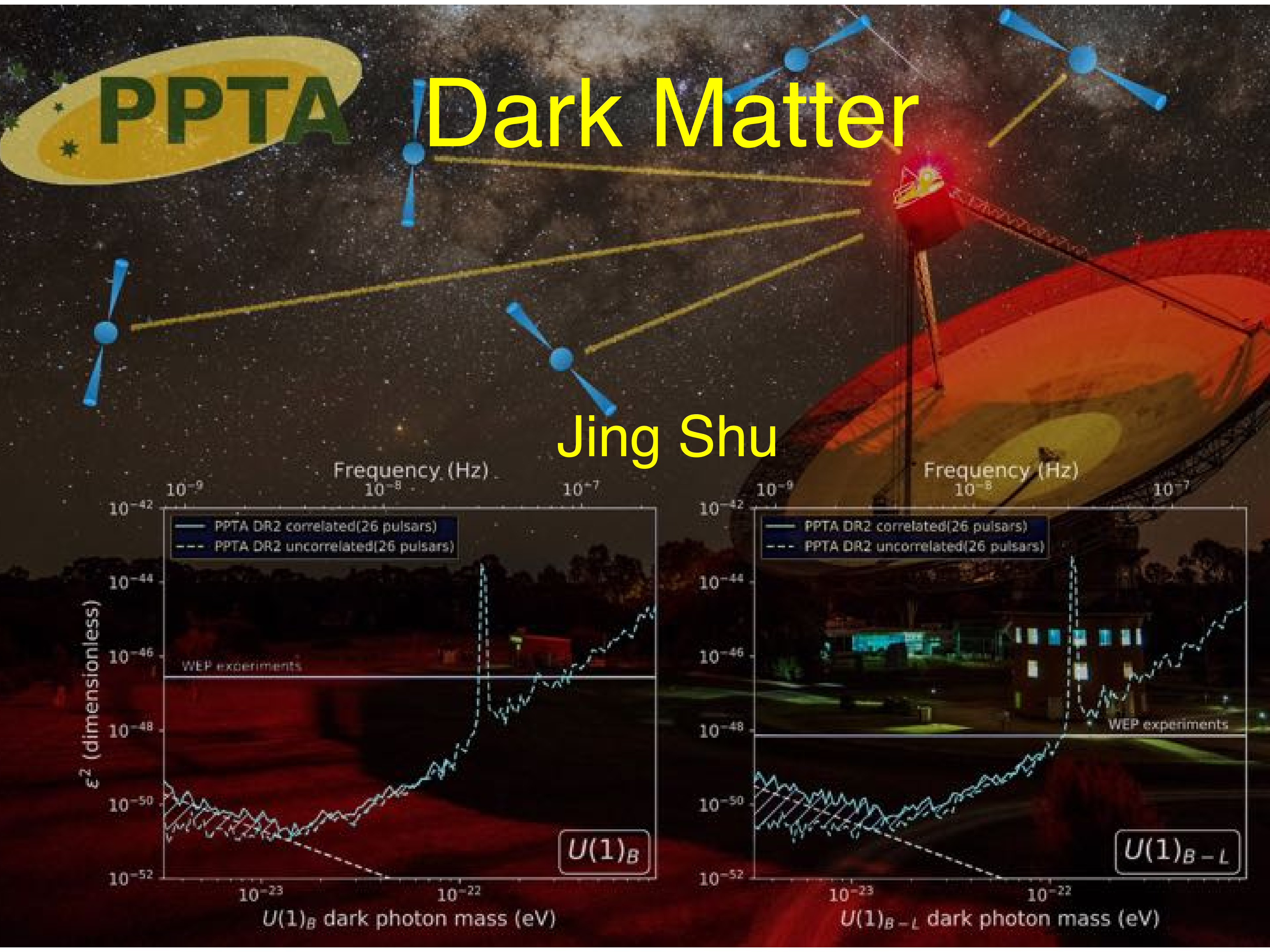

Outlines

- Introduction to DM
- Properties of DM
- Detection Methods of DM
  - Particle-like DM Detection
  - Wave-like DM Detection
- Summary and Outlook

Introduction to DM

Hierarchical Structure of the Universe

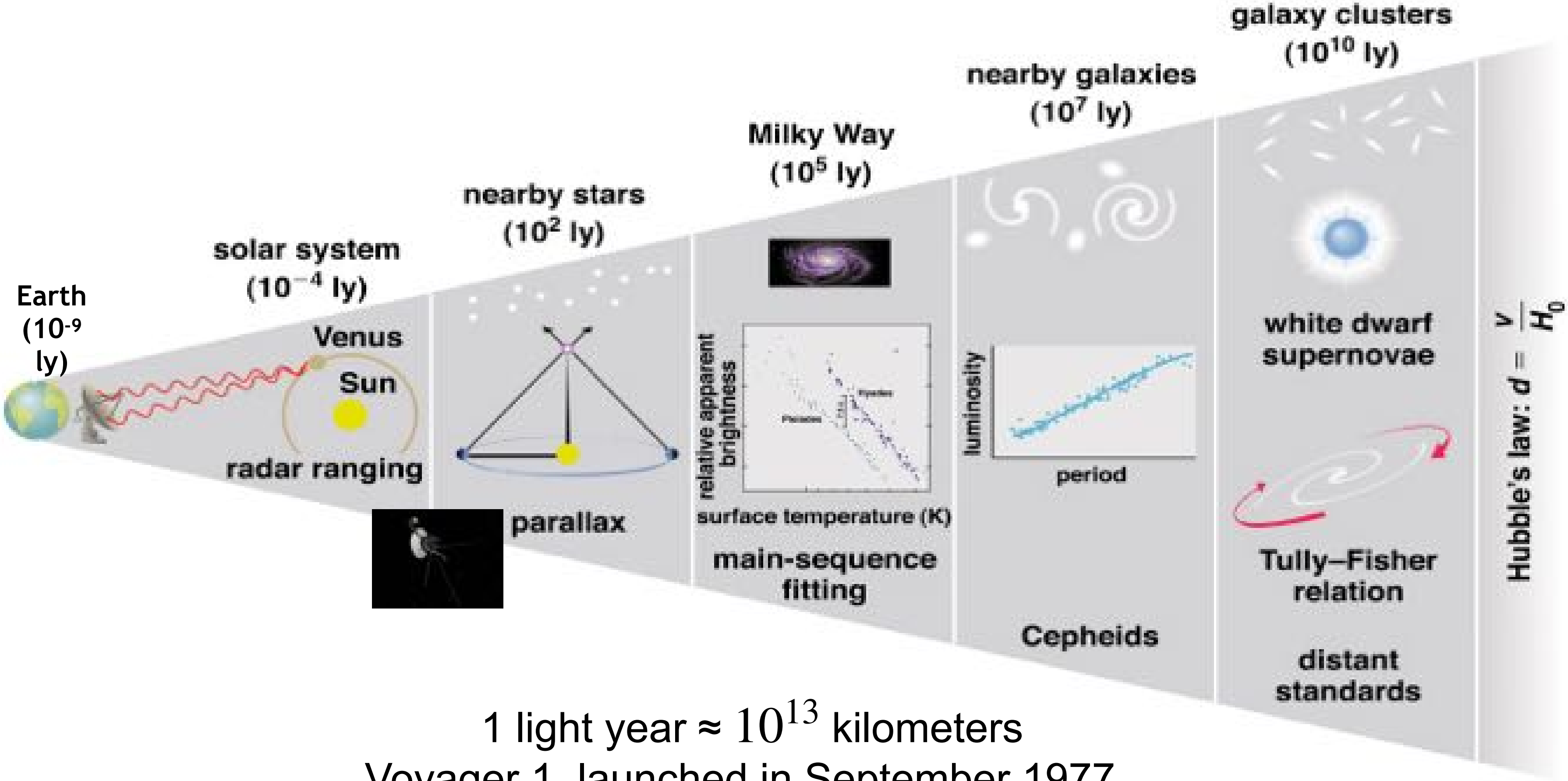

1 light year ≈ 10^{13} kilometers

Voyager 1, launched in September 1977, only exited the solar system in 2012, and is "just" about 20 billion kilometers away from Earth!

How to "Weigh" Celestial Bodies?

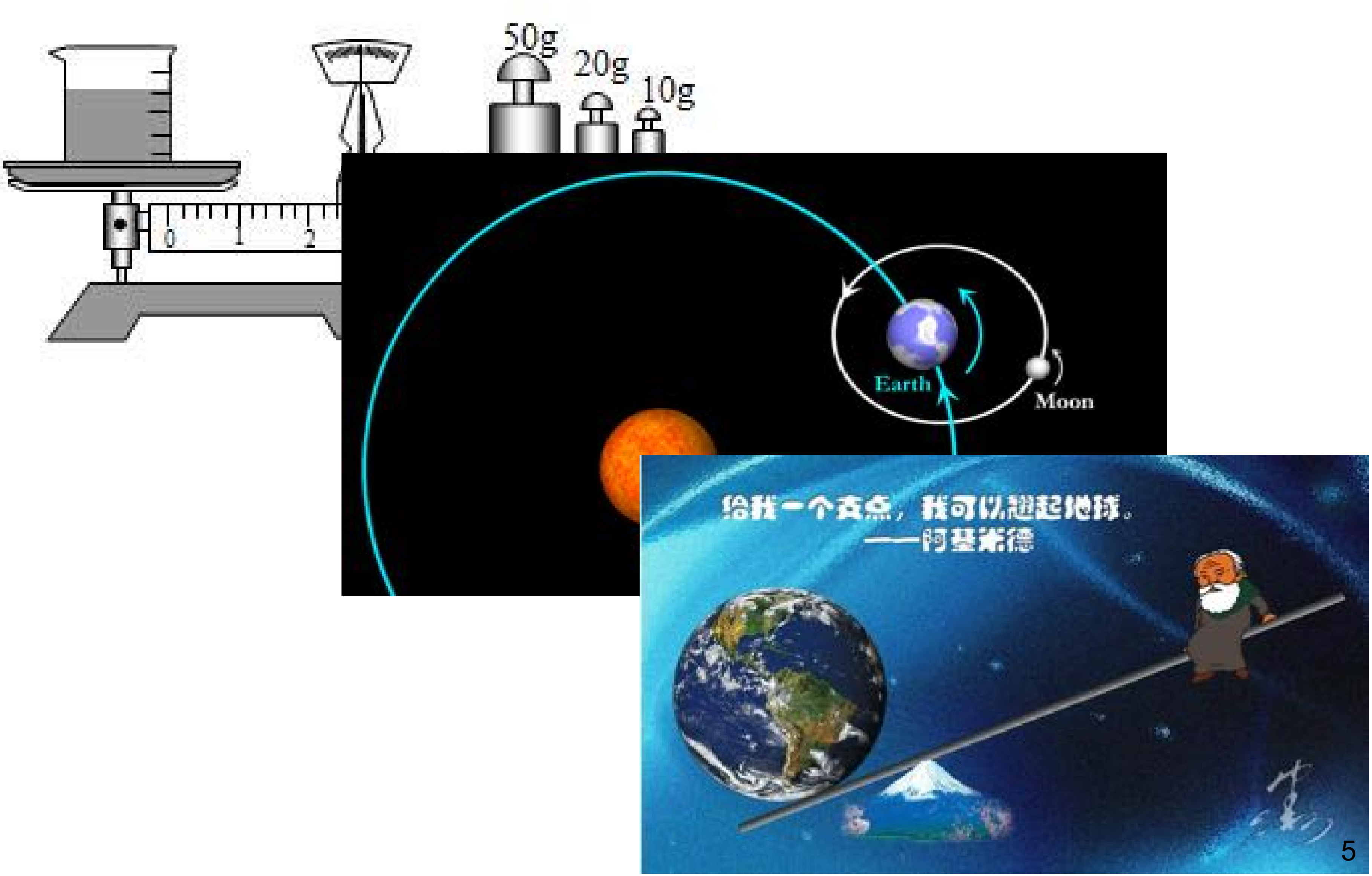

Newton's Laws

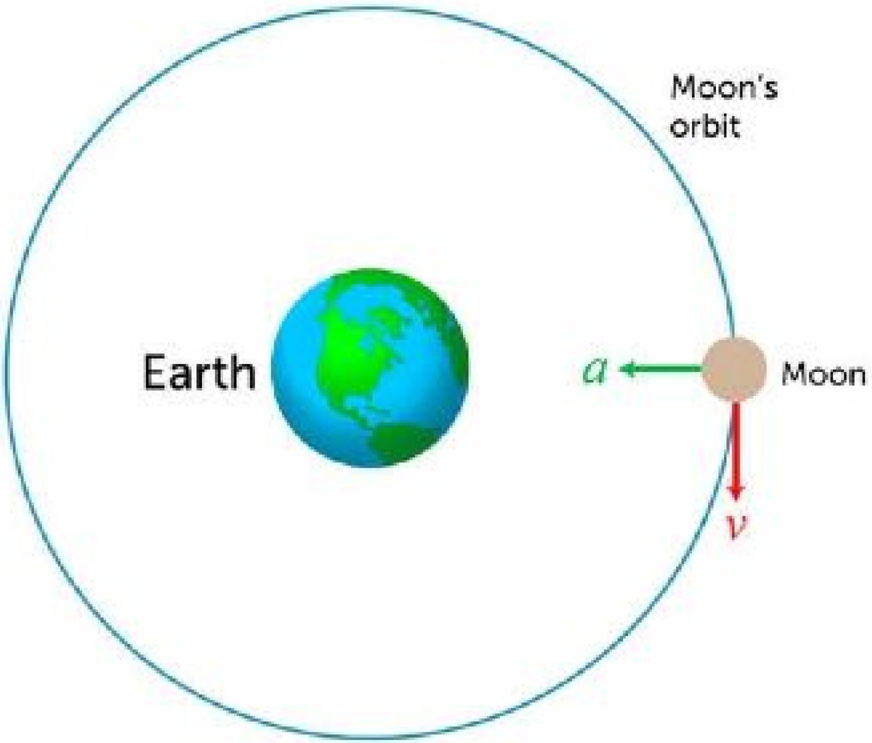

$$\frac{GMm}{r^2} = \frac{mv^2}{r}$$

$$v = \sqrt{\frac{GM}{r}}$$

Rotation Curve in Solar System

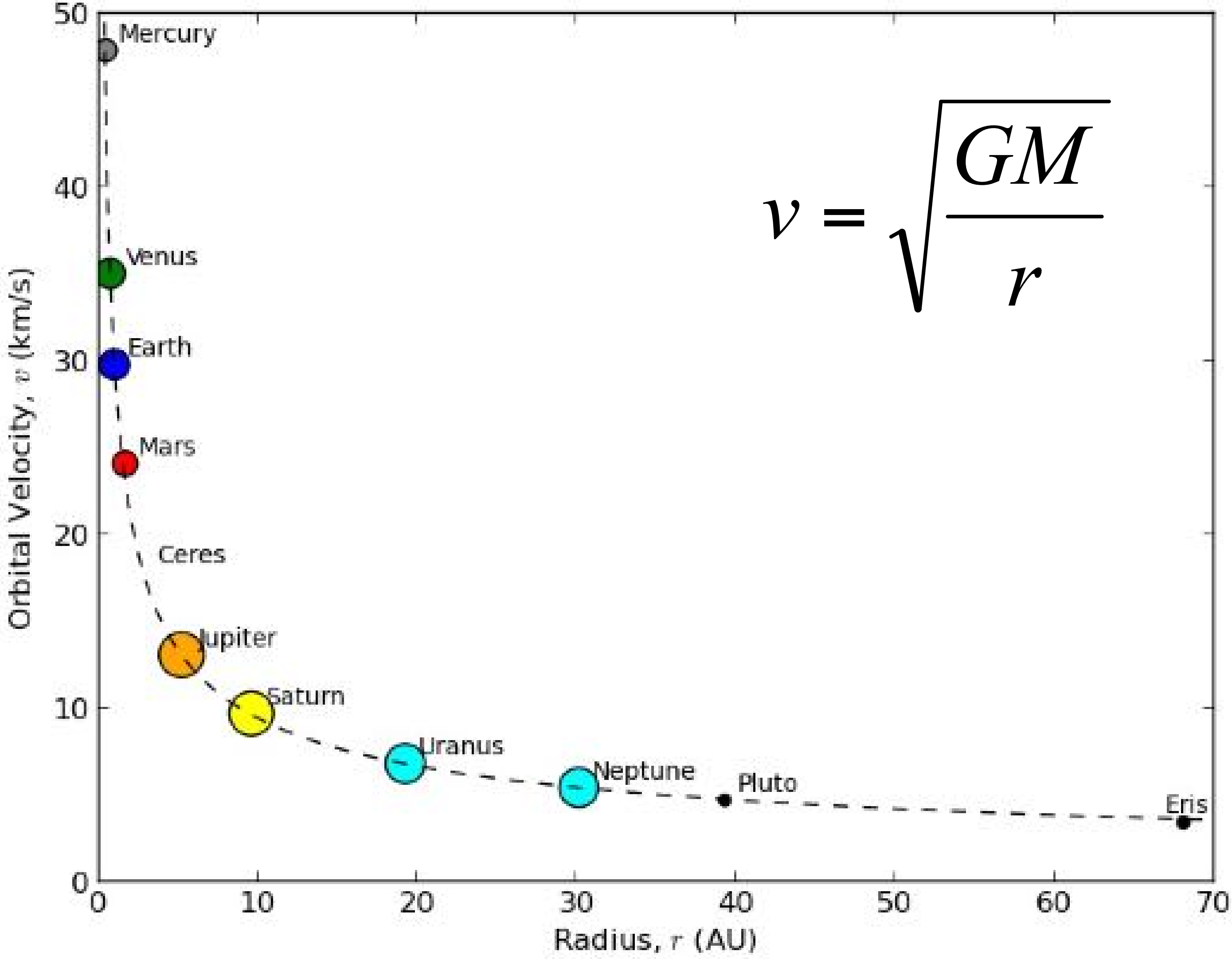

$$v = \sqrt{\frac{GM}{r}}$$

Rotation Curve in Spiral Galaxy

Vera Rubin

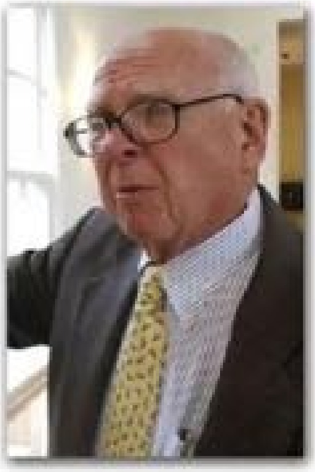

Kent Ford

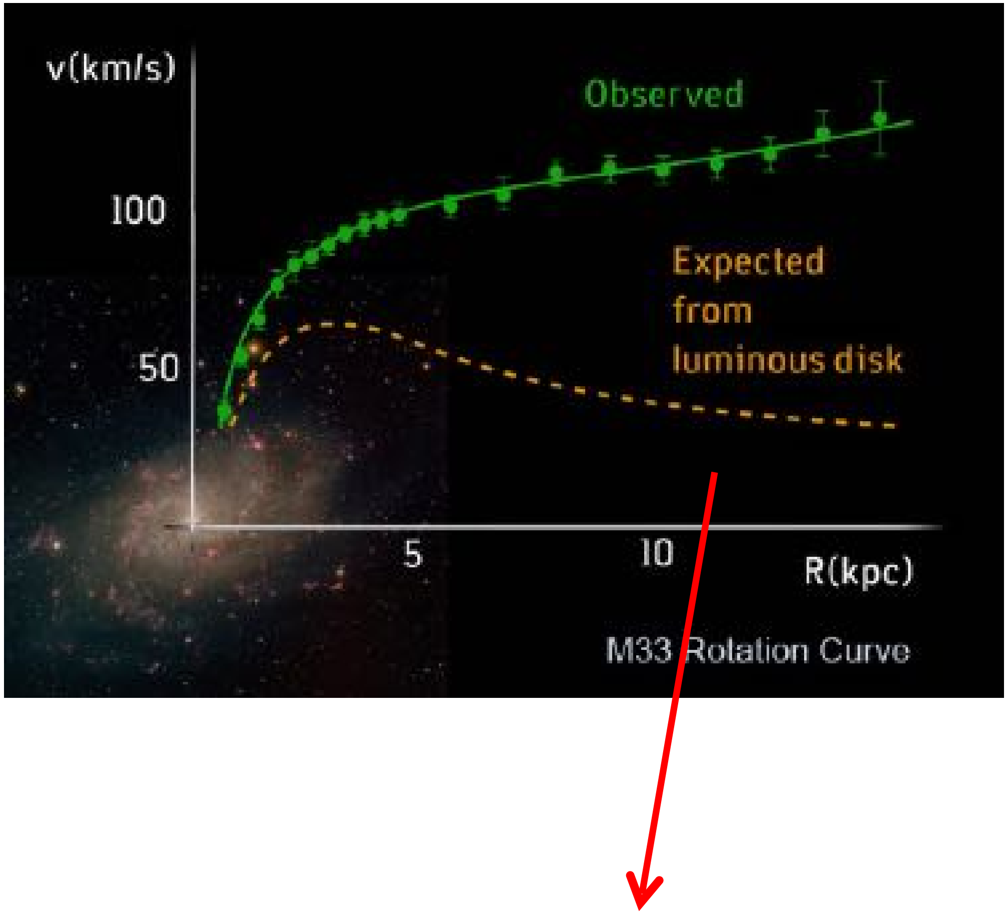

Completely different from the square root decline law (Kepler's laws)!

Possible non-luminous (dark) matter

Gravitational Lensing

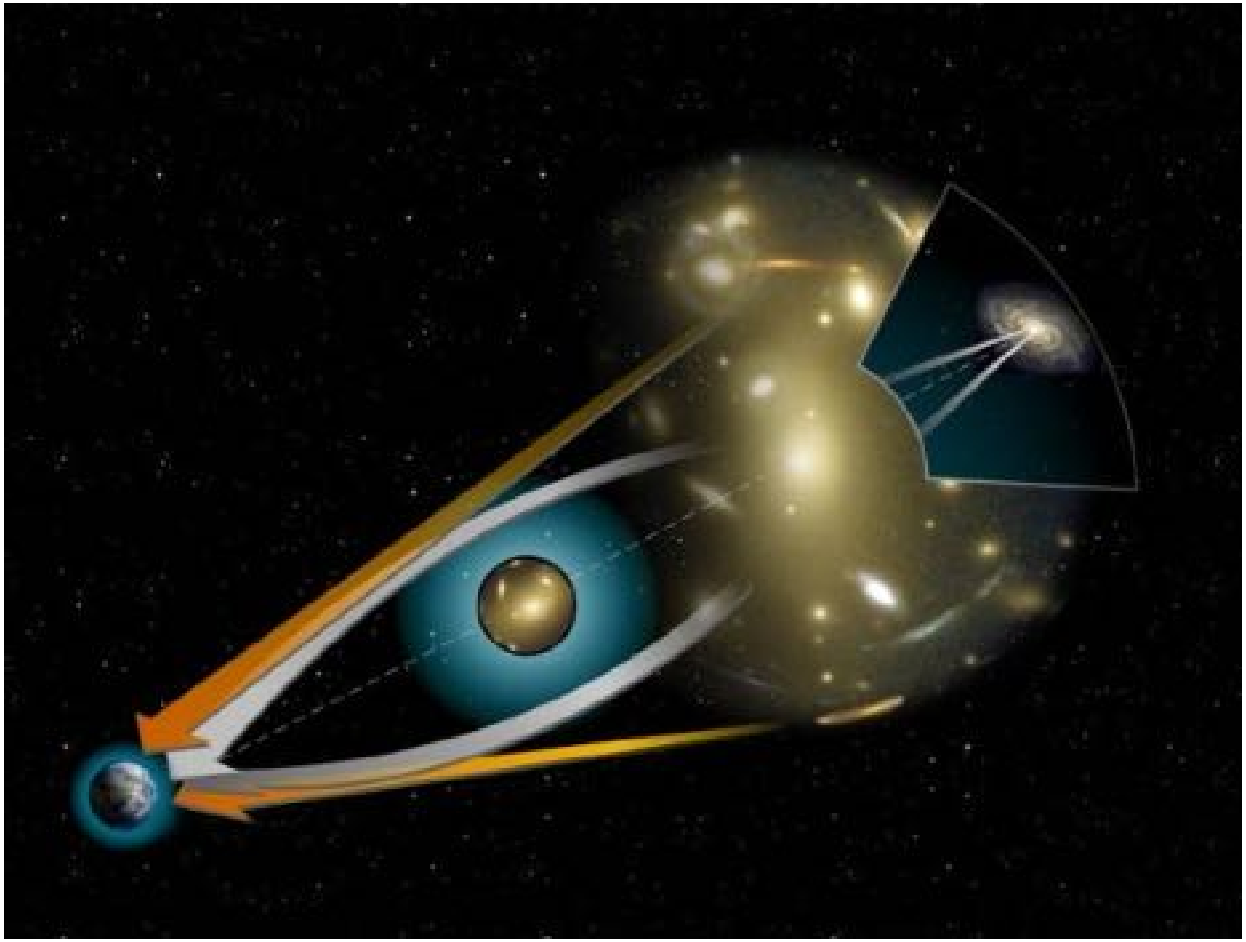

Bullet Cluster: Compelling Evidence for the Existence of Dark Matter

Clowe et al. (2006)

Red: Mass Distribution of X-ray Gas

Blue: Mass Distribution from Gravitational Lensing

Large-Scale Structure: Cold Dark Matter

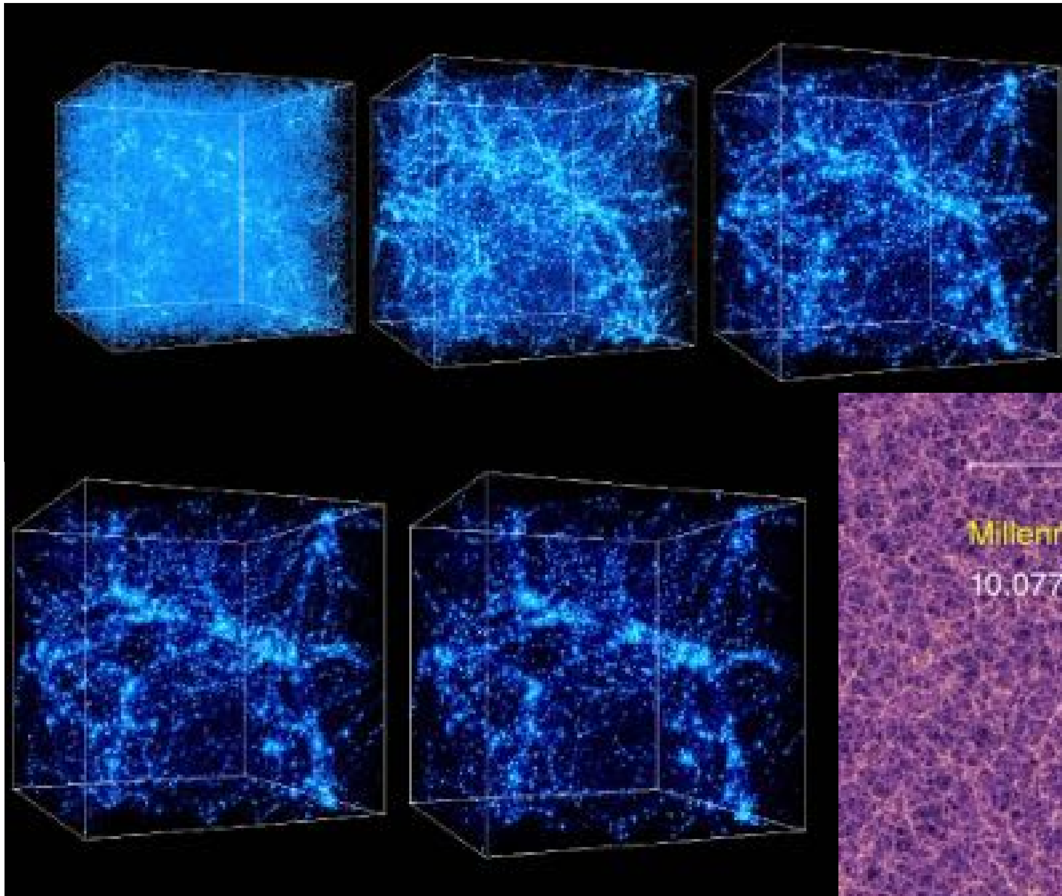

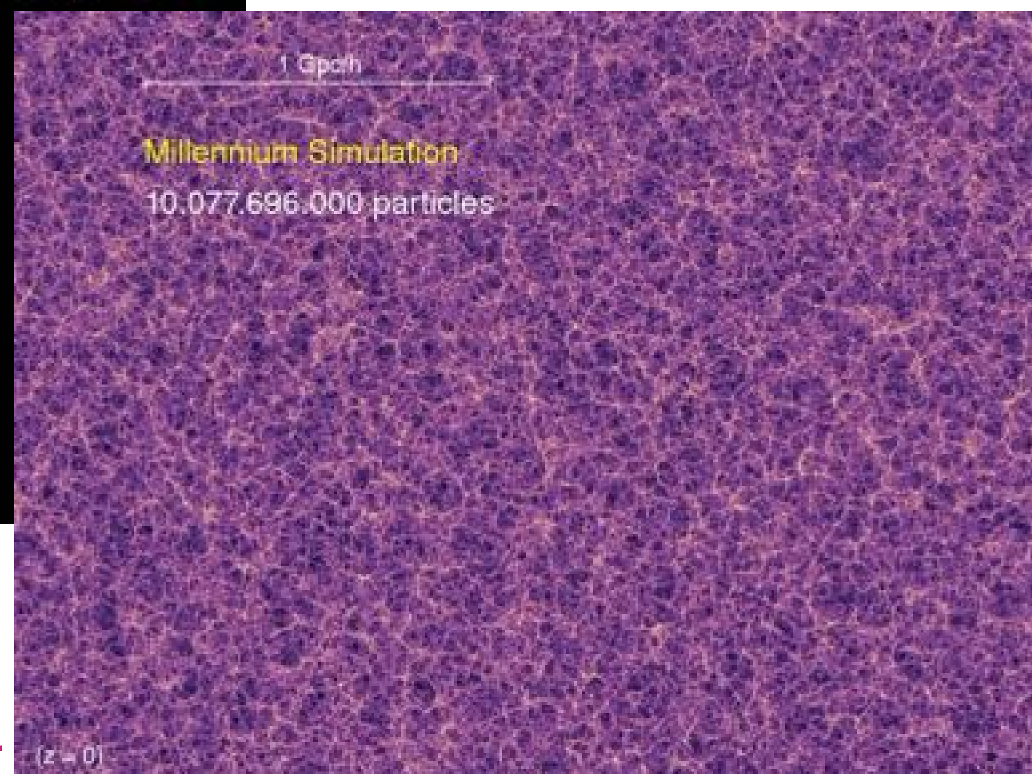

The *Millennium Run* used more than 10 billion particles to trace the evolution of the matter distribution in a cubic region of the Universe over 2 billion light-years on a side.

Composition of the Universe

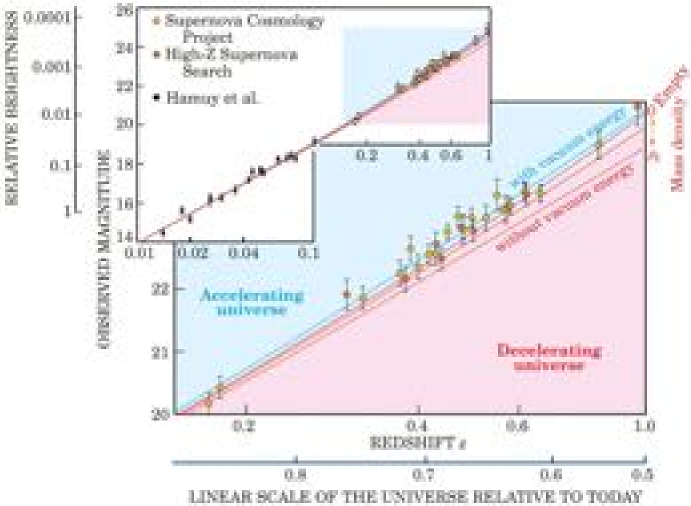

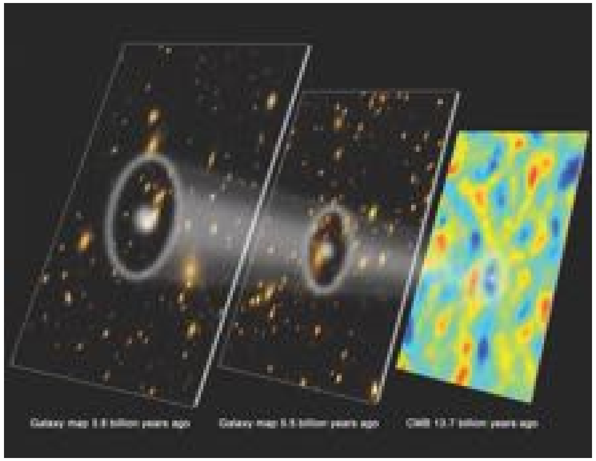

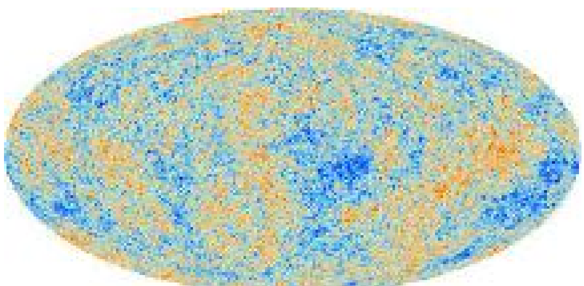

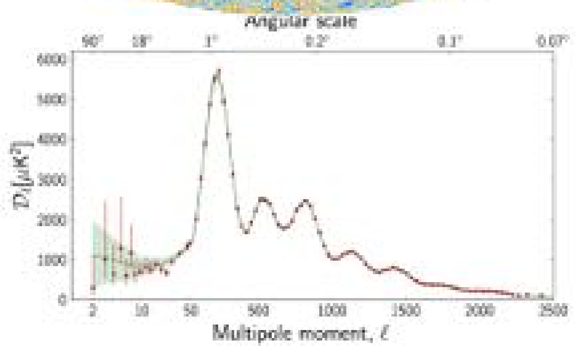

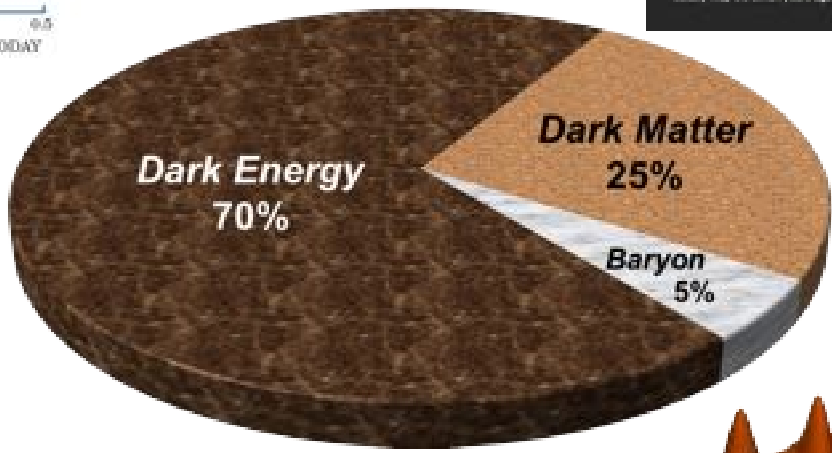

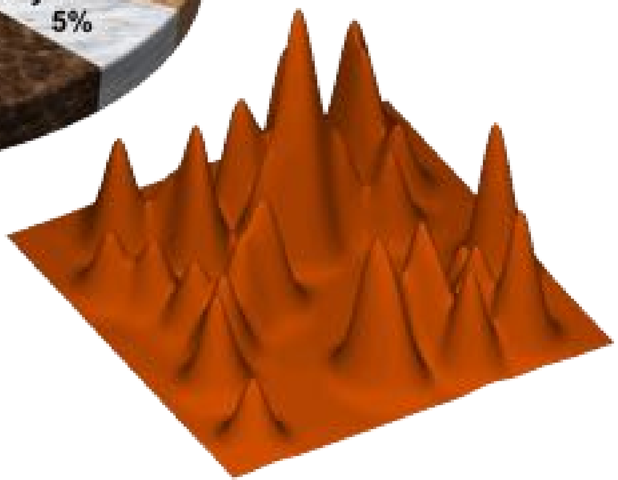

NO!

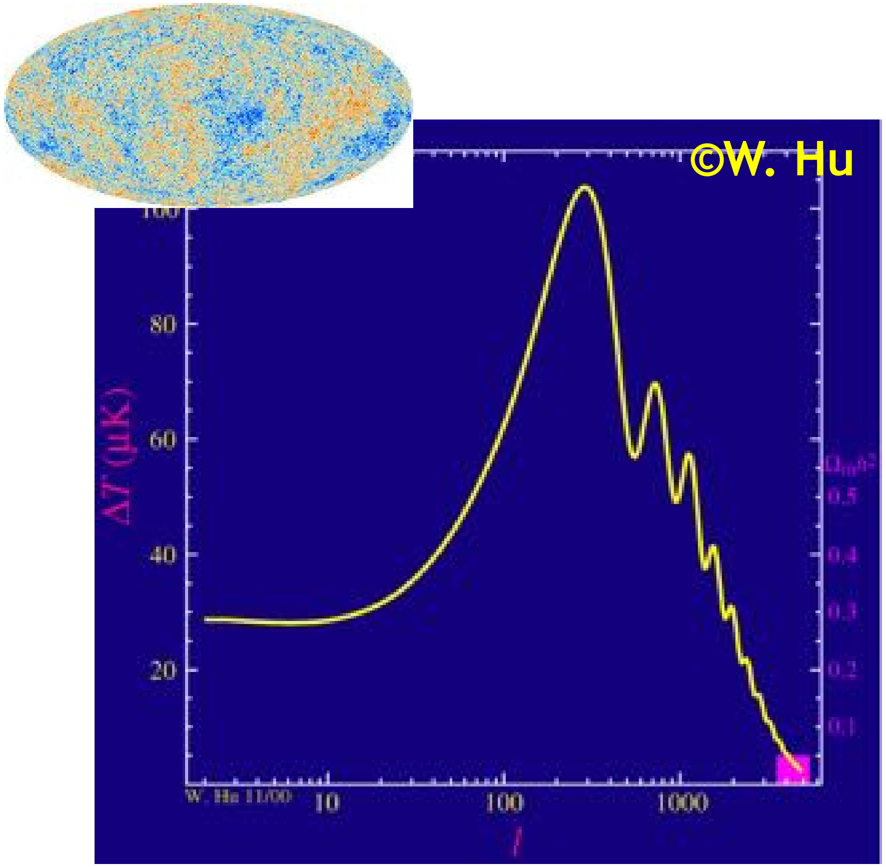

Cosmic Microwave Background(CMB) Radiation Anisotropy:

Ω_b~0.05, Ω_{dm}~0.25

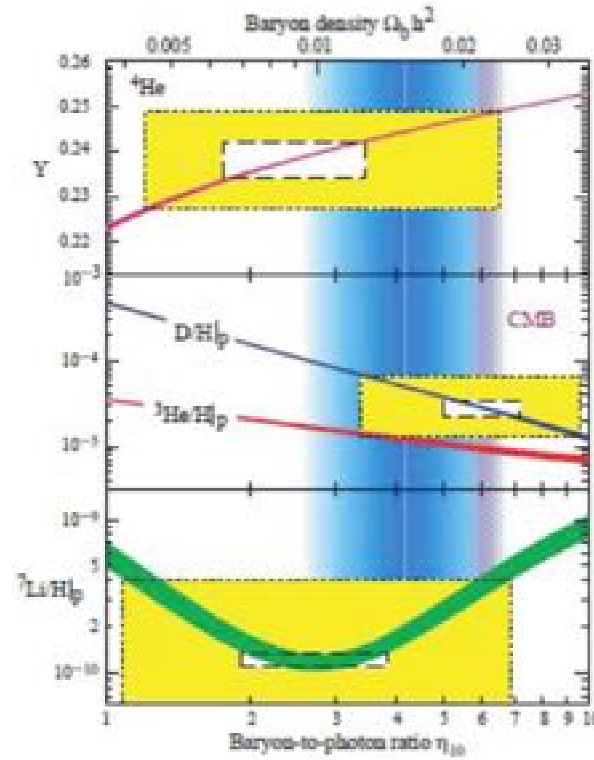

Abundance of light elements predicted by Big Bang Nucleosynthesis(BBN)： Ω_b~0.05 (Fields and Sarkar 2004)

The nature of DM is different from baryonic matter!

Can we see DM with telescopes powerful enough?

Thirty Meter Telescope (TMT)

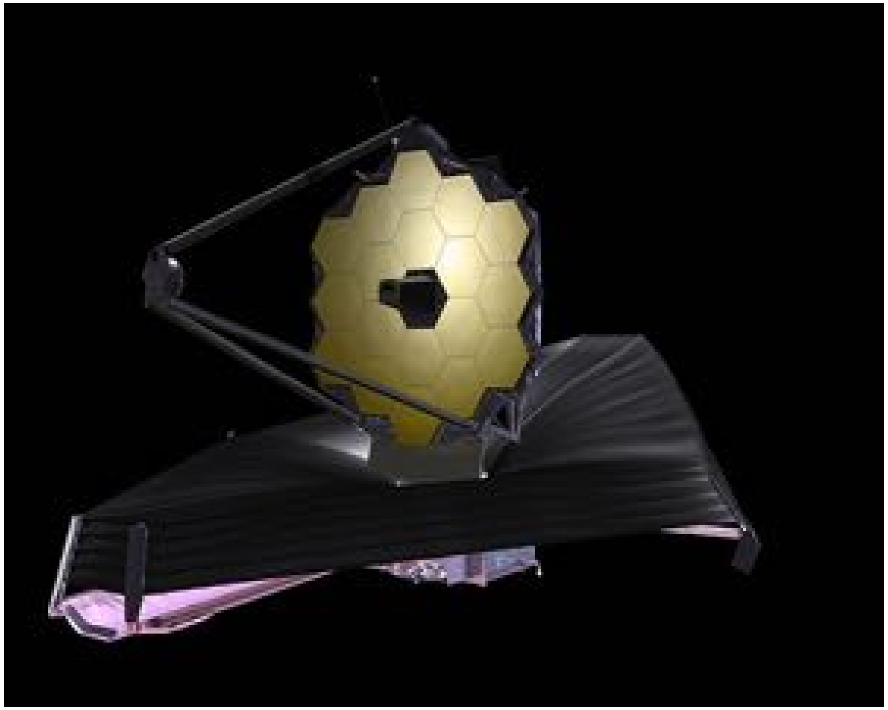

James Webb 6.5-meter Space Telescope

Do the laws of gravity hold true anywhere and anytime?

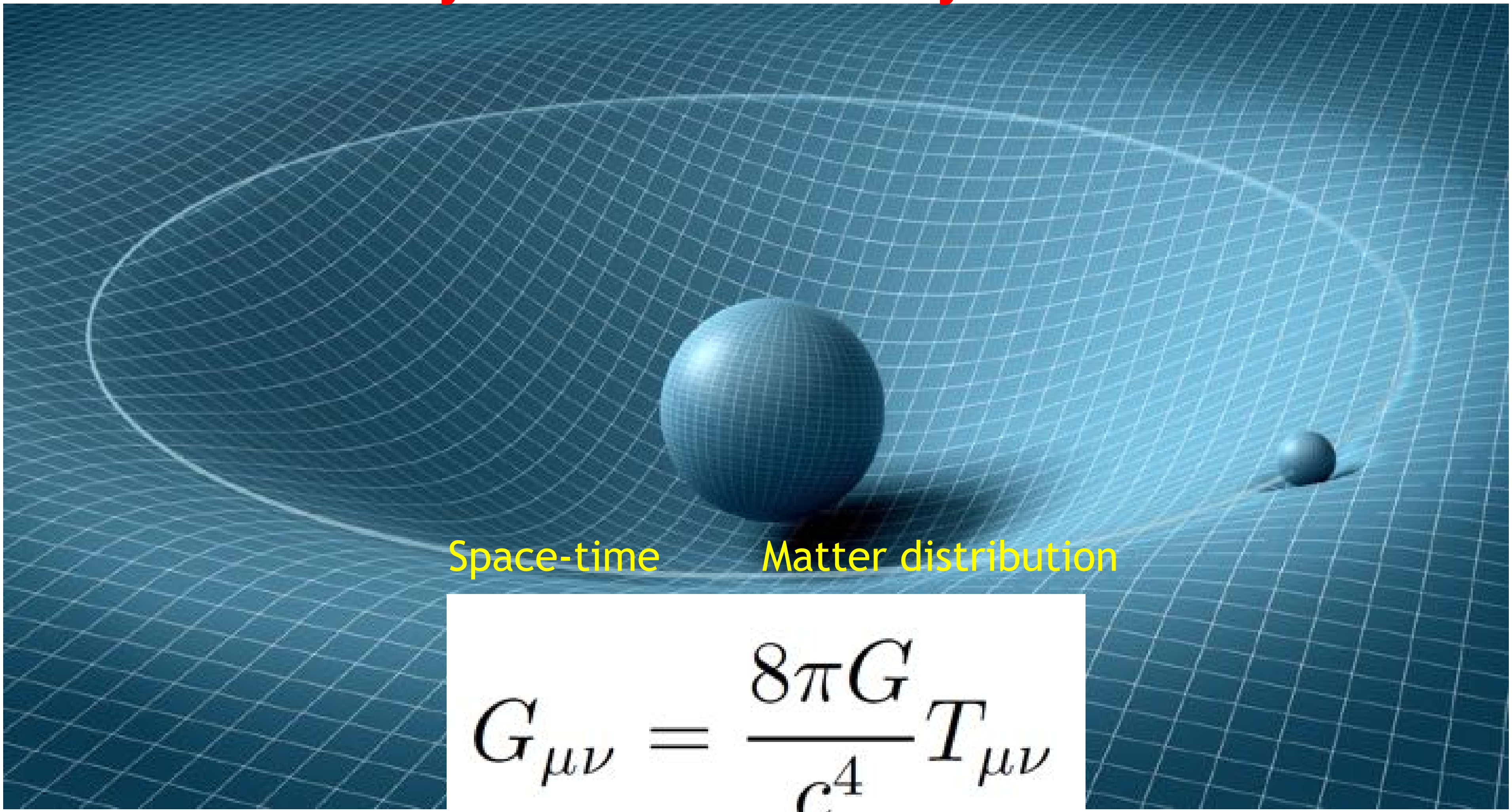

$$G_{\mu\nu} = \frac{8\pi G}{c^4} T_{\mu\nu}$$

Attempts to Modify the Laws of Gravity

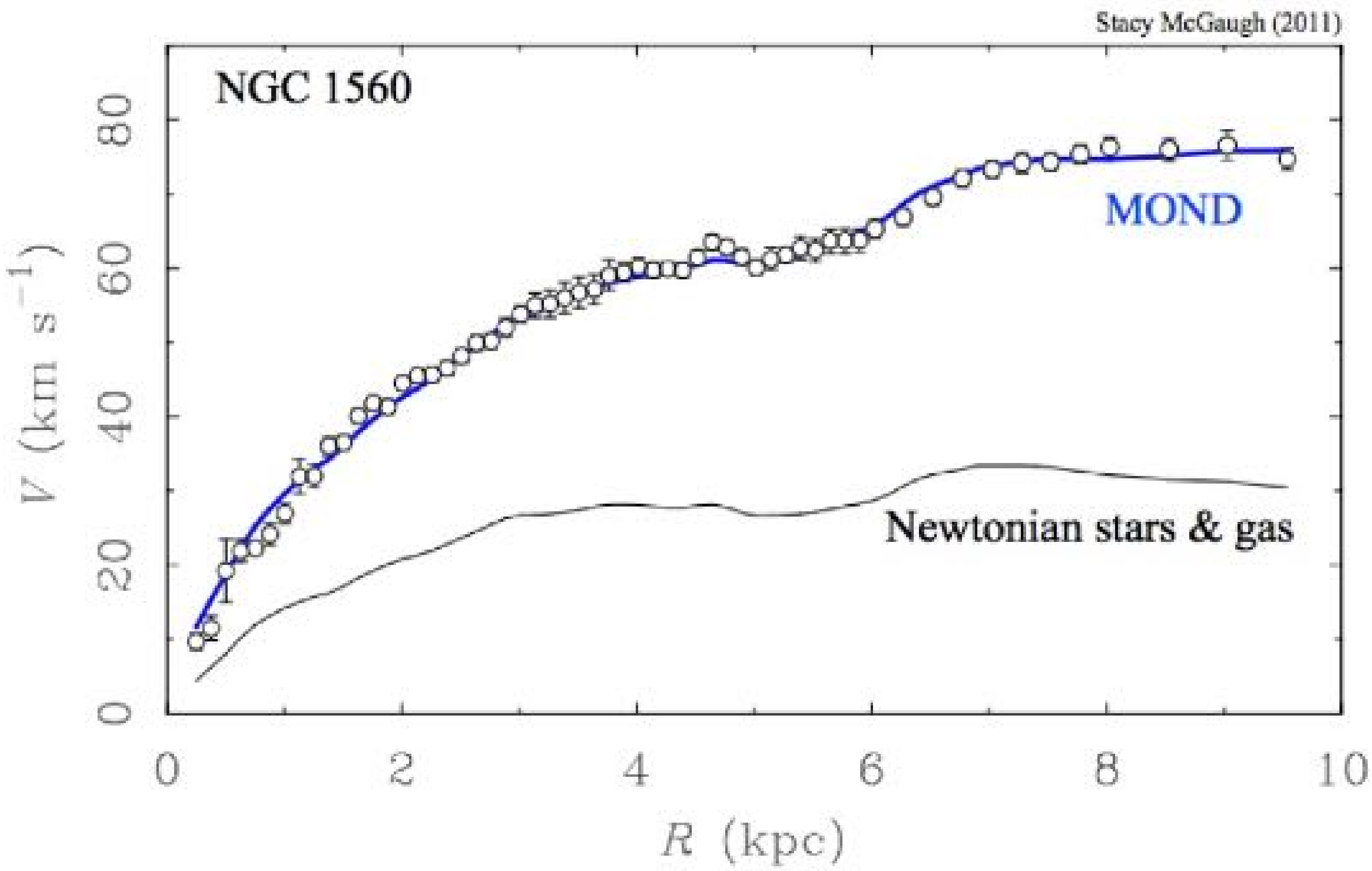

- Sometimes effective, but more often fail.
- Newton/Einstein's laws of gravity have been precisely tested on various scales.

The laws of gravity have undergone rigorous testing.

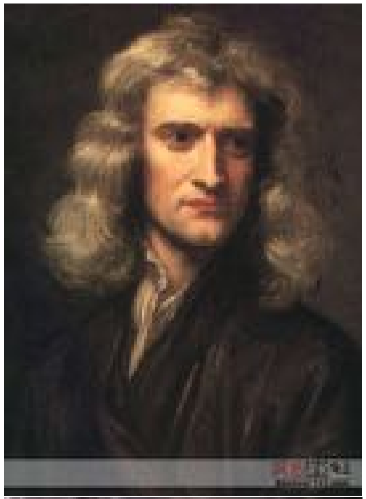

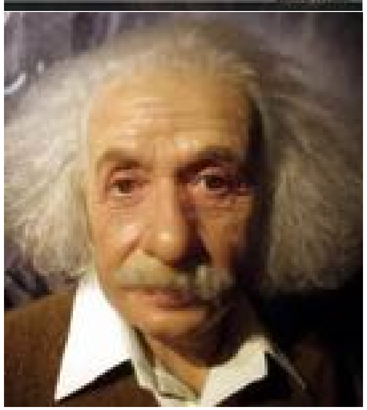

Space-time is swirling around a dead star, proving Einstein right again

News By Charles Q. Choi published January 31, 2020

Space-time is indeed churned by massive rotating bodies, as scientist

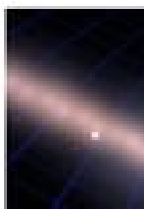

Einstein is right again! Scientists prove that plunging regions exist around black holes - a theory first proposed by the physicist in 1915

- Scientists have proven the existe
- This discovery confirms theoreti

By WILIAM HUNTER
PUBLISHED: 05:05 EDT, 16 May 2024 | U

Share

Over 100 years on, scientists have f
about the nature of black holes.

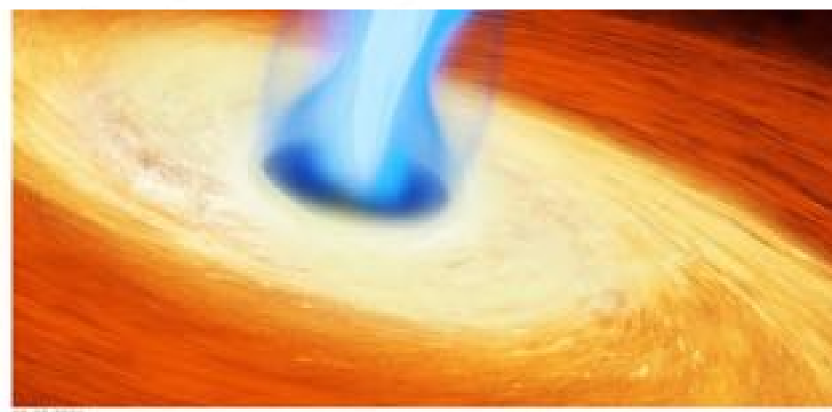

Black hole "waterfall" discovery proves Einstein right again

By Eric Ralls

General Relativity: Prediction and Confirmation of Gravitational Waves

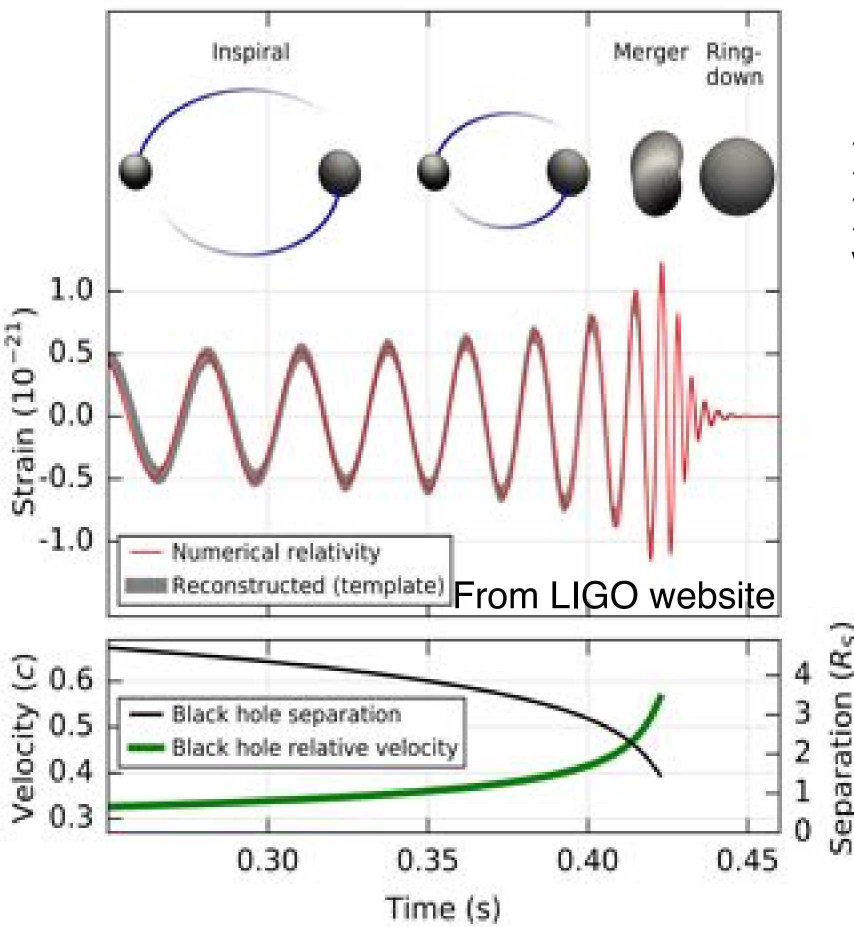

From LIGO website

1916: Einstein predicted gravitational waves based on General Relativity
2015: LIGO/VIRGO detected GW150914
2017: Nobel Prize in Physics awarded to Weiss, Barish, Thorne

General Relativity: Prediction and Confirmation of Black Holes

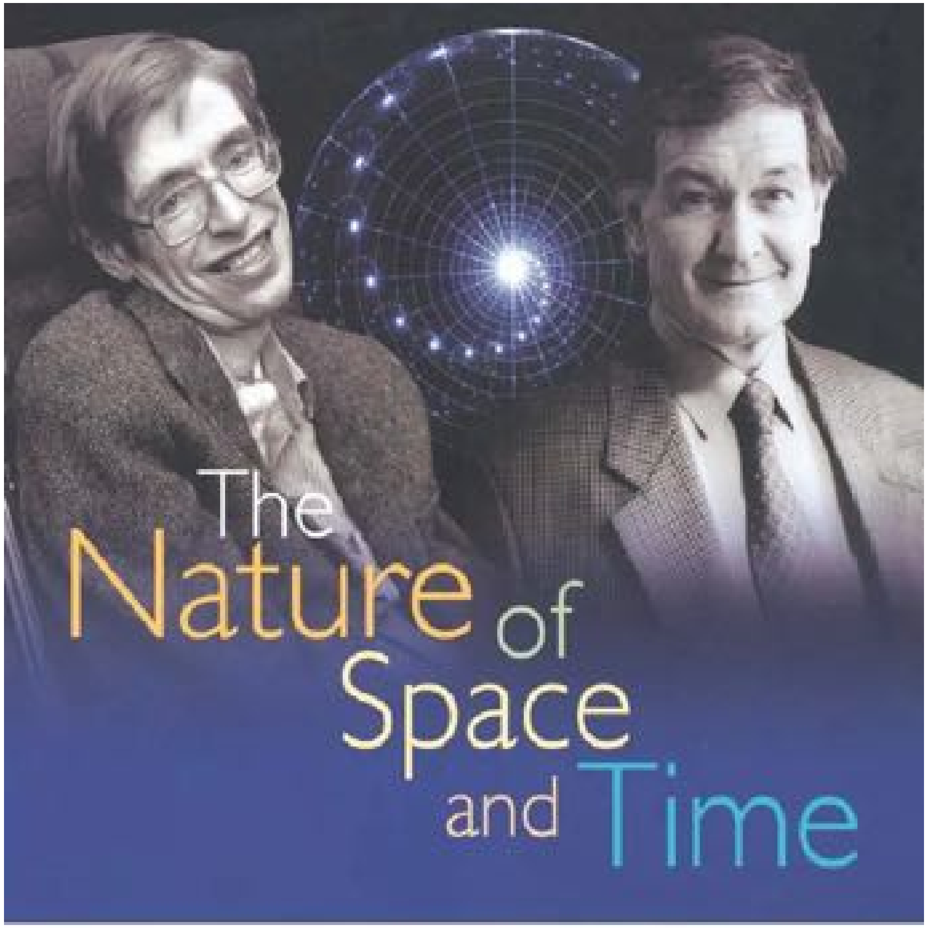

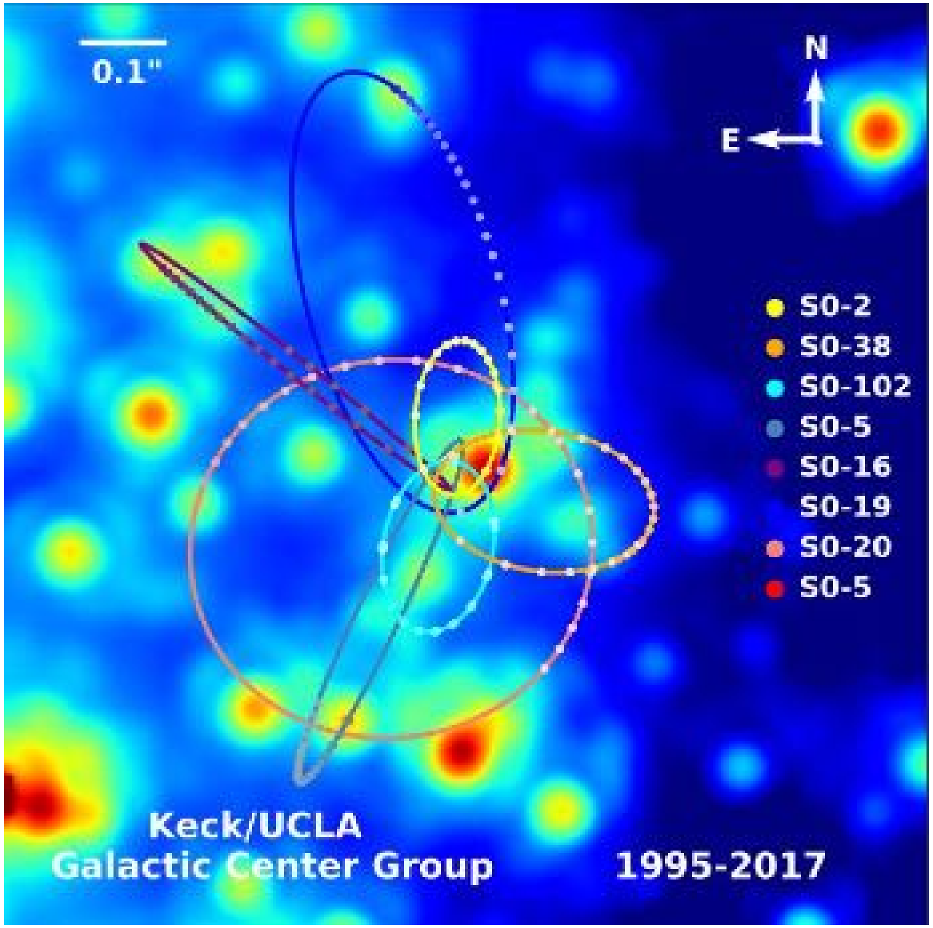

1964-1970: Penrose and Hawking mathematically confirmed the existence of black holes based on General Relativity
1995-2016: Genzel and Ghez discovered and confirmed the supermassive black hole at the center of the Milky Way
2020: Penrose, Genzel, and Ghez received the Nobel Prize in Physics

Precise Testing of General Relativity Near the Galactic Center Black Hole

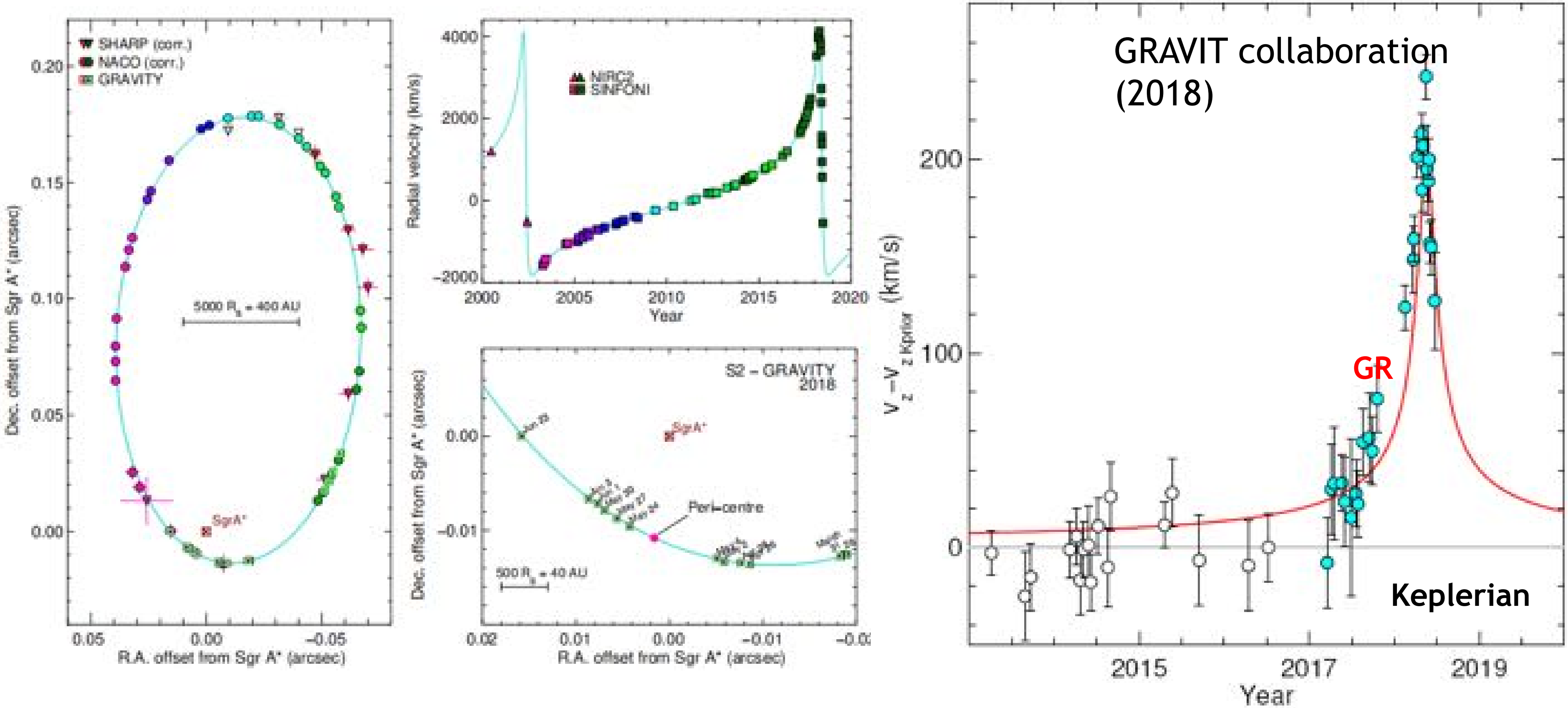

The GRAVITY experiment's measurements of the orbit and velocity of the S2 star around the Galactic Center black hole have precisely validated General Relativity in strong gravitational fields.

Event Horizon Telescope Imaging of a Black Hole

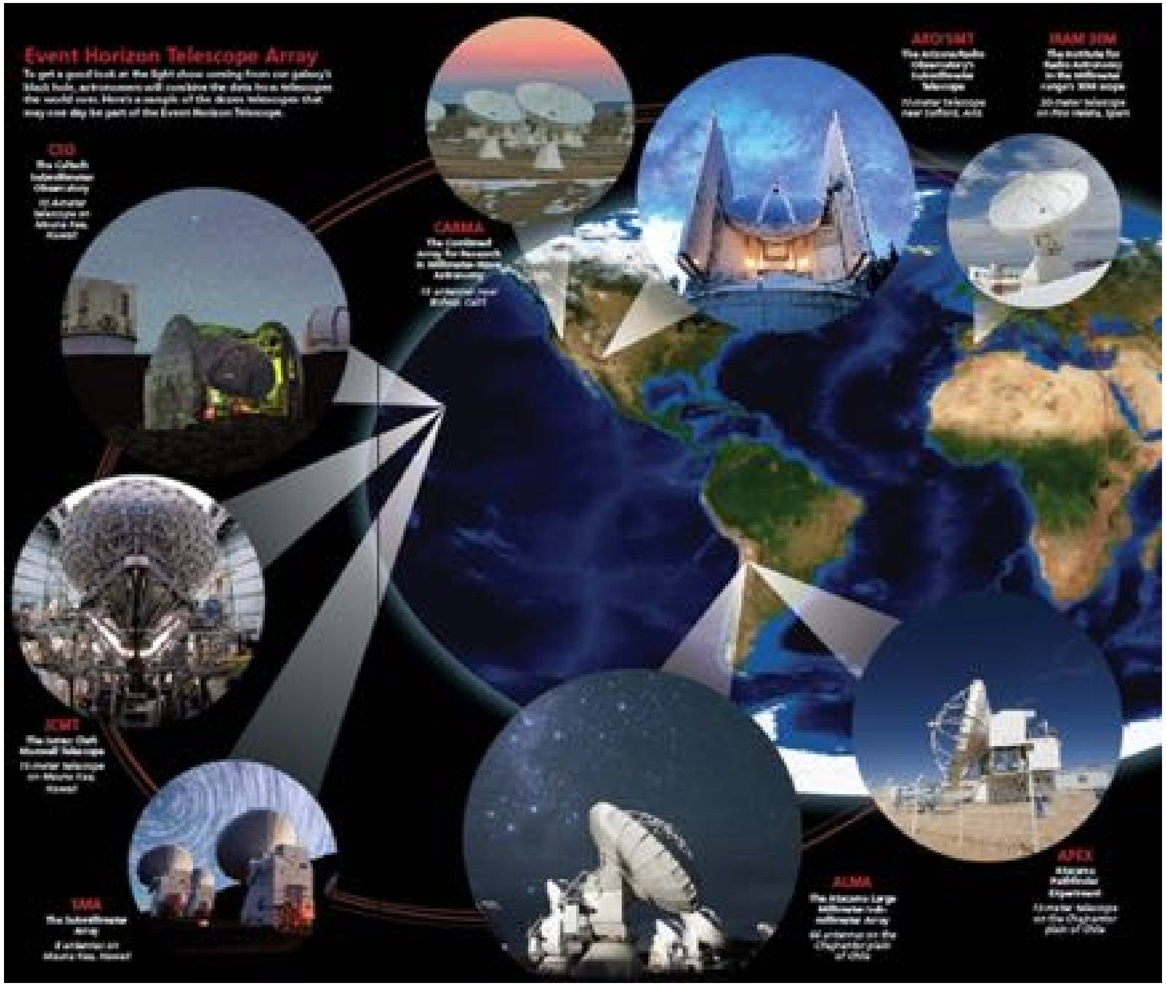

EHT collaboration (2019)

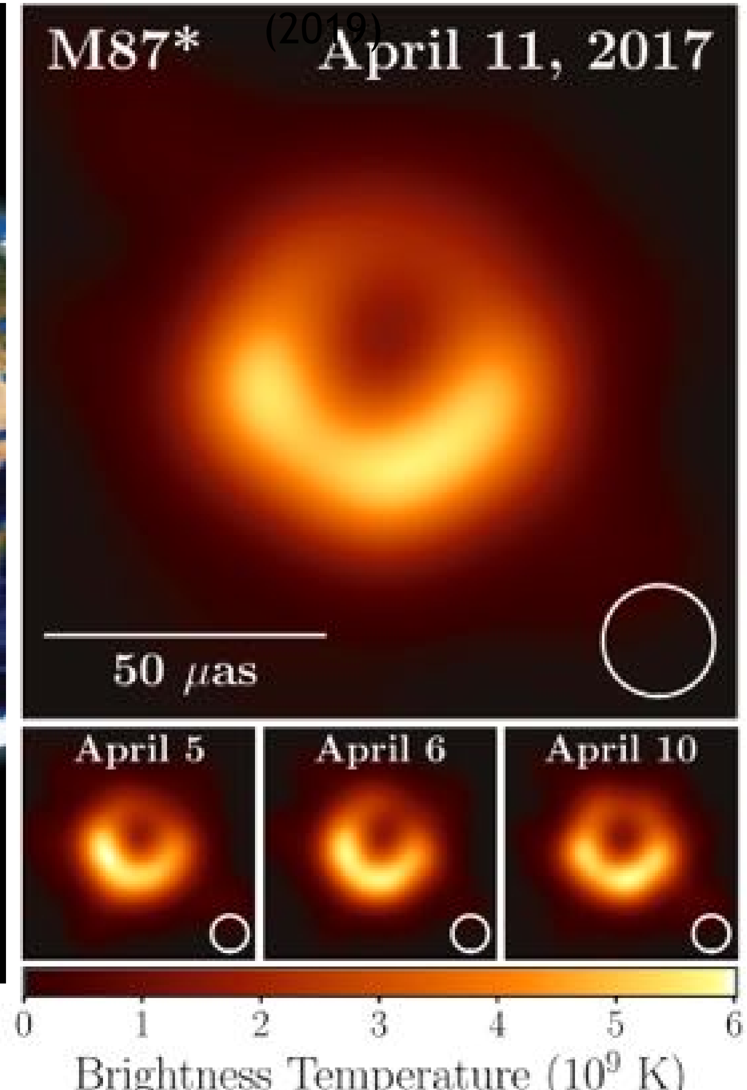

Dark matter matters!

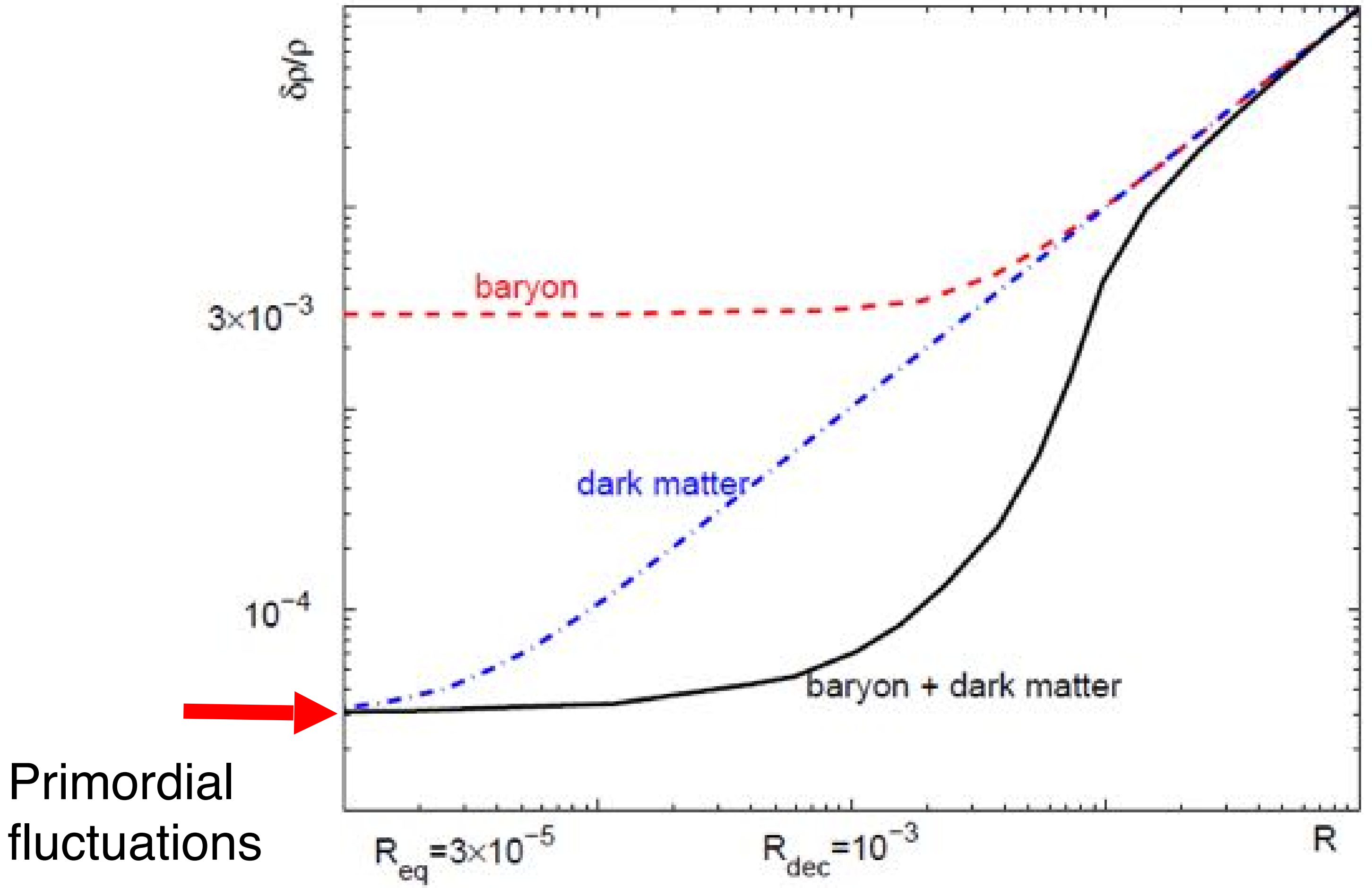

Without DM, galaxies wouldn't have had enough time to form, so there would be no Milky Way, no Solar System, and likely no you or me!

Properties of DM

What is Dark Matter?

DM is an unknown substance inferred from astronomical observations. It doesn't emit light or electromagnetic waves but affects celestial bodies and the universe through gravity on large scales.

DM is unevenly distributed, forming structures of various sizes. Overall, DM has five times the mass of ordinary matter, but its distribution varies greatly.

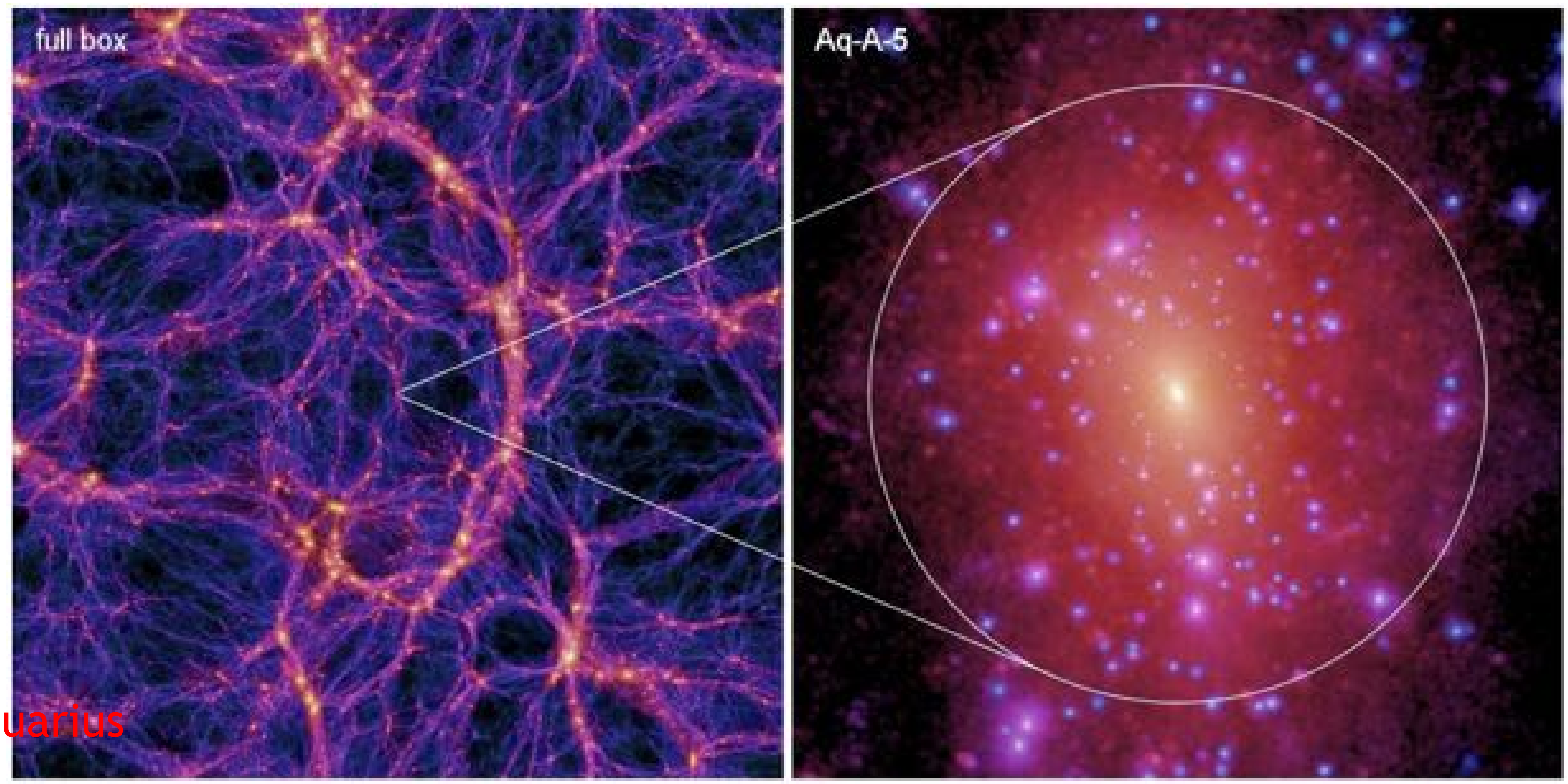

What is Dark Matter?

- Neutral, uncharged
    - Weakly interacts with visible matter
- Stable
- Massive
- Cold

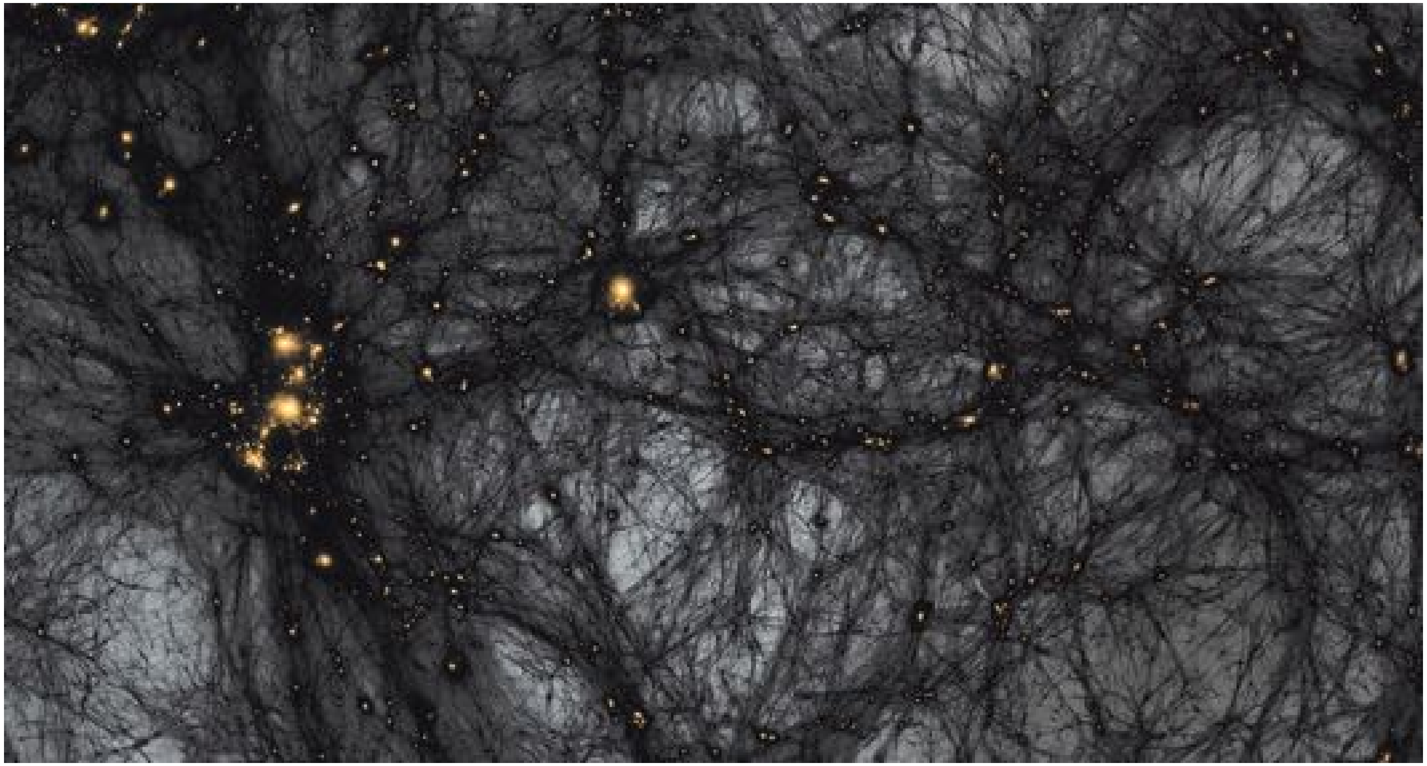

Dark Matter Around Us

- DM density is about 0.3 hydrogen atoms per cm^3.
- Assuming a DM particle mass is 100 times that of a hydrogen atom, there is roughly 1 DM particle in a teacup.
- About 100 million DM particles pass through our bodies every second.
- The total mass of DM within the Earth's volume is approximately 0.5 kilograms.
- In the Milky Way, the mass of DM is about 10 times that of stars and gas.

DM Candidate Models

1904.07915，TASI lecture

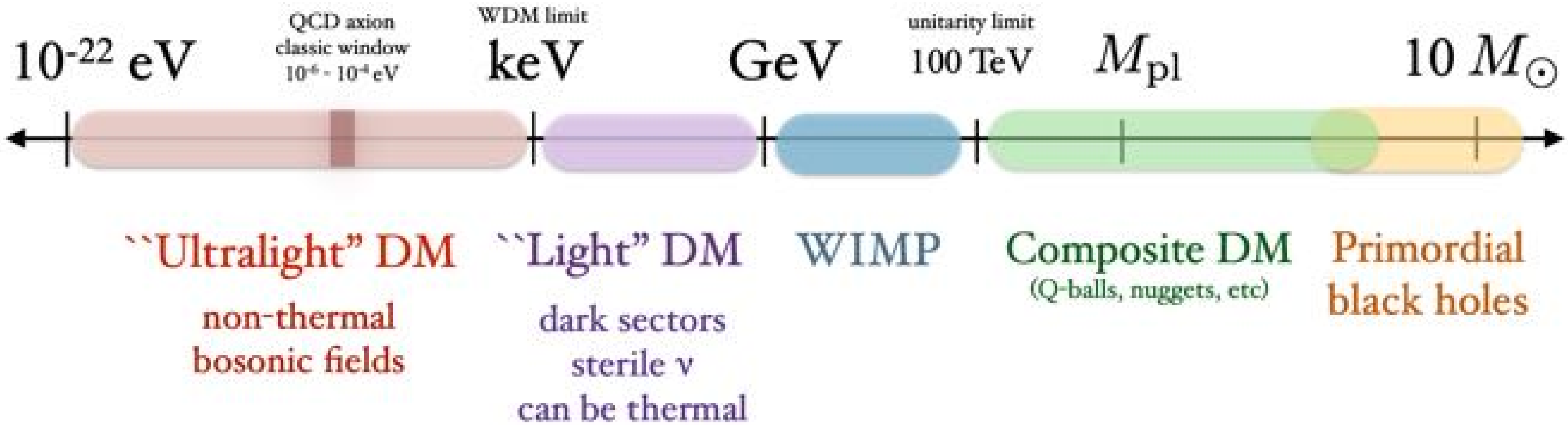

- Primordial Black Hole (PBH)
- Ultralight Dark Matter
- Weakly Interacting Massive Particle (WIMP)

PBH Dark Matter

- Macroscopic Objects
- Primordial Black Holes
- Asteroid-sized primordial black holes could serve as DM.

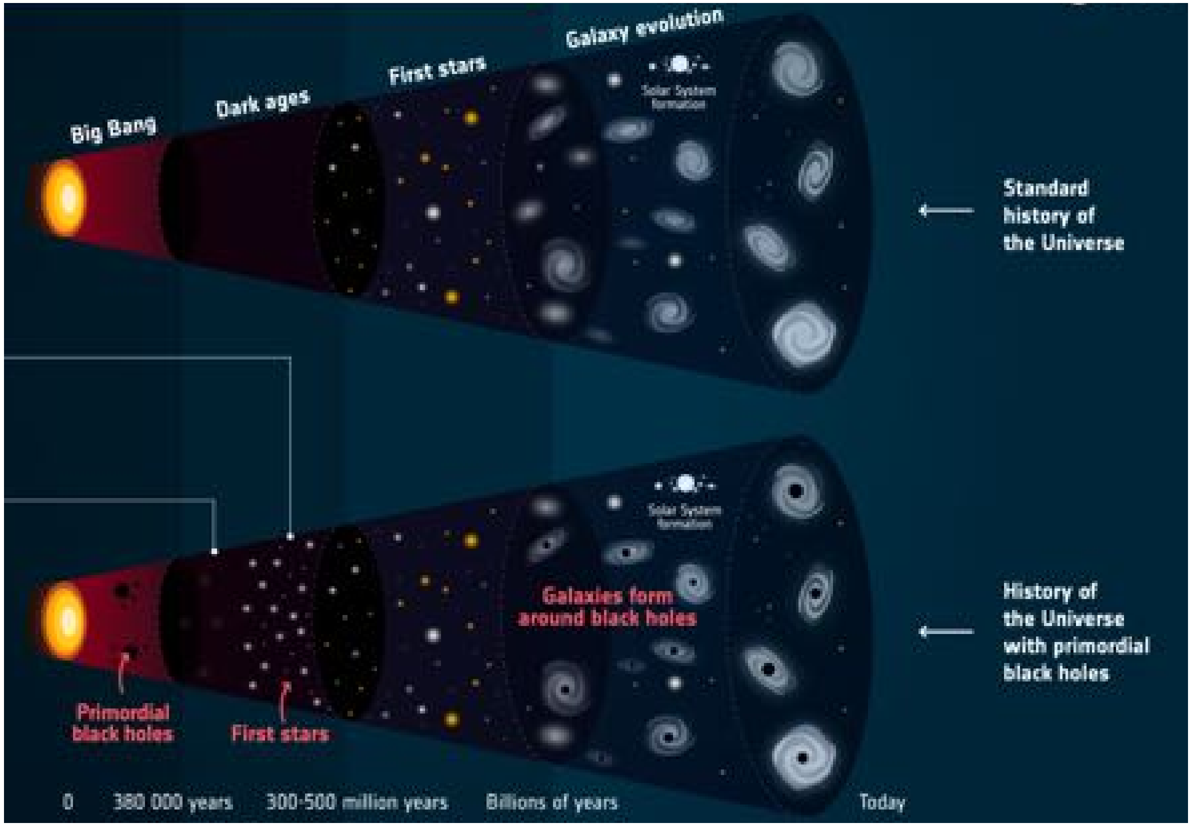

Is DM made of black holes?

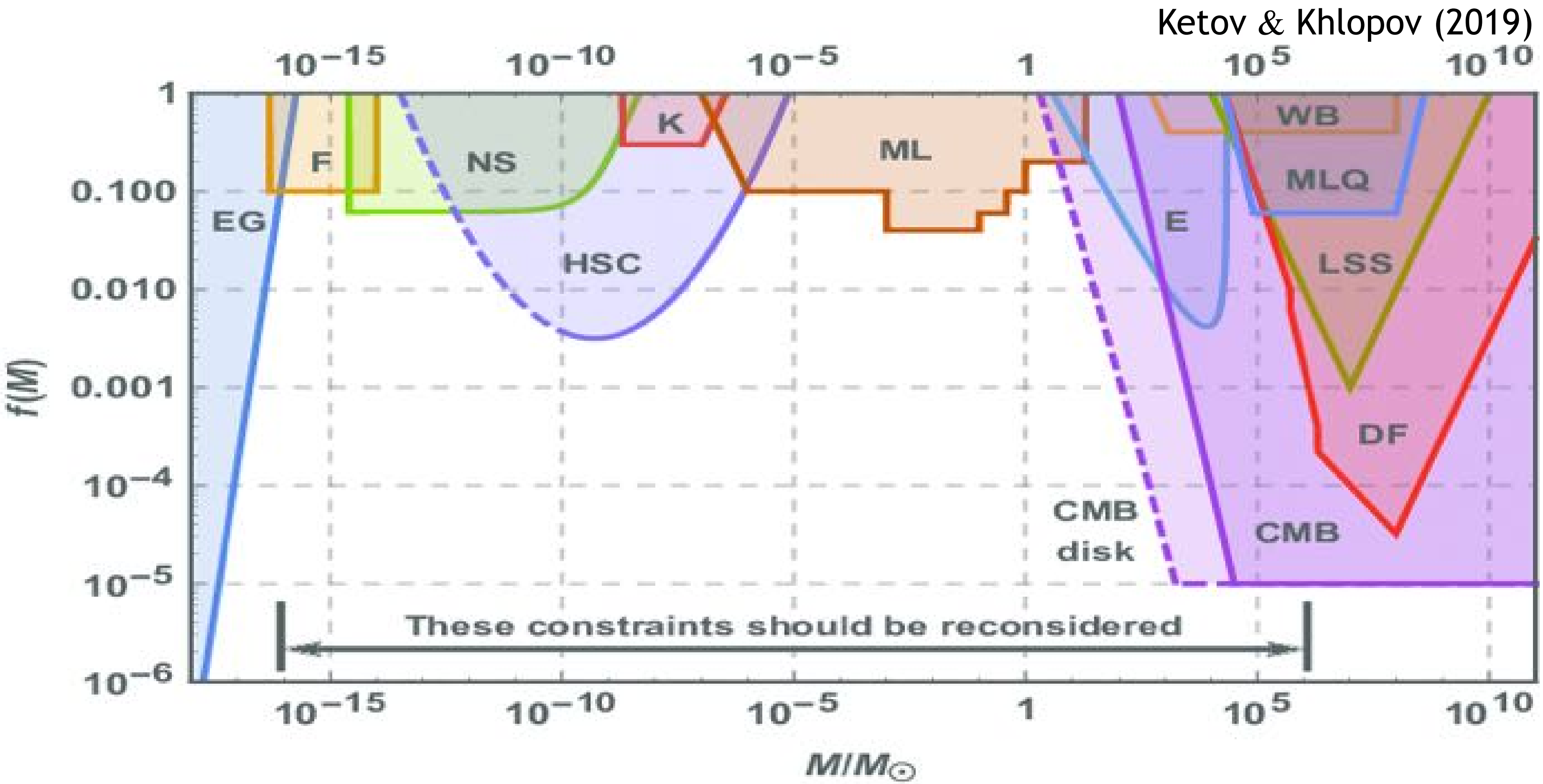

Even if black holes can constitute DM, they can only account for a small fraction of the DM in the universe.

What is Dark Matter?

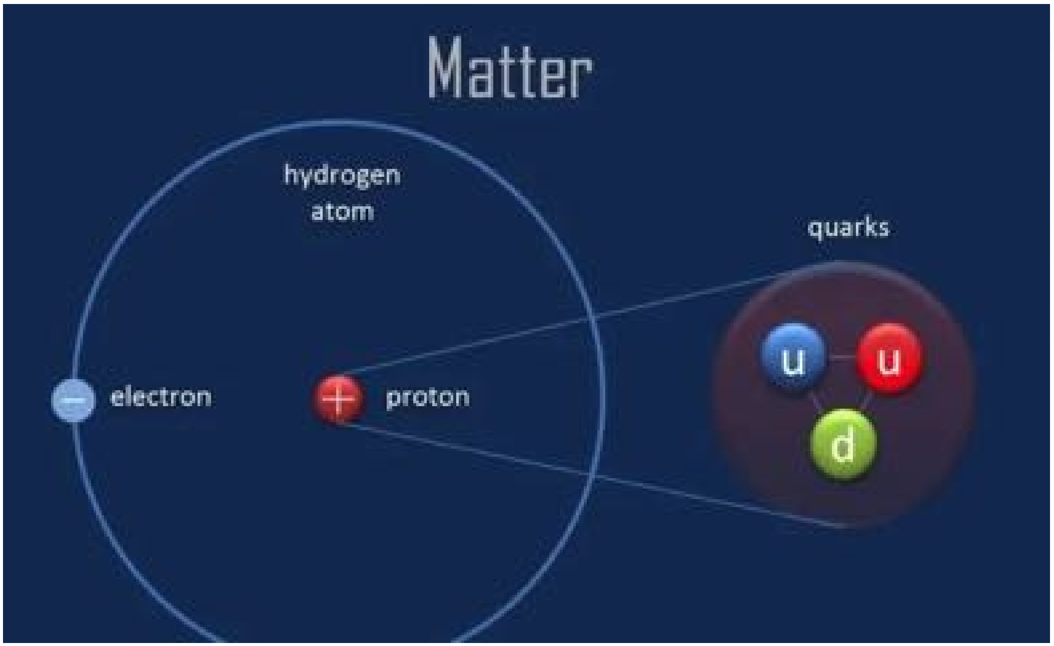

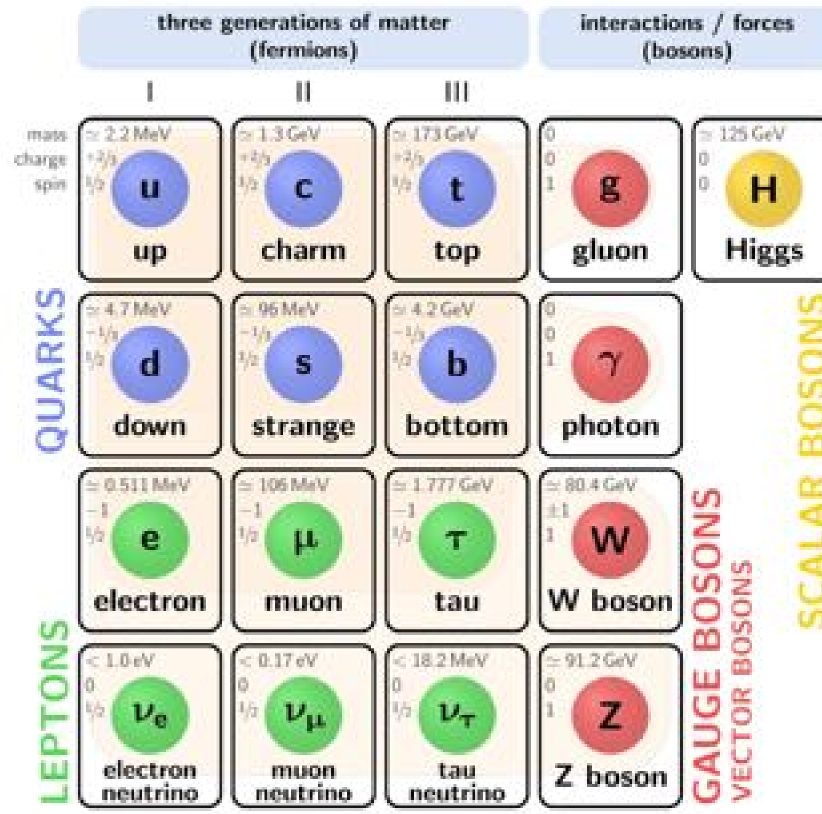

Properties of DM: stable, slow-moving (cold), non-baryonic, weakly interacting

DM is different from any particles in the Standard Model, likely a new particle (or particles) beyond the Standard Model—new physics!

The Standard Model of Particle Physics and DM

- No body knows what DM is
- Not in Standard Model
- There are good guesses

Not neutrinos ✗

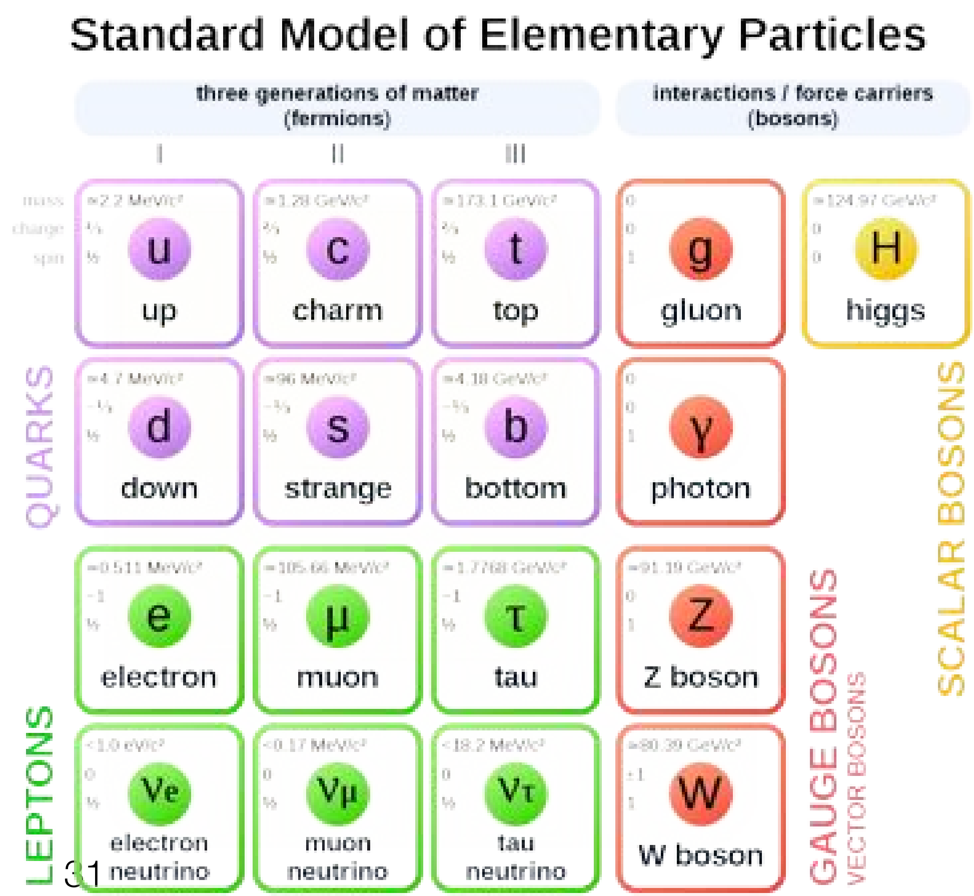

The Standard Model of Particle Physics and DM

- No body knows what DM is
- Not in Standard Model
- There are good guesses

Not neutrinos ✘

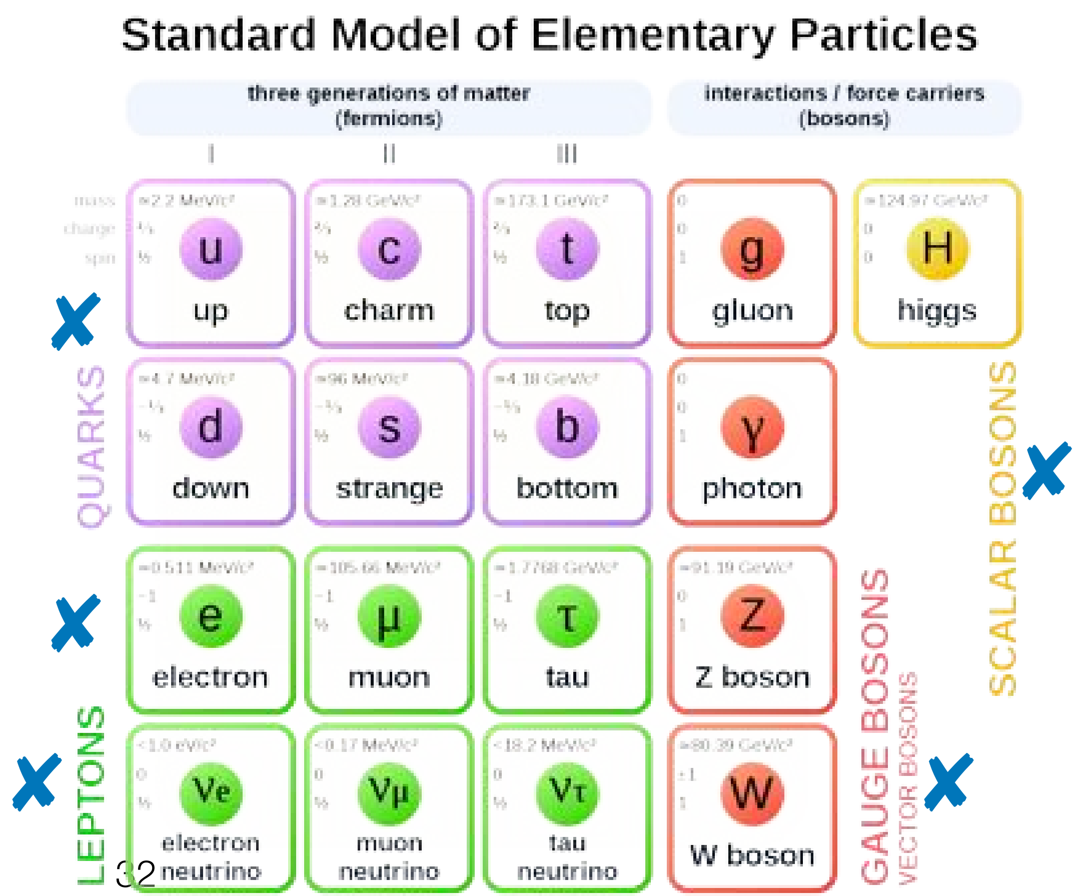

Implications of Large-Scale Structure in the Universe

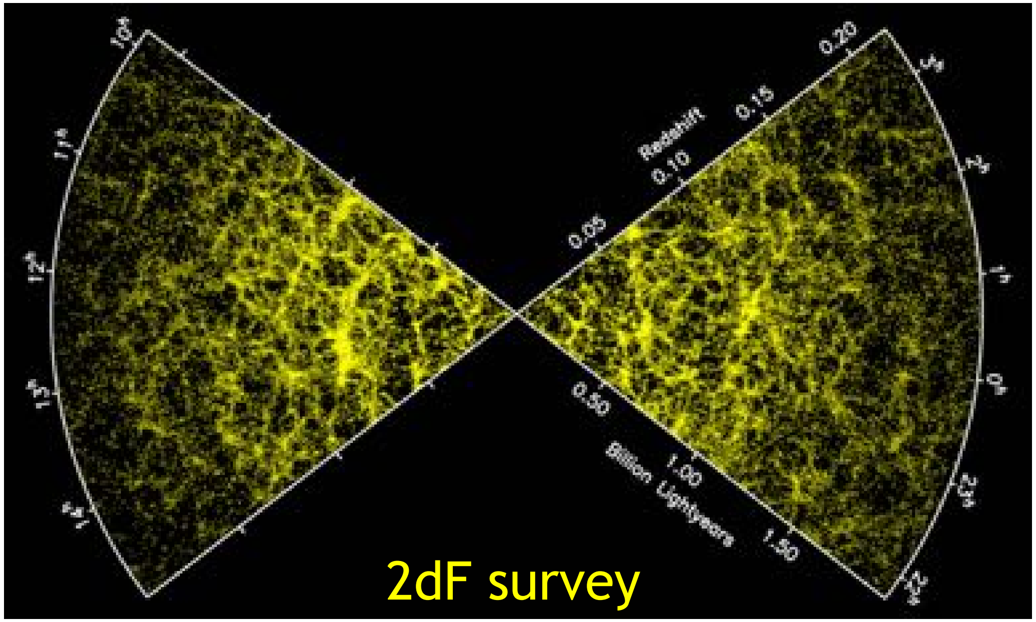

The evolution of structures from small to large implies that DM is cold.
("Cold" means DM has low kinetic energy and short free-streaming distances, forming structures via Jeans instability before spreading out.)

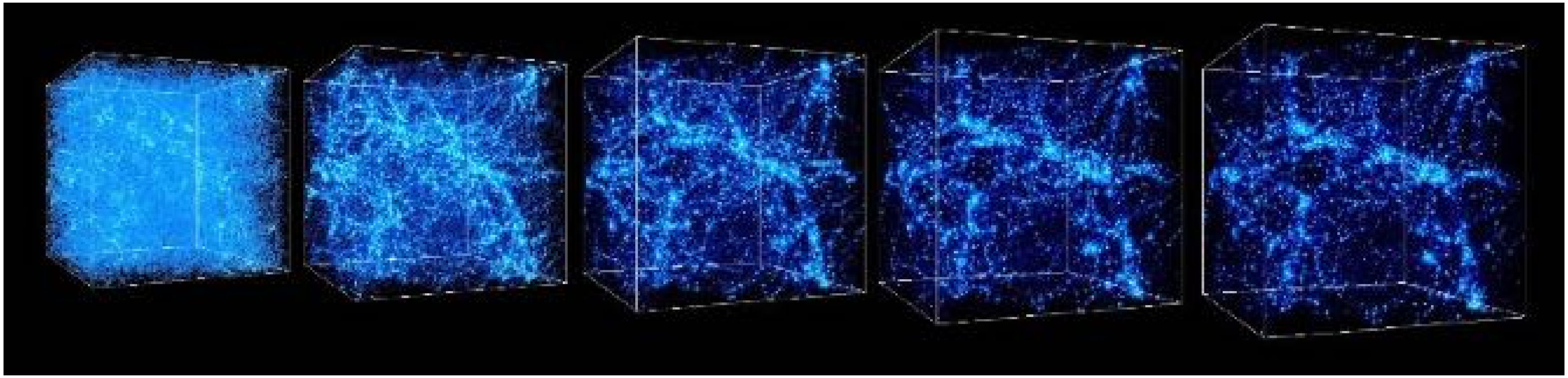

Thermal History of the Universe

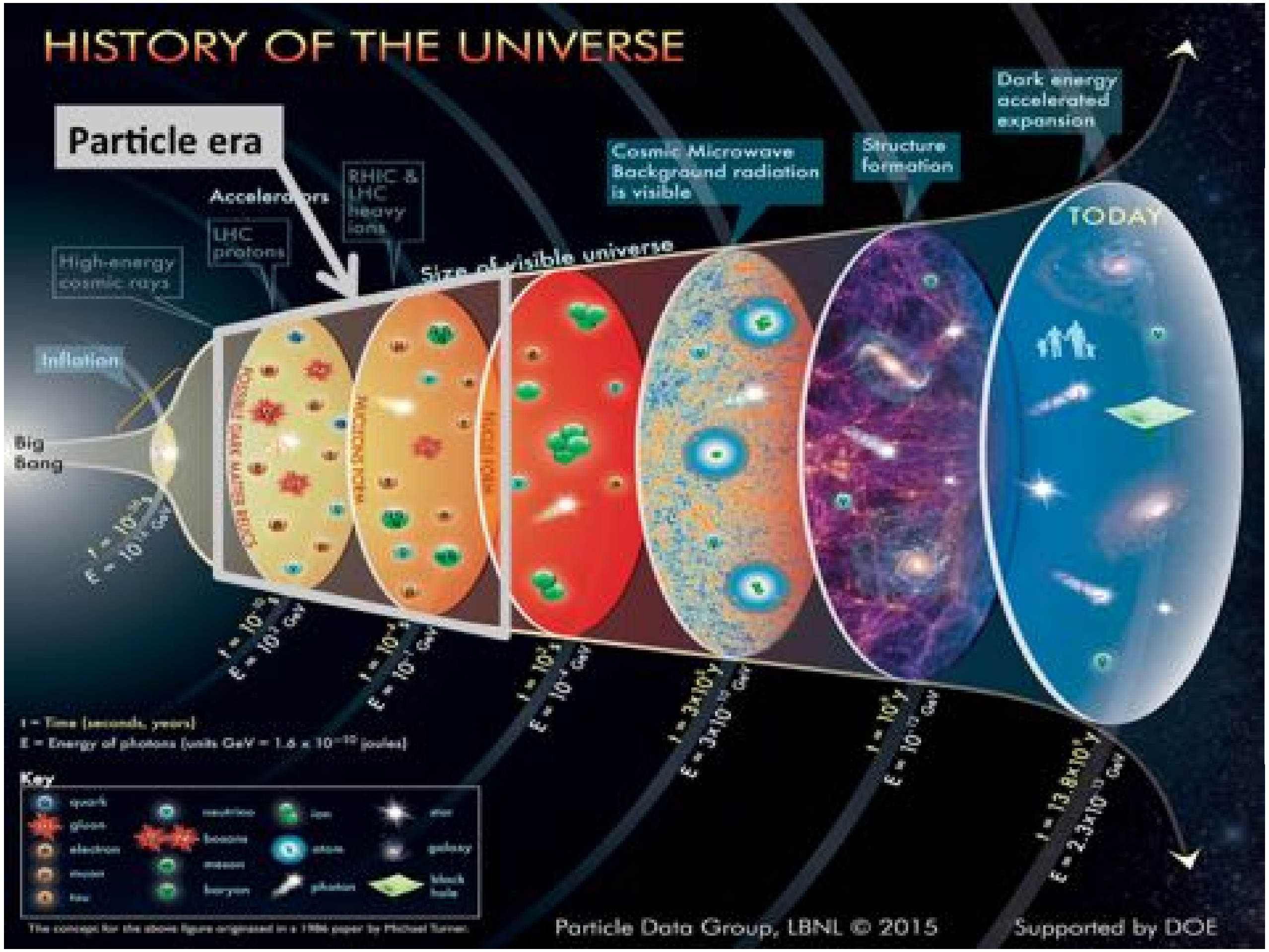

The dark matter distribution

- Astrophysicist knows the distribution of DM by simulation

$$\rho(r) = \frac{\rho_0}{\frac{r}{R_s}\left(1 + \frac{r}{R_s}\right)^2}$$

- Navarro-Frenk-White profile:
- R_s is the "scale radius", $\{\rho_0, R_s\}$ varies from halo to halo
- Integrated mass:

$$M = \int_0^{R_{max}} 4\pi r^2 \rho(r)\, dr = 4\pi\rho_0 R_s^3 \left[\ln\left(\frac{R_s + R_{max}}{R_s}\right) + \frac{R_s}{R_s + R_{max}} - 1\right]$$

$$M = \int_0^{R_{vir}} 4\pi r^2 \rho(r)\, dr = 4\pi\rho_0 R_s^3 \left[\ln(1+c) - \frac{c}{1+c}\right]$$

The dark matter distribution

- Astrophysicist knows the distribution of DM by N-body simulation

- Navarro-Frenk-White profile:

$$\rho(r) = \frac{\rho_0}{\frac{r}{R_s}\left(1 + \frac{r}{R_s}\right)^2}$$

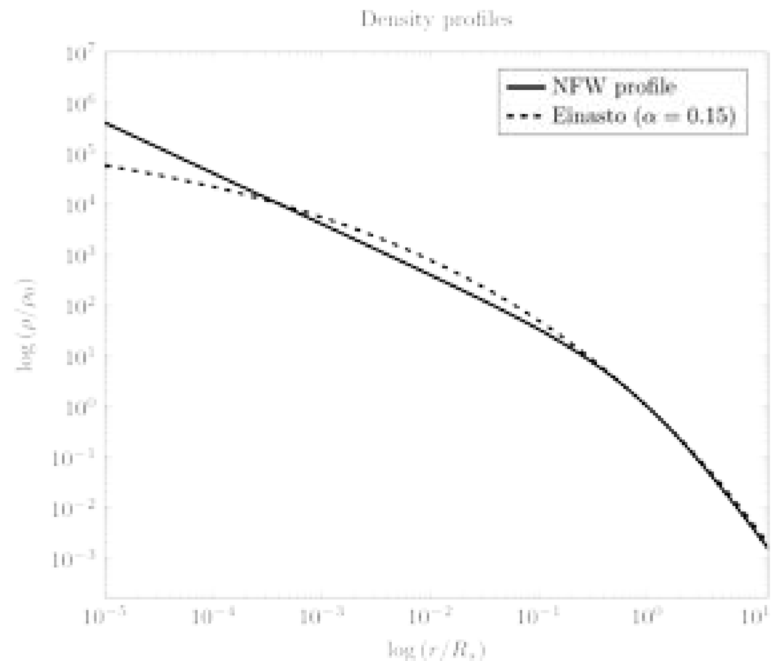

- Other competing profile: Einasto

Small-Scale Structure Problem of DM

- Astrophysicist knows the distribution of DM by N-body simulation
- Navarro-Frenk-White profile:
-

$$\rho(r) = \frac{\rho_0}{\frac{r}{R_s}\left(1 + \frac{r}{R_s}\right)^2}$$

- CDM: very good for large scale, but problems at galactic scale

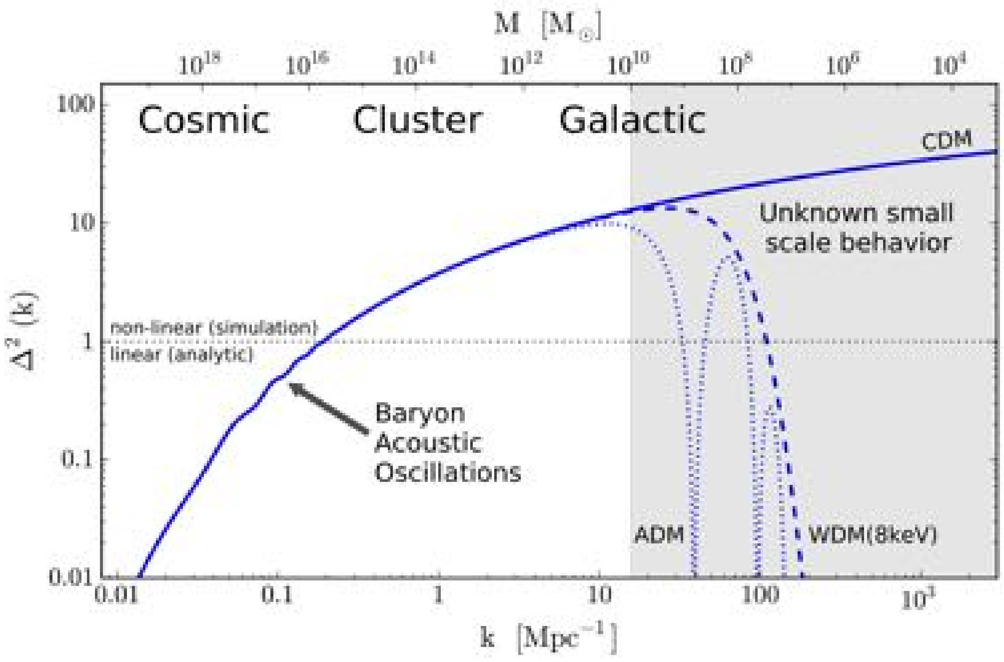

Small-Scale Structure: Cusp-Core Distribution Problem

- Astrophysicist knows the distribution of DM by simulation
- Navarro-Frenk-White profile:
-

$$\rho(r) = \frac{\rho_0}{\frac{r}{R_s}\left(1 + \frac{r}{R_s}\right)^2}$$

- CDM: very good for large scale, but problems at galactic scale
  - Core-Cusp problem of cold dark matter

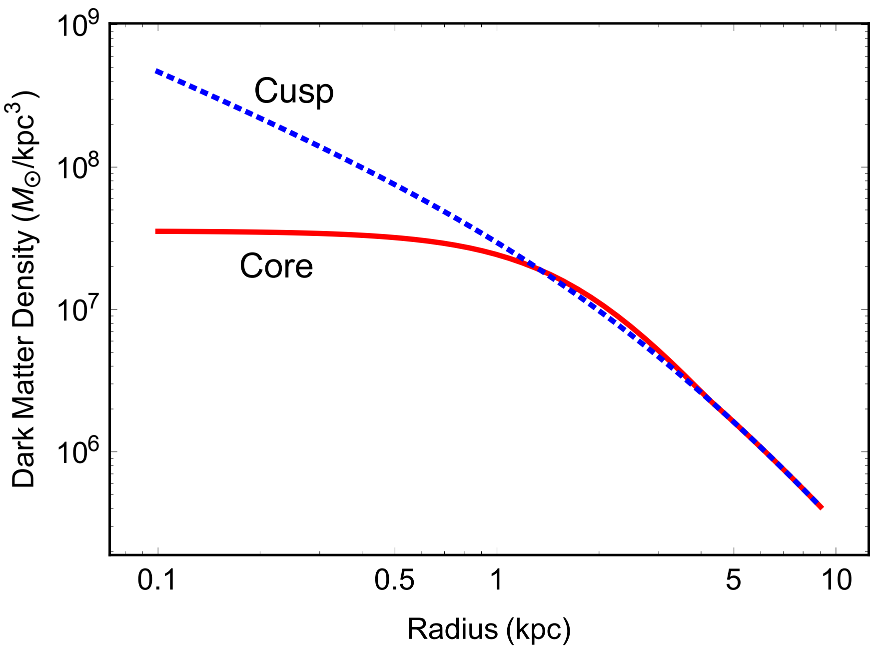

Thermal Evolution History of DM Density

DM+DM ⟷ SM+SM

Garrett & Duta (2011)

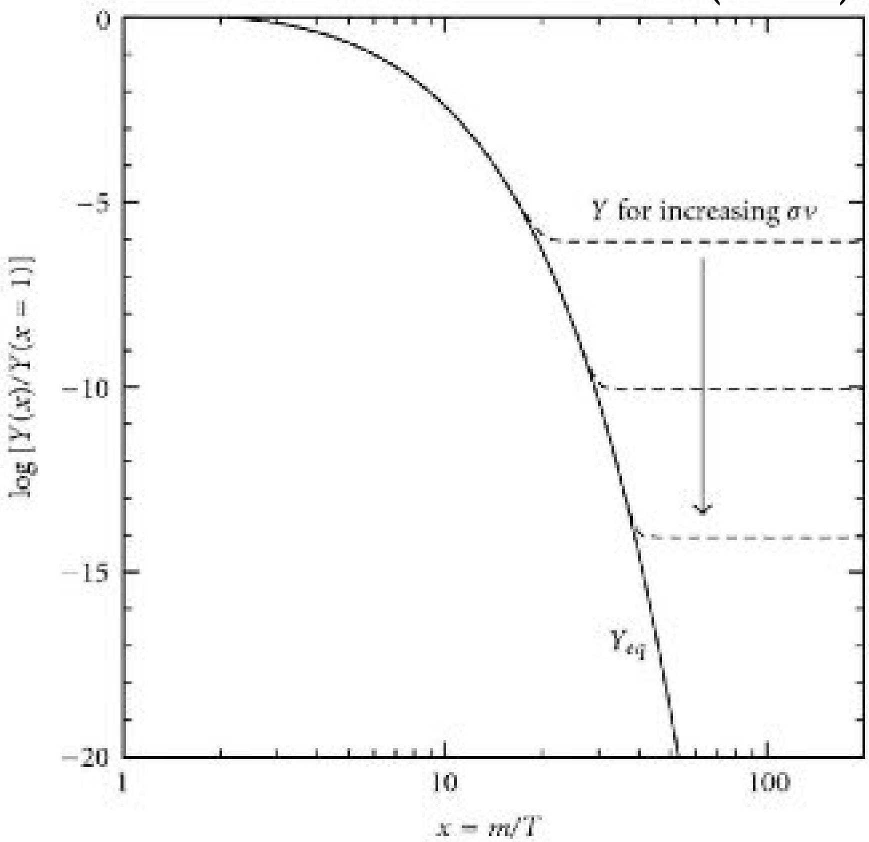

$$\langle \sigma v \rangle \simeq \left(\frac{3 \times 10^{-27} \mathrm{cm}^3 \mathrm{s}^{-1}}{\Omega_\chi h^2} \right)$$

$$\sigma \sim 10^{-35} \mathrm{cm}^2$$

Weak Interaction Cross-Section!

WIMP Miracle: Weakly Interacting Massive Particles (WIMPs) are the best candidates for DM!

Detection Methods of DM

Particle-like DM Detection

Theorists' View of DM

Sterile Neutrinos:
Neutrino Oscillations,
X-ray Astronomy

Black Holes (MACHOs):
Gravitational Lensing,
Gravitational Waves

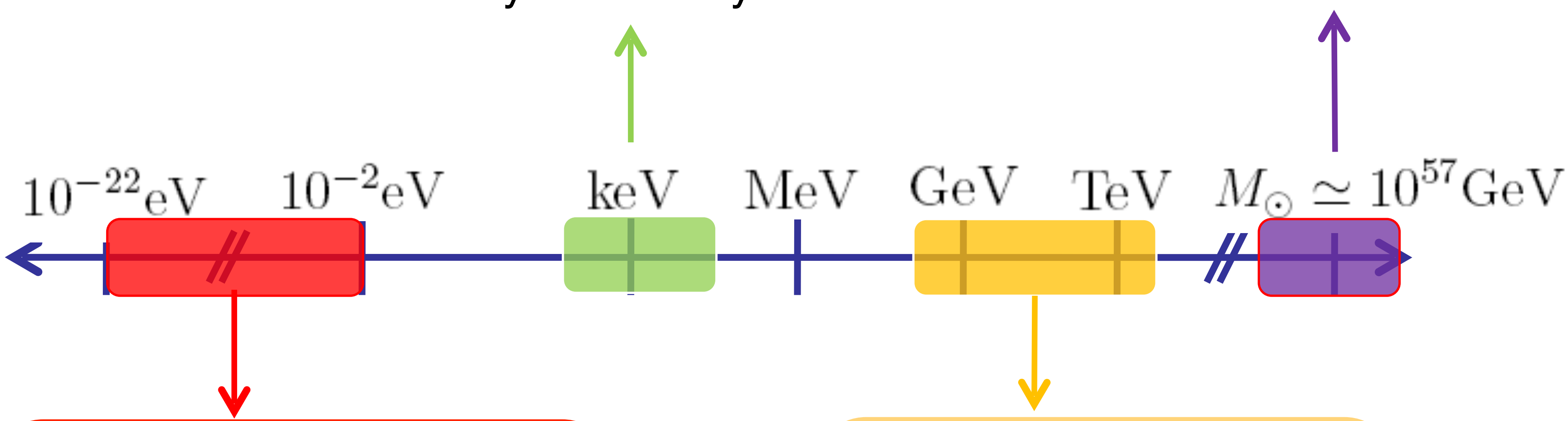

Ultralight DM (Axions, Axion-like Particles, Dark Photons...): Cavity Experiments, Radio Astronomy

Wave-like DM

WIMPs:
Direct Detection, Indirect Detection, Collider Detection

Particle-like DM

Theoretical possibilities for DM are numerous, spanning a wide range of masses and interaction cross-sections, making experimental detection highly challenging.

Detecting WIMP DM from Underground to Space

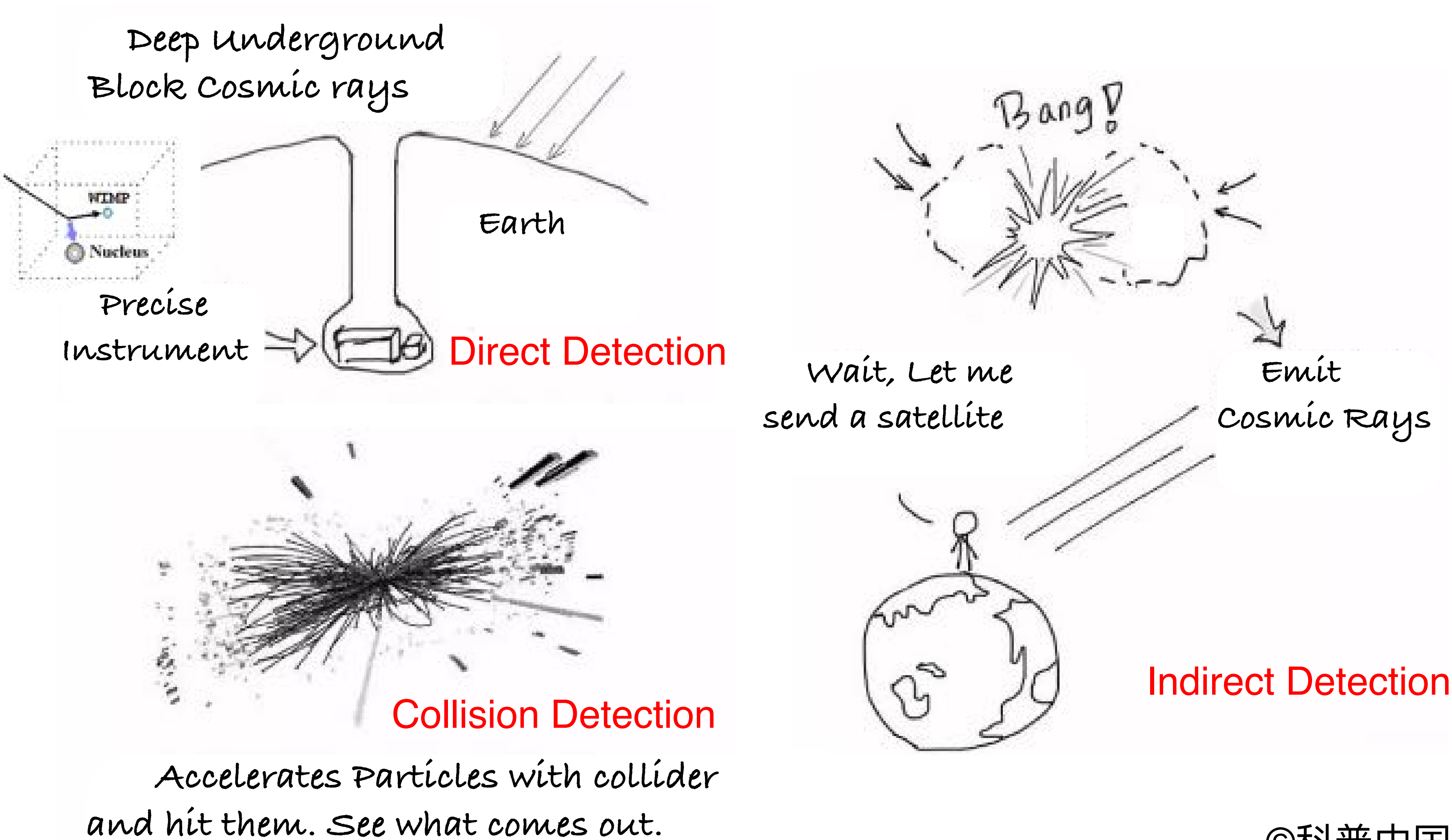

Direct Detection of WIMP DM

Direct Detection of Dark Matter

- Measuring the recoil signal of nuclei after collisions with DM
  - Proposed in 1985 (Goodman & Witten), detection sensitivity has improved by six orders of magnitude over 30 years.

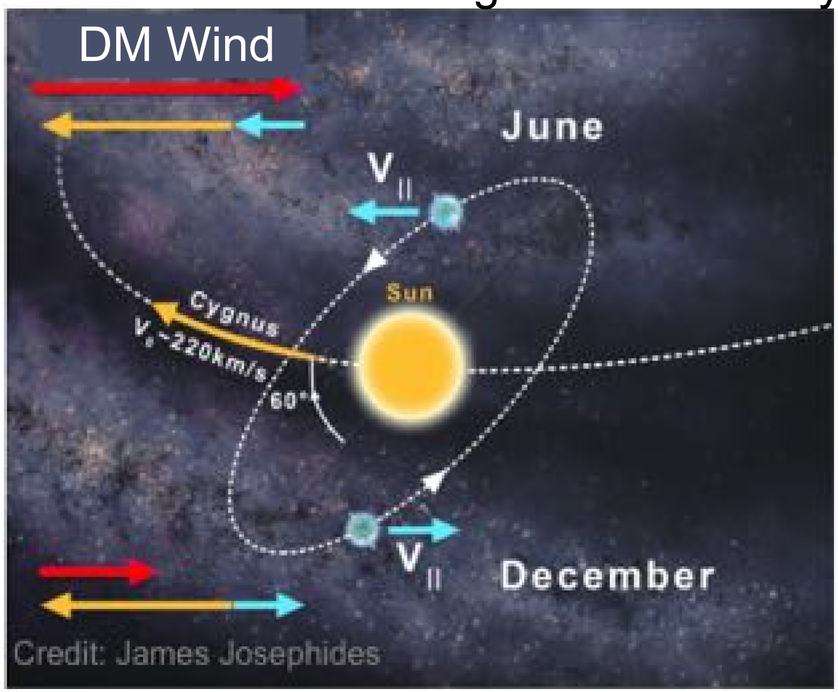

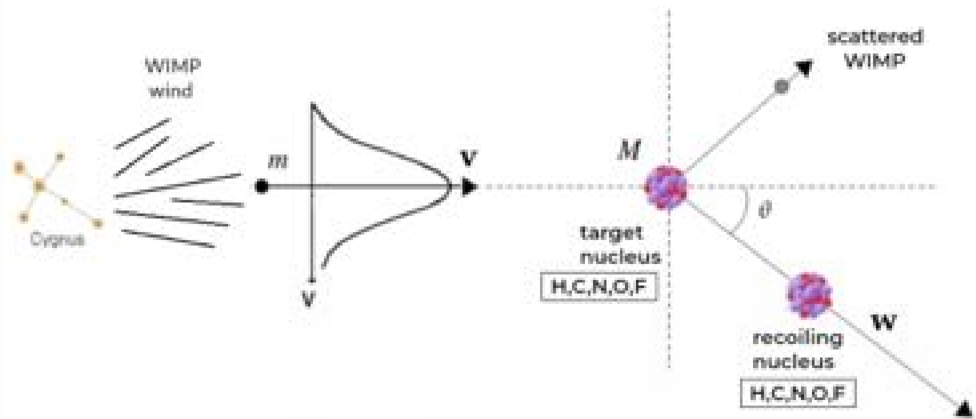

Direct Detection of WIMP DM

What is collision?

- Particle Physicist's language
  - Interaction

- When a ping-pong ball and paddle collide => interaction occurs
  - Dark matter and ordinary matter can interact: collision!
- The stronger the interaction: the easier the collision
  - The size of the paddle hints the strength of interaction: cross-section

Direct Detection of WIMP DM

What is the target matter

- How to detect such weak "interactions"
  - Large amount of atoms => One big piece of ordinary matter
  - Everyone has 100000000000000000000000000000(10^{29}) atoms

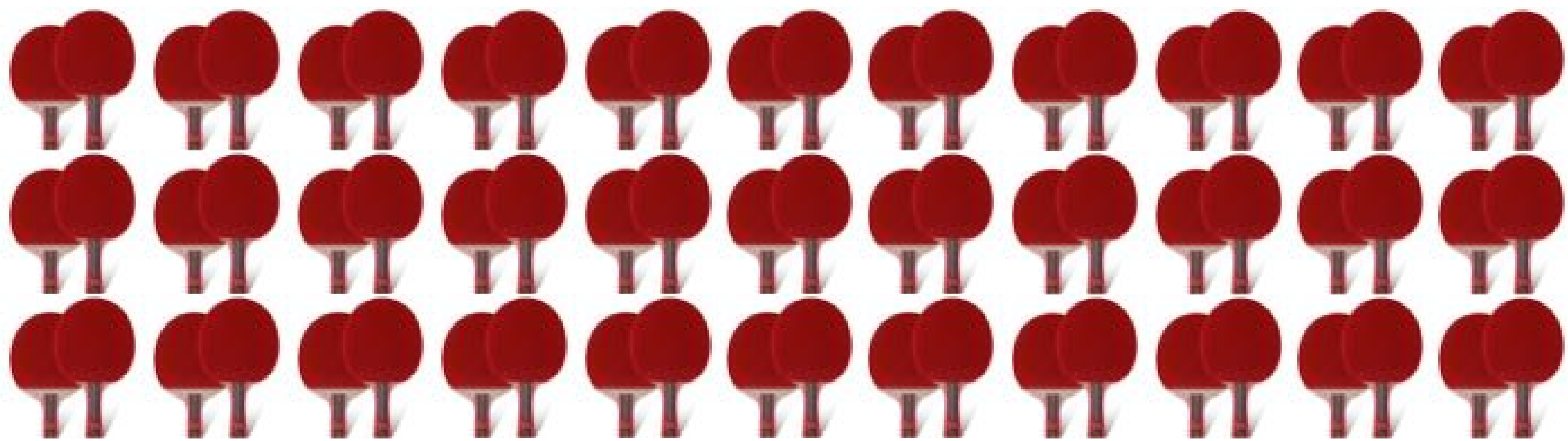

Direct Detection of WIMP DM

What is recoil

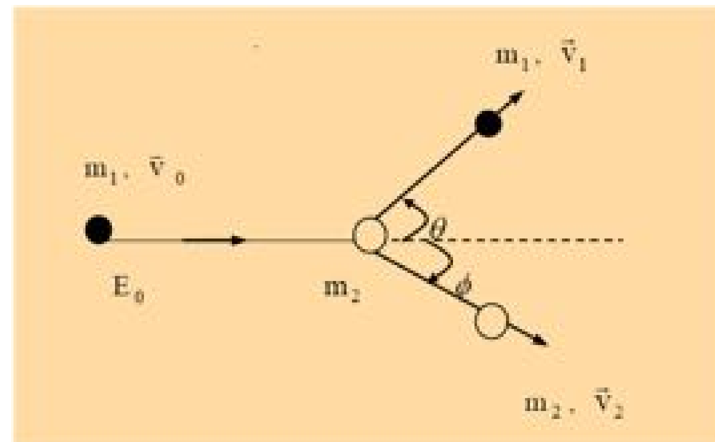

- The recoiled atoms carry energy
- Direct Detection of DM can change recoil into observable signals
  - Infer the mass of the DM particles
  - Measure the interaction strength with ordinary matter

Direct Detection of WIMP DM

Can DM easily collide with ordinary matter

- 100000000(10^8) DM particles travel through us each second
- Each person has 10^{29} target particles
- Each person collides with dark matter < 1 time each year

ELSEVIER

Physics Letters B

Volume 717, Issues 1–3, 22 October 2012, Pages 25-28

Dark matter collisions with the human body

Katherine Freese [a], Christopher Savage [b]

[a] Michigan Center for Theoretical Physics, Department of Physics, University of Michigan, Ann Arbor, MI 48109, United States

[b] The Oskar Klein Centre for Cosmoparticle Physics, Department of Physics, Stockholm University, AlbaNova, SE-106 91 Stockholm, Sweden

Received 6 September 2012, Accepted 19 September 2012, Available online 24 September 2012.

Editor: S. Dodelson

Current Direct Detection of WIMP DM

Calculate the DM Event Rate

- For a 1ton Xenon Detector
- Assumptions for DM
  - DM mass-100GeV
  - DM cross-section with xenon nucleus-$10^{-38}\mathrm{cm}^2$
  - DM relative velocity-200km/s
  - DM density near the earth-0.3GeV/cm^3
- Please estimate, how many collision signals on the device each year?

1

Direct Detection of WIMP DM

Where to find the Dark Matter

- Our body collides with cosmic rays and gamma rays 10^8 times each day
  - Cosmic rays: high energy particles from the universe
  - Gamma rays: from adjacent nucleus decay
  - Those fake signals are called “background noise”
- Hide the detector into deep underground, and cover the detector with thick screening material

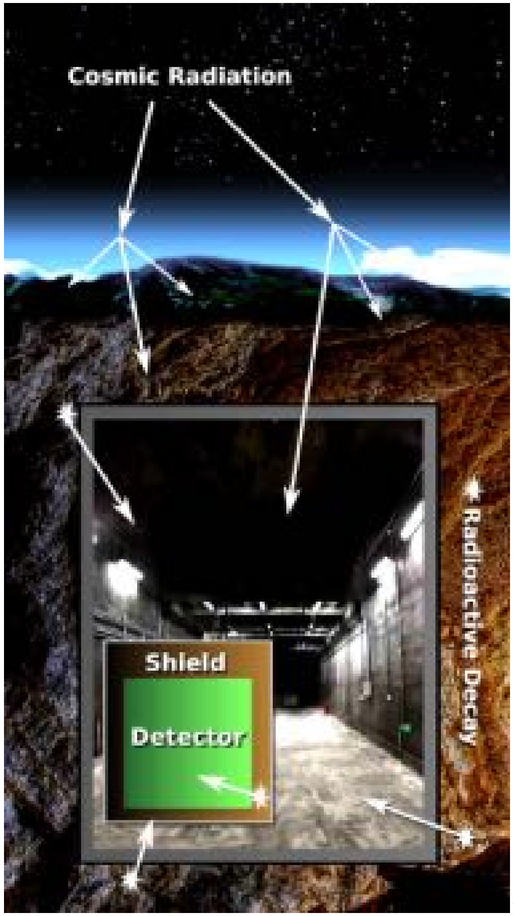

Direct Detection of WIMP DM

DM scatter with nucleus of atoms

- DM particles elastically scatter with target nucleus
- Recoil energy of nucleus $E_R = \frac{4m_\chi m_N}{(m_\chi+m_N)^2} E_\chi^{kin}$
  - $E_\chi^{kin} \sim \frac{1}{2} m_\chi v^2 \sim 50\ \mathrm{keV} \frac{m_\chi}{100\ \mathrm{GeV}}$

Low detection threshold

- Event Rate of unit target mass scattering with DM
  - $\frac{dR}{dE_R} \propto \sigma_N \frac{\rho_{DM}}{m_{DM}} \int_{v_{min}}^{v_{esc}} \frac{dv}{v} f(v)$
- Spin-unrelated $\sigma_N^{SI}(E_R) \propto \boldsymbol{A}^2 F^2(E_R)\sigma_n$

Heavy target nucleus

- Spin-related $\sigma_N^{SD}(E_R) \propto \frac{1}{2\boldsymbol{J}+1} S(E_R)\sigma_n$

Target nucleus with spin

Direct Detection of WIMP DM

Calculate signatures of DM signal

- Assumptions for DM
  - DM mass-100GeV
  - DM cross-section with xenon nucleus-$10^{-38}\mathrm{cm}^2$
  - DM relative velocity-200km/s
  - DM density near the earth-0.3GeV/cm^3
- Please estimate the recoil energy of nucleus scattering with DM

Direct Detection of WIMP DM

Signatures of DM signal

- **Scattering cross section on nuclei**
  - Spin-independent, $\propto A^2$, Form factor
  - Spin-dependent, spin structure factor

$$\frac{dR}{dE_R} = \frac{\rho_0}{m_\chi m_N} \int_{v_{min}}^{v_{esc}} \frac{d\sigma_{\chi N}}{dE_R}(v, E_R) v f(v) dv$$

$$\frac{d\sigma_{\chi N}}{dE_R} = \frac{m_N}{2\mu_N^2 v^2}(\sigma_0^{SI} F_{SI}^2(E_R) + \sigma_0^{SD} F_{SD}^2(E_R))$$

Recoil energy spectrum

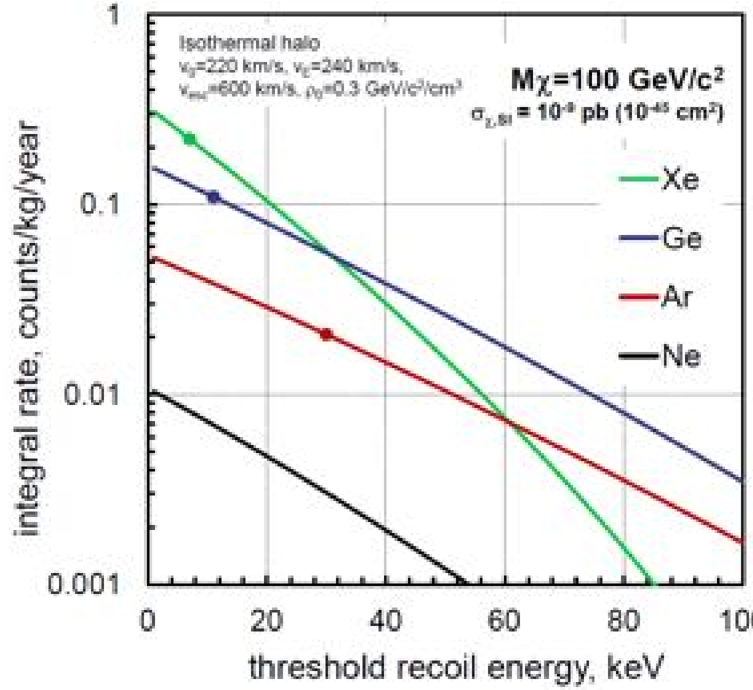

19

Underground Direct Detection

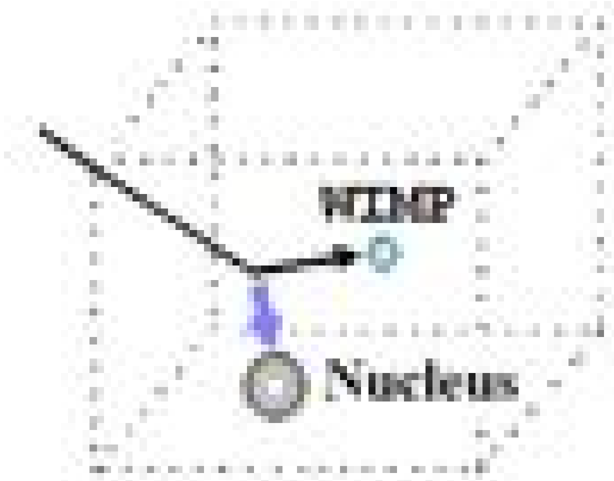

- ➢ Detect the recoil energy of nucleus scattered by DM
- ➢ Deep underground, to block the cosmic ray background

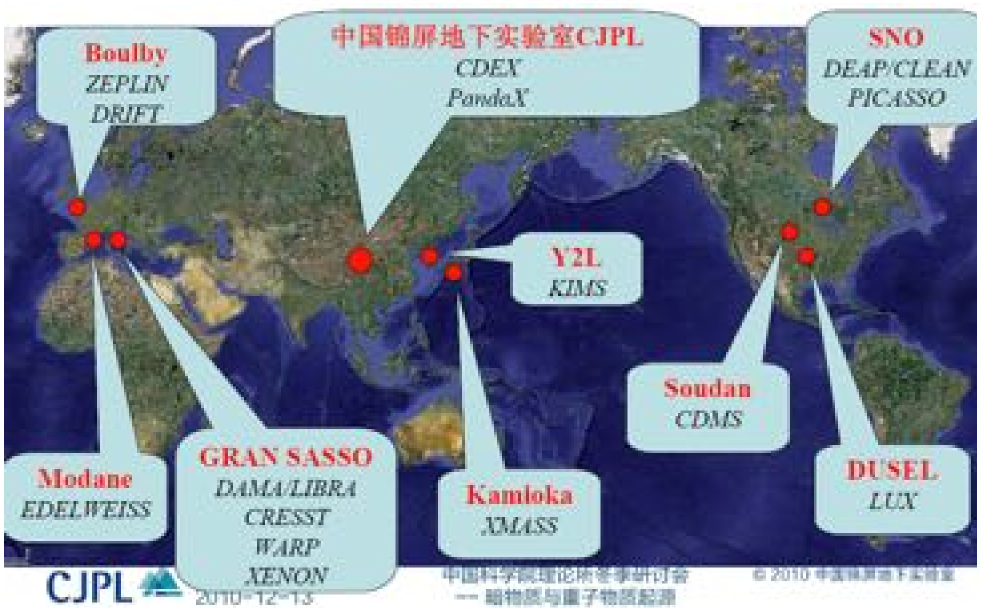

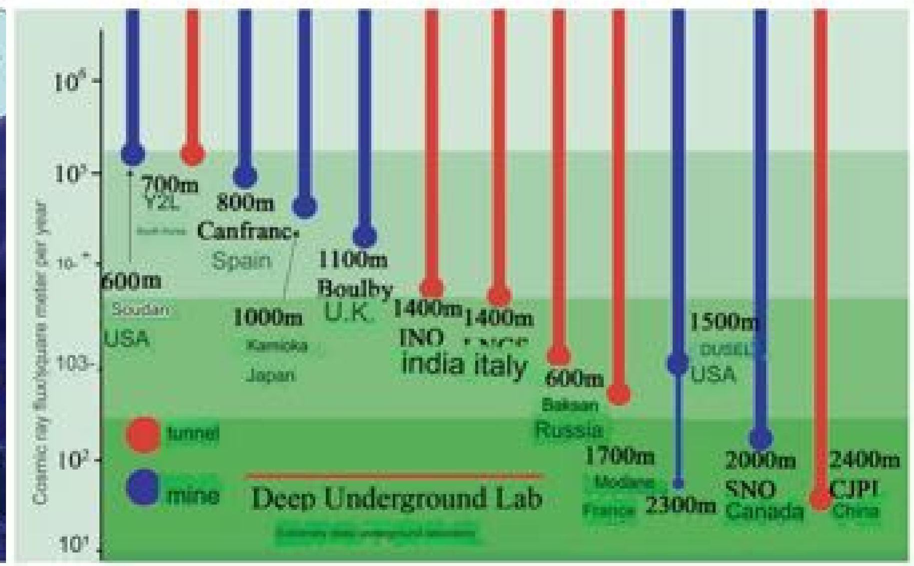

Annual modulation observed by DAMA

DAMA (2008)

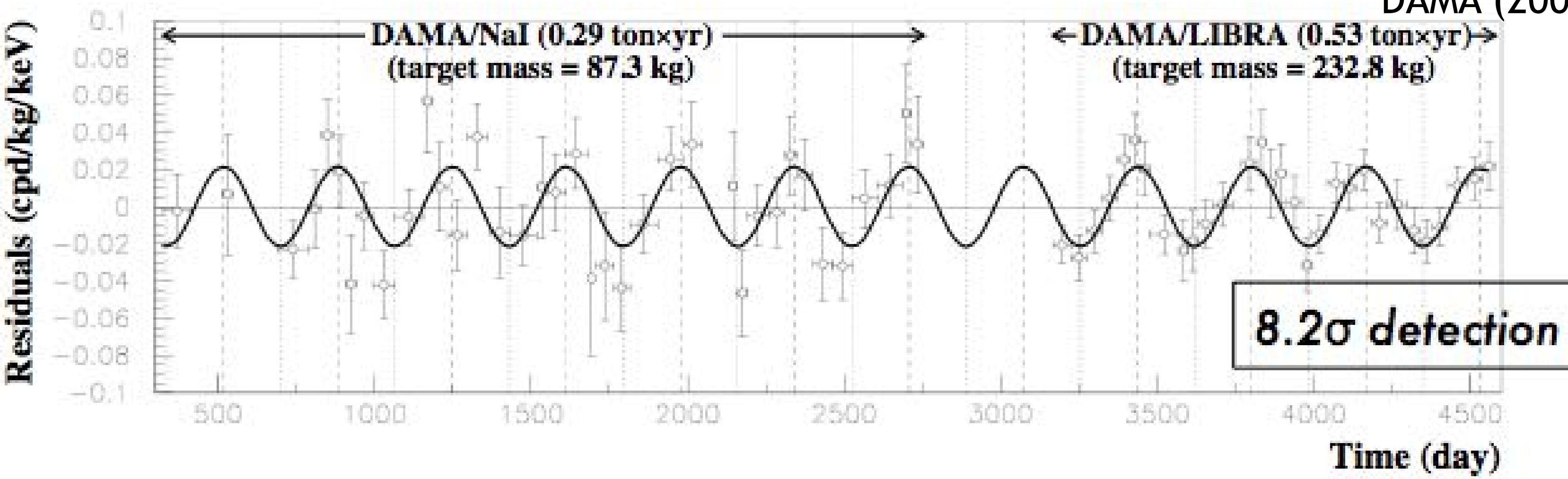

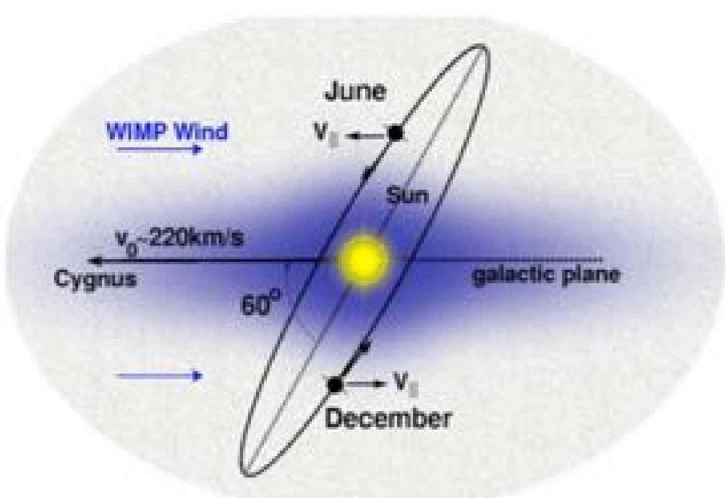

COSINE (2018)

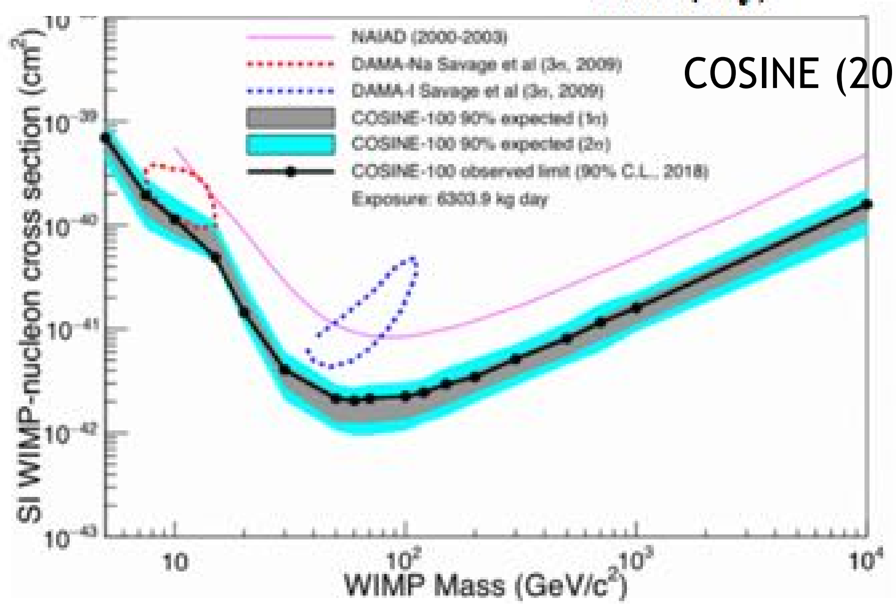

Inconsistent with other experiments!

PandaX in Jinping

Direct DM detection in PandaX

PandaX-4T (2021)

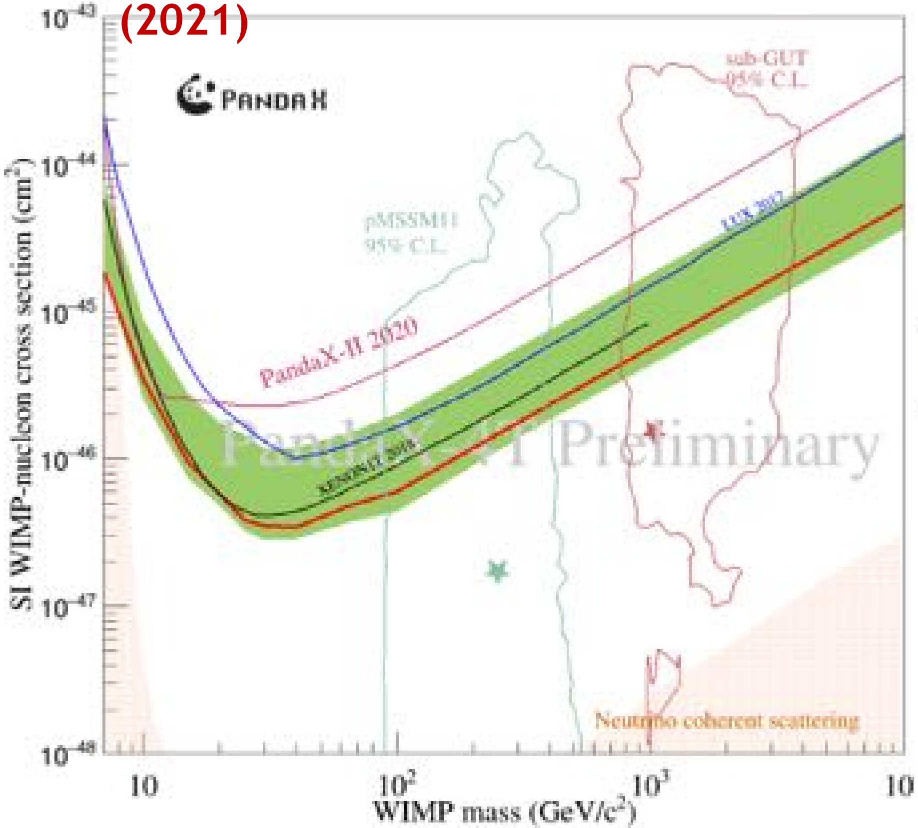

CDEX (2018)

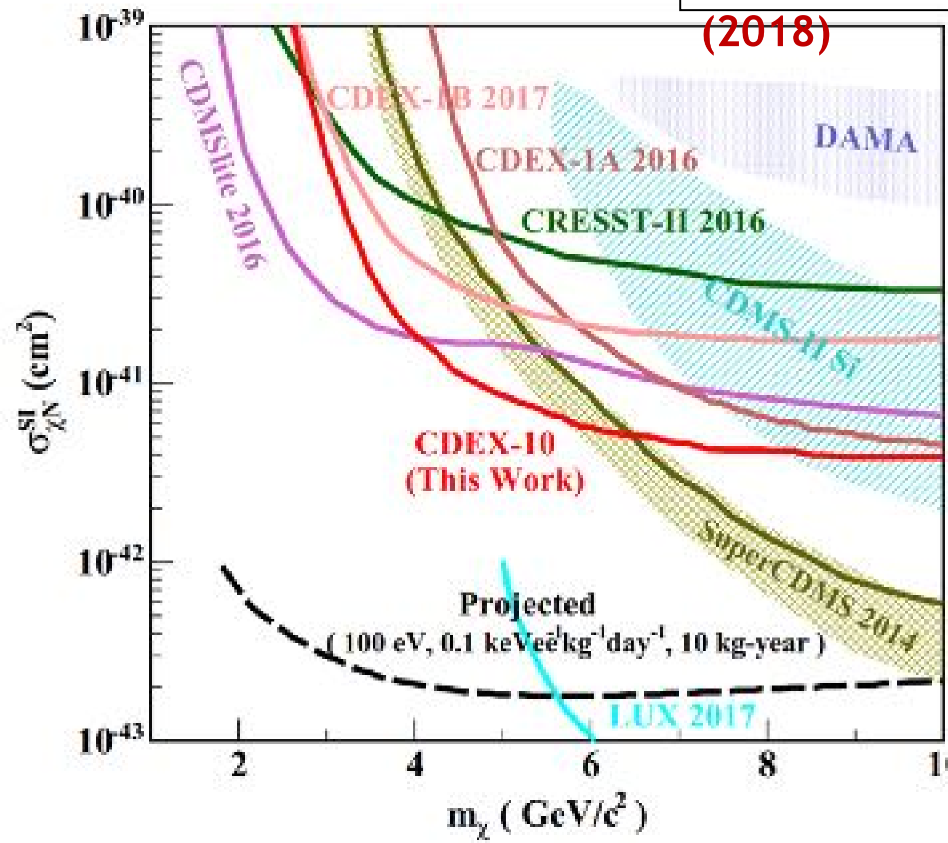

XENON1T excess of electron recoil

Aprile et al., PRD, 102, 072004 (2020)

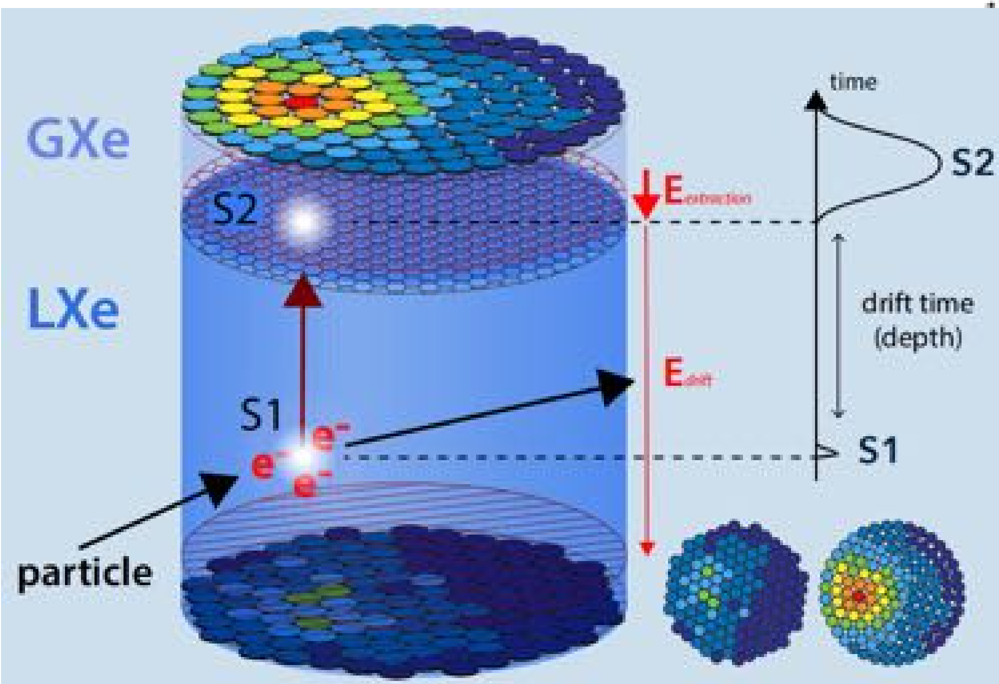

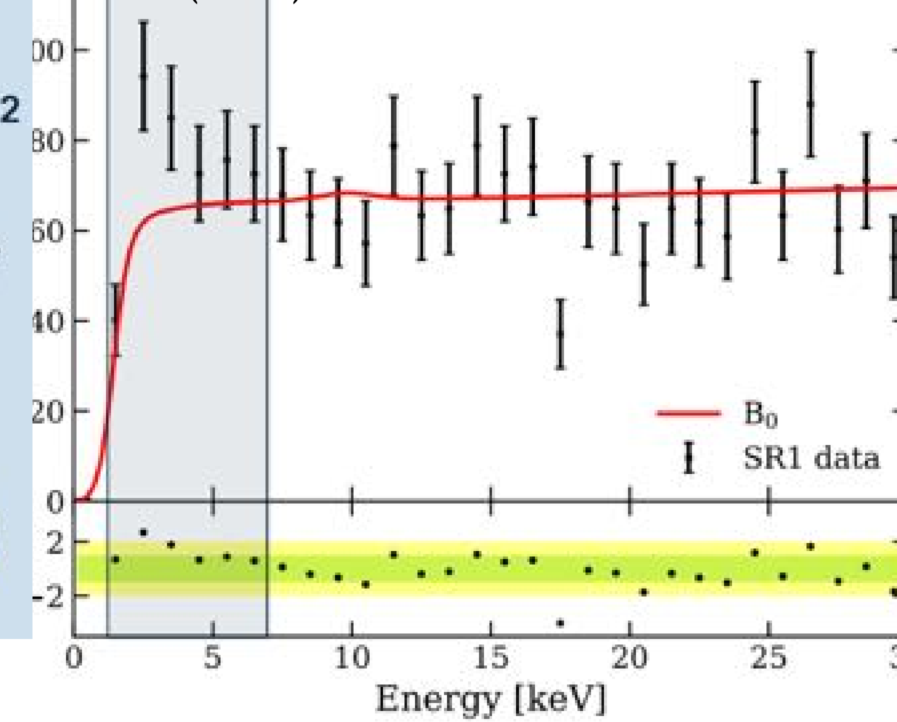

XENON1T reported its latest analysis results of electron recoil events in June 2020, finding an excess of about 3.5σ in the 2-7 keV energy range. Possible explanations include tritium background, solar axions, neutrino magnetic moment, dark matter, etc.

PandaX-II results of electron recoil

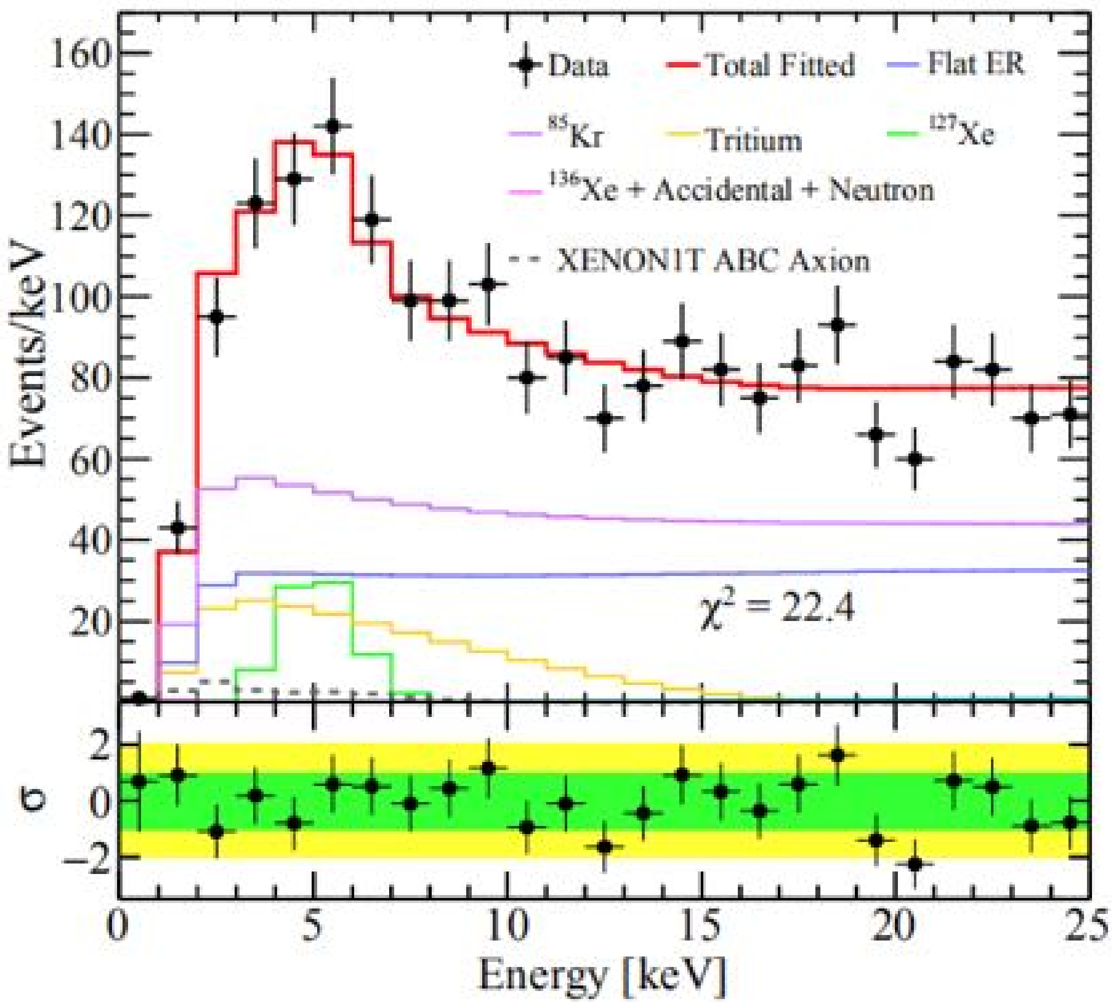

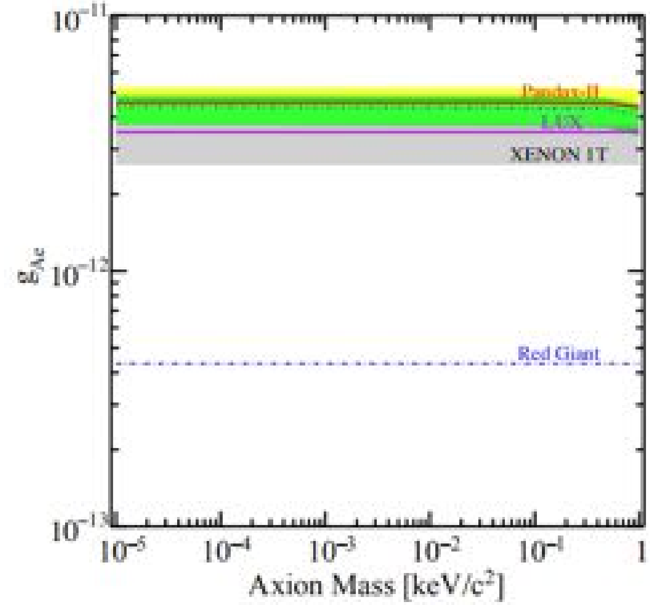

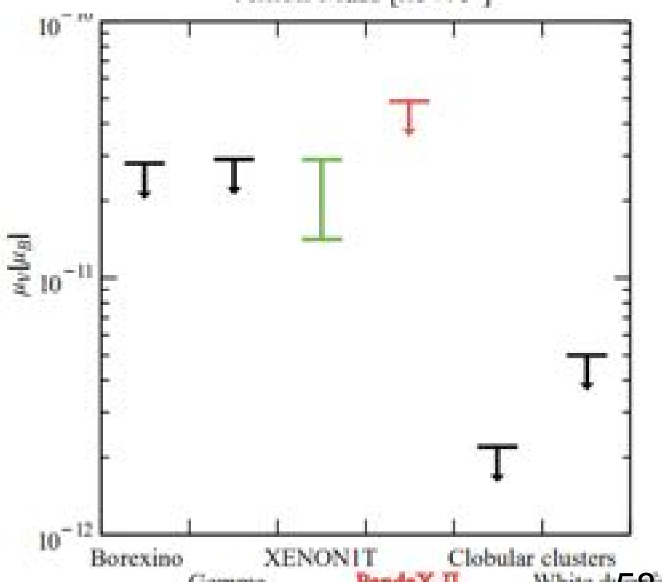

Consistent with expected background, but can't exclude the XENON1T results. Zhou et al., Chin. Phys. Lett., 38, 011301 (2020)

Current Direct Detection of WIMP DM

- Lower threshold
- Boosted DM

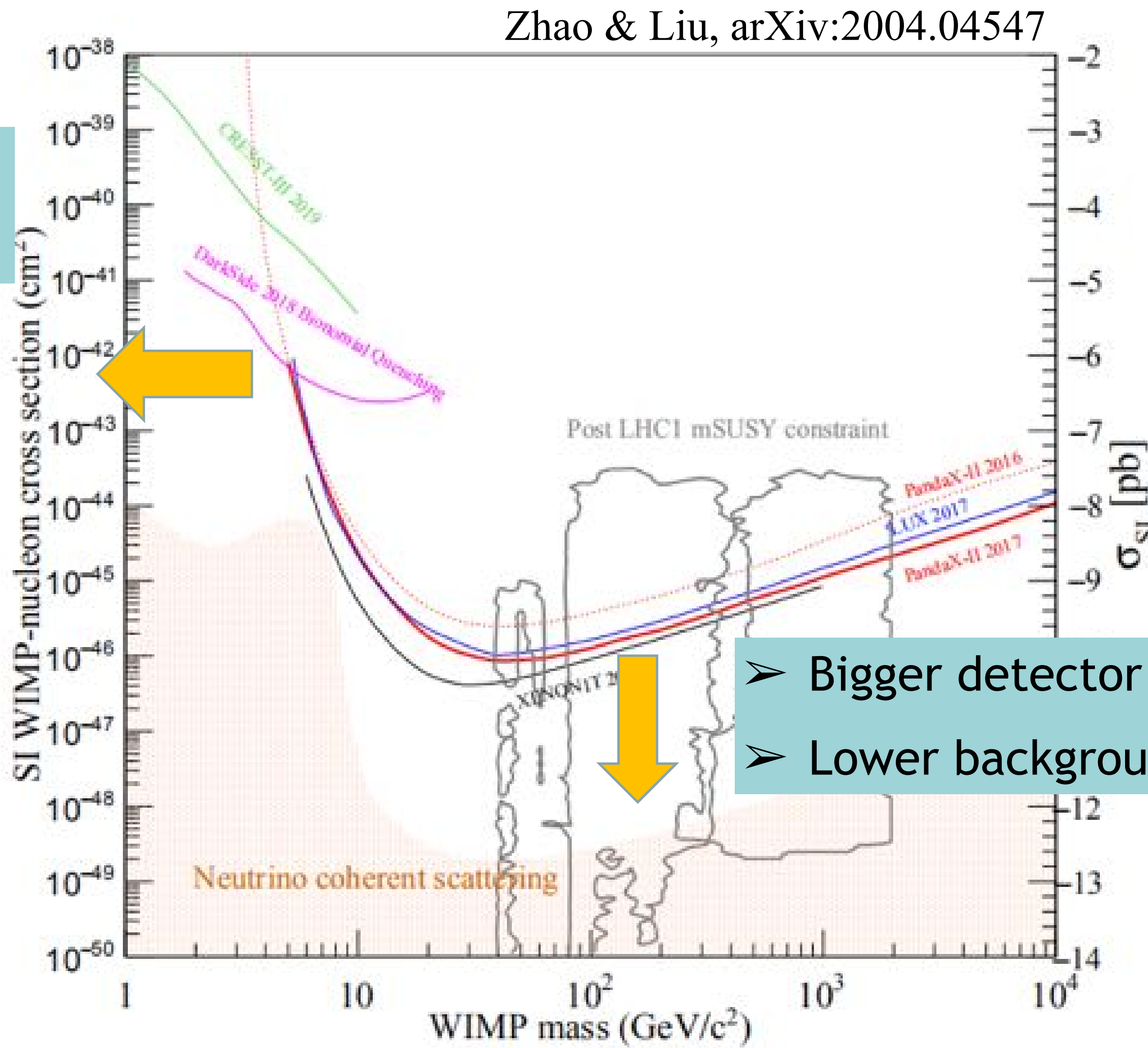

- Bigger detector
- Lower background

Detect DM from Large particle collision experiment

dark matter production in association with X

- dark matter escape detection
- X: visible particles
- E_T^{miss}: momentum imbalance in transverse plane

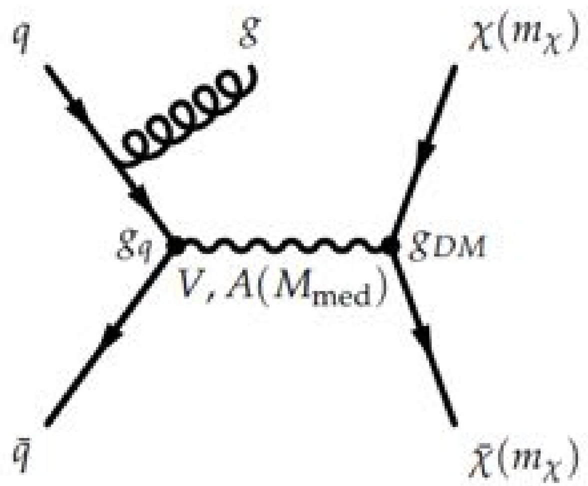

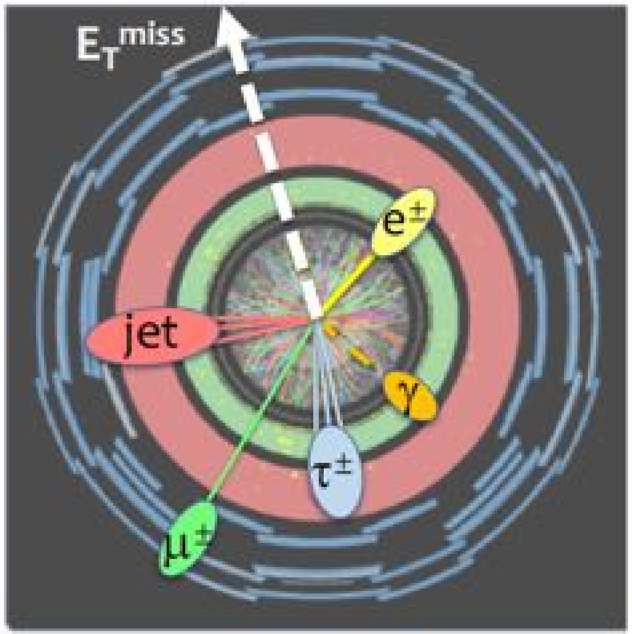

From Ning Zhou

Detect DM from Large particle collision experiment

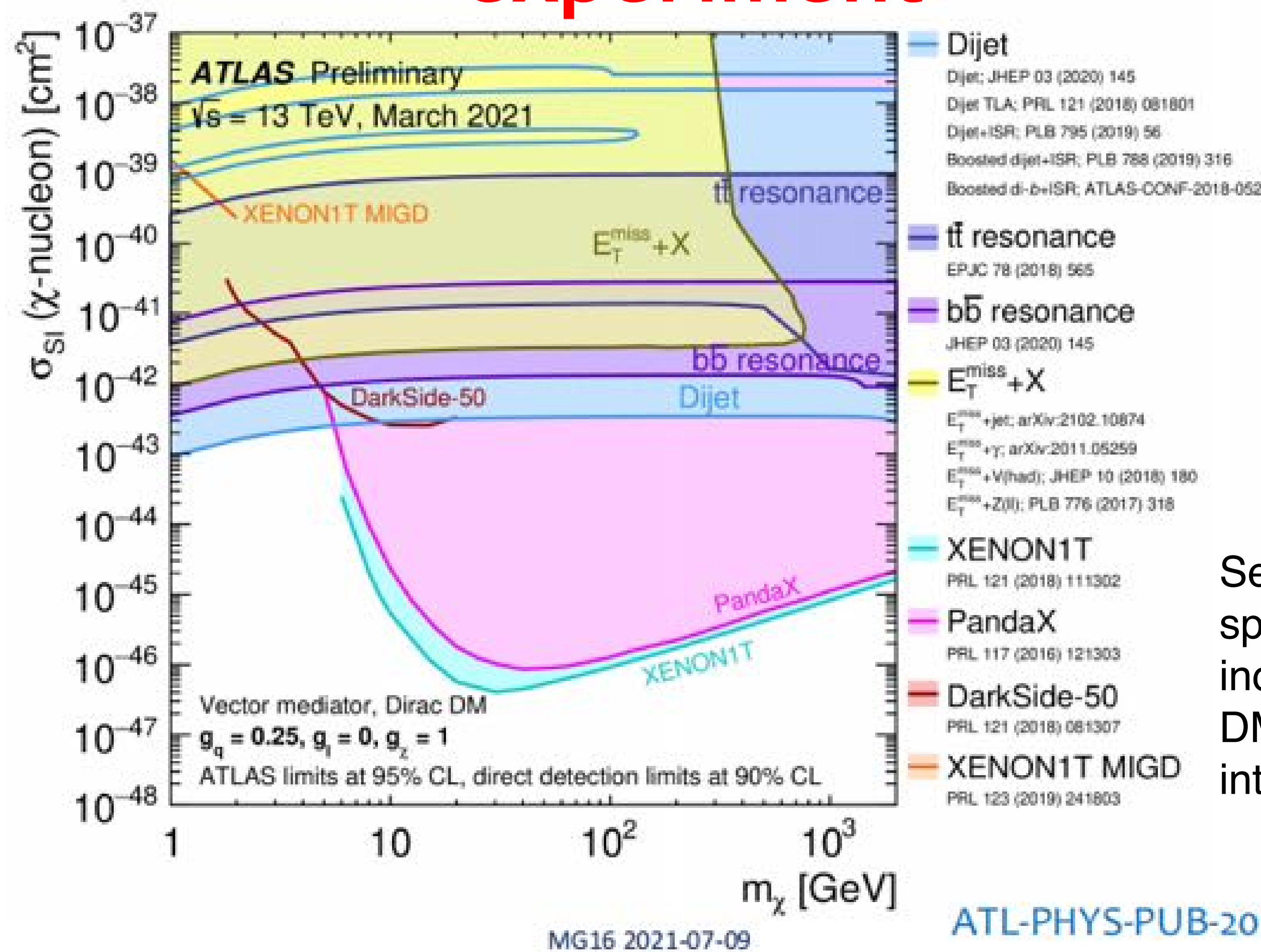

Search for spin-independent DM-nucleus interaction

ATL-PHYS-PUB-2021-006

From Ning Zhou

Detect DM from Large particle collision experiment

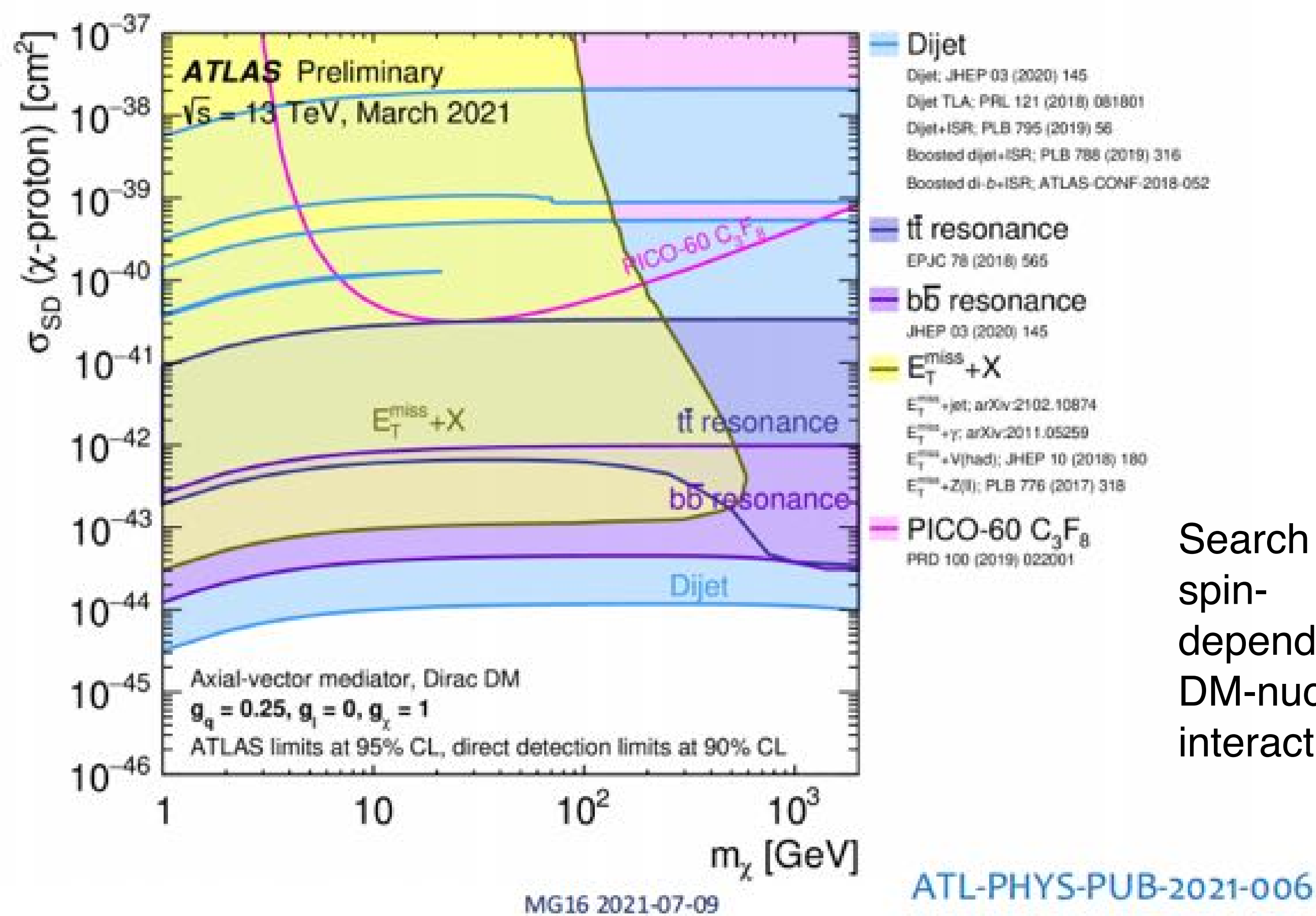

Search for spin-dependent DM-nucleus interaction

From Ning Zhou

Indirect detection of Cosmic Rays

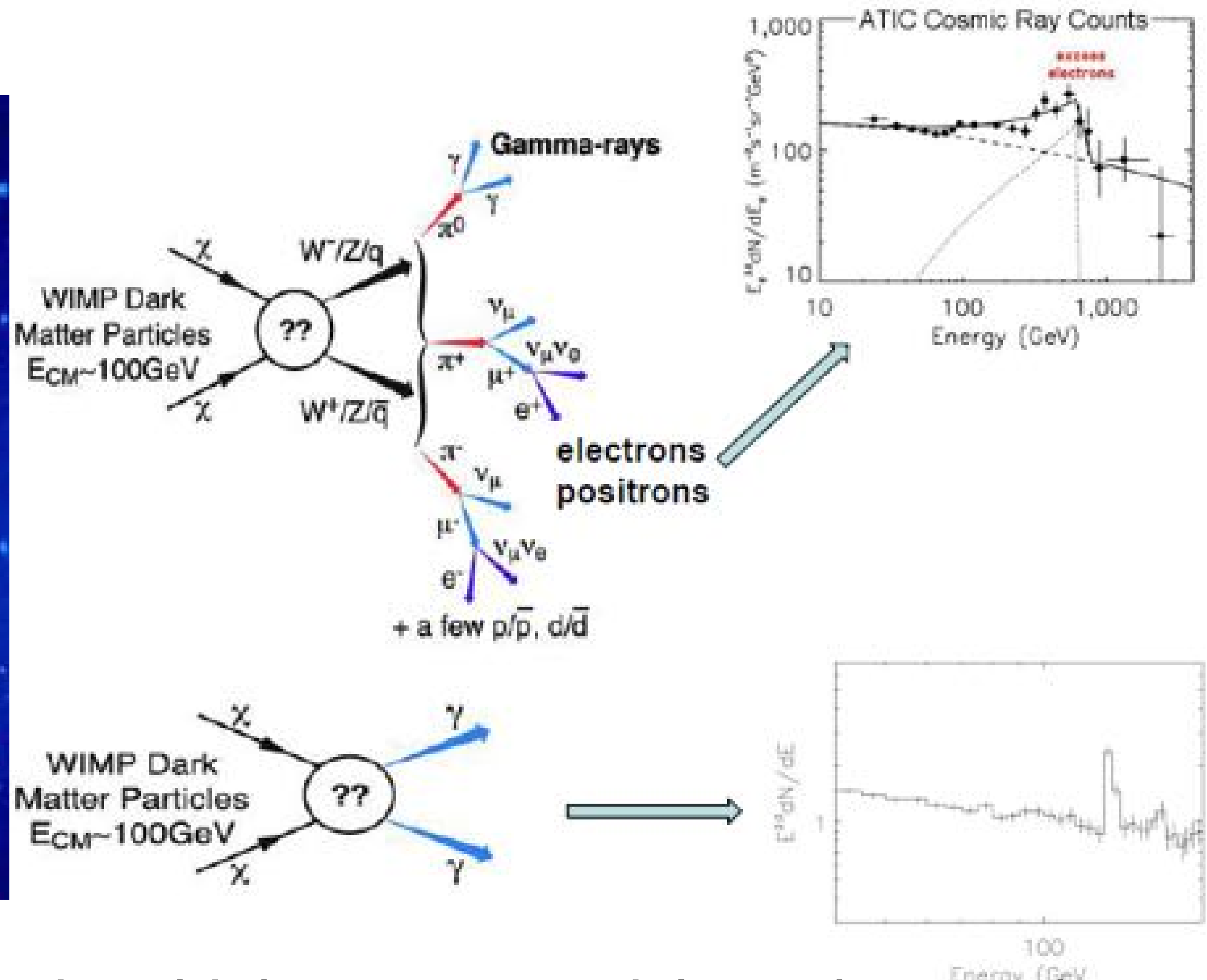

DM annihilate or decay into high energy particle and secondary radiation, contributing into the cosmic ray and gamma rays we observed.

Summary of cosmic ray detection

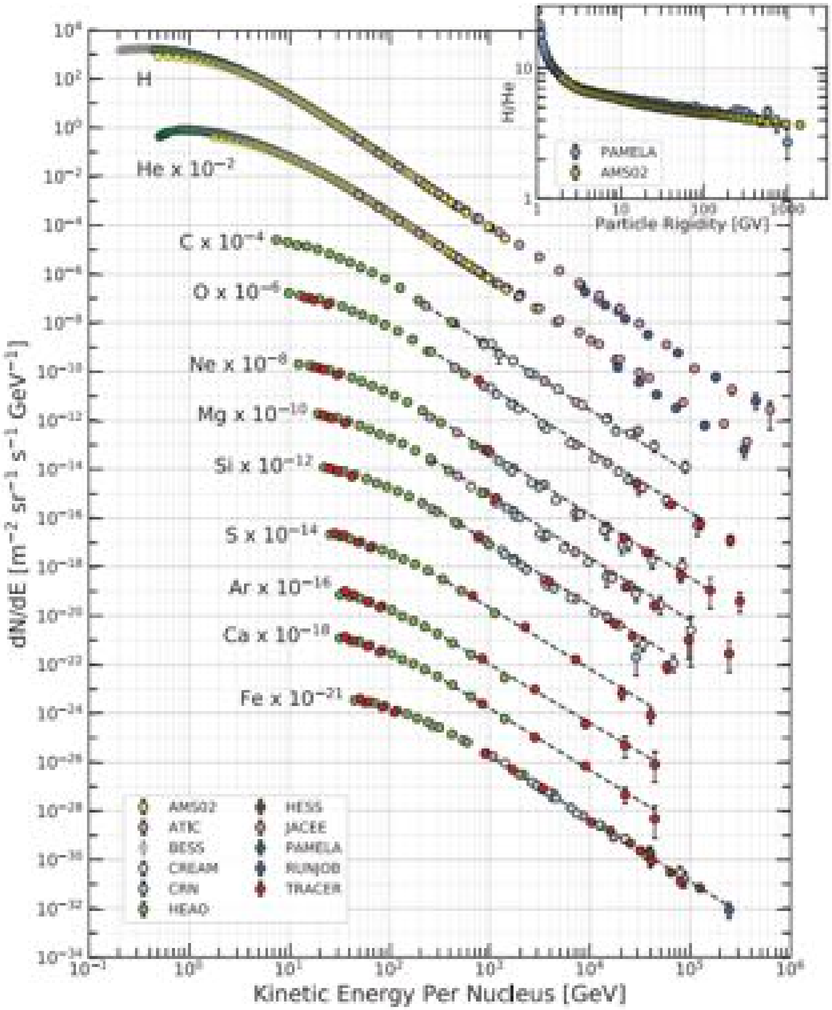

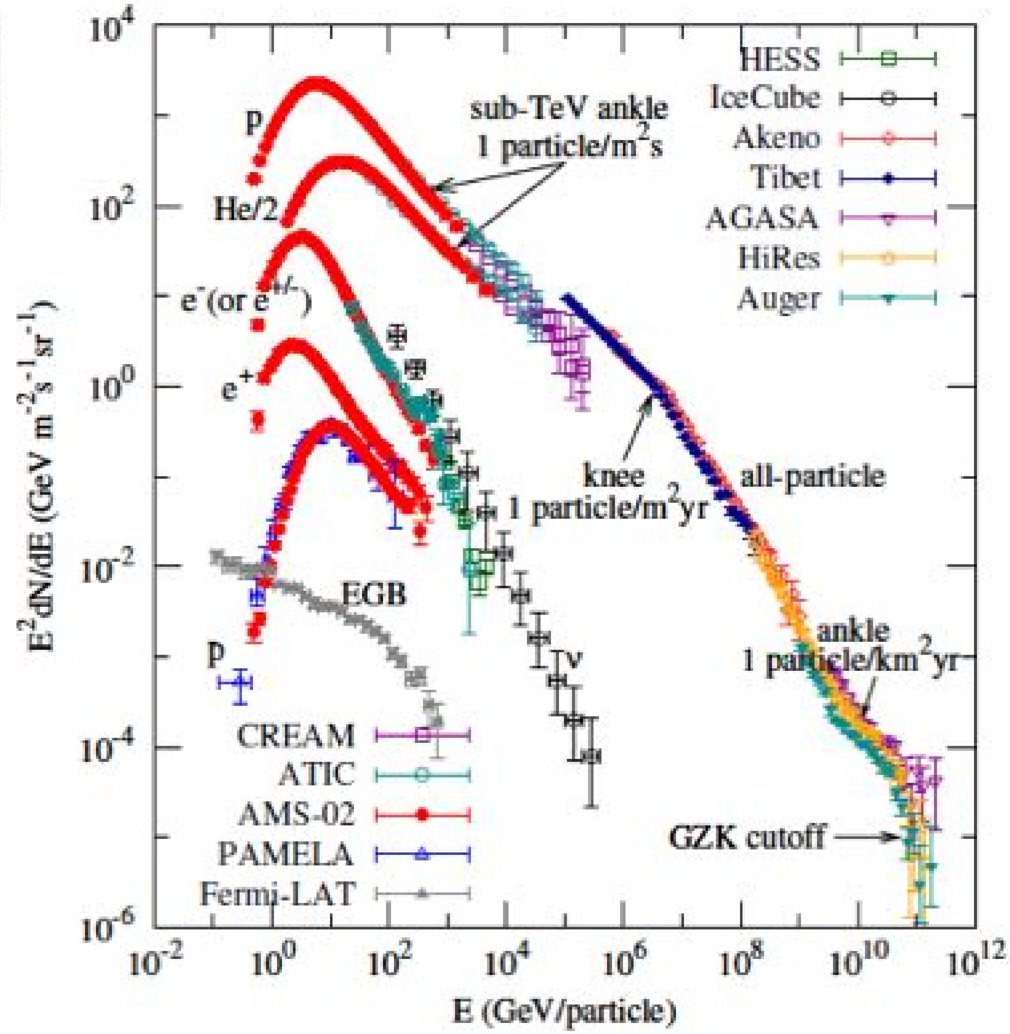

Signatures of DM indirect detection

- Gamma ray line spectrum: unique features
- Spatial distribution of gamma rays: tracing DM distribution
- Cosmic ray positrons and antiprotons: secondary products with low flux, and their flux can be predicted from cosmic ray models

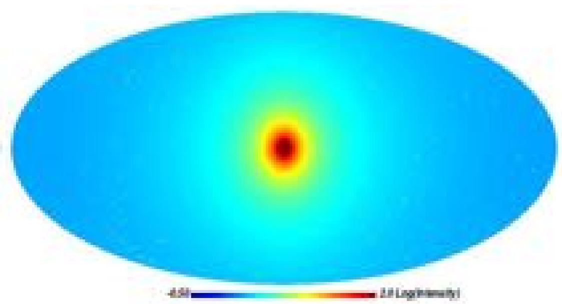

- Cosmic ray electrons: 10 times higher flux than positrons'. Good sensitivity for dark matter detection.

Spatial Indirect Search for DM

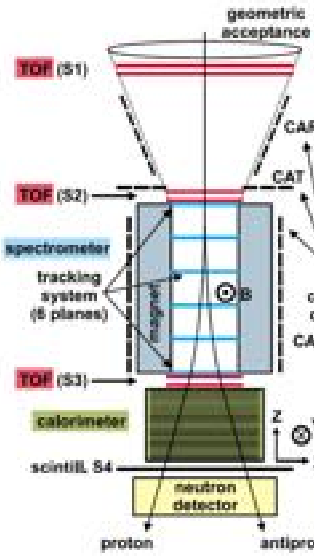

PAMELA

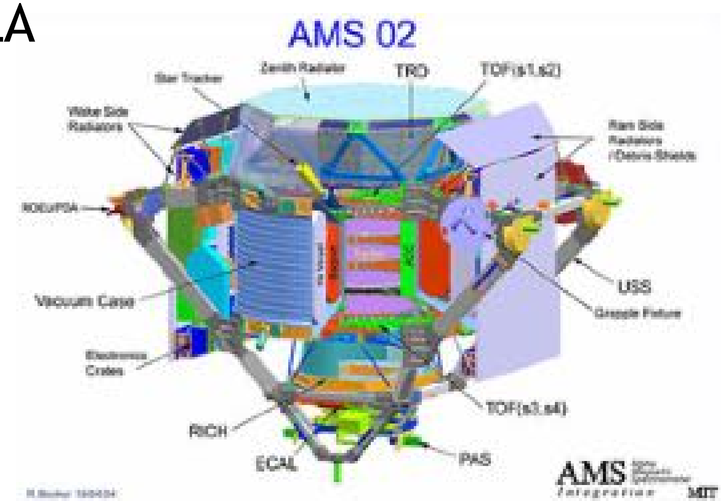

Fermi

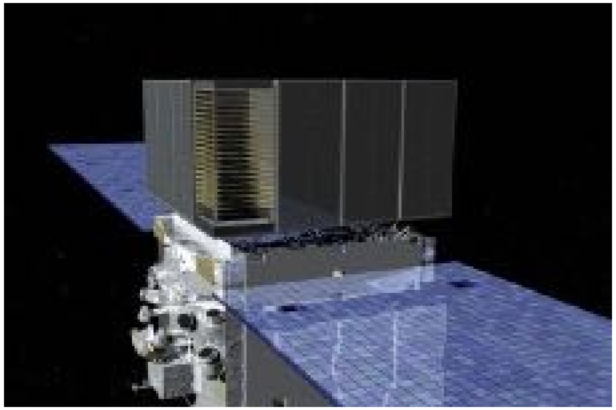

CALET

DAMPE

Possible gamma ray spectrum from Fermi

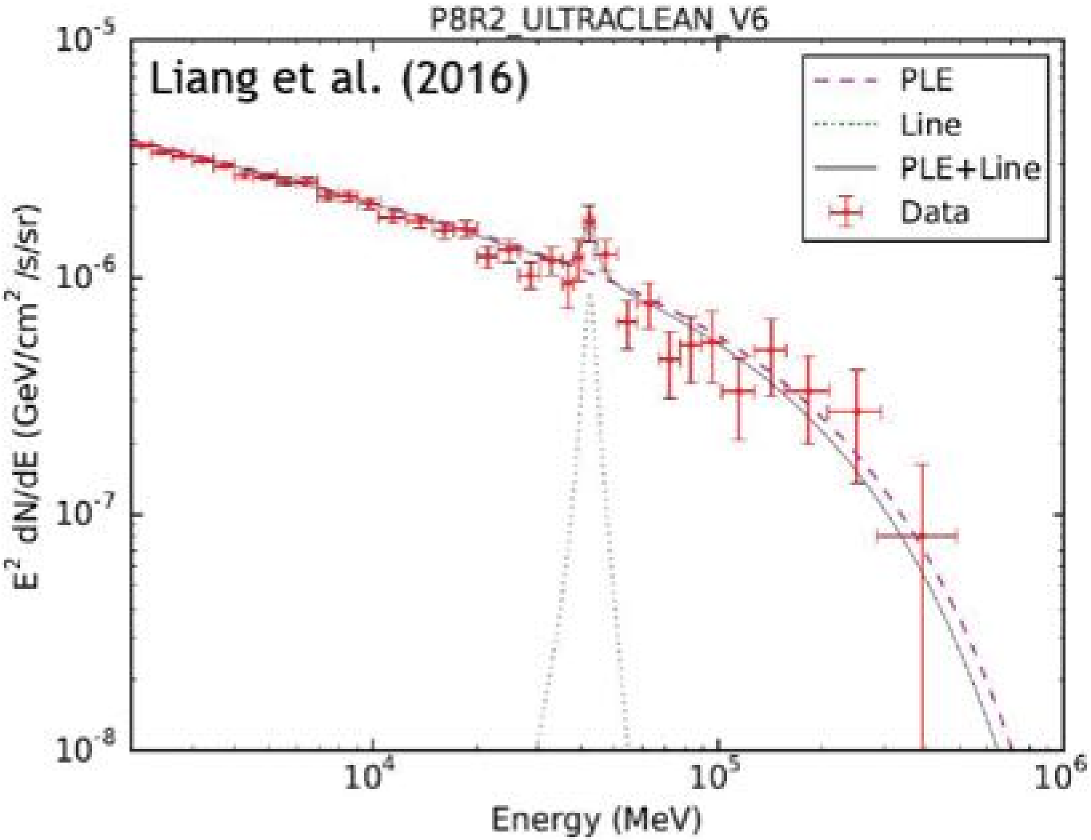

- E~43 GeV
- From a galaxy cluster
- No similar line spectrum radiation in places where dark matter is concentrated, such as the center of the Milky Way and dwarf spheroidal galaxies.
- Possibly statical fluctuation or instrument error?

Positron Excess

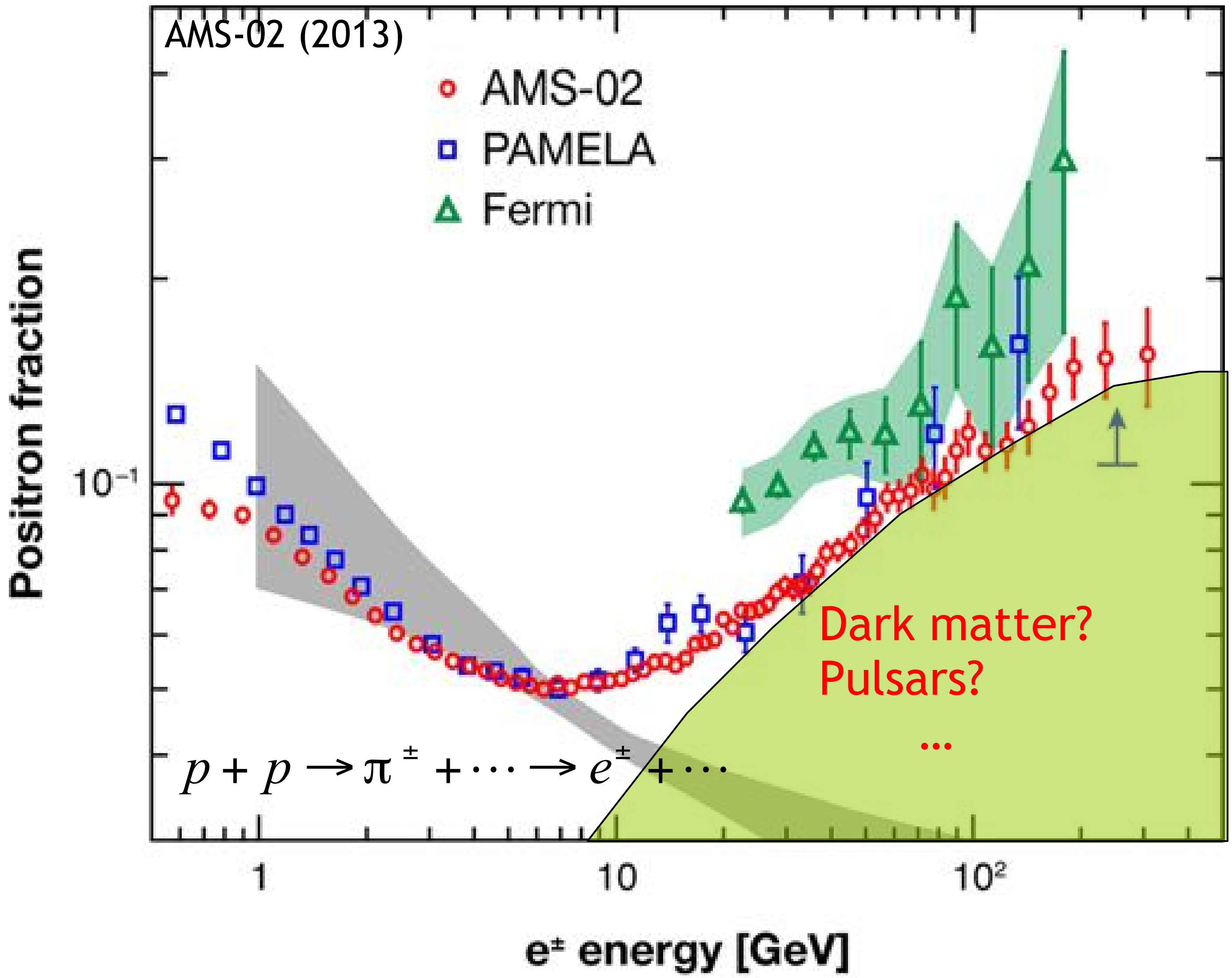

Gamma Ray Excess from Galactic Center

Gordon & Macias (2013)

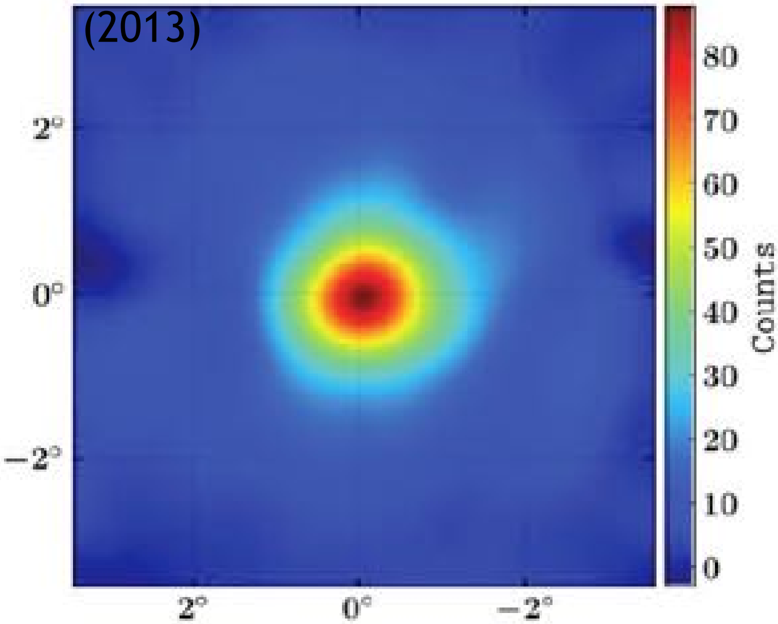

Goodenough & Hooper (2009)
Vitale & Morselli (2009)
Hooper & Goodenough (2011) ...

Calore et al. (2015)

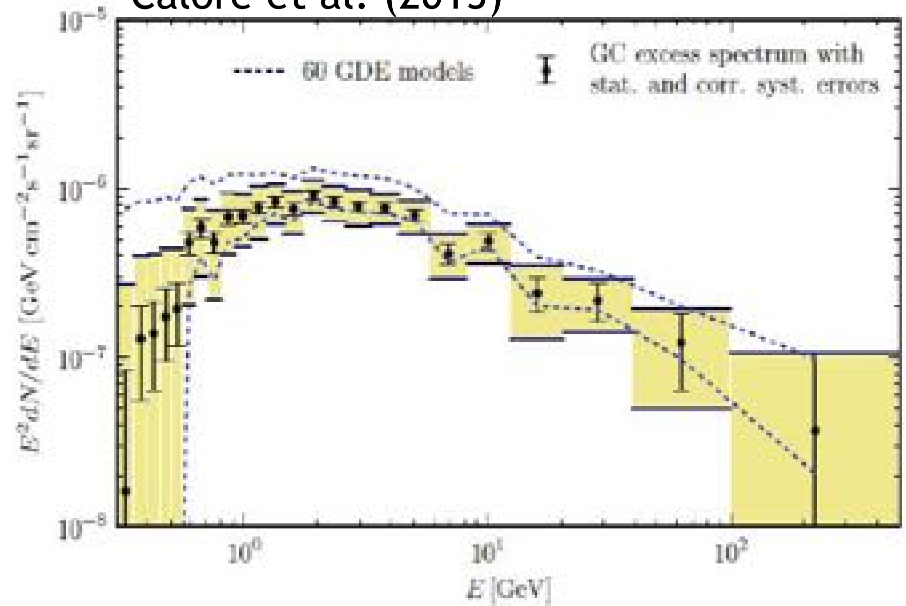

- ➢ Fermi gamma-ray observations of the Milky Way center reveal a circularly symmetric excess. Highly consistent with dark matter model expectations!
- ➢ DM model is not the only explanation.

Possible excess of anti-proton

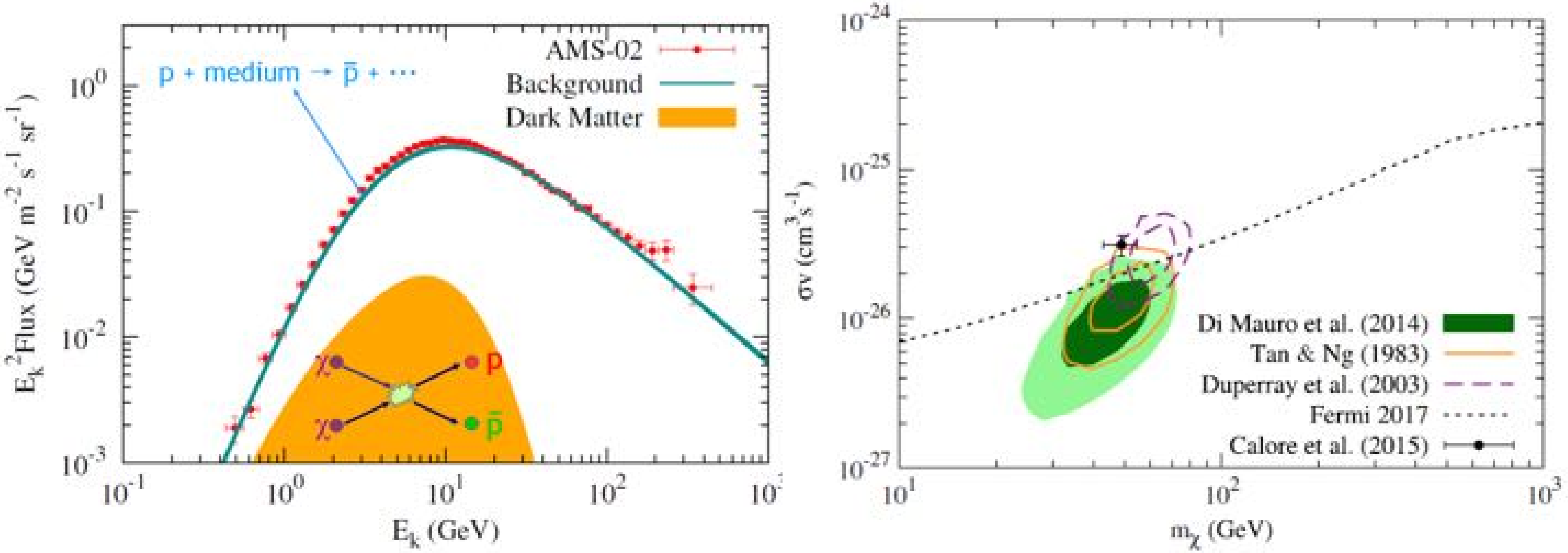

➢ Antiprotons from the secondary effects of cosmic rays is slightly lower than experiment. Could be resolved by DM, with highly consistent parameters with GC center excess!

➢ Still uncertainties in the antiproton production cross section and the modulation effect of the solar system on protons and antiprotons, calling for further research.

Cui et al. (2017); Cuoco et al. (2017)

Summary of DM detection

- Colliders： null results
- Direct Detection： null results
- Indirect detections：
  1. Positron excess
  2. GC gamma ray excess
  3. Gamma Ray spectrum excess
  4. Anti-proton excess

  Large uncertainties from astronomy! Results still unclear!

- Astronomical observations discover dark matter through "invisibility"
- Physics experiments try to "see" dark matter, but so far no one has seen it

Dark Matter Detection Satellites

Dark Matter Detection Satellites

Launched 17 Dec. 2015

Three scientific goals:

- DM Indirect search (precise measure of electron and gamma ray directional spectrum)
- Cosmic Ray origin and acceleration (precise measure of nucleus cosmic ray spectrum and anisotropy)
- Gamma ray astronomy (gamma ray temporal spectrum)

DAMPE Detector

- Plastic Scintillator Array Detector: particle charge (IMP)
- Silicon Tracker: charge and direction (IHEP, UNIGE, UNIPG)
- BGO Calorimeter: energy, direction and particle species (USTC, PMO)
- Neutron Detector: particle species (PMO)

Classical Events

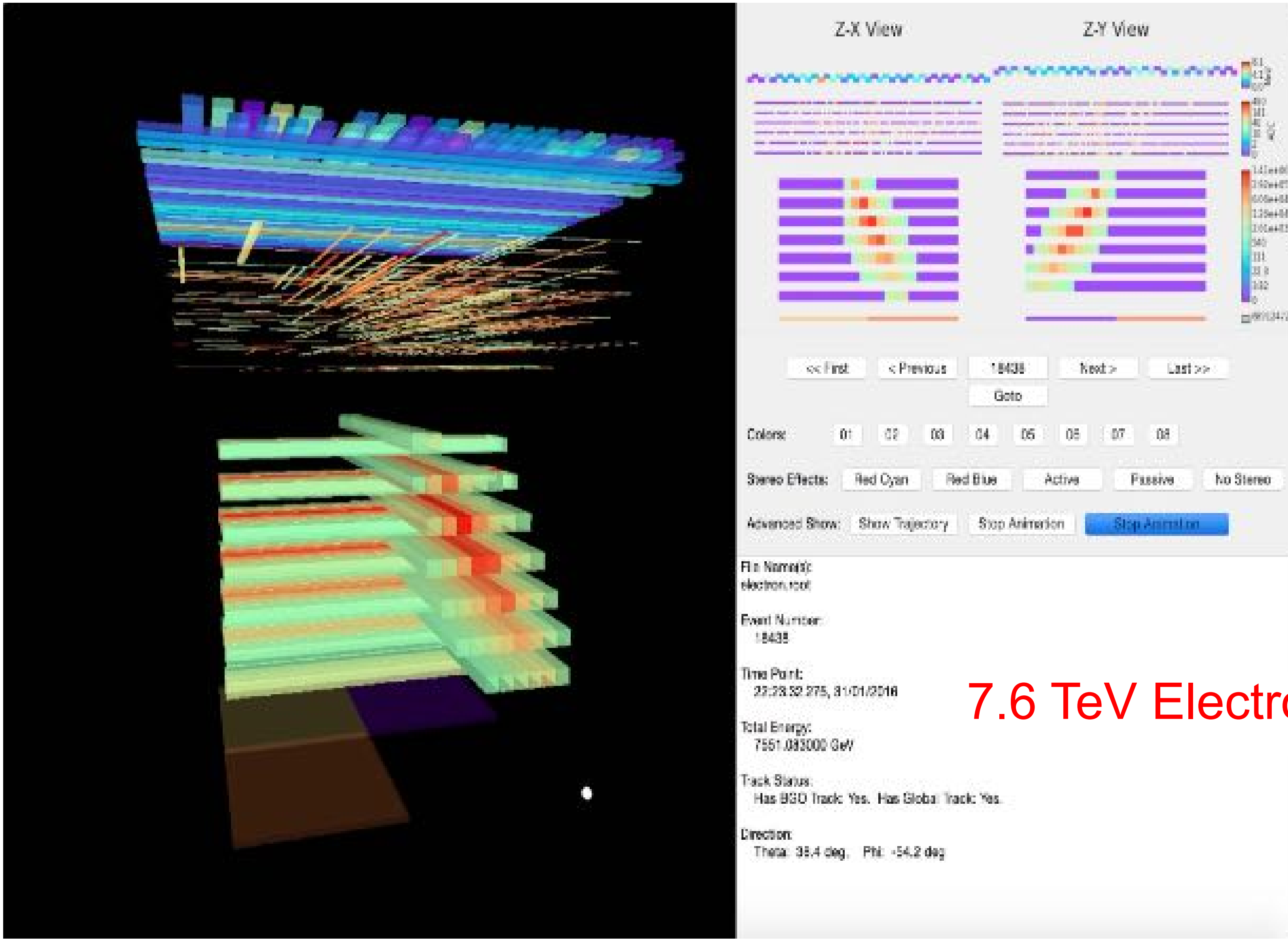

7.6 TeV Electrons

Particle Classifications

Electrons | Gamma | Protons

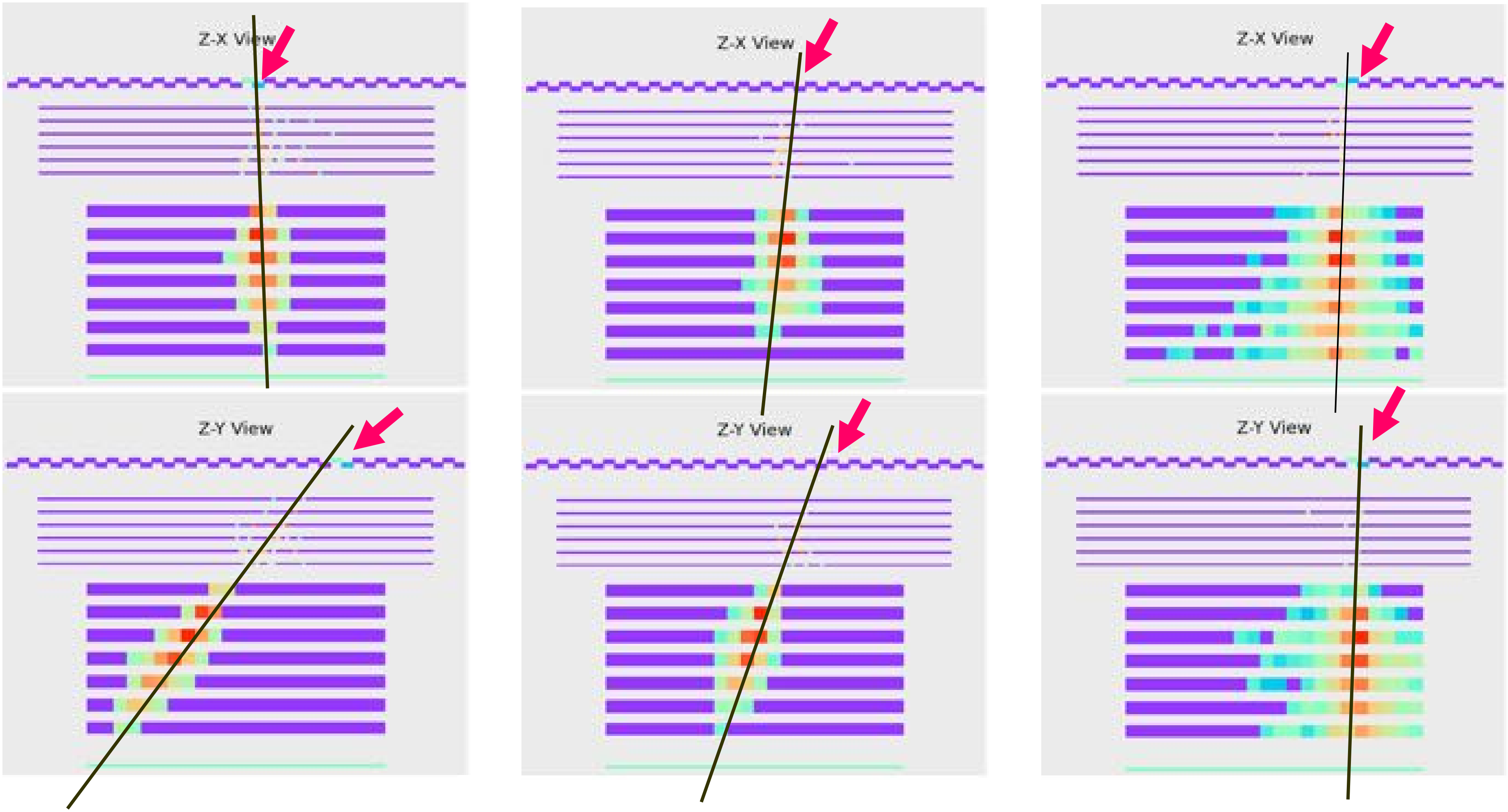

Detector Stability

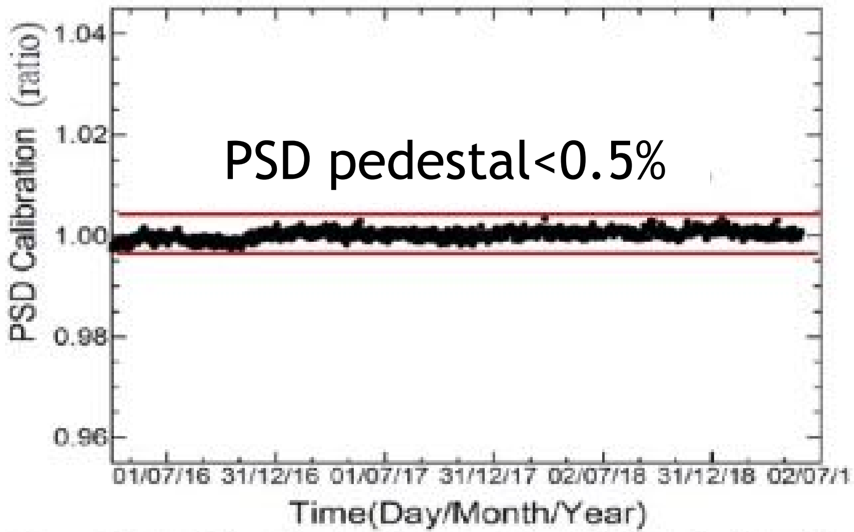

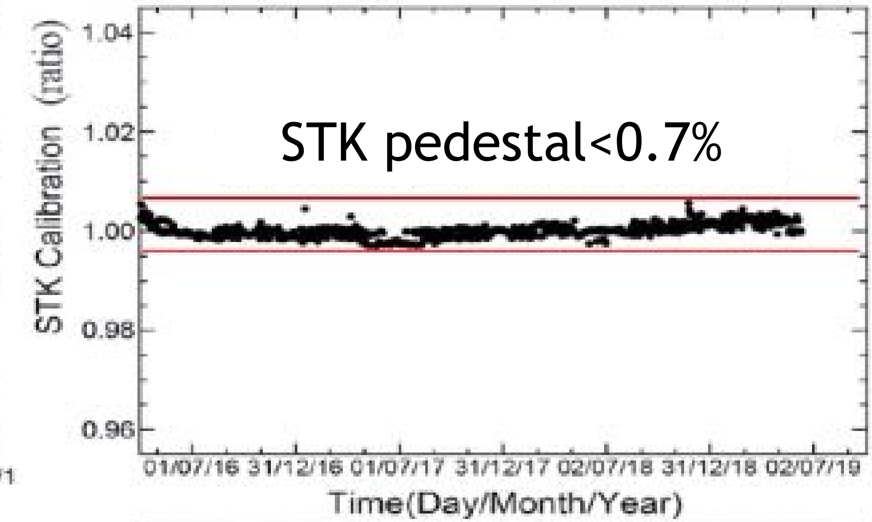

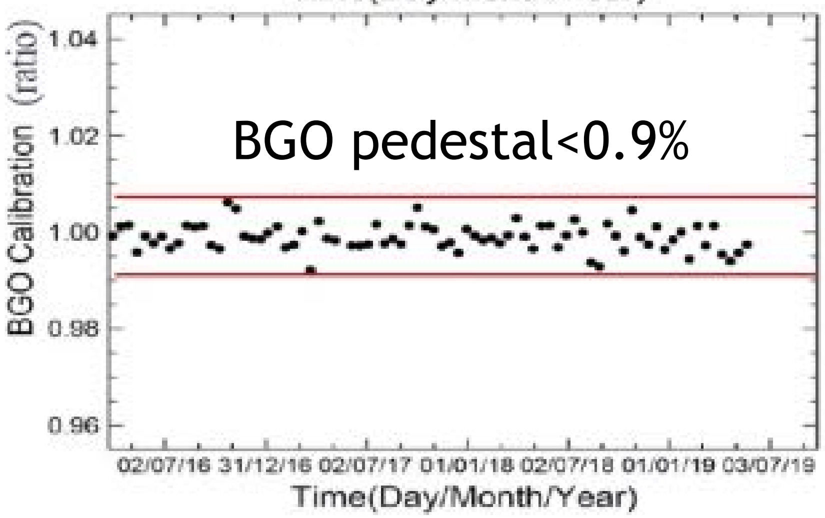

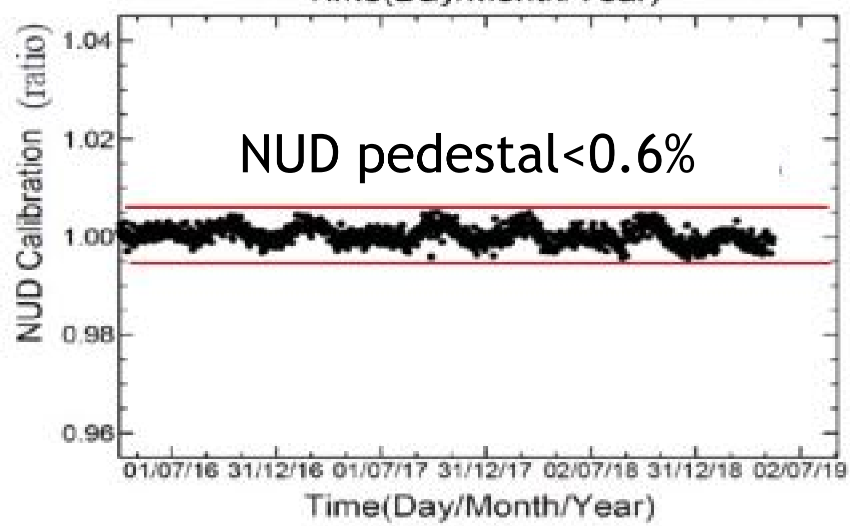

Charge Measurement

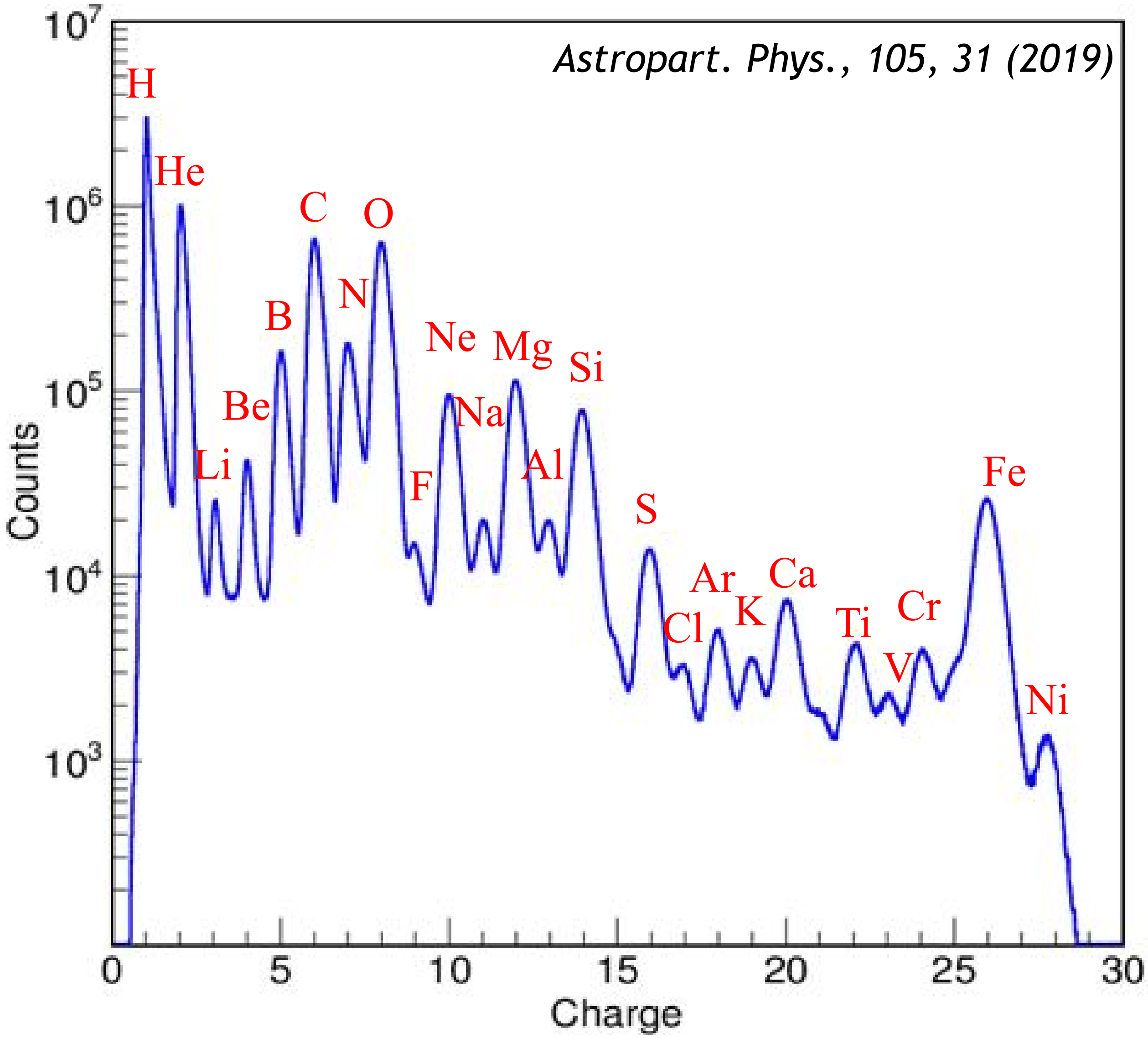

Species	Charge Res.
P	0.06
He	0.10
Li	0.14
Be	0.21
B	0.17
C	0.18
N	0.21
O	0.20

Directional Measurements

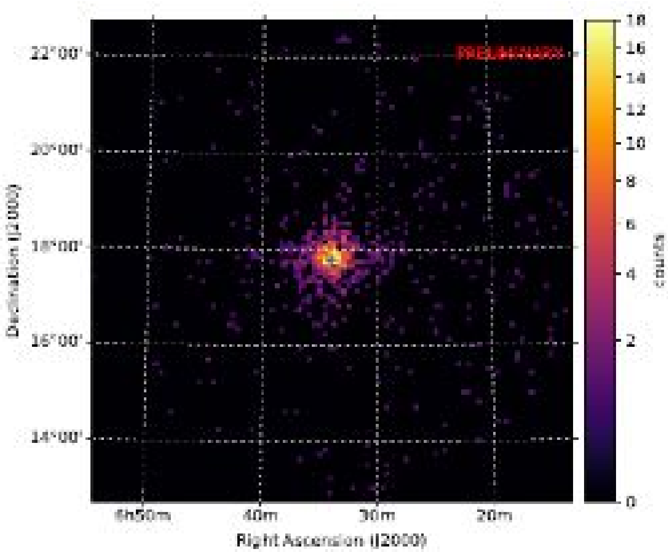

Geminga

AGNs

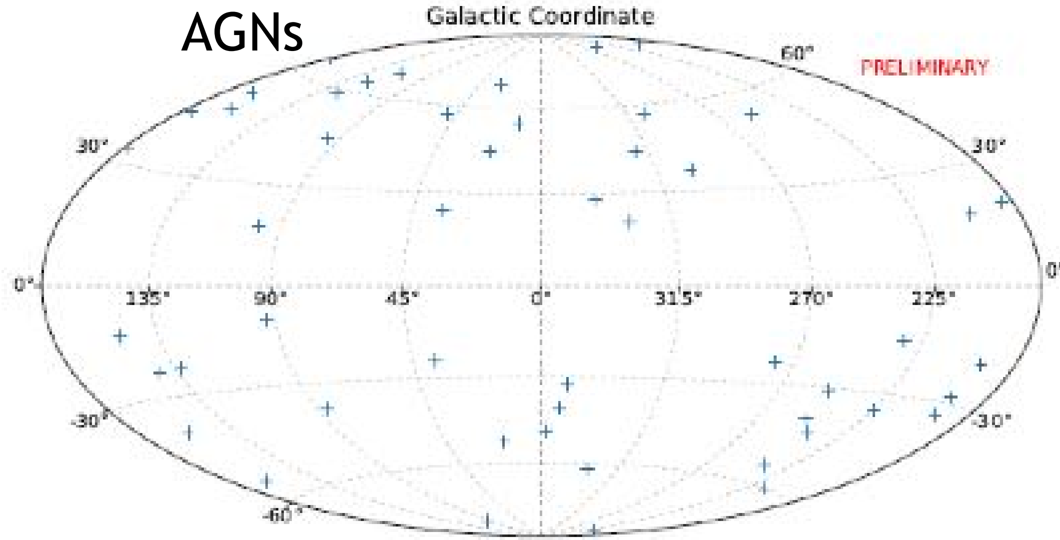

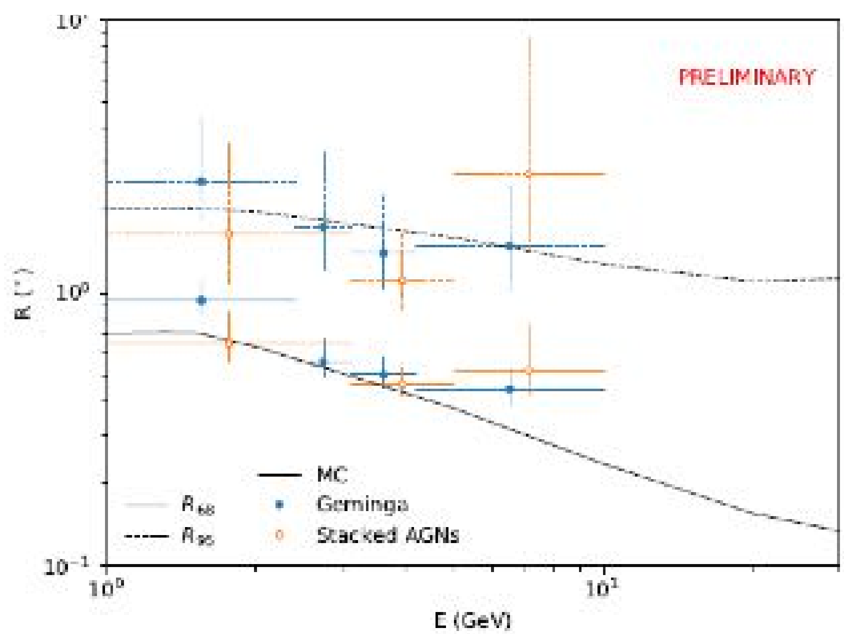

Gamma point source calibrated angular resolution: 0.5° at 5 GeV

Energy Measurements

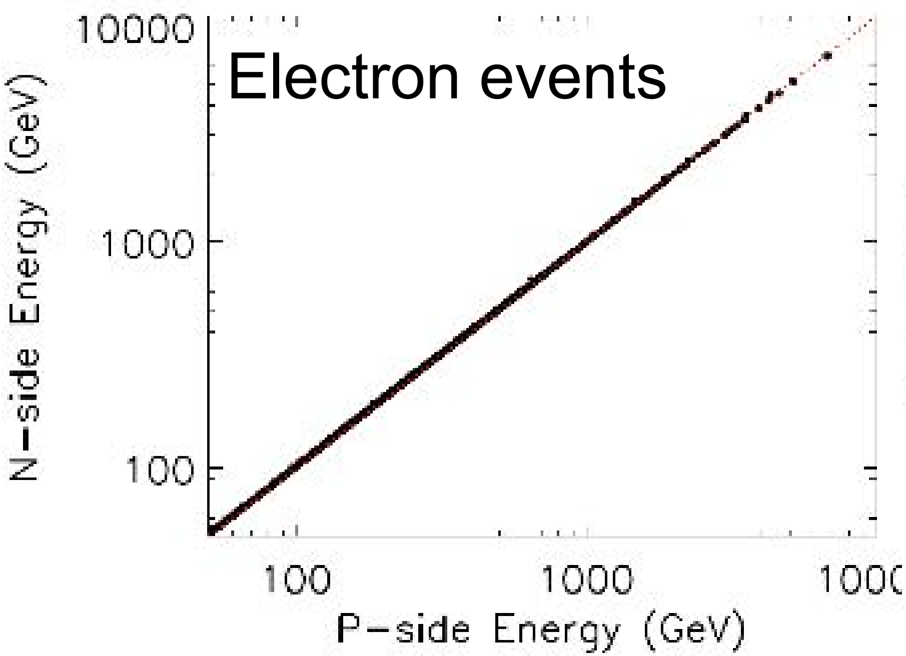

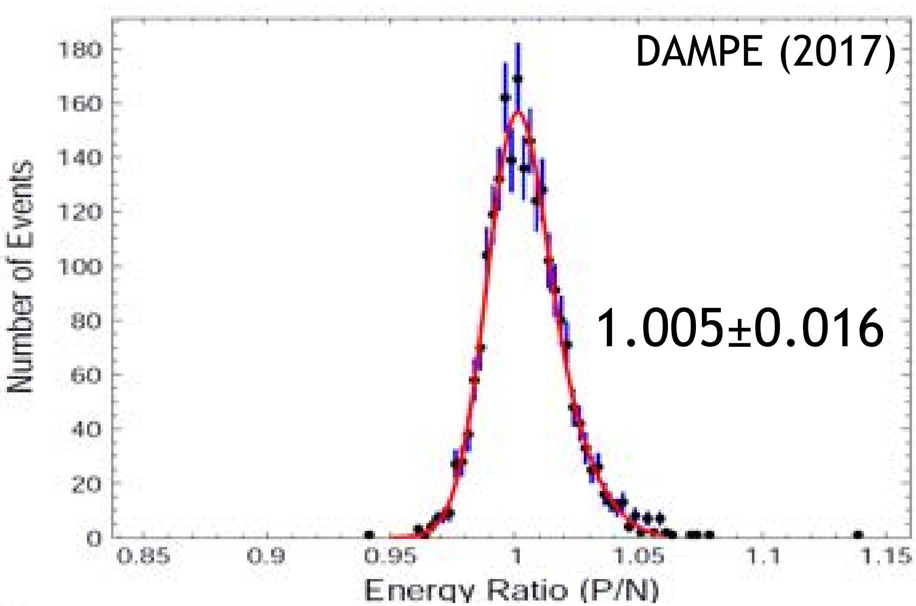

- ➢ Great linearity on both sides (to ~ 10TeV)
- ➢ Energy measurement precision ~1% at TeV (Highest resolution)

Electron-proton classification

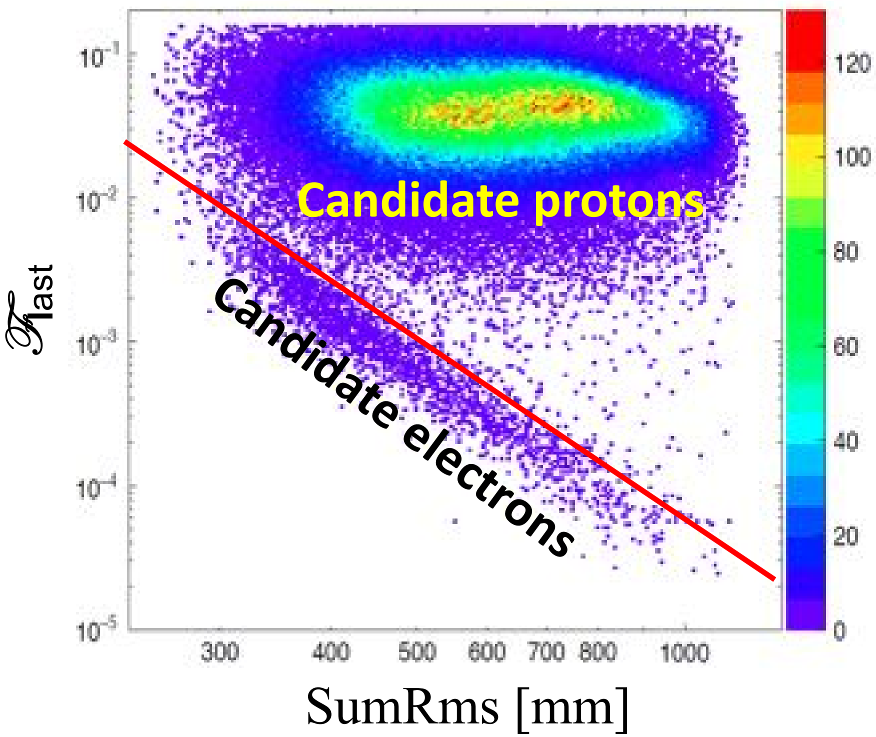

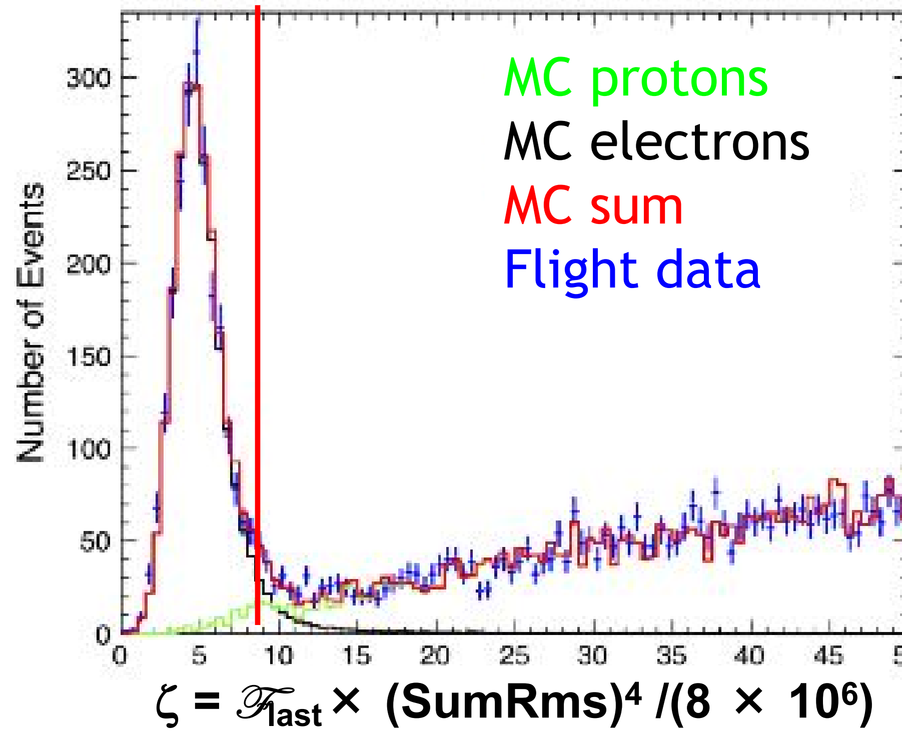

- Identify electrons and proton by horizontal and vertical progression of particle beans
- Maintaining 90% electron efficiency, proton background ~ 2% at TeV, ~5% at 2 TeV, ~10% at 5 TeV (best background level)

Electron-proton classification—comparison

DAMPE
悟空号：Nature, 552, 63 (2017)

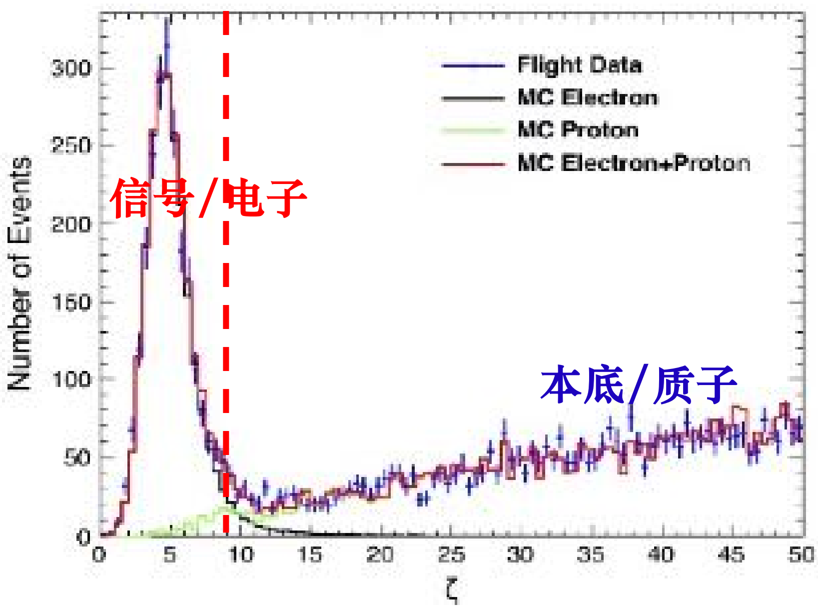

Proton contamination rate ~ 2.5% at 1TeV, best in the world!

CALET： Phys. Rev. Lett. 120, 261102 (2018)

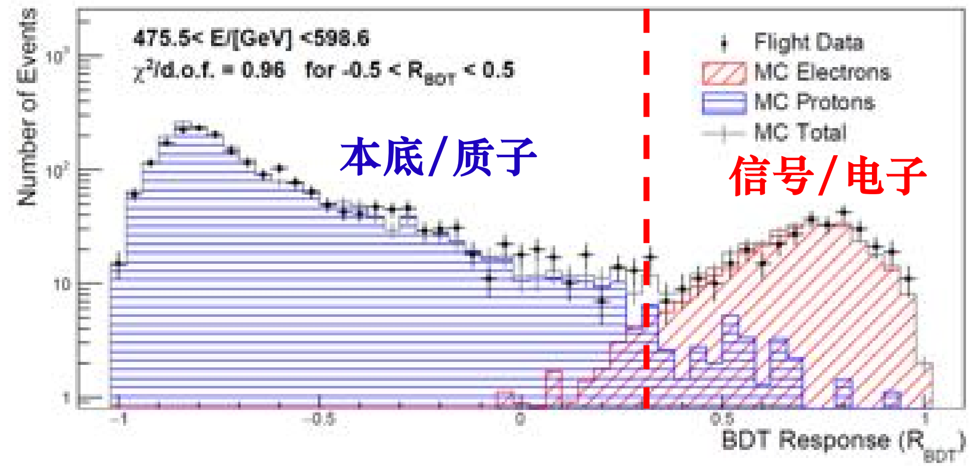

FERMI： Phys. Rev. D 95, 082007 (2017)

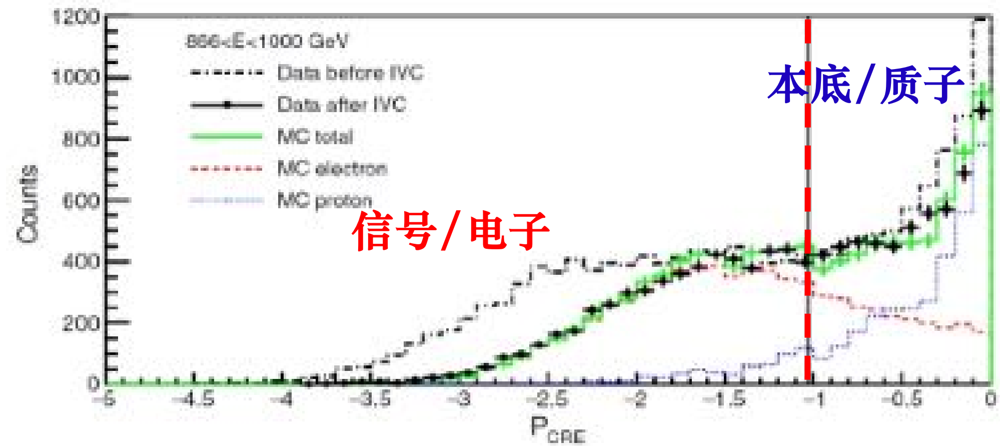

Precise electron-positron spectrum

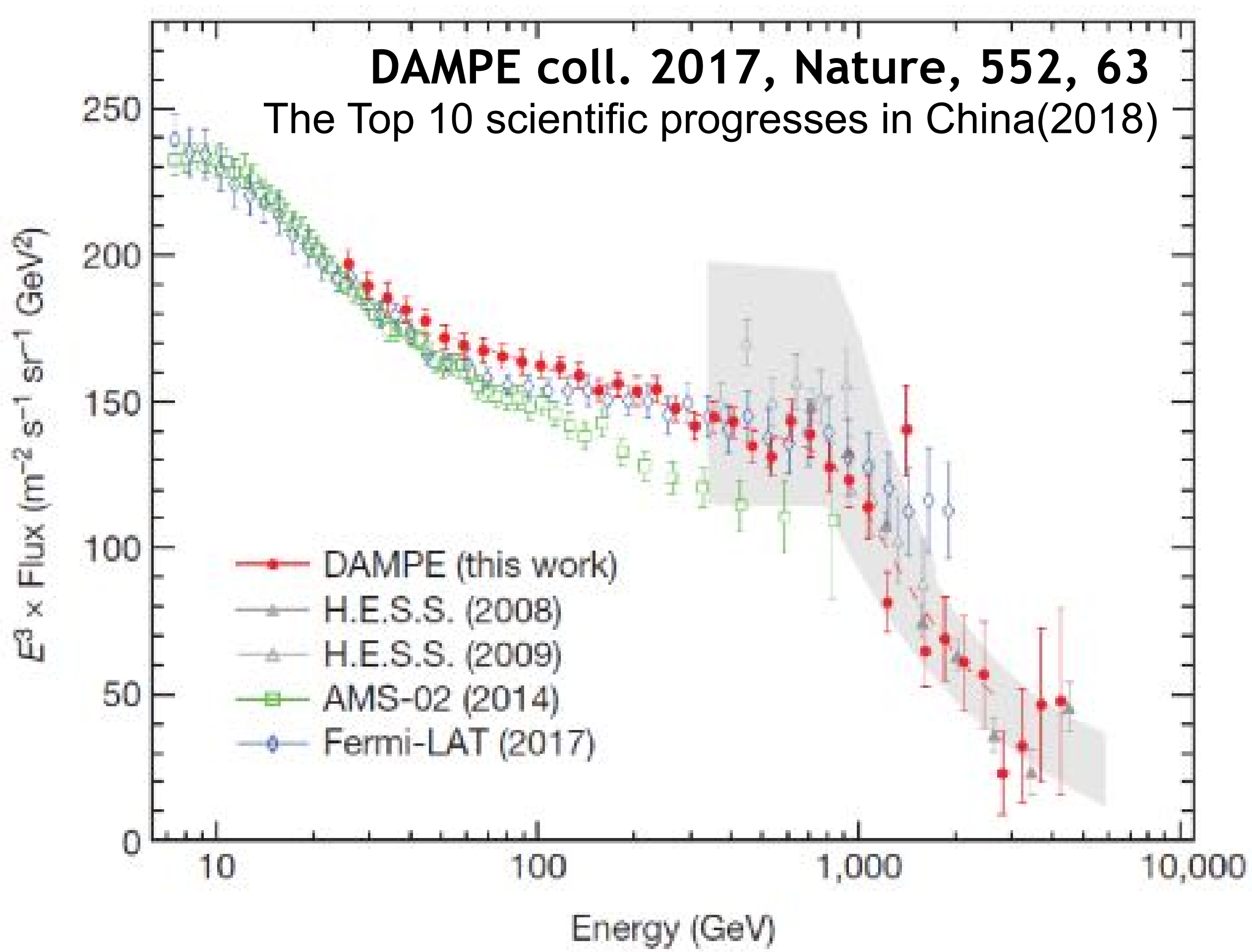

- DAMPE is most precise, with lowest background, lowest error at TeV
- Direct Measurement of the 0.9TeV turning point at ~0.9TeV
- First sign of fine structure in spectrum.

3-components model of electron-positron

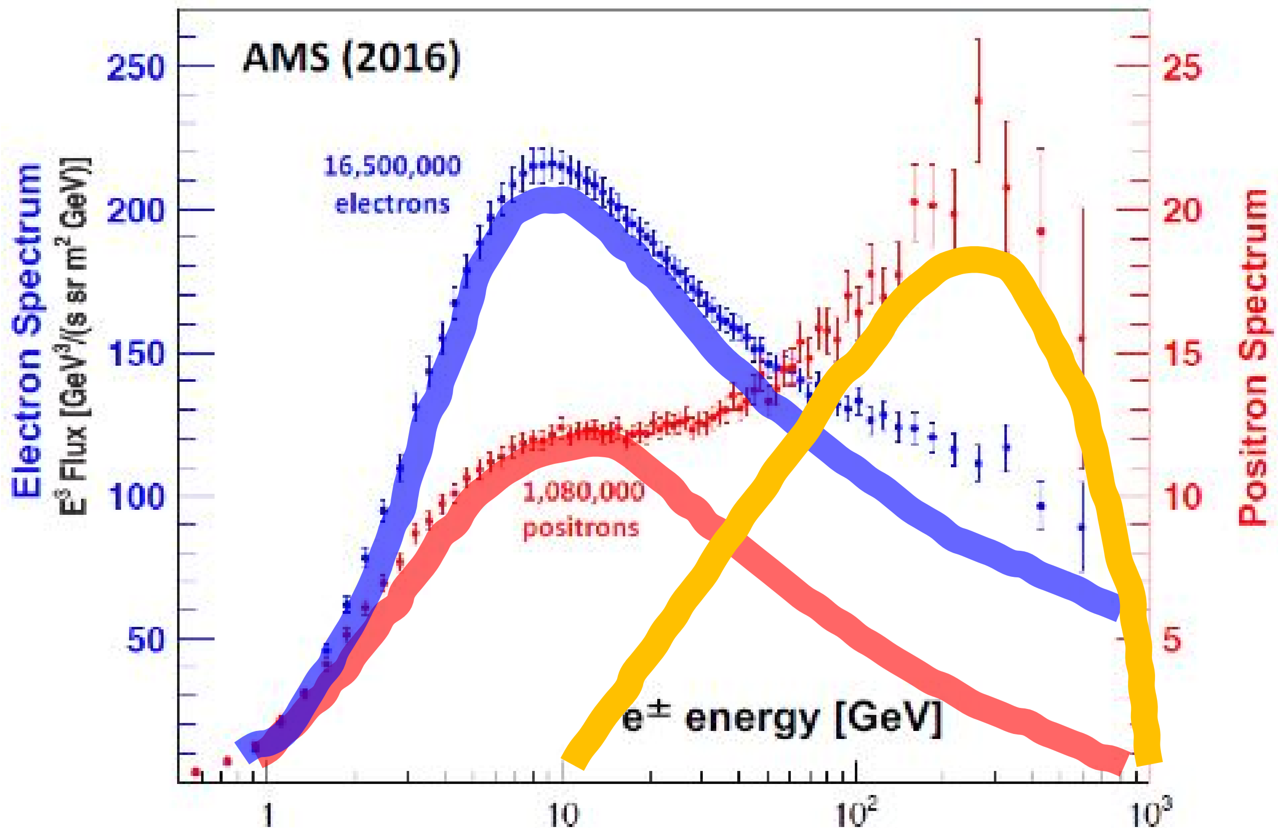

- Primordial electrons accelerated by cosmic ray source
- Secondary e^-e^+s from cosmic ray collisions with stellar matter
- Extra sources producing the e^-e^+ excess.

DAMPE data can strength constraints on the 1st and the 3rd components

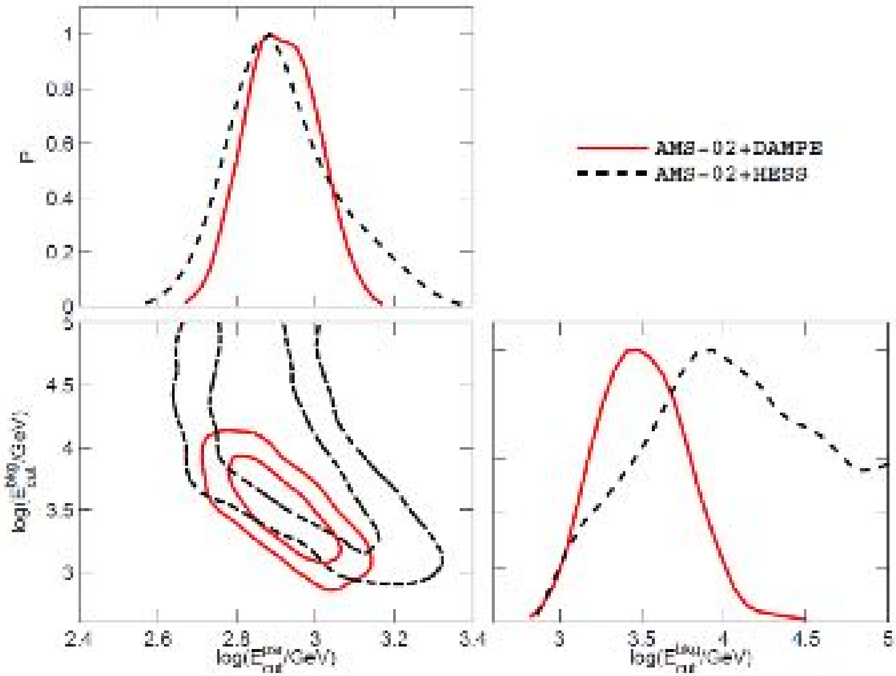

bkg cutoff energy vs. pulsar cutoff

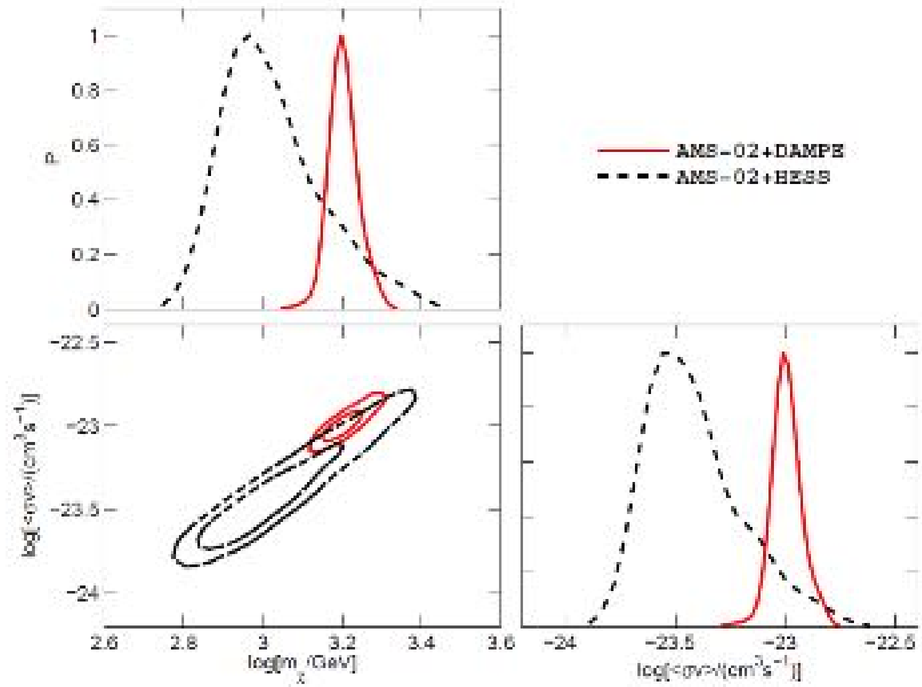

mchi vs. <σv>

Yuan et al. (2017)

DAMPE search for gamma ray line spectrum

Science Bulletin, 67, 679 (2022)

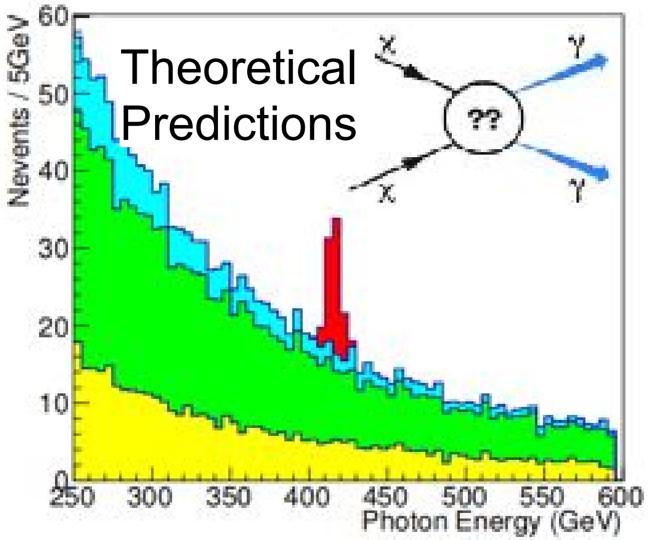

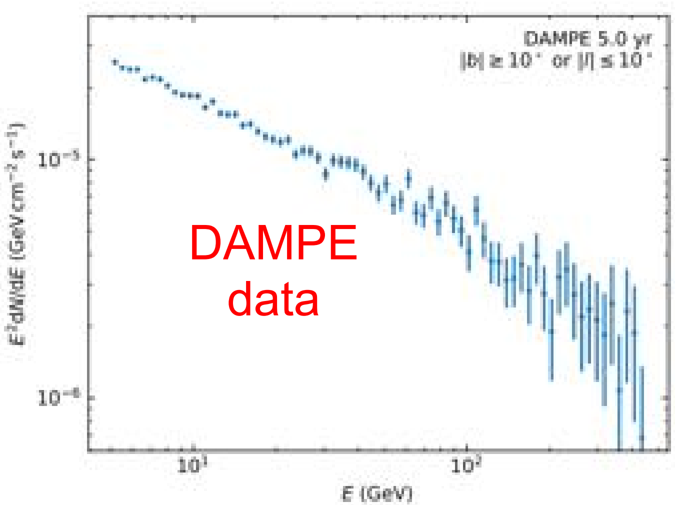

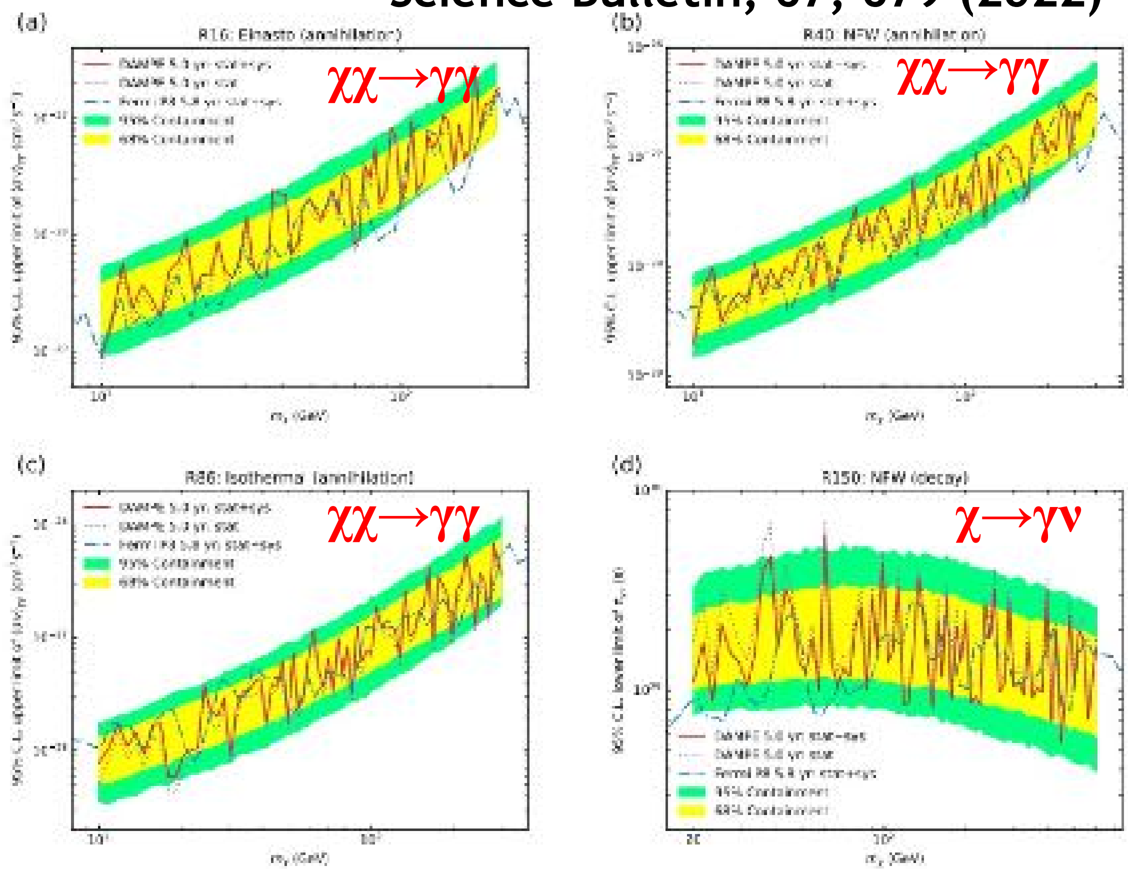

- DAMPE excels in high energy resolution, suitable for gamma ray line spectrum
- Best constraints on dark matter decay lifetime; similar constraints on annihilation with Fermi.

Cosmic Ray Scientific Research

DAMPE 2019, Sci. Adv., 5, eaax3793

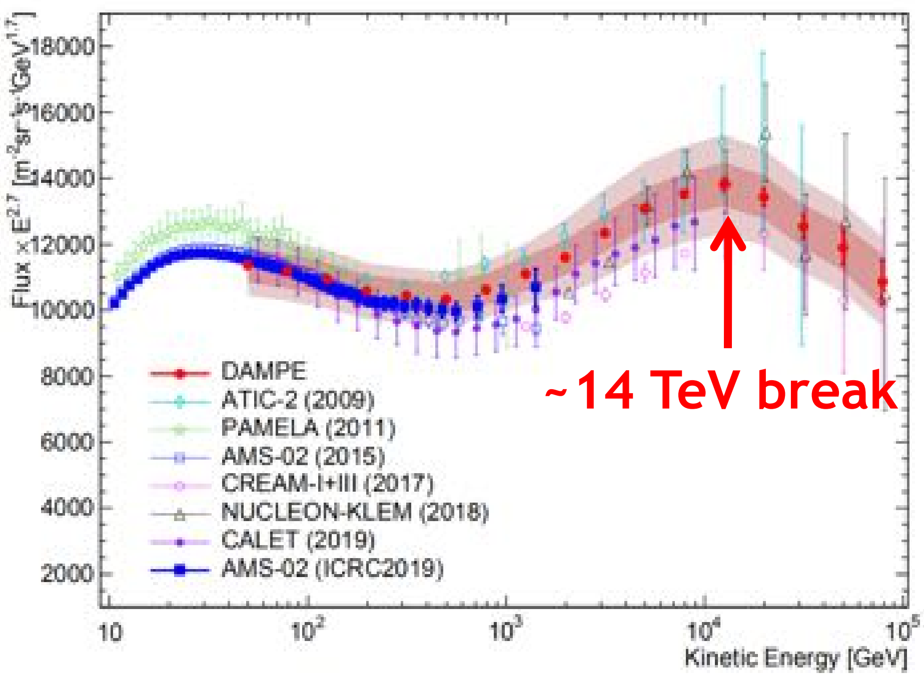

DAMPE 2021, PRL, 126, 201102

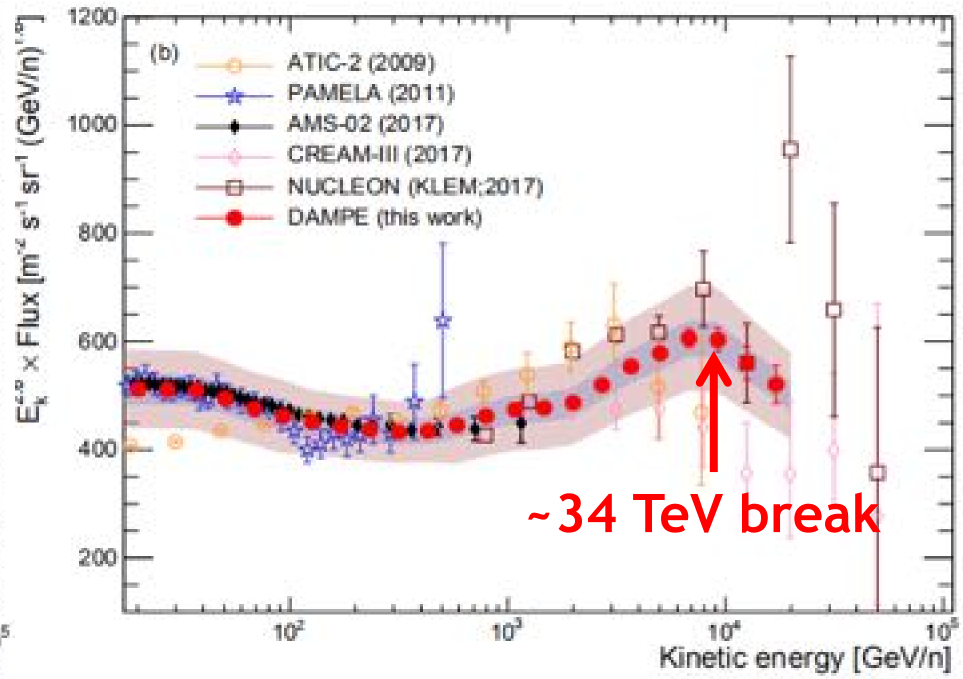

- DAMPE found new turning points at 14TeV for cosmic ray protons and 34TeV for helium nucleus at 34TeV, enriching the cosmic ray observational results.
- Possibly meaning a close cosmic ray accelerator near Earth.

Gamma Ray Astronomy

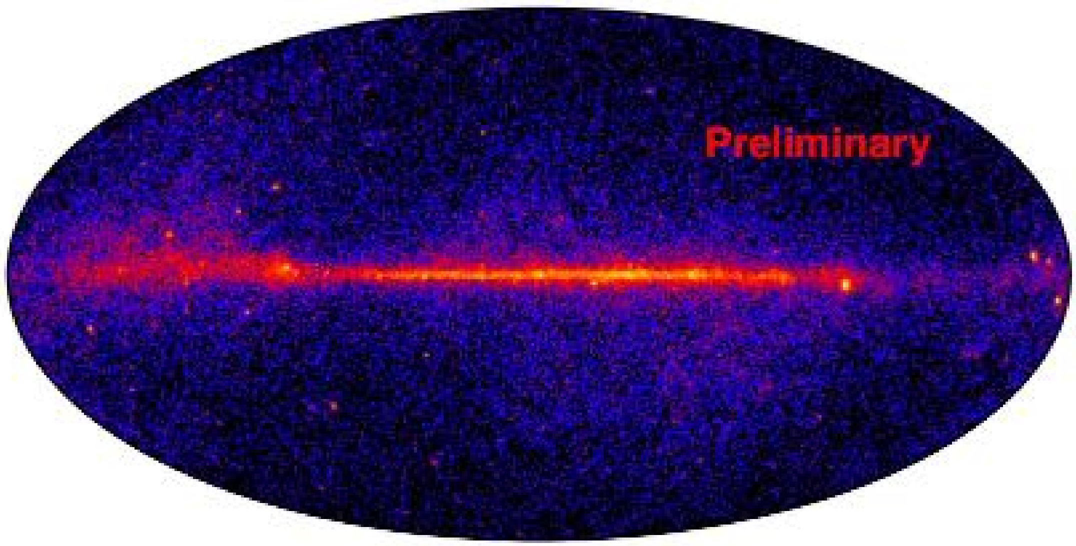

Source Name	3FGL Name	Type	RA (°)	DEC (°)	Flux[a] (10^{-8} ph/cm^2/s)
s5 1044+71	3FGL J1048.4+7144	FSRQ	162.12	71.74	1.102 ± 0.186
3C 454.3	3FGL J2254.0+1608	FSRQ	343.50	16.15	4.563 ± 0.603
CTA 102	3FGL J2232.5+1143	FSRQ	338.14	11.72	11.008 ± 0.885
Vela	3FGL J0835.3-4510	Pulsar	128.84	-45.18	52.630 ± 1.520
Geminga	3FGL J0633.9+1746	Pulsar	98.48	17.77	33.058 ± 1.385
Crab	3FGL J0534.5+2201	Pulsar	83.64	22.02	9.086 ± 0.707
Mkn501	3FGL J1653.9+3945	BL Lac	253.48	39.75	0.414 ± 0.134
Mkn421	3FGL J1104.4+3812	BL Lac	166.12	38.21	2.165 ± 0.317
IC443	3FGL J0617.2+2234e	SNR	94.31	22.58	3.659 ± 0.517
PSR J1836+5925	3FGL J1836.2+5925	Pulsar	279.06	59.43	4.419 ± 0.354
PSR J0007+7303	3FGL J0007.0+7302	Pulsar	1.77	73.05	3.459 ± 0.305
PSR B1706-44	3FGL J1709.7-4429	Pulsar	257.43	-44.49	8.246 ± 0.652

Line spectrum search

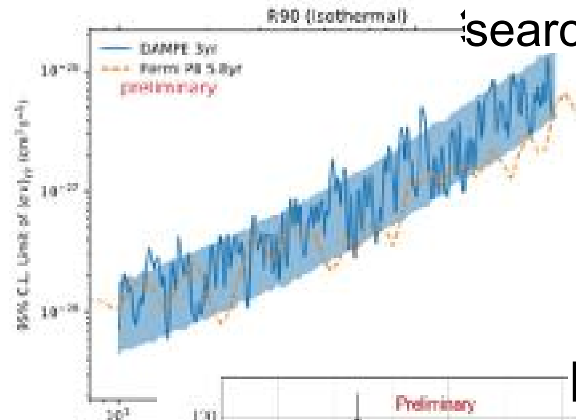

Pulsar

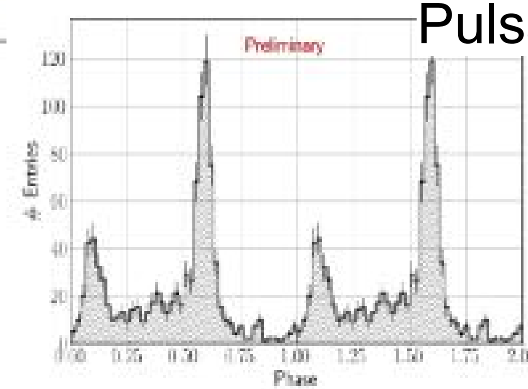

Active Galatic Nucleus

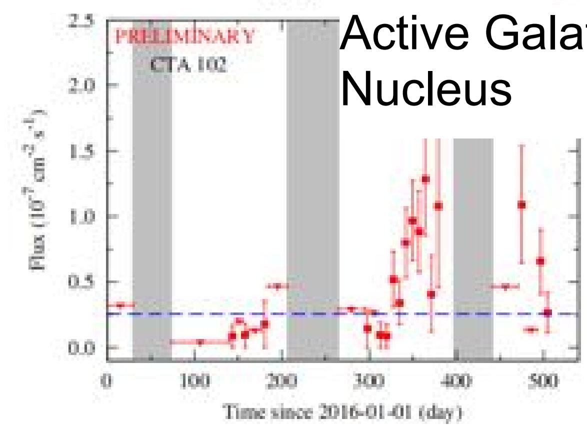

Next Generation DM Particle detector satellite: Very Large Area gamma ray Space Telescope (VLAST)

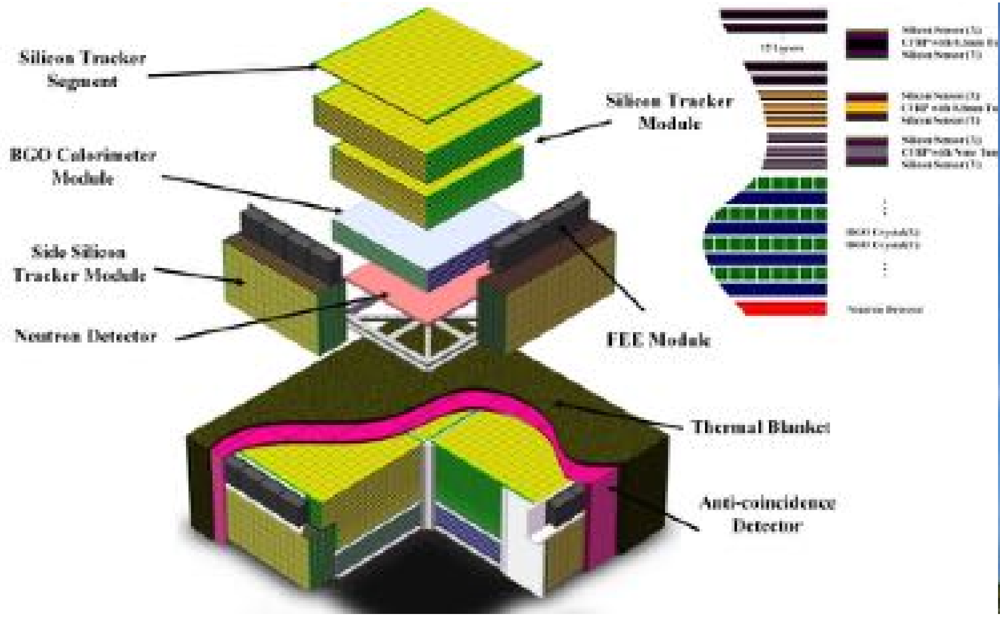

VLAST: The world's first 10 m² sr high-energy detection satellite, dedicated to leading dark matter indirect detection

Abundance of Thermal Dark Matter

Excellent Production Mechanism: Thermal Freeze-out

- DM is a massive elementary particle
- DM has an electroweak-scale coupling
    - DM starts with thermal distribution
    - Relic abundance is determined by freeze-out mechanism
    - DM Annihilation into
        - X = Standard Model particles (direct coupling)

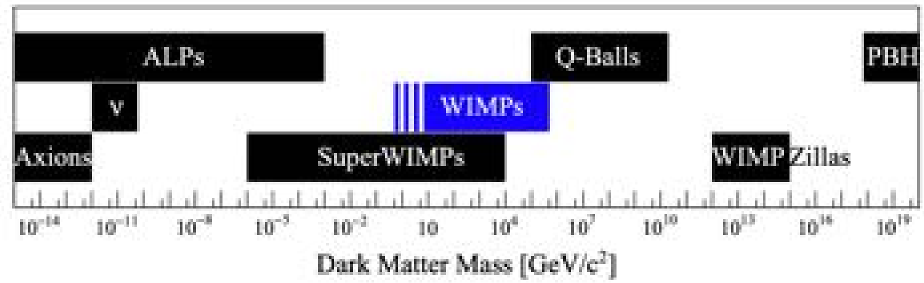

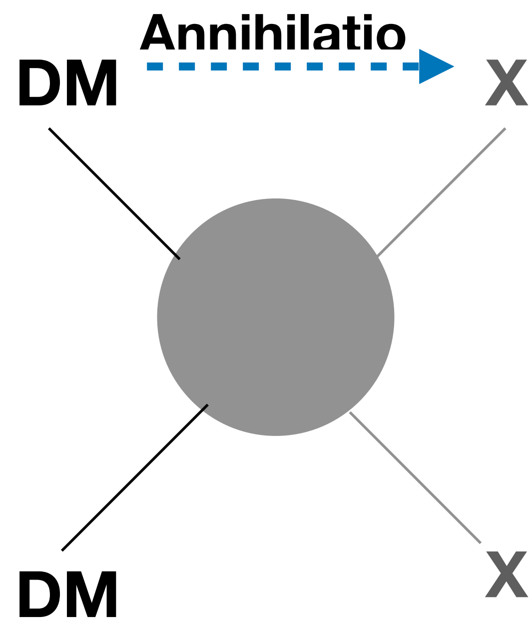

Thermal Decoupling Annihilation Cross-Section of WIMP DM

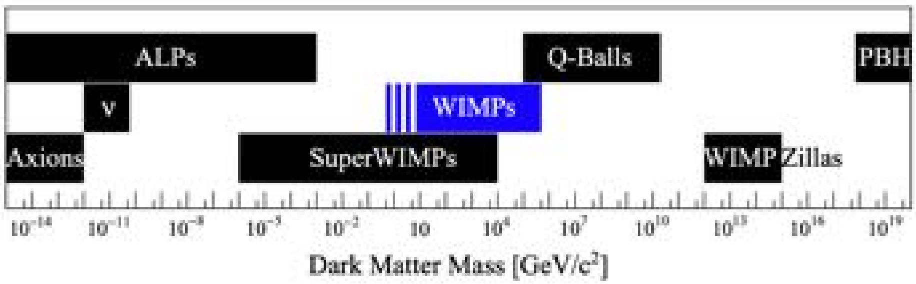

- The thermal decoupling annihilation cross-section matches the strength and scale of electroweak interactions.

$$\langle \sigma v \rangle \sim \frac{\alpha^2}{m_W^2} \sim 3 \times 10^{-26} \mathrm{cm}^3 \mathrm{s}^{-1}$$

Such match is called WIMP miracle

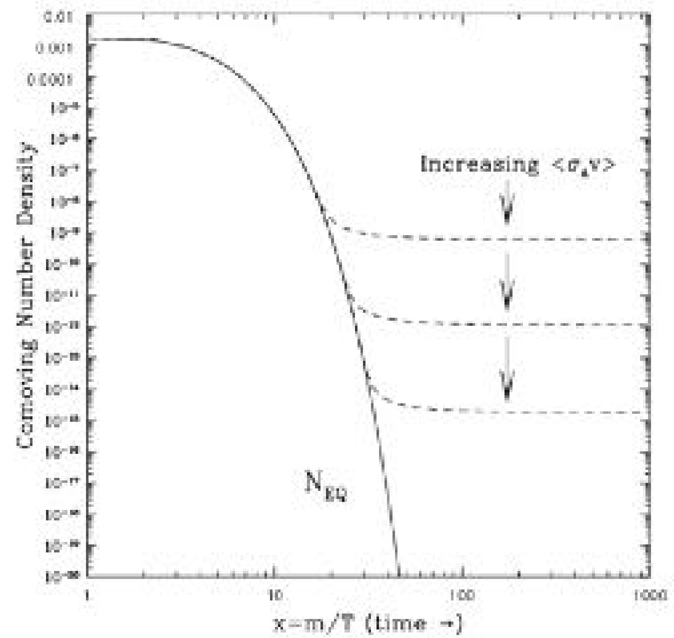

Jungman *et al* hep-ph/9506380

Thermal Freeze-out: Excellent!

- Naturally yields the relic abundance
  - No need for UV information (starts with thermal equilibrium distribution)
  - Annihilation cross-section at the electroweak scale
  - Similar story to other Standard Model particles (decoupling, ratio, nuclear elements)
    - (ν decoupling, n_p/n_n ratio, nuclear elements)
  - Predicts direct/indirect/collider experimental signals

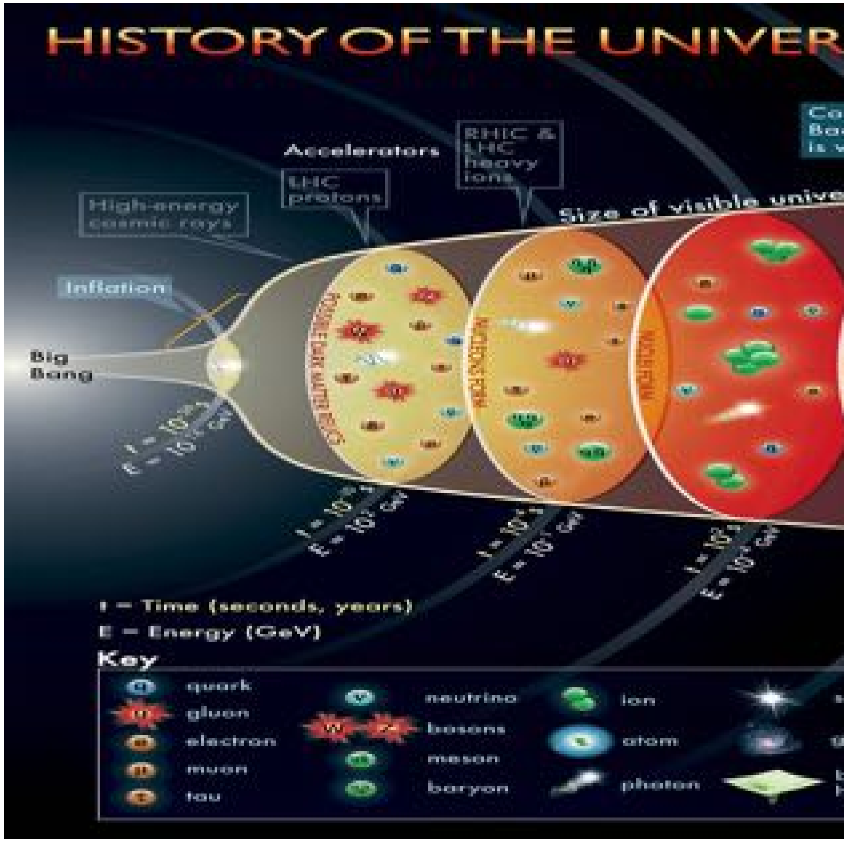

Background Knowledge：
Phase Space and Cross-sections

- Particle's phase space
- 4D Lorentz-invariance： phase-space of a single on-shell particle

$$dPS = \Theta(E)\delta(p\cdot p - m^2)d^4p = \frac{d^3\vec{p}}{(2\pi)^3 2E}$$

  - Why the factor $(2E)^{-1}$?
  - Normalize to 2E particle in the volume

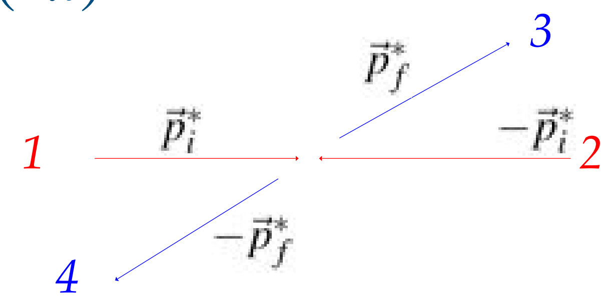

- Interaction Cross-section： $1 + 2 \to 3 + 4$ (DM + DM > SM SM)

$$\sigma = \frac{1}{2E_1 2E_2 \left|v_1 - v_2\right|}\int\left(\prod_f \frac{d^3p_f}{(2\pi)^3}\frac{1}{2E_f}\right)\times\left|\mathscr{M}\left(p_1, p_2 \to \left\{p_f\right\}\right)\right|^2 (2\pi)^4\delta^{(4)}\left(p_1 + p_2 - \sum p_f\right)$$

Background Knowledge 2：
Phase Space Density of particles

- Phase space distribution function $f(\vec{x}, \vec{p}, t) d\vec{x} d\vec{p}$

- Distribution under thermal equilibrium $f_{\text{eq}} = \dfrac{1}{e^{E/T} \pm 1} \approx e^{-E/T}$

- Number density $n_{\text{eq}} = \int d\vec{p} f_{\text{eq}} = \int \dfrac{d\vec{p}}{(2\pi)^3} e^{-\frac{E}{T}}$

  - High temperature $T \gg m$ limit (relativistic) $n_{\text{eq}} = T^3$

  - High temperature $T \ll m$ limit (non-relativistic) $n_{\text{eq}} = \left(\dfrac{mT}{2\pi}\right)^{3/2} e^{-\frac{m}{T}}$

Background Knowledge 3：
Cosmic Metric and radiation-dominated universe

- Expansion Rate of a Radiation-Dominated Universe

$$H_{\rm rad}^2 = \frac{8\pi^3}{90}\frac{g_* T^4}{m_{\rm PL}^2}$$

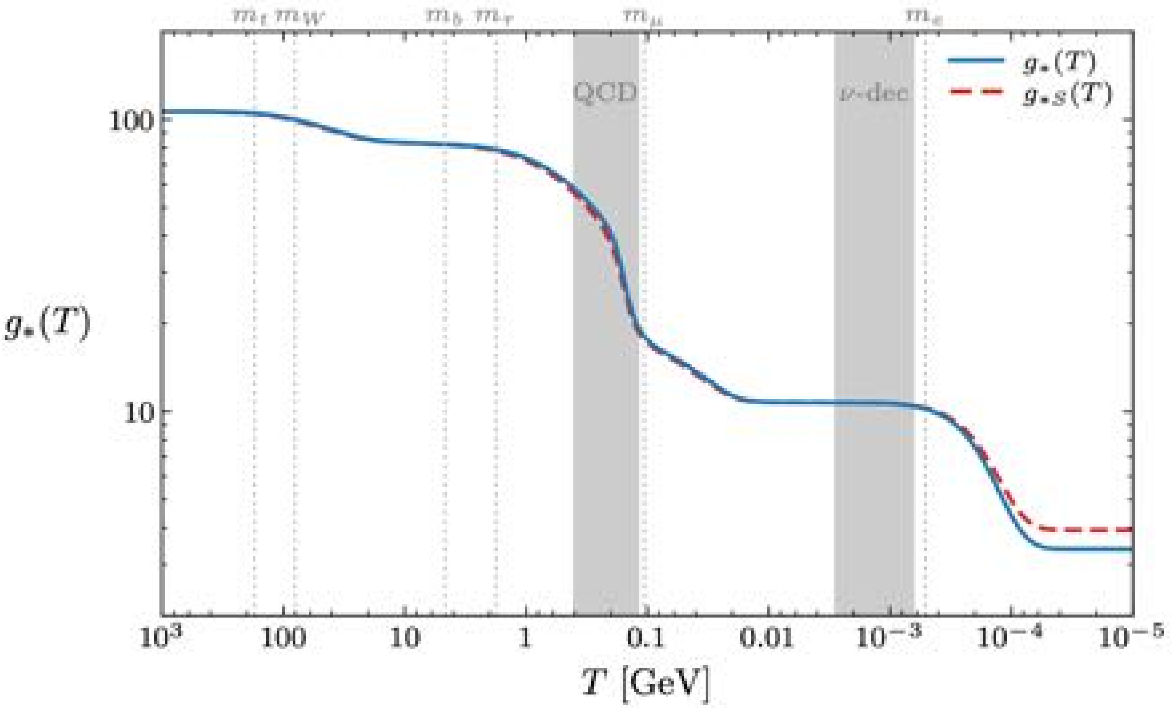

- Temperature Redshift in a Radiation-Dominated Universe

$$T \propto a(t)^{-1}$$

$$\rho_{\rm rad} \propto a(t)^{-4}$$

DM freeze-out: Boltzmann Equation

- Final Evolution of DM: The Boltzmann Equation

$$a^{-3}\frac{d(na^3)}{dt} = n_1^{\rm eq} n_2^{\rm eq}\langle \sigma v\rangle \left(\frac{n_3 n_4}{n_3^{\rm eq} n_4^{\rm eq}} - \frac{n_1 n_2}{n_1^{\rm eq} n_2^{\rm eq}} \right)$$

$$\dot{n} + 3Hn = \langle \sigma v\rangle (n_{\rm eq}^2 - n^2)$$

- Thermally Averaged DM Annihilation Cross-Section

$$\langle \sigma v\rangle \equiv \frac{1}{n_1^{\rm eq} n_2^{\rm eq}} \int \Pi_{i=1}^4 d{\rm PS}_i \times (2\pi)^4 \delta^4(p_1 + p_2 - p_3 - p_4) |\mathscr{M}|^2 \times e^{-\frac{E_1+E_2}{T}}$$

Solving the DM freeze-out Boltzmann Equation

- Behavior of DM number density

$$n_{\rm eq}^{\rm rad} \sim T^3 \sim a^{-3}, \quad n_{\rm eq}^{\rm mat} \sim (mT)^{3/2} e^{-m/T}$$

$$n_{\rm freeze-out} \sim a^{-3}$$

- Useful variable: DM Yield and temperature x

$$Y_{\rm dm} \equiv n_{\rm dm}/s, \quad x \equiv m_{\rm dm}/T$$

- DM Evolution: Boltzmann Equation

$$\frac{dY}{dx} = \frac{\langle \sigma v \rangle x s}{\sqrt{\frac{8\pi^3 g_\star}{90 m_{\rm Pl}^2}}\, m^2} \left(Y_{\rm eq}^2 - Y^2\right) \qquad dx/dt = (8\pi^3 g_\star/(90 m_{\rm Pl}^2))^{1/2} m^2/x$$

Solving the DM freeze-out Boltzmann Equation

- DM Evolution: Boltzmann Equation

$$\frac{dY}{dx} = \frac{\langle \sigma v \rangle x s}{\sqrt{\frac{8\pi^3 g_\star}{90 m_{\rm Pl}^2}} m^2} \left(Y_{\rm eq}^2 - Y^2\right)$$

- DM thermal freeze-out temperature

$$n_{\rm fo} \langle \sigma v \rangle \approx H_{\rm fo}$$

$$x_{\rm fo} \sim 25$$

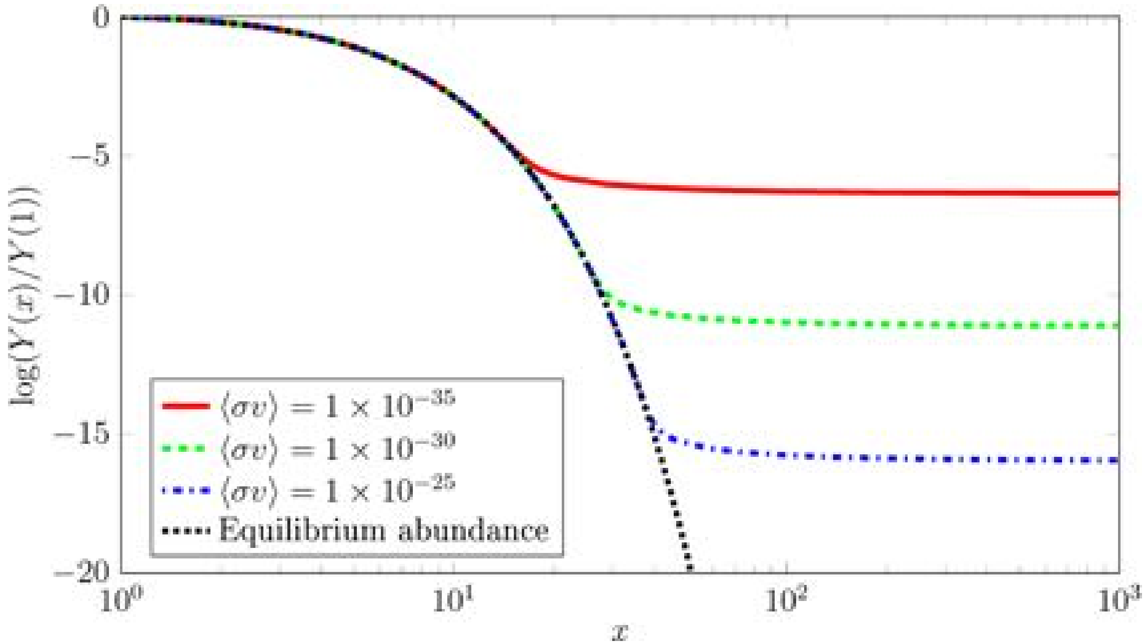

Approximately Solving the DM freeze-out Boltzmann Equation

- Approximately Solving the Boltzmann Equation

$$\frac{dY}{dx} = -\frac{\lambda}{x^2}(Y^2 - Y_{\rm eq}^2)$$

$$\frac{\lambda}{x^2} \equiv \langle \sigma v \rangle \frac{xs}{H_{\rm rad}(T = m_{\rm DM})}$$

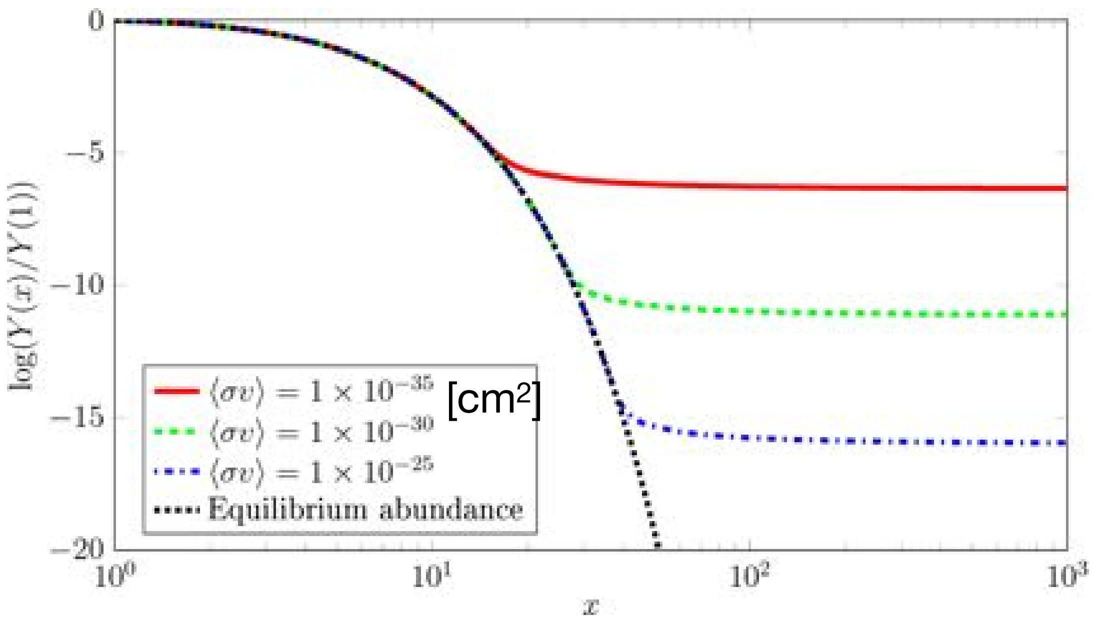

- For $x \gg 1$

$$\frac{dY}{dx} \approx -\frac{\lambda}{x^2}Y^2$$

$$\implies Y_\infty^{-1} - Y_{\rm fo}^{-1} = \frac{\lambda}{x_{\rm fo}} \implies Y_\infty^{-1} = \frac{\lambda}{x_{\rm fo}}$$

Approximately Solving the DM freeze-out Boltzmann Equation

- Approximately Solving the Boltzmann Equation $Y_\infty^{-1} = \frac{\lambda}{x_{\rm fo}}$
- Today's DM energy fraction $\Omega_{\rm dm} = 26.8\,\%$

$$\Omega_{\rm dm} h^2 = \frac{Y_0 s_0 m_{\rm dm}}{\rho_{\rm cr}} h^2 \approx \frac{Y_\infty s_0 m_{\rm dm}}{\rho_{\rm cr}} h^2 \approx 0.3 \left(\frac{m_{\rm dm}}{\rm eV}\right) Y_\infty$$

$$\rho_{\rm cr} = 3H_0^2 m_{\rm Pl}^2/8\pi \approx 8\times 10^{-47} h^2\,{\rm GeV}^4 \text{ and } s_0 \approx 2970\,{\rm cm}^{-3}$$

- Magnitude of DM Annihilation Cross-Section at Thermal Decoupling

$$\Omega h^2 \approx 0.1 \left(\frac{x_f}{25}\right)\left(\frac{g_\star}{80}\right)^{-1}\left(\frac{3\times 10^{-26}{\rm cm}^3{\rm s}^{-1}}{\langle\sigma v\rangle}\right)$$

WIMP Dark Matter Miracle

- Magnitude of DM Annihilation Cross-Section at Thermal Decoupling

$$\Omega h^2 \approx 0.1 \left(\frac{x_f}{25}\right)\left(\frac{g_\star}{80}\right)^{-1}\left(\frac{3\times 10^{-26}\mathrm{cm}^3\mathrm{s}^{-1}}{\langle\sigma v\rangle}\right)$$

$$\langle\sigma v\rangle \sim 3\times 10^{-26} cm^3/s$$

$$\sim 10^{-8}\ \mathrm{GeV}^{-2} \sim \frac{\alpha^2}{m_W^2}$$

- DM might be associated with the electroweak interaction scale.

WIMP DM crisis

- Null result from direct detection
  - Maybe discovery in the corner?
  - Neutrino floor and beyond: directional ..
  - The rise of light dark matter ($\lesssim$ 10 GeV)

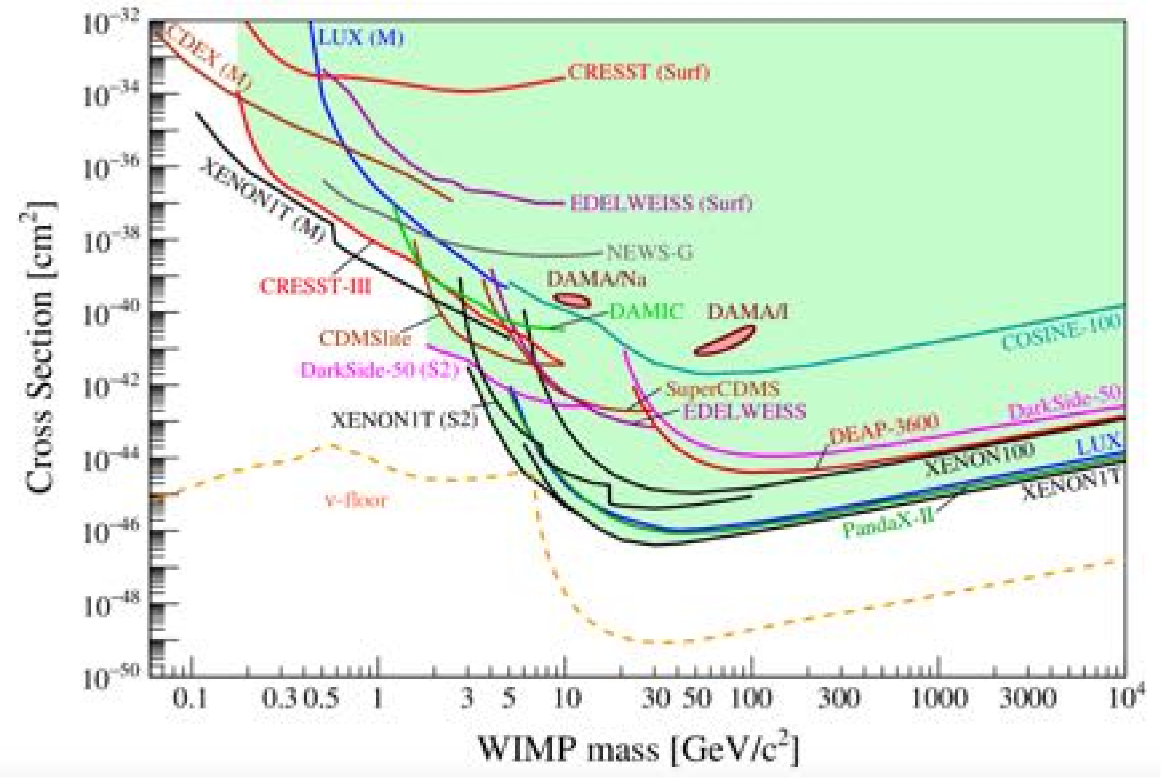

APPEC Committee Report: 2104.07634

Detection Methods of DM

Wave-like DM Detection

Theorists' View of DM

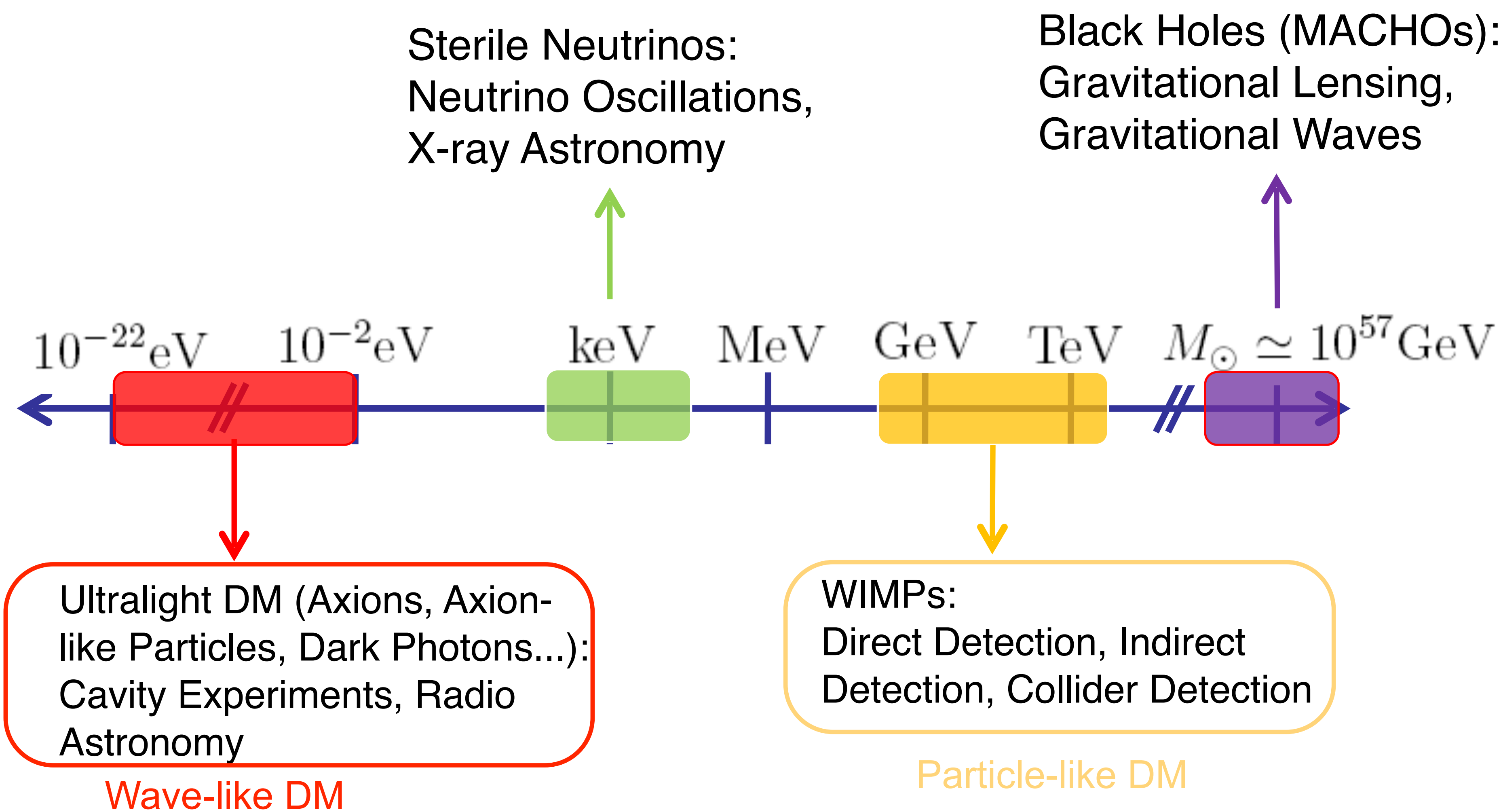

Theoretical possibilities for DM are numerous, spanning a wide range of masses and interaction cross-sections, making experimental detection highly challenging.

(Wavy) Ultra-light DM

Quantum Mechanics： Matter behave both like waves and particles

($m \sim 10^{-22}$ eV)

de Broglie wavelength reaches galactic scales (kpc)

- Dependent on astrophysical observations (location, time)

Astrophysical experiments

Ultralight DM has a macroscopic wavelength, manifesting as a fluctuating background field on a macroscopic scale.

Unlike traditional DM detection (no longer based on particle scattering)

Huge potential for development

Similar to gravitational waves

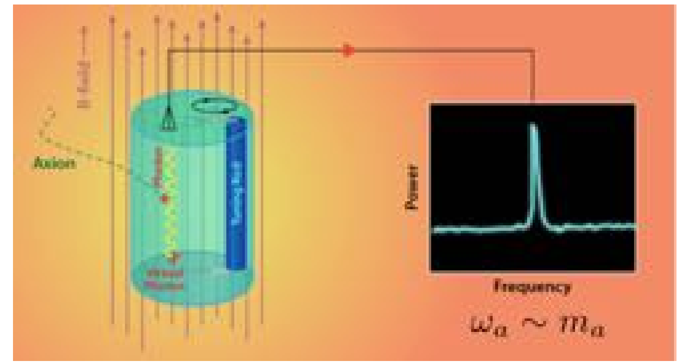

$$m_a \sim \mathrm{GHz} \sim 10^{-6}\ \mathrm{eV}$$

Compton wavelength is laboratory scale(m)

Resonant Cavity Quantum Amplifier

Propose new quantum detection method

Fussy Dark Matter

Ultra-light DM: solve small-structure problem

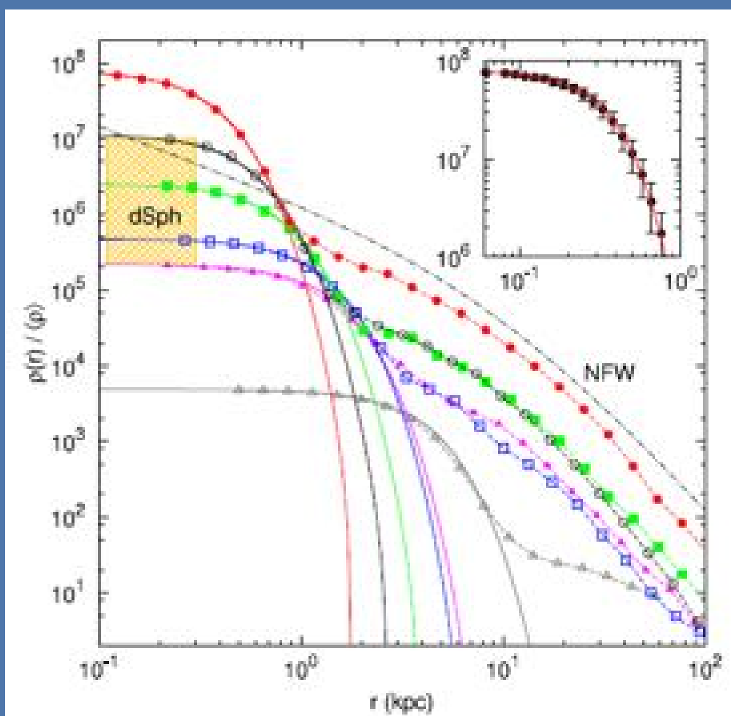

Ultralight DM (bosons) can form Bose-Einstein condensates, resembling cold DM on large scales.

On small scales (around $m \approx 10^{-22}$eV, $\lambda \approx$ kpc), it can addresse the cusp-core problem in dwarf galaxy observations.

Hu et al., 2000

Ultralight DM energy distribution follows the soliton core profile, with the central region density not being very high (non-divergent).

$$\rho(x) = \begin{cases} 0.019\left(\frac{m_a}{m_{a,0}}\right)^{-2}\left(\frac{l_c}{1\mathrm{kpc}}\right)^{-4} M_\odot \mathrm{pc}^{-3}, & \text{for } r < l_c \\ \frac{\rho_0}{r/R_H(1+r/R_H)^2}, & \text{for } r > l_c \end{cases}$$

soliton solution

NFW profile

Ultra-light Wavy Dark Matter

- Ultralight Dark Matter
    - QCD axion, ALP, dark photon, etc.
    - Production mechanism: Misalignment
        - $\ddot{a} + 3H\dot{a} + m_a^2 a = 0$

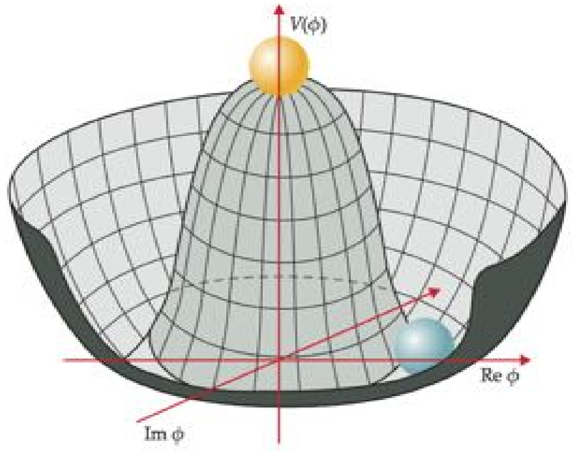

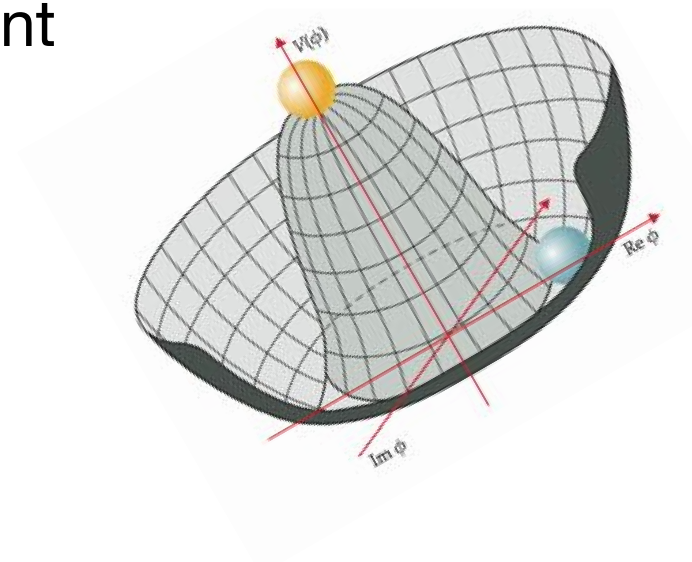

Ultra-light DM: axion

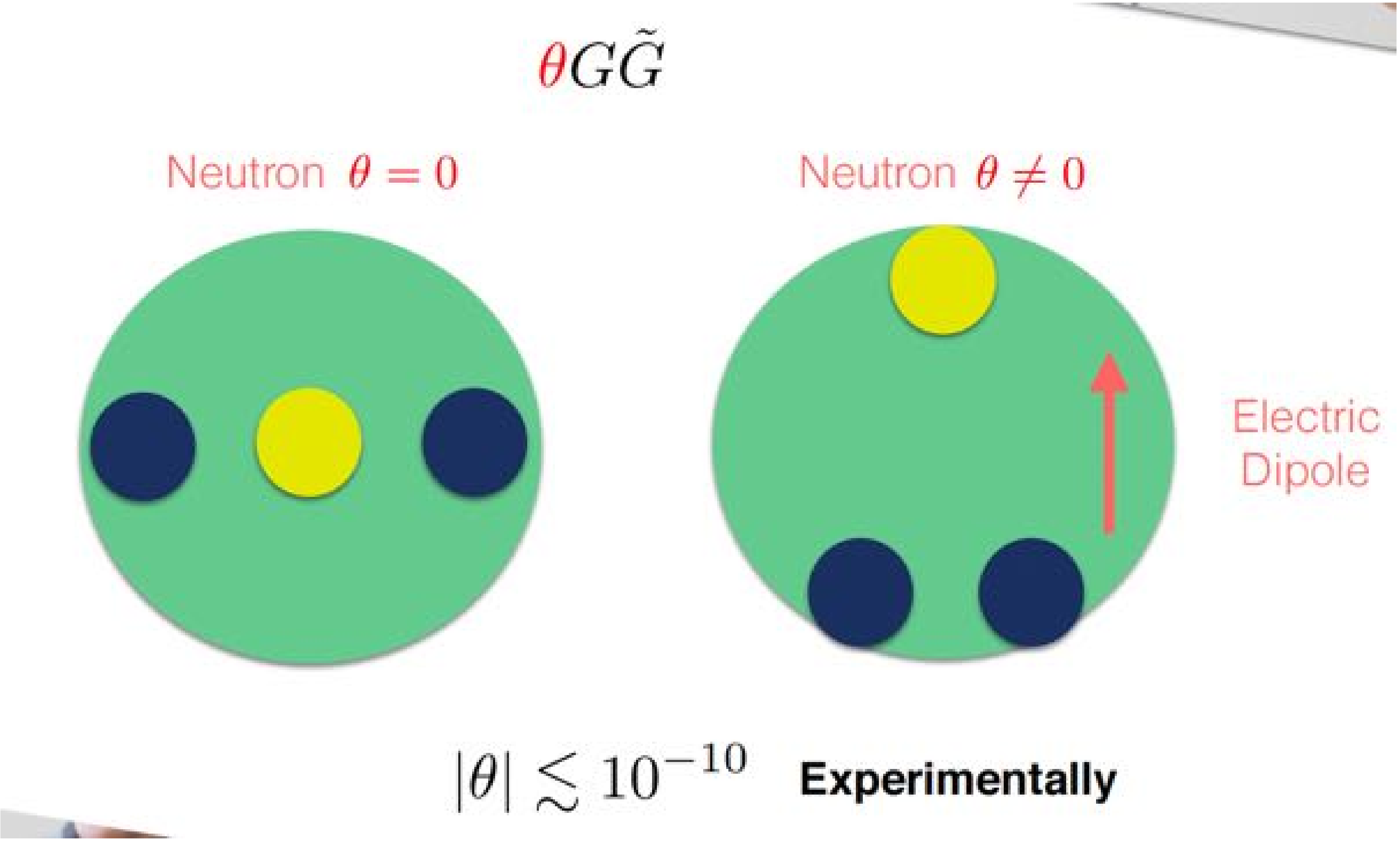

Ultra-light DM: axion

Introduce a new global symmetry (PQ symmetry) broken at energ

$$\theta G\tilde{G} \longrightarrow \left(\theta + \frac{a}{f_a}\right) G\tilde{G}$$

breaking PQ shift symmetry

Potential energy term $\cos(\theta + a/f_a)$

At the minimum

$$\langle a \rangle = -\theta f_a$$

Self-adjust to 0

The QCD axion and the Strong CP problem

$$\mathscr{L} \supset -\frac{\theta g_s^2}{32\pi^2} G\tilde{G} - \left(\bar{u}_L M_u u_R + \bar{d}_L M_d d_R + \mathrm{h.c.}\right)$$

- The CKM matrix from $M_{u,d}$
  - CP violating phase θ_{CP} ~ 1.2 radian
- QCD induced CP violating phase, $\bar{\theta}$

$$\bar{\theta} = \theta + \arg\left[\det\left[M_u M_d\right]\right]$$

- $\bar{\theta}$ is invariant under quark chiral rotation $d^n_{\mathrm{EDM}} \sim \theta \times 10^{-16}$ e cm
- According to neutron EDM experiment $d^n_{\mathrm{exp}} < 10^{-26}$ e cm

$$\bar{\theta} \lesssim 1.3 \times 10^{-10} \text{ radian}$$

The Peccei-Quinn solution to Strong CP problem

- Experiment requires $\bar{\theta} = \theta + \arg\left[\det\left[M_u M_d\right]\right] \lesssim 10^{-1}\mathrm{rad}$
- PQ: promote the constant $\bar{\theta}$ to a dynamical field, a
- Vafa-Witten theorem: vector-like theory (QCD) has ground state $\langle\theta\rangle = 0$
- Introduce a *global* PQ-symmetry $U(1)_{\mathrm{PQ}}$, *anomalous* under the QCD
    - The massless Goldstone boson a is called *axion*
        - $a \to a + \kappa f_a \;\Rightarrow \mathcal{S} \to \mathcal{S} + \frac{\kappa}{32\pi^2}\int d^4x G\tilde{G}$, cancels $\bar{\theta}$
        - Low energy: $\mathscr{L} = \sum_q \bar{q}\left(iD_\mu\gamma^\mu - m_q\right)q - \frac{1}{4}GG + \frac{g_s^2}{32\pi^2}\frac{a}{f_a}G\tilde{G} + \frac{1}{2}\left(\partial_\mu a\right)^2 + \mathscr{L}_{\mathrm{int}}[\partial_\mu a]$

https://arxiv.org/abs/hep-ph/0011376

Model independent visible axion properties

- For two flavor QCD, $q = (u, d)^T$
  - $\mathscr{L} \supset \frac{1}{2}\left(\partial_\mu a\right)^2 + \frac{g_s^2}{32\pi^2}\frac{a}{f_a}G\tilde{G} + \frac{1}{4}g^0_{a\gamma}F\tilde{F} - \bar{q}_L M_q q_R + \frac{\partial_\mu a}{2f_a}\bar{q}c^0_q\gamma^\mu\gamma_5 q + h.c.$
  - The three QCD related terms can be eliminated to 2 d.o.f.
  - Choose to eliminate $G\tilde{G}$ term by quark field redefinition in a-related chiral rotation

$q \to e^{i\alpha} q \qquad \bar{q} \to e^{-i\alpha}\bar{q}$

- A new quark field: $q' = \exp\left(i\frac{a}{2f_a}\gamma_5 Q_a\right) q$

anomalous U(1) axial transformation

a: transformation angle

- $\mathscr{L} \supset \frac{1}{2}\left(\partial_\mu a\right)^2 + \frac{1}{4}g_{a\gamma}F\tilde{F} - \bar{q}'_L M_{q'} q'_R + \frac{\partial_\mu a}{2f_a}\bar{q}' c_q \gamma^\mu\gamma_5 q' + h.c.$

Model independent visible axion properties

- In the new basis
  - $\mathscr{L} \supset \frac{1}{2}\left(\partial_\mu a\right)^2 + \frac{1}{4} g_{a\gamma} F\tilde{F} - \bar{q}'_L M_a q'_R + \frac{\partial_\mu a}{2f_a}\bar{q}' c_q \gamma^\mu \gamma_5 q' + h.c.$
  - $c_q = c_q^0 + Q_q\,,\; g_{a\gamma} = g_{a\gamma}^0 - 2N_c \frac{\alpha_{em}}{2\pi f_a}\mathrm{Tr}[Q_a Q^2]$
  - Quark mass is complex:

$$M_a = \exp\left(i\frac{a}{2f_a}Q_a\right) M_q \exp\left(i\frac{a}{2f_a}Q_a\right)$$

Induce cos(a) potential term

  - There is a phase a in the mass if we define away $\frac{g_s^2}{32\pi^2}\frac{a}{f_a}G\tilde{G}$

The axion and Chiral Lagrangian

- The generic low energy Lagrangian is

$$\mathcal{L} \supset \frac{1}{2}\left(\partial_\mu a\right)^2 + \frac{1}{4} g_{a\gamma} F\tilde{F} - \bar{q}_L M_a q_R + \frac{\partial_\mu a}{2f_a} \bar{q} c_q \gamma^\mu \gamma_5 q + h.c.$$

Induce cos(a) potential term

- Two flavor quarks $q = (u, d)$; quark mass term $M_a = e^{i\frac{aQ_a}{2f_a}} M_q e^{i\frac{aQ_a}{2f_a}}$
- Below the QCD scale, one needs the chiral axion Lagrangian

$$\mathcal{L}_a^{\chi PT} = \frac{f_\pi^2}{4} \mathrm{Tr}\left[(D^\mu U)^\dagger D_\mu U + 2B_0(UM_a^\dagger + M_a U^\dagger)\right] + \frac{\partial^\mu a}{4f_a} \mathrm{Tr}[c_q \sigma^a] J_\mu^a$$

$$U \equiv e^{i\pi^a \sigma^a / f_\pi}$$

$$J_\mu^a \equiv e^{i\pi^a \sigma^a / f_\pi}$$

Axion mass and interaction with pions

$$\mathcal{L}_a^{\chi PT} = \frac{f_\pi^2}{4}\mathrm{Tr}\left[(D^\mu U)^\dagger D_\mu U + 2B_0(UM_a^\dagger + M_a U^\dagger)\right] + \frac{\partial^\mu a}{4f_a}\mathrm{Tr}[c_q\sigma^a]J_\mu^a$$

- Axion mass: $m_a^2 \simeq (Q_u + Q_d)^2 \frac{m_u m_d}{(m_u+m_d)^2}\frac{m_\pi^2 f_\pi^2}{f_a^2}$
- Axion-π^0 mixing: $\theta_{a\pi} \simeq \frac{(Q_d m_d - Q_u m_u)}{(m_u+m_d)}\frac{f_\pi}{f_a}$
- Axion-pion couplings: $-\frac{3}{2}\frac{\epsilon}{f_a f_\pi}\partial_\mu a\left(2\partial^\mu\pi^0\pi^+\pi^- - \pi^0\partial^\mu\pi^+\pi^- - \pi^0\pi^+\partial^\mu\pi^-\right)$
    - Coefficient: $\epsilon = -\frac{1}{2}\left(\frac{Q_d m_d - Q_u m_u}{m_u+m_d} + c_d^0 - c_u^0\right)\frac{f_\pi}{f_a}$

Experimental searches for Axion-Like Particles axion

Methodology:

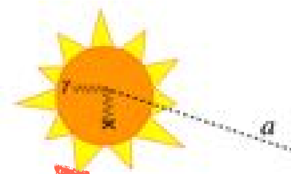
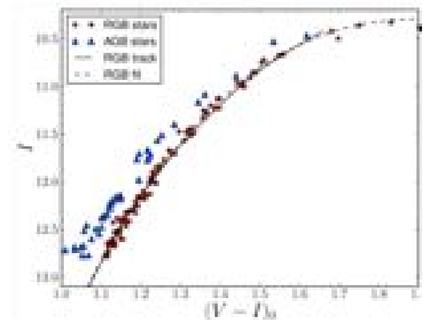

- Dark Matter Axion: haloscopes …
- Axion independent searches:
  - Rare meson decays
  - Stellar cooling
  - Supernova
  - Helioscopes: solar axion (CAST, IAXO, or DM direct detection searches)
  - Light shining through walls
  - Polarization
  - Fifth force
  - Radio wave detection


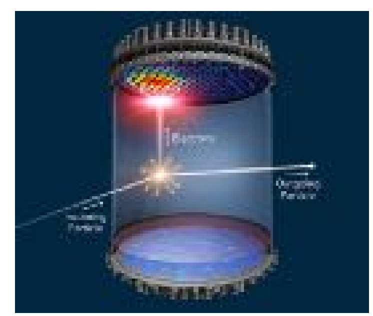

Experimental searches for Axion-Like Particles axion

$$\mathcal{L}_{\rm ALP} = g_{ag}\frac{a}{f_a}G\tilde{G} + g_{a\gamma}\frac{a}{f_a}F\tilde{F} + g_{af}\frac{\partial_\mu a}{2f_a}\bar{f}\gamma^\mu\gamma_5 f$$

- ALP couplings:

$$g_{a\gamma\gamma}aF_{\mu\nu}\epsilon^{\mu\nu\alpha\beta}F_{\alpha\beta} \sim g_{a\gamma\gamma}a\overrightarrow{E}\cdot\overrightarrow{B}$$

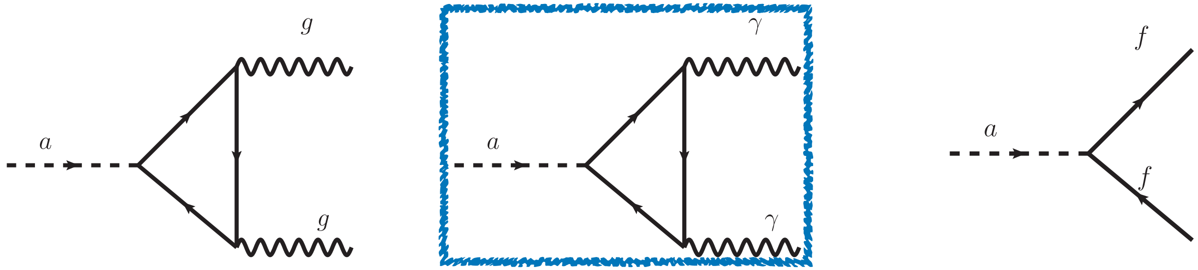

$$f = q, \ell, N$$

Ultralight light bosonic dark matter

- Ultralight Dark Matter
  - Axion and ALPs: coupling to spins, inducing time varying EDM
  - Dark photon: coupling to EM currents, leading to dark E and B fields
  - Dark scalar： coupling to fermion mass, time varying masses
  - Relic abundance： Misalignment etc …
  - Motivations：
    - Small structure problems from CDM
    - Dark sector and dark matter
    - Very small mass from
      - pseudo-Nambu-Goldstone, QCD axion

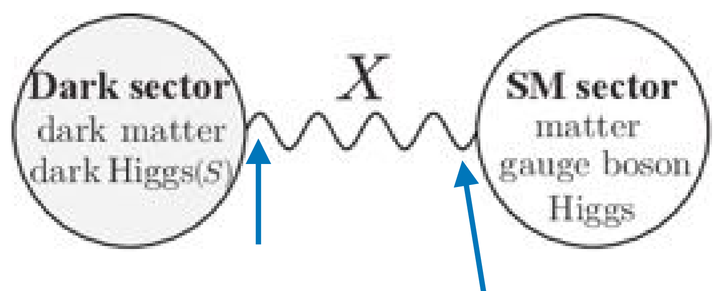

Normal couplings

Very small couplings

Dark Matter Cosmic Evolution

Axion DM

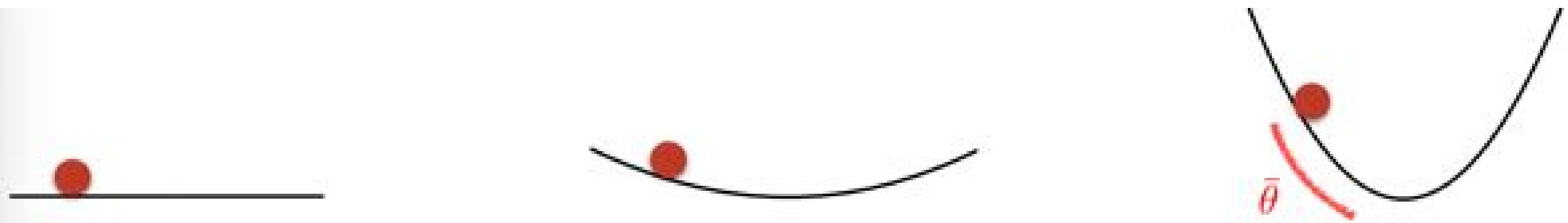

$$\theta \equiv a/f_a$$

$$\ddot{\theta} + 3H\dot{\theta} + m_a^2(T)\theta = 0$$

"Friction" "String"

Decay term

Dark Matter Mass Evolution

$$\ddot{\theta} + 3H\dot{\theta} + m_a^2(T)\theta = 0$$

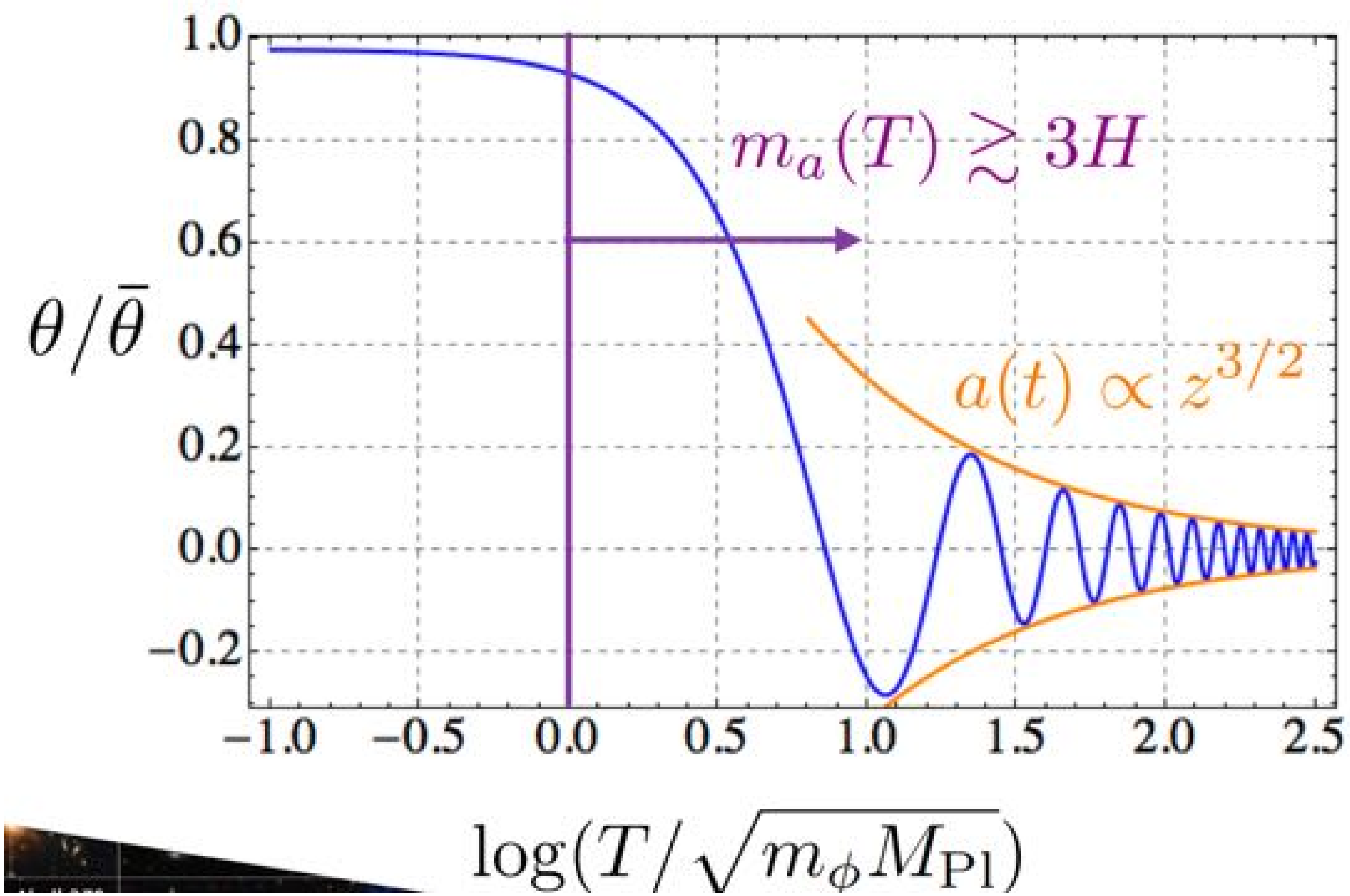

Dark Matter Mass Evolution

The number of ultralight DM particles within a unit de Broglie volume is enormous => must be bosons.

$$a(t) = \frac{\sqrt{2\rho_{\rm DM}}}{m_a} \cos(m_a t + \phi)$$

Gravitational virialization determines the correlation time and length of ultralight DM.

$$\tau_a \sim 1/m_a \langle v_{\rm DM}^2 \rangle \sim Q_a/m_a \sim 10^6/m_a$$

$$\lambda_a \sim 1/m_a \sqrt{\langle v_{\rm DM}^2 \rangle} \sim 10^3/m_a$$

Spectrum of Ultra-light Dark Matter

$$a(t) = \frac{\sqrt{2\rho_{\rm DM}}}{m_a}\cos(m_a t + \phi)$$

Frequency: $\omega_a \simeq \text{GHz}\,\frac{m_a}{10^{-6}\ \text{eV}}$

Coherence: $\tau_a \simeq \text{ms}\,\frac{10^{-6}\ \text{eV}}{m_a}$

Max Exp. Size: $\lambda_a \simeq 200\ \text{m}\,\frac{10^{-6}\ \text{eV}}{m_a}$

DM coherence time

$$\tau_a \sim 1/m_a \langle v_{\rm DM}^2 \rangle \sim Q_a/m_a \sim 10^6/m_a$$

Energy Spectrum Width 10^{-6}

$$\lambda_a \sim 1/m_a \sqrt{\langle v_{\rm DM}^2 \rangle} \sim 10^3/m_a$$

Momentum Width 10^{-3}

Ultra-light DM: Astrophysical Test

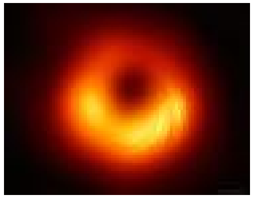

- Pulsar-Timing-Array search for ULDM

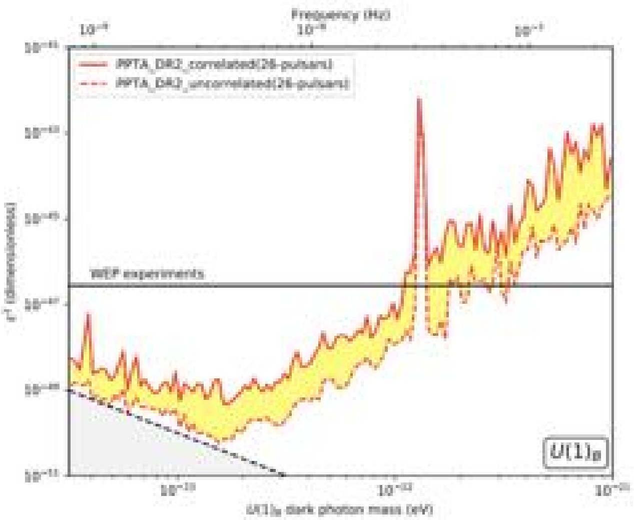

"No Man's Land", Best results now

China's FAST, future Square Kilometer Array (SKA)

- Using Event Horizon Telescope polarization observation to detect axion ULDM.

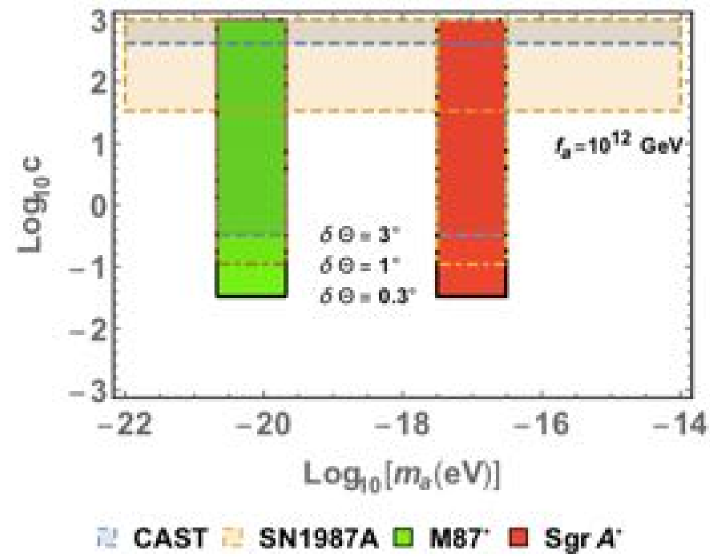

- Gaia satellite's precise measurement of stellar positions within the Milky Way.

- Accurate measurements of orbits in binary systems (Sun-Mercury, Earth-Moon, neutron star-white dwarf, etc.).

Pulsar

A pulsar is a highly magnetized rotating neutron star that emits strong electromagnetic radiation along its magnetic axis, periodically sending out pulse signals.

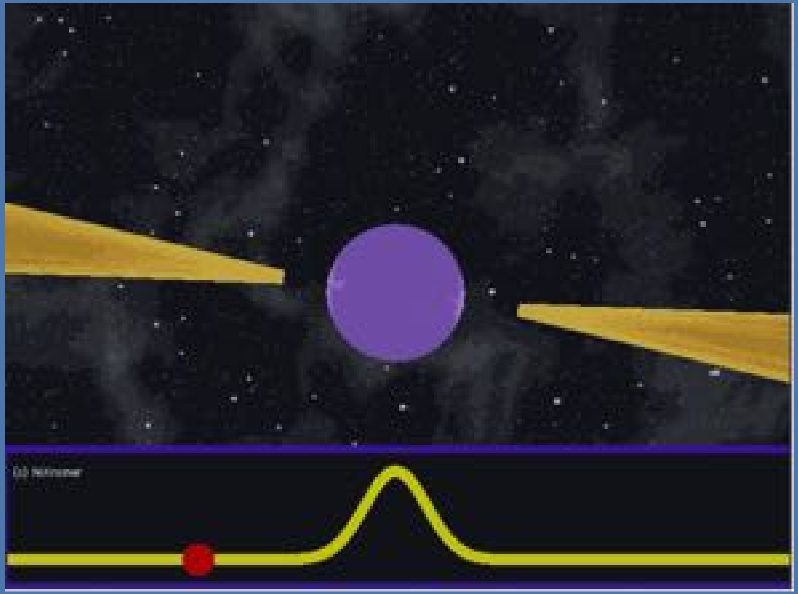

Pulsar-Timing-Array

PTA observation involves recording a series of pulsar pulse arrival times at a fixed observation frequency, referencing atomic time as a reference, compared with pulsar timing models.

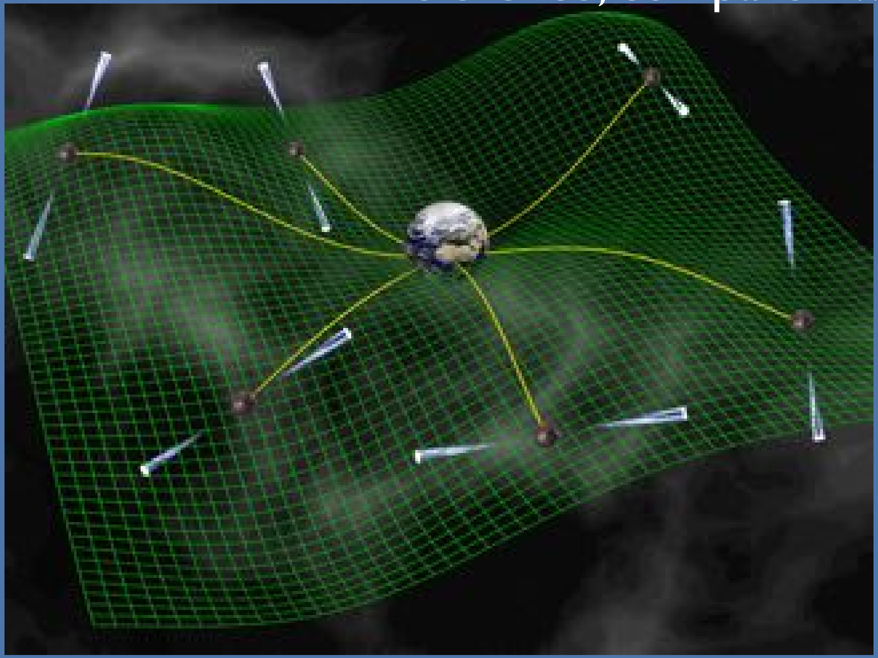

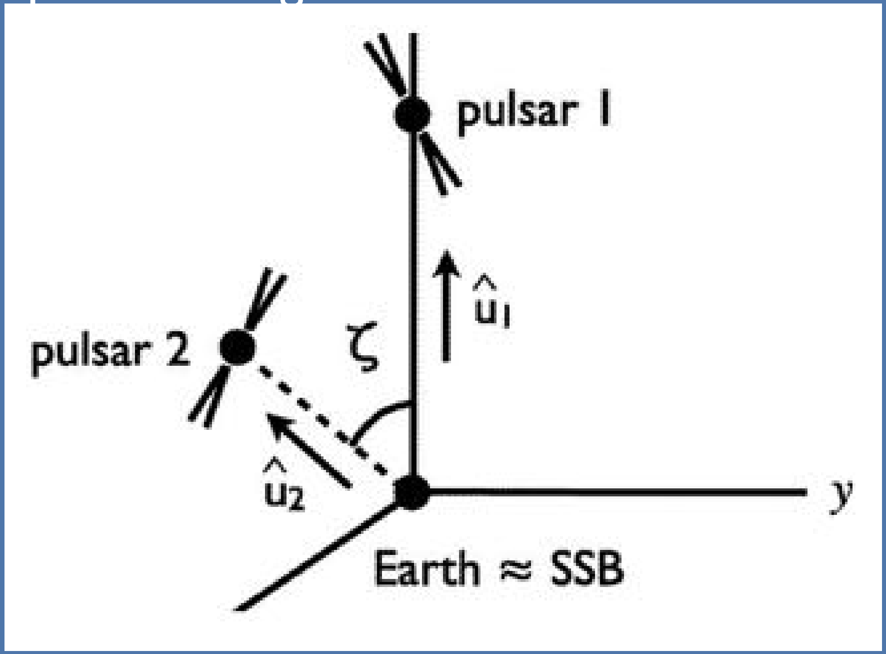

PTA measures the timing of pulses from multiple pulsars to analyze correlations between their signals.

The pulsar timing array (PTA)

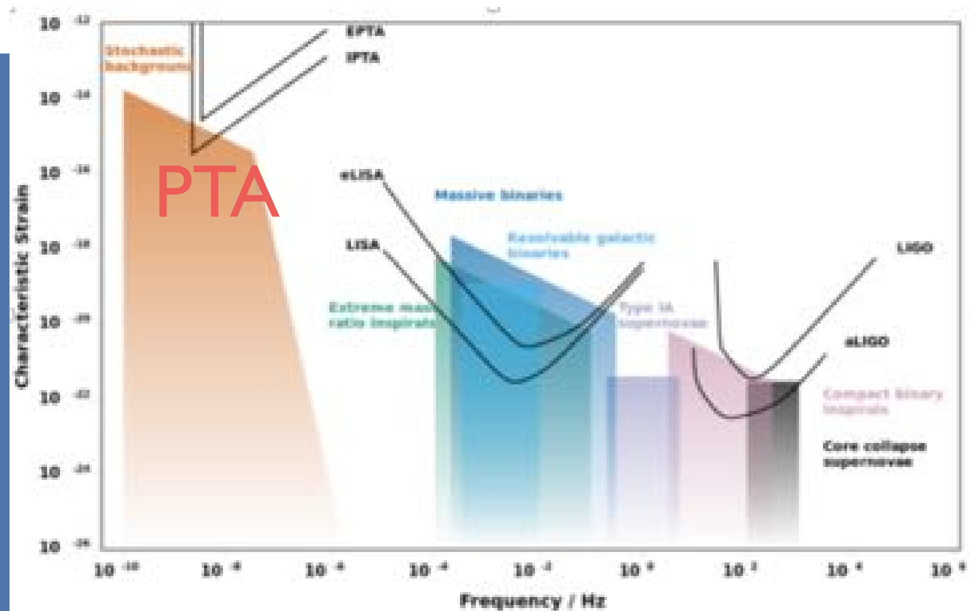

Precise measurement of pulsar pulse timing can detect gravitational waves in the nHz range and can also be used to measure ultralight DM.

PPTA, EPTA, IPTA, NanoGrav, CPTA(FAST)?

Ultra-light DM: Astrophysical Test

FAST in China

Observing
Pulsars,
binaries, etc.

future Square Kilometer Array (SKA)

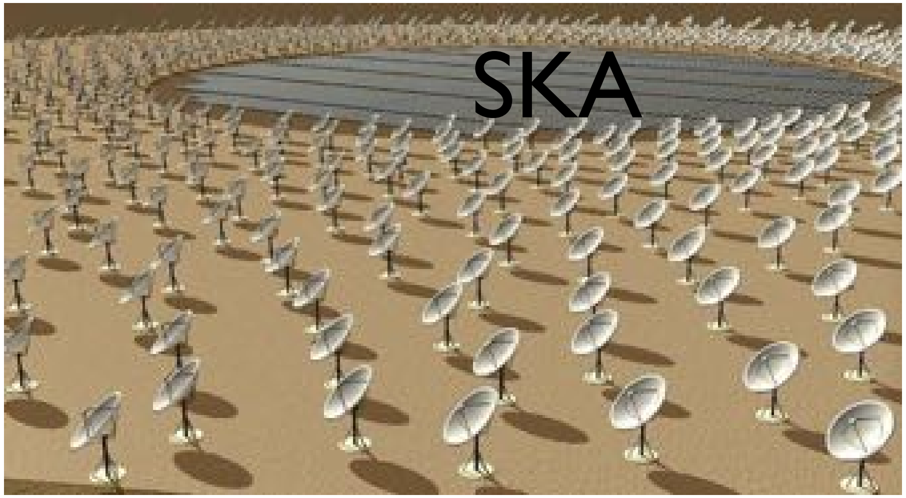

FAST & SKA?

PPTA search for scalar fuzzy DM

Parkes Pulsar Timing Array constraints on ultralight scalar-field dark matter

Nataliya K. Porayko,[1,*] Xingjiang Zhu,[2,3,4,†] Yuri Levin,[5,6,2] Lam Hui,[5] George Hobbs,[7] Aleksandra Grudskaya,[8] Konstantin Postnov,[8,9] Matthew Bailes,[10,4] N. D. Ramesh Bhat,[11] William Coles,[12] Shi Dai,[7] James Dempsey,[13] Michael J. Keith,[14] Matthew Kerr,[15] Michael Kramer,[1,14] Paul D. Lasky,[2,4] Richard N. Manchester,[7] Stefan Osłowski,[10] Aditya Parthasarathy,[10] Vikram Ravi,[16] Daniel J. Reardon,[10,4] Pablo A. Rosado,[10] Christopher J. Russell,[17] Ryan M. Shannon,[10,4] Renée Spiewak,[10] Willem van Straten,[18] Lawrence Toomey,[7] Jingbo Wang,[19] Linqing Wen,[3,4] and Xiaopeng You[20]
(The PPTA Collaboration)

1810.03227

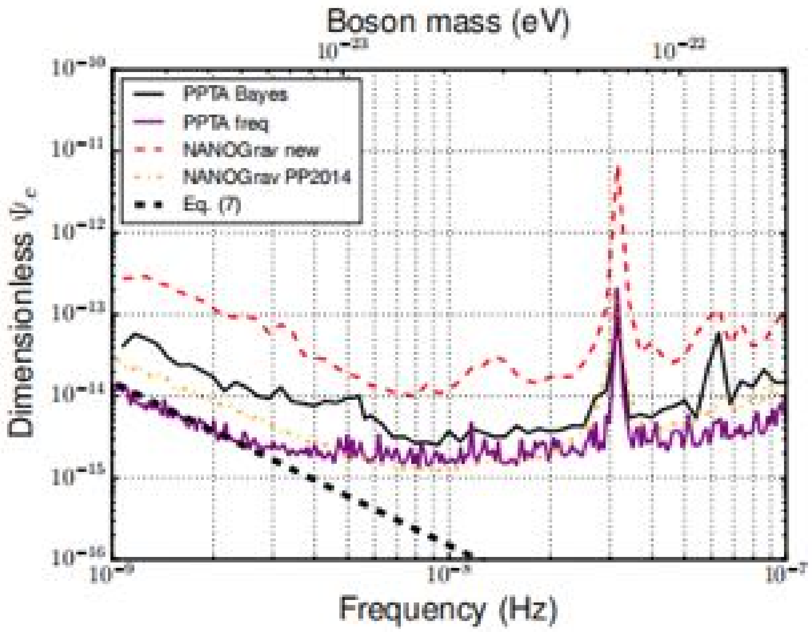

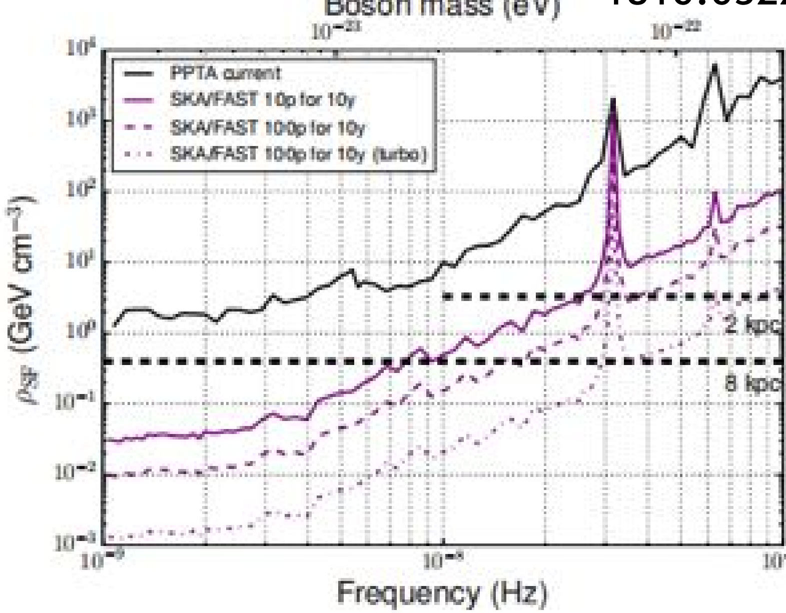

Future SKA can have much better results!

Effects of Gravity from ULDM

The gravitational potential of oscillating DM fields will alter the surrounding energy-momentum tensor, thereby changing the gravitational deflection of incoming electromagnetic pulses.

Scalar DM:

$$s(t) = \frac{\Psi_c}{\pi f} \sin(\alpha_e - \theta_p) \cos(2\pi f t + \alpha_e + \theta_p)$$

Vector DM:

$$\begin{aligned} R_V = & \; R_\Psi + R_h \\ = & \; \frac{h_{osc}}{\pi f} \left\{ \frac{1}{2} \left[(\hat{p} \cdot \hat{l})^2 + (\hat{p} \cdot \hat{n})^2 - 2(\hat{p} \cdot \hat{k})^2 \right] - \frac{1}{8} \right\} \\ & \; \sin(\alpha_e - \alpha_p) \cos(2\pi f t + \alpha_e + \alpha_p) \end{aligned}$$

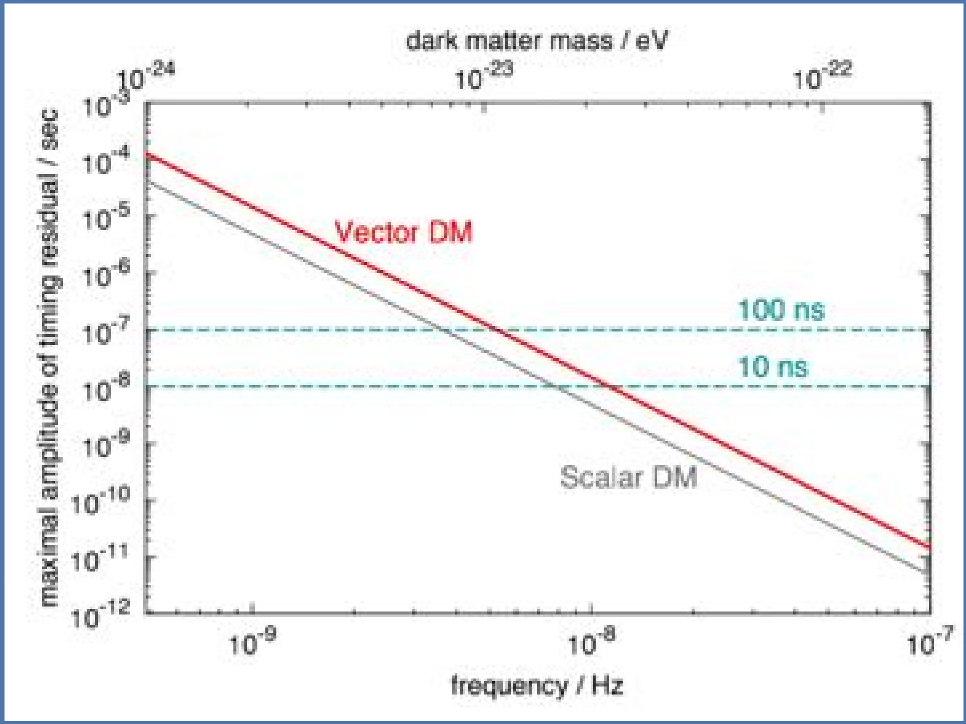

Effects of ULDM's Direct Coupling with Matter

ULDM can directly interact with matters to produce acceleration

$$a(t, x) \simeq \epsilon e \frac{q}{m} m_A A_0 \cos(m_A t - k \cdot x + \alpha(x)),$$

Change of pulsar timing series

Acceleration induce displacement

$$\Delta x(t, x) = -\frac{\epsilon e q}{m m_A} A_0 \cos(m_A t - k \cdot x + \alpha(x)).$$

(A) Completely uncorrelated: The phases and amplitudes of dark photon background for each pulsar are independent.

(B) Completely correlated: The phases are independent phases but with a common amplitude.

$$\Delta t^{(B)}_{\text{DPDM}} = -\frac{\epsilon e}{m_A}\left(\frac{q_p^{(B)}}{m_p} A_0{}^p \cos(m_A t + \alpha_p) - \frac{q_e^{(B)}}{m_e} A_0{}^e \cos(m_A t + \alpha_e)\right) \cdot n,$$

$$\Delta t^{(B-L)}_{\text{DPDM}} = -\frac{\epsilon e}{m_A}\left(\frac{q_p^{(B-L)}}{m_p} A_0{}^p \cos(m_A t + \alpha_p) - \frac{q_e^{(B-L)}}{m_e} A_0{}^e \cos(m_A t + \alpha_e)\right) \cdot n,$$

Parkes PTA data

Pulsars	N_{obs}	T(years)	$\overline{\sigma} \times 10^{-6}(s)$	$\log_{10} A_{SN}$	γ_{SN}	$\log_{10} A_{DM}$	γ_{DM}
J0437-4715	29262	15.03	0.296	$-15.76^{+0.17}_{-0.18}$	$6.63^{+0.17}_{-0.13}$	$-13.05^{+0.10}_{-0.08}$	$2.26^{+0.32}_{-0.44}$
J0613-0200	5920	14.20	2.504	$-14.63^{+0.77}_{-0.68}$	$4.93^{+1.33}_{-1.61}$	$-13.02^{+0.08}_{-0.08}$	$0.95^{+0.33}_{-0.31}$
J0711-6830	5547	14.21	6.197	$-12.85^{+0.14}_{-0.16}$	$0.97^{+0.64}_{-0.55}$	$-14.54^{+0.72}_{-0.89}$	$4.43^{+1.68}_{-1.72}$
J1017-7156	4053	7.77	1.577	$-12.89^{+0.07}_{-0.07}$	$0.54^{+0.53}_{-0.37}$	$-12.72^{+0.06}_{-0.06}$	$2.18^{+0.45}_{-0.44}$
J1022+1001	7656	14.20	5.514	$-12.79^{+0.12}_{-0.13}$	$0.54^{+0.55}_{-0.37}$	$-13.04^{+0.10}_{-0.12}$	$0.58^{+0.47}_{-0.36}$
J1024-0719	2643	14.09	4.361	$-14.28^{+0.27}_{-0.20}$	$6.51^{+0.35}_{-0.60}$	$-14.53^{+0.54}_{-0.56}$	$5.22^{+1.14}_{-1.18}$
J1045-4509	5611	14.15	9.186	$-12.75^{+0.24}_{-0.40}$	$1.58^{+1.28}_{-0.93}$	$-12.18^{+0.09}_{-0.08}$	$1.86^{+0.36}_{-0.32}$
J1125-6014	1407	12.34	1.981	$-12.64^{+0.11}_{-0.12}$	$0.51^{+0.55}_{-0.37}$	$-13.14^{+0.19}_{-0.21}$	$3.36^{+0.73}_{-0.66}$
J1446-4701	508	7.36	2.200	$-16.46^{+2.88}_{-3.17}$	$2.74^{+2.49}_{-1.89}$	$-13.49^{+0.32}_{-1.87}$	$2.48^{+1.92}_{-1.45}$
J1545-4550	1634	6.97	2.249	$-17.33^{+2.50}_{-2.55}$	$3.25^{+2.45}_{-2.18}$	$-13.40^{+0.24}_{-0.38}$	$3.90^{+1.61}_{-1.09}$
J1600-3053	7047	14.21	2.216	$-17.63^{+2.10}_{-2.29}$	$3.28^{+2.34}_{-2.15}$	$-13.27^{+0.12}_{-0.13}$	$2.79^{+0.43}_{-0.40}$
J1603-7202	5347	14.21	4.947	$-12.82^{+0.14}_{-0.16}$	$1.01^{+0.67}_{-0.60}$	$-12.66^{+0.10}_{-0.09}$	$1.44^{+0.40}_{-0.38}$
J1643-1224	5941	14.21	4.039	$-12.32^{+0.08}_{-0.09}$	$0.51^{+0.42}_{-0.34}$	$-12.27^{+0.07}_{-0.07}$	$0.55^{+0.32}_{-0.29}$
J1713+0747	7804	14.21	1.601	$-14.09^{+0.25}_{-0.38}$	$2.98^{+1.00}_{-0.64}$	$-13.35^{+0.08}_{-0.08}$	$0.53^{+0.32}_{-0.31}$
J1730-2304	4549	14.21	5.657	$-17.39^{+2.39}_{-2.51}$	$3.05^{+2.59}_{-2.12}$	$-14.11^{+0.40}_{-0.57}$	$4.22^{+1.42}_{-1.04}$
J1732-5049	807	7.23	7.031	$-16.51^{+3.04}_{-2.97}$	$3.29^{+2.37}_{-2.97}$	$-13.38^{+0.54}_{-0.84}$	$4.07^{+1.96}_{-1.93}$
J1744-1134	6717	14.21	2.251	$-13.39^{+0.14}_{-0.15}$	$1.49^{+0.66}_{-0.57}$	$-13.35^{+0.09}_{-0.09}$	$0.86^{+0.40}_{-0.33}$
J1824-2452A	2626	13.80	2.190	$-12.56^{+0.13}_{-0.12}$	$3.61^{+0.41}_{-0.39}$	$-12.18^{+0.11}_{-0.10}$	$1.64^{+0.46}_{-0.59}$
J1832-0836	326	5.40	1.430	$-16.47^{+2.63}_{-3.09}$	$3.66^{+2.33}_{-2.52}$	$-13.07^{+0.24}_{-0.63}$	$3.77^{+2.00}_{-1.05}$
J1857+0943	3840	14.21	5.564	$-14.76^{+0.74}_{-0.50}$	$5.75^{+0.91}_{-1.53}$	$-13.40^{+0.20}_{-0.25}$	$2.66^{+0.83}_{-0.67}$
J1909-3744	14627	14.21	0.672	$-13.60^{+0.13}_{-0.12}$	$1.60^{+0.43}_{-0.46}$	$-13.48^{+0.09}_{-0.08}$	$0.69^{+0.38}_{-0.35}$
J1939+2134	4941	14.09	0.468	$-14.38^{+0.22}_{-0.18}$	$6.24^{+0.49}_{-0.62}$	$-11.59^{+0.07}_{-0.07}$	$0.13^{+0.19}_{-0.10}$
J2124-3358	4941	14.21	8.863	$-14.79^{+0.82}_{-0.67}$	$5.07^{+1.37}_{-1.97}$	$-13.35^{+0.18}_{-0.33}$	$0.95^{+1.11}_{-0.66}$
J2129-5721	2879	13.88	3.496	$-15.48^{+1.92}_{-3.54}$	$2.91^{+2.29}_{-1.83}$	$-13.31^{+0.13}_{-0.14}$	$1.07^{+0.65}_{-0.65}$
J2145-0750	6867	14.09	5.086	$-12.82^{+0.10}_{-0.11}$	$0.62^{+0.50}_{-0.40}$	$-13.33^{+0.14}_{-0.16}$	$1.38^{+0.54}_{-0.55}$
J2241-5236	5224	8.20	0.830	$-13.40^{+0.09}_{-0.08}$	$0.44^{+0.40}_{-0.30}$	$-13.79^{+0.10}_{-0.10}$	$1.42^{+0.61}_{-0.59}$

64m Parkes telescope in Australia

Results from Parkes PTA in Australia

Results for ULDM $U(1)_B$ and ULDM $U(1)_{B-L}$

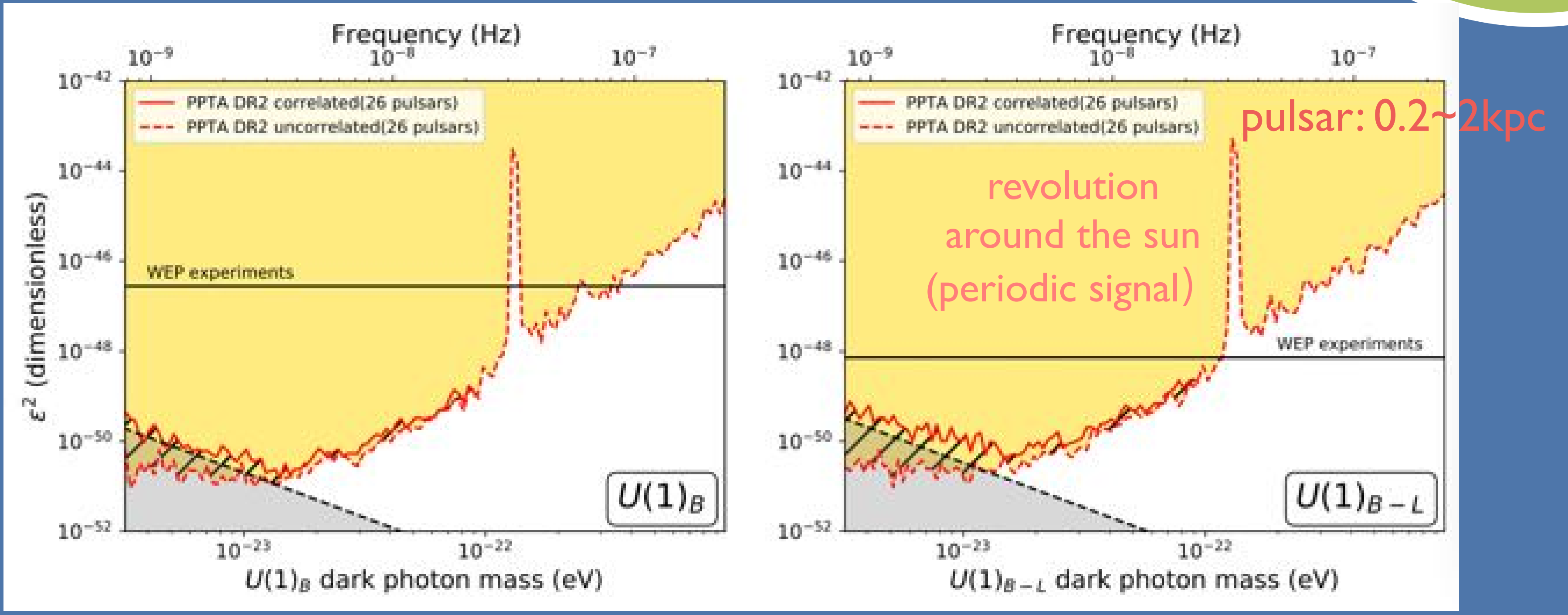

X. Xiao, Z-j. Xia, J. Shu., Q. Yuan, Y. Zhao, X-j. Zhu, with PPTA collaboration, Phys.Rev.Res. 4 (2022) 1, L012022

The best experiment test results up till now.

Gaia Stellar Position Measurements

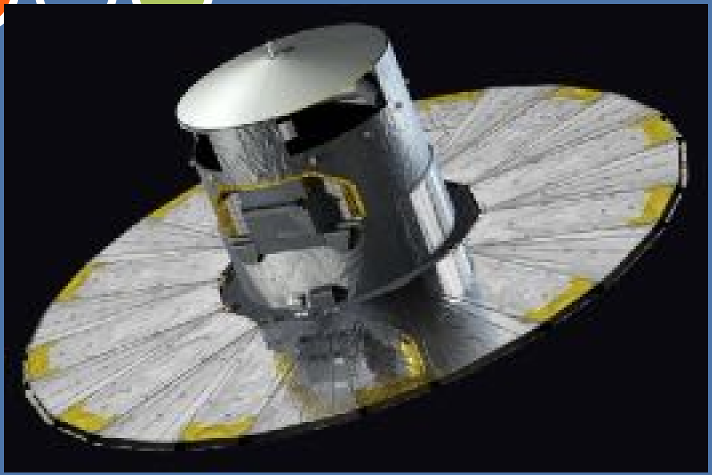

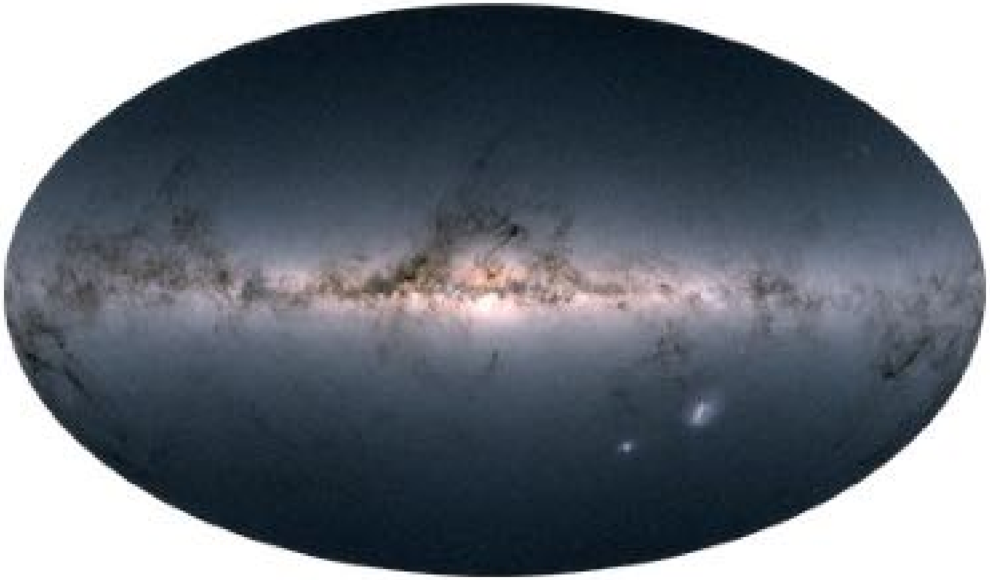

The Gaia satellite (launched in 2003) precisely measures the positions and velocities of ~1% of stars within the Milky Way (~10^9 stars).

Study the structure of the Milky Way, stellar evolution, new planets, fundamental physics, etc.

Bending the light

(Gaia Satellite) experiences a dragging effect under an ultralight DM background field.

$$a(t, x) \simeq \epsilon e \frac{q}{m} m_A A_0 \cos(m_A t - k \cdot x)$$

Acceleration causes periodic changes in velocity, leading to changes in the observed angle.

$$\Delta v(t, x) \simeq \epsilon e \frac{q}{m} A_0 \sin(m_A t - k \cdot x).$$

$$\Delta\theta \simeq -\Delta v \sin\theta$$

Lower precision in the radial direction.

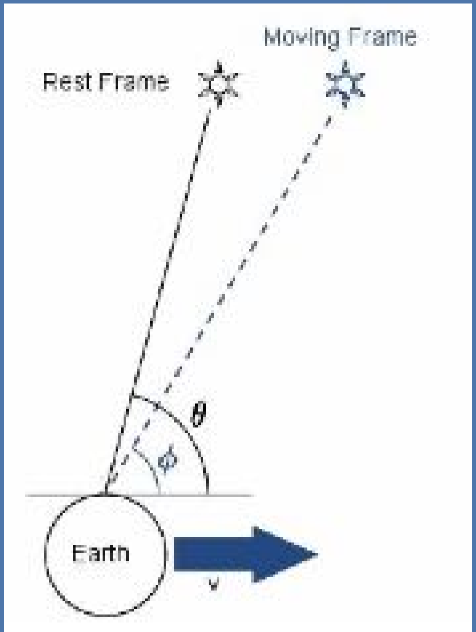

Global Periodically changes on star position

Neglecting star position changes

Search for ULDM with Gaia

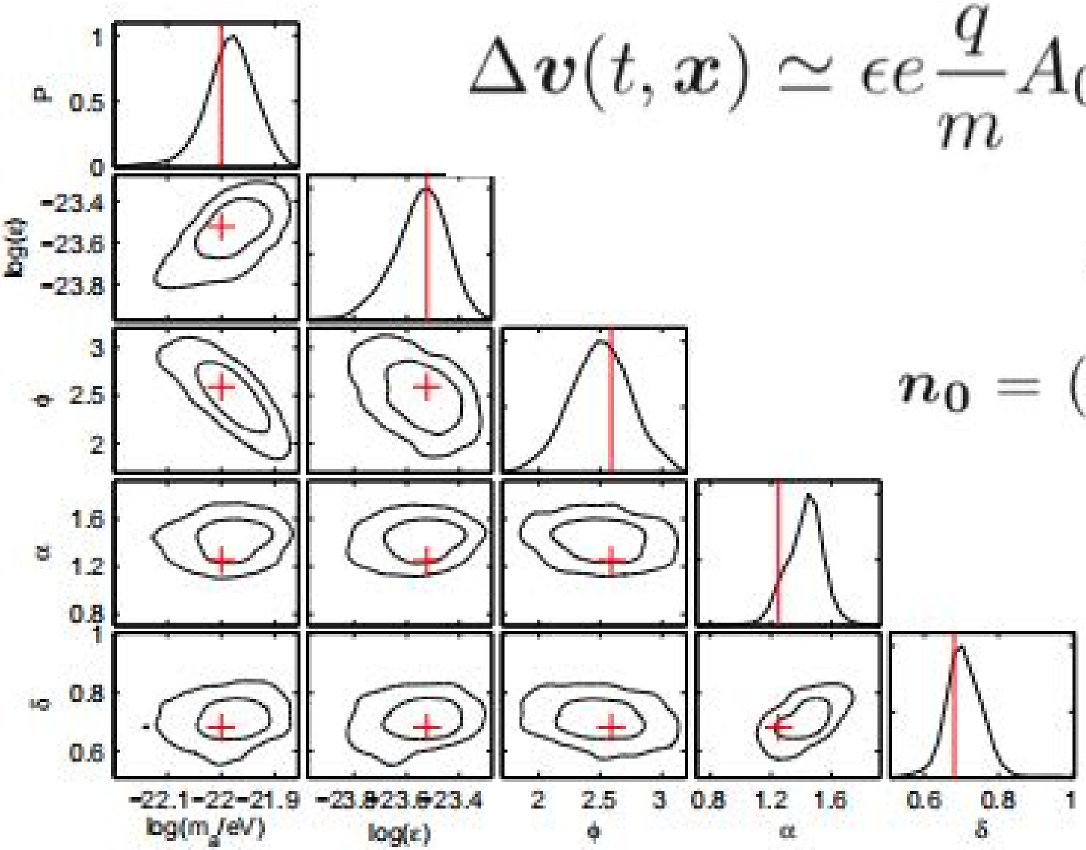

$$\Delta \boldsymbol{v}(t, \boldsymbol{x}) \simeq \epsilon e \frac{q}{m} A_0 \boldsymbol{n_0} \sin[m_A(t - t_0) + \phi],$$

equatorial coordinate (α, δ)

$$\boldsymbol{n}_0 = (\cos\delta\cos\alpha,\ \cos\delta\sin\alpha,\ \sin\delta),$$

Data Processing
Compression

$$\sigma = 100\ \mu\text{as}/\sqrt{10^5}.$$

mock data

H-k. Guo, Y-q. Ma, J. Shu., X. Xiao, Q. Yuan, Y. Zhao, JCAP 1905 (2019) 015

$$(m_A, \epsilon, \phi, \alpha, \delta) = (10^{-22}\ \text{eV}, 3\times 10^{-24}, 2.59, 1.25, 0.68).$$

Search for ULDM with Gaia

95% C.L. Exclusion Line (Expected Value)

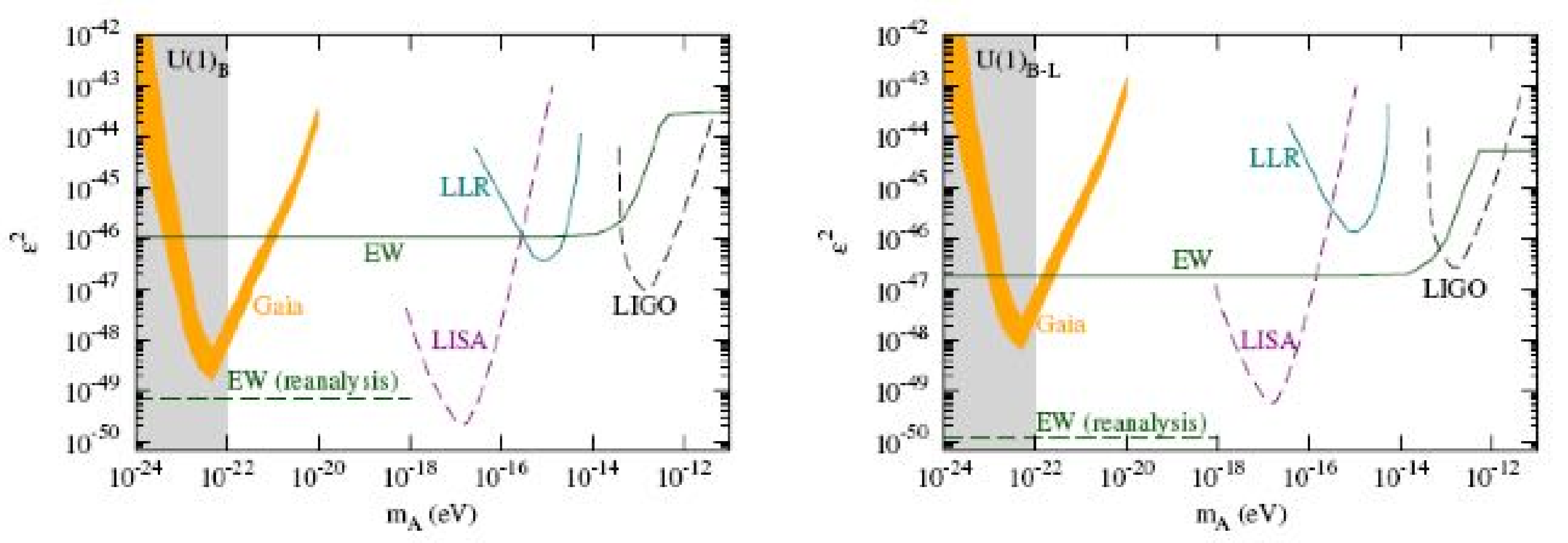

H-k. Guo, Y-q. Ma, J. Shu., X. Xiao, Q. Yuan, Y. Zhao, JCAP 1905 (2019) 015

Gaia's 2025 data release includes temporal variations, which can be used for actual measurements.

M87* Black Hole Polarization Observations

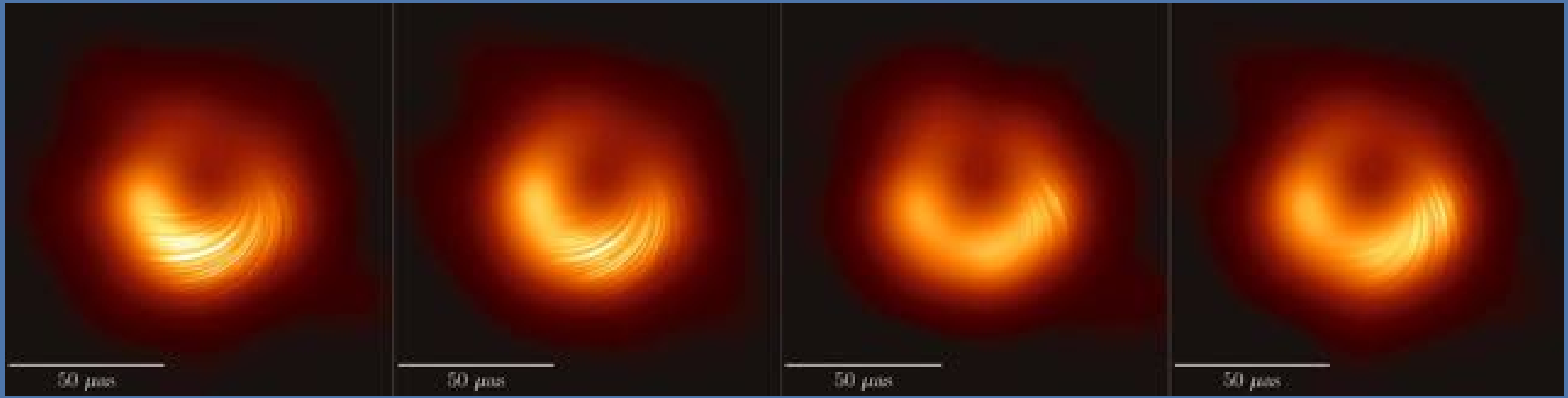

4 days of polarimetry observation of *M87**

Event Horizon Telescope

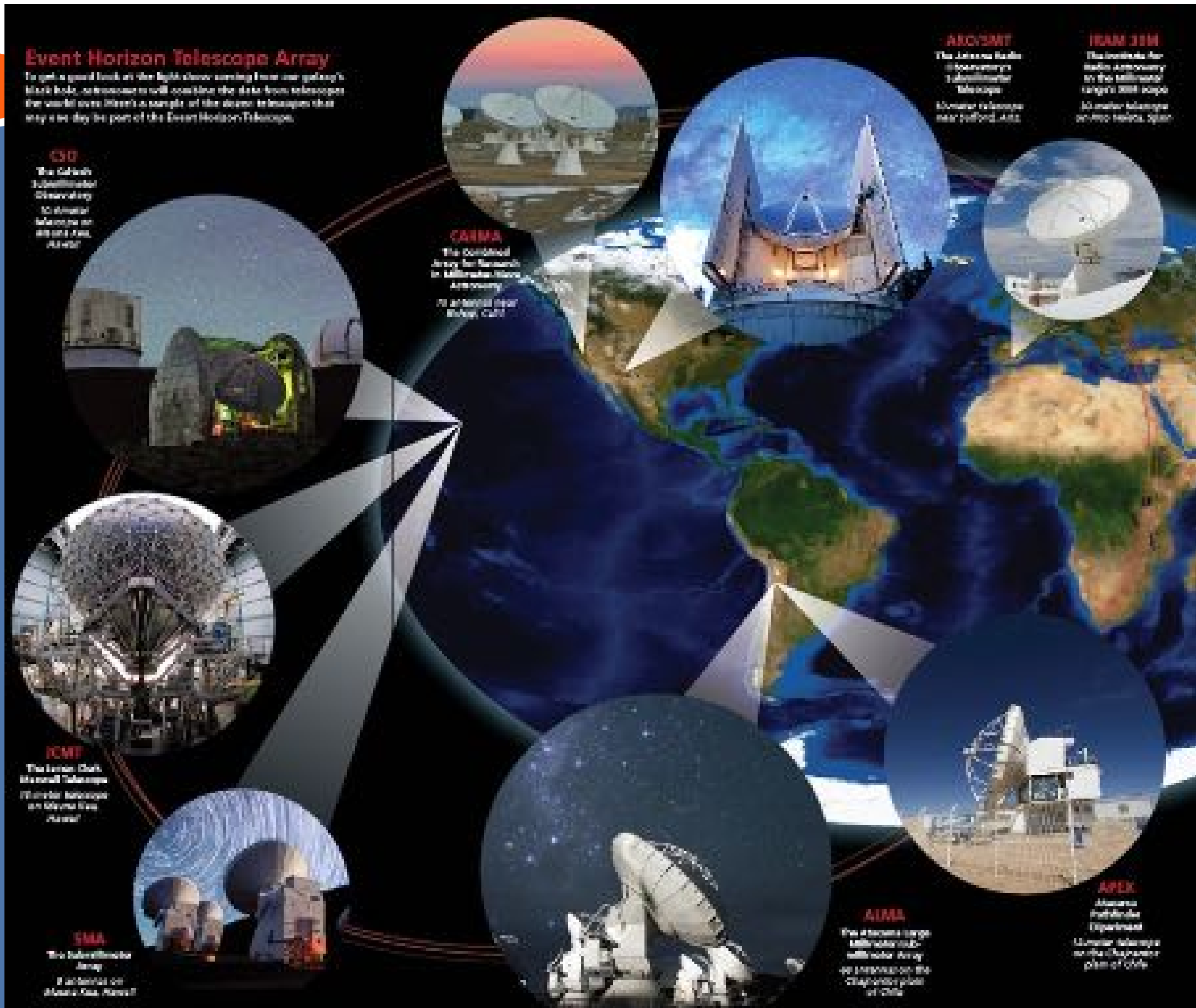

Western Hemisphere mm-Wave Telescope Array

mm-Wave Band is Suitable for Precise Polarization Angle Measurements

Axion-Electromagnetic Equation

Axion-induced bi-refringence effect

$$\mathcal{L} = -\frac{1}{4}F_{\mu\nu}F^{\mu\nu} - \frac{1}{2}g_{a\gamma}aF_{\mu\nu}\tilde{F}^{\mu\nu} + \frac{1}{2}\nabla^{\mu}a\nabla_{\mu}a - V(a),$$

$$\nabla\cdot\boldsymbol{E} = g\nabla\varphi\cdot\boldsymbol{B}, \quad \nabla\times\boldsymbol{E} + \frac{\partial\boldsymbol{B}}{\partial t} = 0,$$

$$\nabla\times\boldsymbol{B} - \frac{\partial\boldsymbol{E}}{\partial t} = g\left(\boldsymbol{E}\times\nabla\varphi - \boldsymbol{B}\frac{\partial\varphi}{\partial t}\right),$$

$$\nabla\cdot\boldsymbol{B} = 0,$$

$$\Box\varphi = \frac{\partial^2\varphi}{\partial t^2} - \nabla^2\varphi = -g\boldsymbol{E}\cdot\boldsymbol{B}.$$

The CP-odd axion field affects the phase velocity of left and right circularly polarized electromagnetic waves.

Maxwell's equations with axion field

Bi-refringence Effect

Axion-induced bi-refringence effect

$$\Box A_{\pm} = \pm 2 i g_{a\gamma}[\partial_z a \dot{A}_{\pm} - \dot{a}\partial_z A_{\pm}],$$

$$\omega_{\pm} \approx k \pm \tfrac{1}{2} g\left(\frac{\partial\varphi}{\partial t} + \nabla\varphi\cdot\frac{\boldsymbol{k}}{k}\right)$$

different phase velocities for +/- helicities

For linear-polarized photons

$$\begin{aligned}\Delta\Theta &= g_{a\gamma}\Delta a(t_{\rm obs}, \mathbf{x}_{\rm obs}; t_{\rm emit}, \mathbf{x}_{\rm emit}) \\ &= g_{a\gamma}\int_{\rm emit}^{\rm obs} ds\ n^{\mu}\ \partial_{\mu}a \\ &= g_{a\gamma}[a(t_{\rm obs}, \mathbf{x}_{\rm obs}) - a(t_{\rm emit}, \mathbf{x}_{\rm emit})],\end{aligned}$$

The polarization angle shift is the difference between the initial and final expectation values of the axion field.

Therefore, precise measurements of the polarization angle is needed.

Superradiance

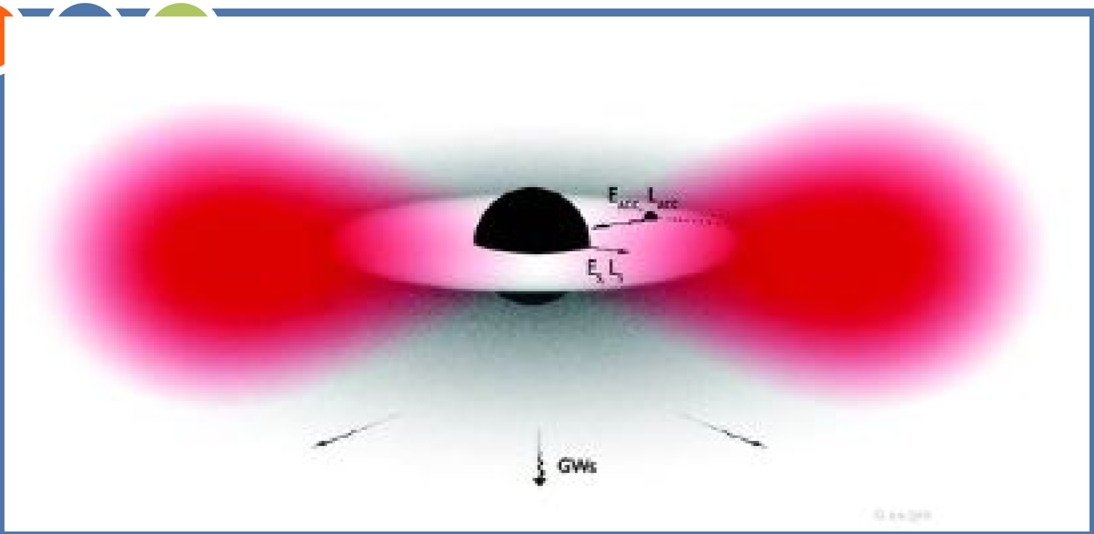

Superradiance condition

$$\omega < \omega_c = \frac{a_J m}{2r_+}$$

Effective Frequency range for Superradiance: when the axion wavelength is comparable to the black hole's event horizon.

$$\frac{r_g}{\lambda_C} = \mu M \equiv \alpha \in (0.1, 1),$$

Rapidly rotating black holes lose energy and angular momentum by radiating axion fields.

Axion cloud induced near the black hole

The energy of the axion cloud could be comparable to that of the black hole.

Superradiance Field Equation Solution

Axion Could

K-G equation solution under kerr background

Similar to hydrogen atom energy level (non-relativistic):

$$a(x^\mu) = e^{-i\omega t} e^{im\phi} S_{lm}(\theta) R_{lm}(r)$$

$$\alpha \equiv \mu M$$

$$\mathrm{Re}(\omega) \simeq \left(1 - \frac{\alpha^2}{2\bar{n}^2}\right)\mu$$

Reduce to spherical harmonics Y_{lm} in the non-relativistic limit.

The imaginary part of the field provides superradiance conditions.

Axion cloud production is more effective in lower l-modes

Black Hole Superradiance

Radial Solution

$$r_\pm = r_g\left(1 \pm \sqrt{1 - a_J^2}\right)$$

The brightest position of the electromagnetic radiation ring observed by EHT is approximately where the radial solution reaches its maximum.

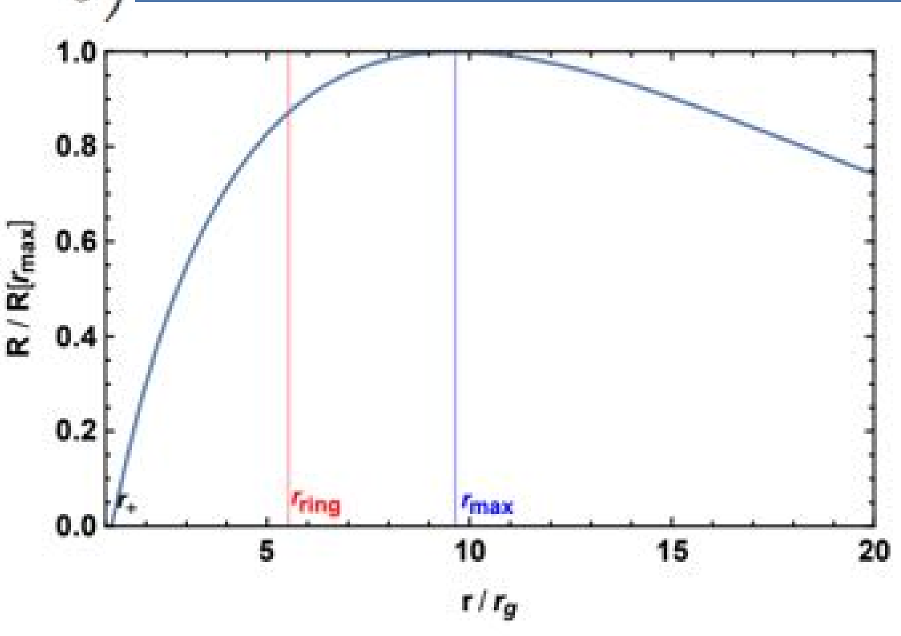

Y-f. Chen, J. Shu., X. Xiao, Q. Yuan, Y. Zhao, Phys.Rev.Lett. 124 (2020) 061102

Self-Interaction of Axion Cloud

Besides gravity, the self-interaction of ultralight DM field matters.

$$S = \int d^4x\sqrt{-g}[-\frac{1}{2}(\nabla a)^2 - \mu^2 f_a^2(1-\cos\frac{a}{f_a})]$$

Ansatz: $$a = \frac{1}{\sqrt{2\mu}}(e^{-i\mu t}\psi + e^{i\mu t}\psi^*)$$

Simulation results suggest that axion clouds can stably exist.

Gravity potential

$$S_{\rm NR} = \int d^4x \left(i\psi^*\partial_t\psi - \frac{1}{2\mu}\partial_i\psi\partial_i\psi^* - \frac{\alpha}{r}\psi^*\psi + \frac{(\psi^*\psi)^2}{16f_a^2}\right)$$

Self-interaction

Position angle change

We use $a_0 \approx f_a$ and $\omega \approx \mu$

Neglect the axion field near earth

$$\Delta\Theta_{\max} \simeq -b g_{a\gamma} f_a \cos\left[\mu t_{\rm emit} + \beta(|\mathbf{x}_{\rm emit}| = r_{\max})\right],$$

$$b \equiv a_{max}/f_a$$

$$\Delta\Theta(t, r, \theta, \phi) \approx -\frac{b g_{a\gamma} f_a R_{11}(r)}{R_{11}(r_{\max})} \sin\theta \cos\left[\omega t - m\phi\right]. \quad (17)$$

Spatial and temporal resolution

$$g_{a\gamma} \equiv \frac{c}{2\pi f_a} \equiv \frac{c_\gamma \alpha_{em}}{4\pi f_a},$$

fermion loop $\quad c_\gamma \sim NQ^2.$

clockwork $\quad c_\gamma \sim 2Q^2 q^{N-M}.$

Huge

Expected Limit

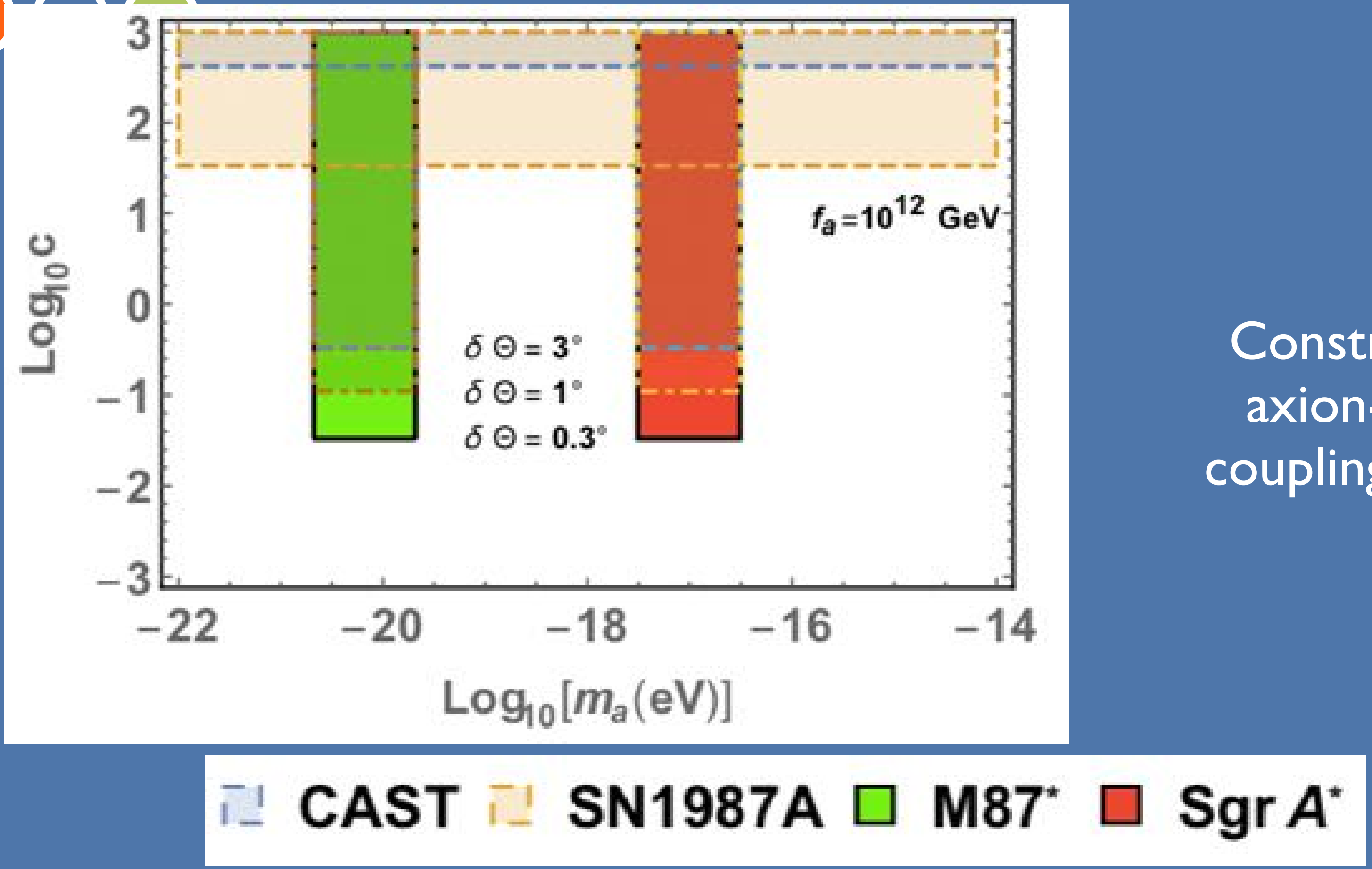

Constraints on axion-photon coupling strength

Y-f. Chen, J. Shu., X. Xiao, Q. Yuan, Y. Zhao, Phys.Rev.Lett. 124 (2020) 061102

Polarization Parameters

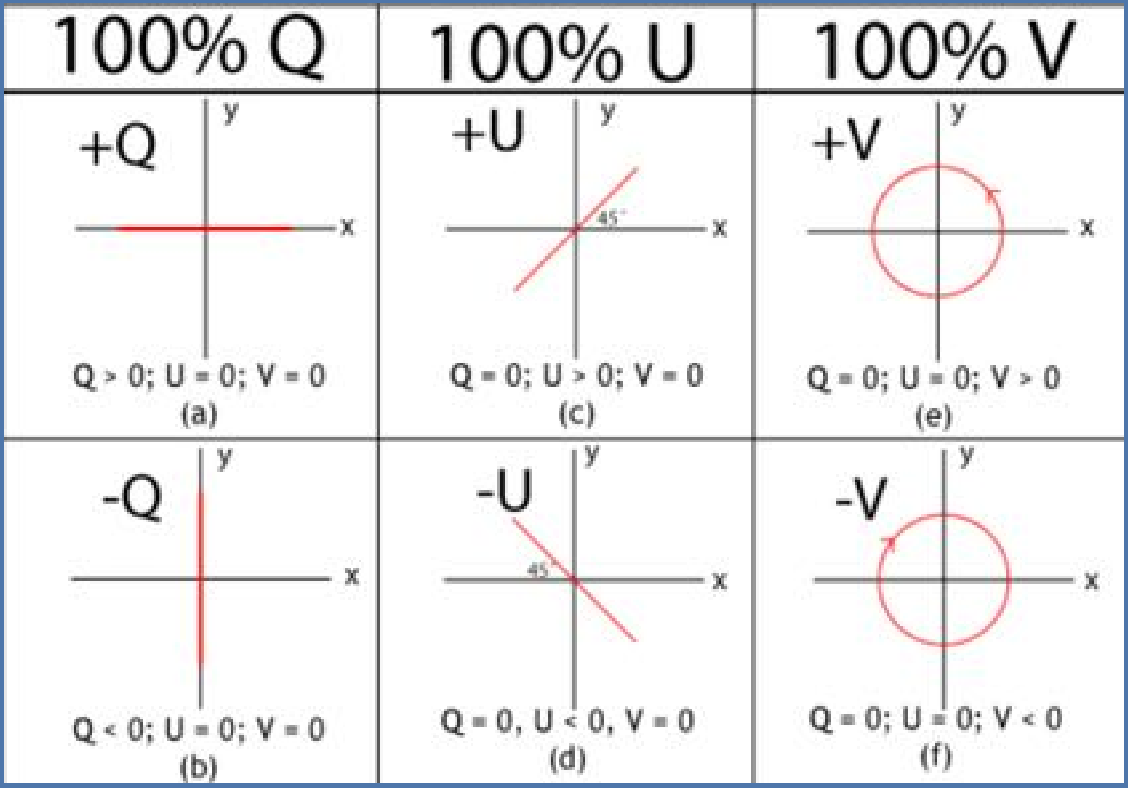

4 Stokes parameters
(I, Q, U,V):

I: total intensity;
Q, U: linear polarization;
V: circular polarization.

Radiative Transfer

$$\frac{d}{ds}\begin{pmatrix} I \\ Q \\ U \\ V \end{pmatrix} = \begin{pmatrix} j_I \\ j_Q \\ j_U \\ j_V \end{pmatrix} - \begin{pmatrix} \alpha_I & \alpha_Q & \alpha_U & \alpha_V \\ \alpha_Q & \alpha_I & \rho_V & \rho_U \\ \alpha_U & -\rho_V & \alpha_I & \rho_Q \\ \alpha_V & -\rho_U & -\rho_Q & \alpha_I \end{pmatrix} \begin{pmatrix} I \\ Q \\ U \\ V \end{pmatrix}$$

Considering curved spacetime and plasma effects, we use Stokes parameters for radiative transformation. The axion birefringence effect is similar to the Faraday rotation effect (without periodic time variation).

$$\rho_V = \rho_V^{\mathrm{FR}} - 2g_{a\gamma}\frac{da}{ds},$$

EVPA $$\chi \equiv \frac{1}{2}\arg(Q + iU).$$

Change of EVPA

RIAF model

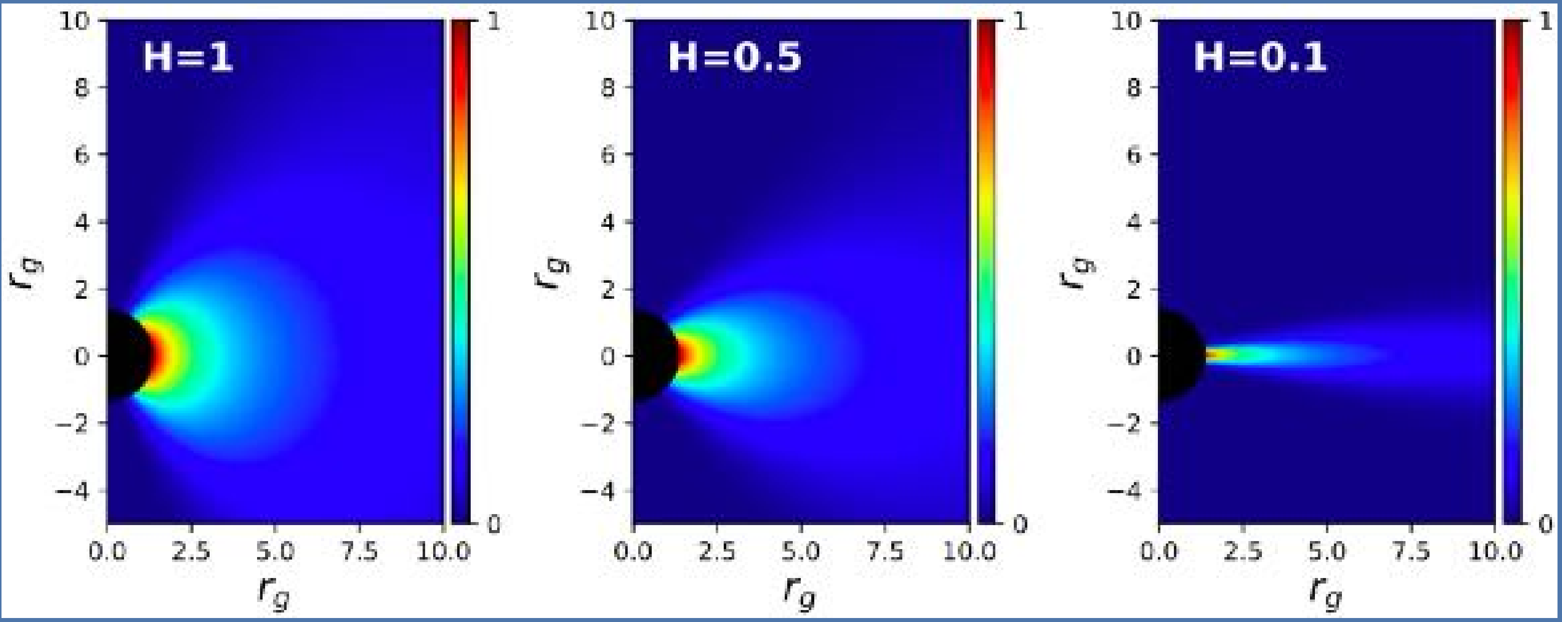

Color indicate the electron number density

H stands for the average thickness of the accretion disk

RIAF Model, thin accretion disk give smaller background

Demonstration

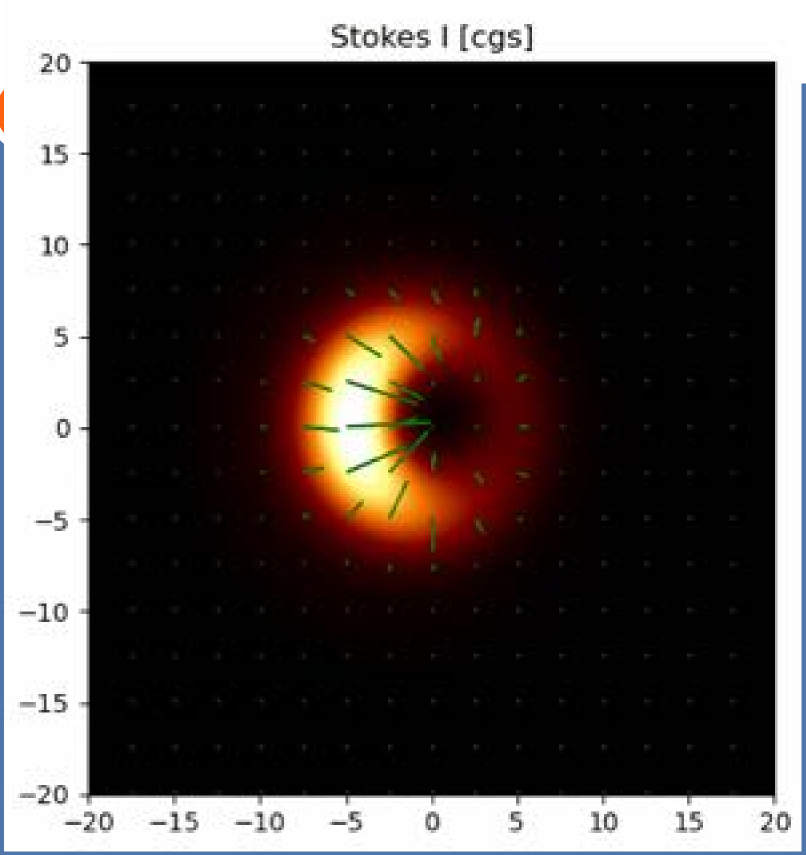

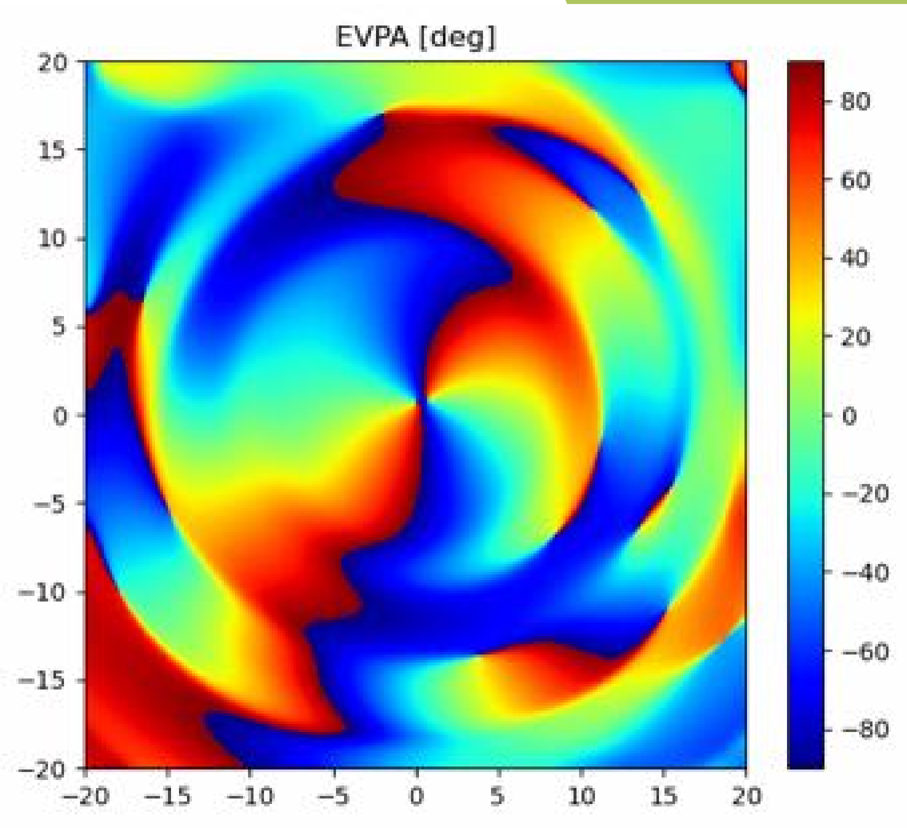

Numerical results from analytical RIAF model

Y-f. Chen, Y-x. Liu, R-s. Lu, Y. Mizauno, J. Shu., X. Xiao, Q. Yuan, Y. Zhao, Nature Astronomy

EHT's Observation

Polarization Data released on March, 2021

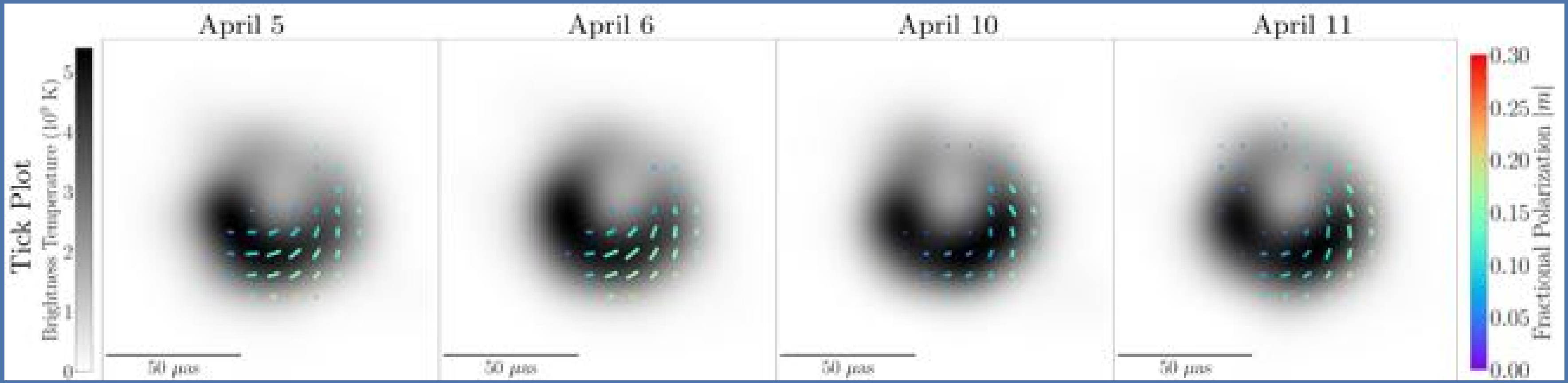

4 days of Polarization Data

Results

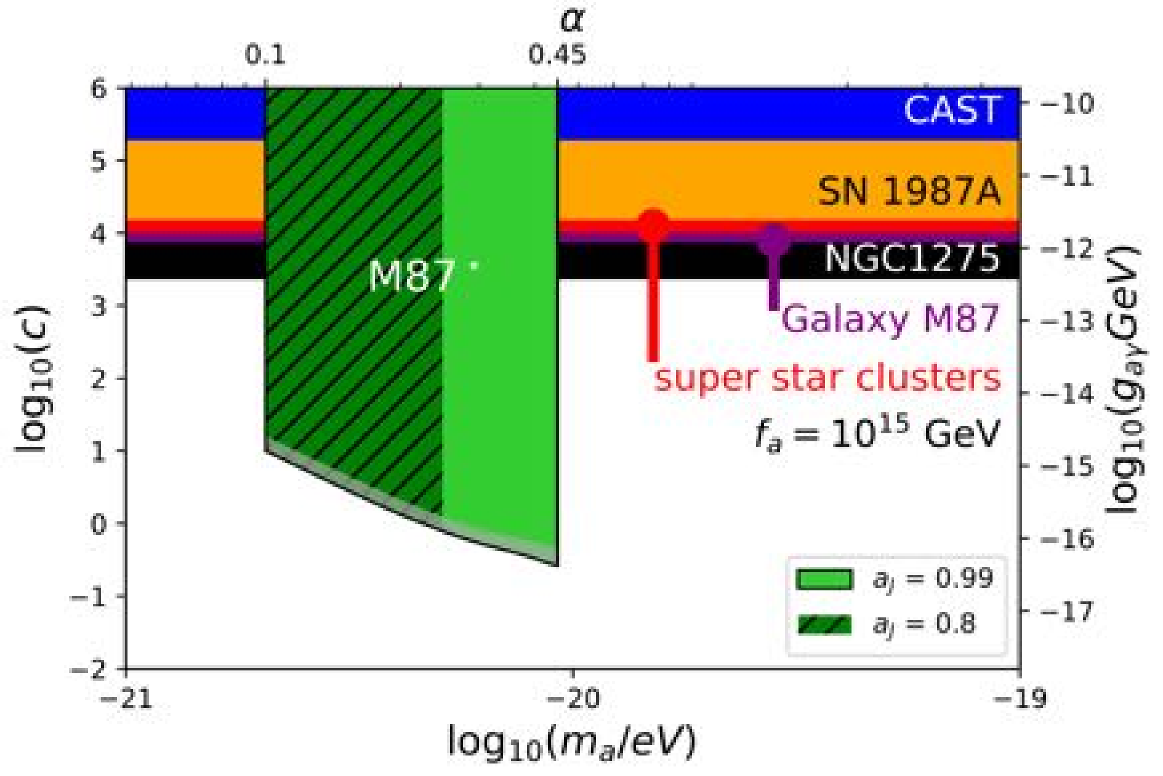

Smaller mass,
longer wavelength,
longer period.

Long periods, with smaller amplitude changes over four days of subtraction, reducing sensitivity.

Y-f. Chen, Y-x. Liu, R-s. Lu, Y. Mizuno, J. Shu., X. Xiao, Q. Yuan, Y. Zhao, Nature Astronomy 2022

Current status

- Axon dark matter detection competition :
  - Traditional resonant cavity: ADMX, CAPP, HAYSTACK
  - LC circuit: DM Radio, ABRACADABRA
  - Nuclear Magnetic Resonance: CASPER, Spin amplifier (USTC) …

- The main experimental limits come from the resonant cavity, CAST, and stellar cooling.

A huge parameter space to be explored!

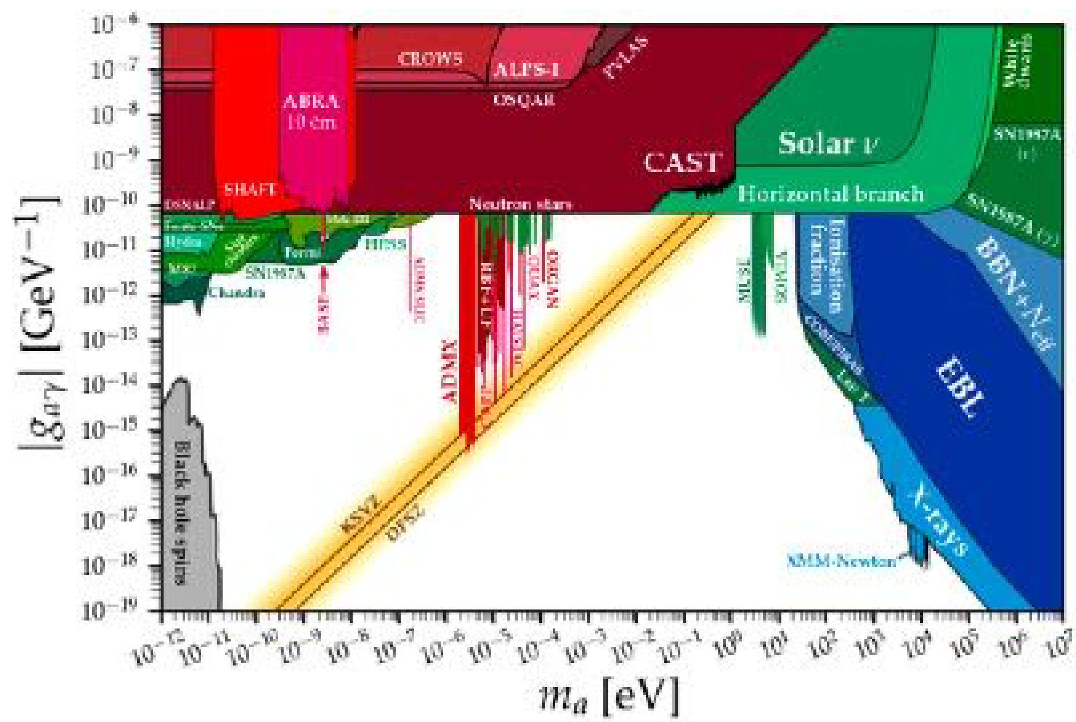

Inverse Primakoff Effect

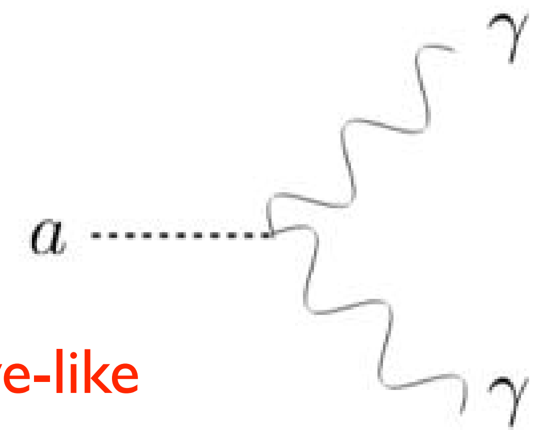

Wave-like dark matter

Under strong magnetic field background

$$\nabla \times \mathbf{B} \simeq \partial_t \mathbf{E} + \mathbf{J} + g_{a\gamma\gamma} \mathbf{B}\, \partial_t a$$

Axion dark matter induces an effective current under strong magnetic field.

$$J_{\rm eff}(t) \sim g_{a\gamma\gamma} B_0(t) \sqrt{\rho_{\rm DM}} \cos m_a t$$

Cavity with static B field

$$\left(\partial_t^2 + \frac{m_a}{Q_1}\partial_t + m_a^2\right)\mathbf{E}_1 \sim m_a \cos m_a t$$

$$Q_a \sim 10^6$$

Quantum amplifier to readout the signal.

$$m_a \sim \mathrm{GHz} \sim 10^{-6}\,\mathrm{eV}$$

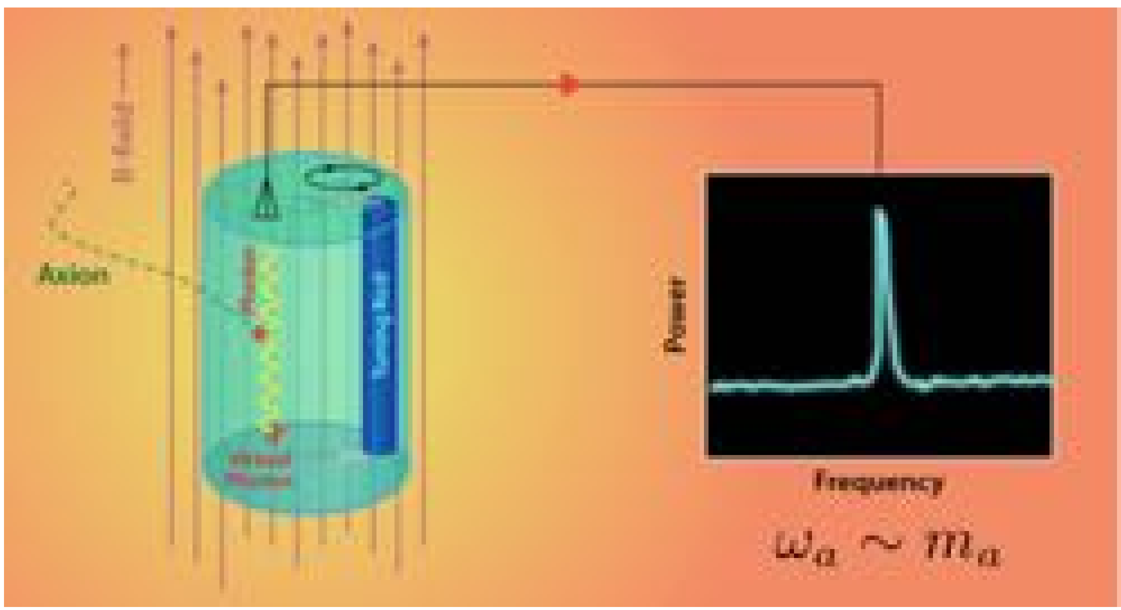

Cavity size ~ (axion mass)^-1

Signal power decreases with axion mass

e.g. ADMX, HAYSTACK

Resonant EM detection of axion dark matter

Cavity mode equation

Source: **a**
(almost monochromatic)

$$\sum_n \left(\partial_t^2 + \frac{\omega_n}{Q_n}\partial_t + \omega_n^2\right)\mathbf{E}_n = g_{a\gamma\gamma}\partial_t(\mathbf{B}\partial_t a)$$

Signal Mode: $\mathbf{E}_n$

Pump Mode: **B**

- Traditional resonant detection matches axion mass with the resonant frequency by using a static B field.

$$\omega_1 \simeq m_a \qquad \partial_t(\mathbf{B}) \simeq 0$$

$$\left(\partial_t^2 + \frac{m_a}{Q_1}\partial_t + m_a^2\right)\mathbf{E}_1 = g_{a\gamma\gamma}\mathbf{B}\sqrt{\rho_{\rm DM}}\, m_a \cos m_a t$$

LC Circuit with static B field

- Resonant conversion happens when

$$m_a = \omega = \frac{1}{\sqrt{LC}}$$

- Scan the mass from 100 Hz to 100 MHz by tuning the capacitor C

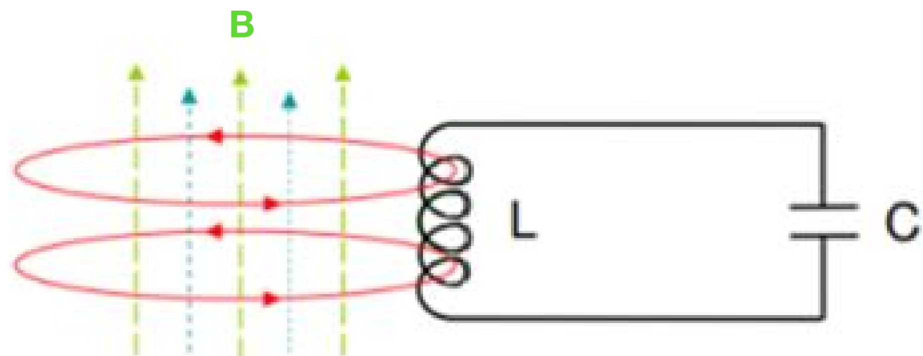

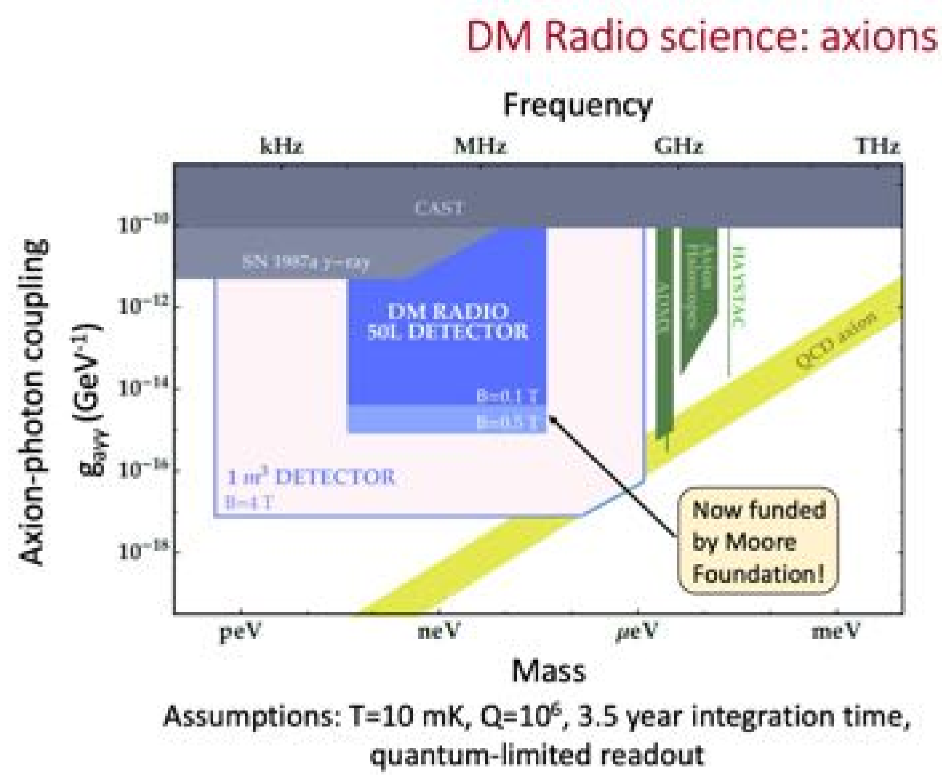

e.g. DM radio, ADMX-SLIC

Broadband Detection

- ABRACADABRA: no capacitor, **simultaneous scan of broad frequencies using SQUID**. [Y.Kahn, B. Safdi, J. Thaler 16']

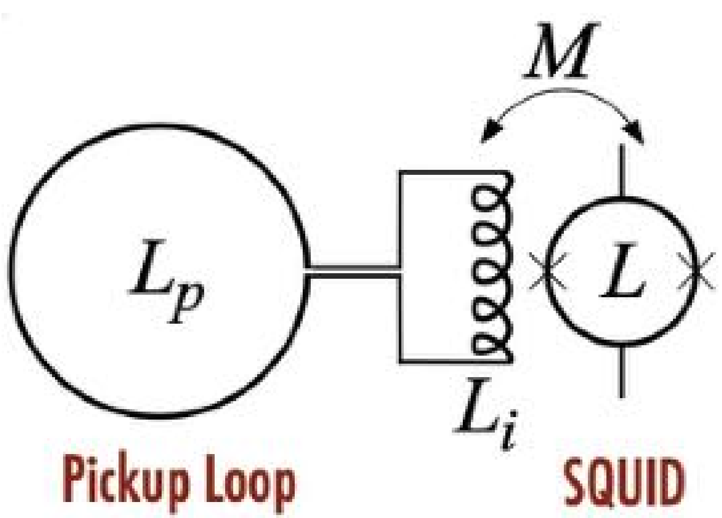

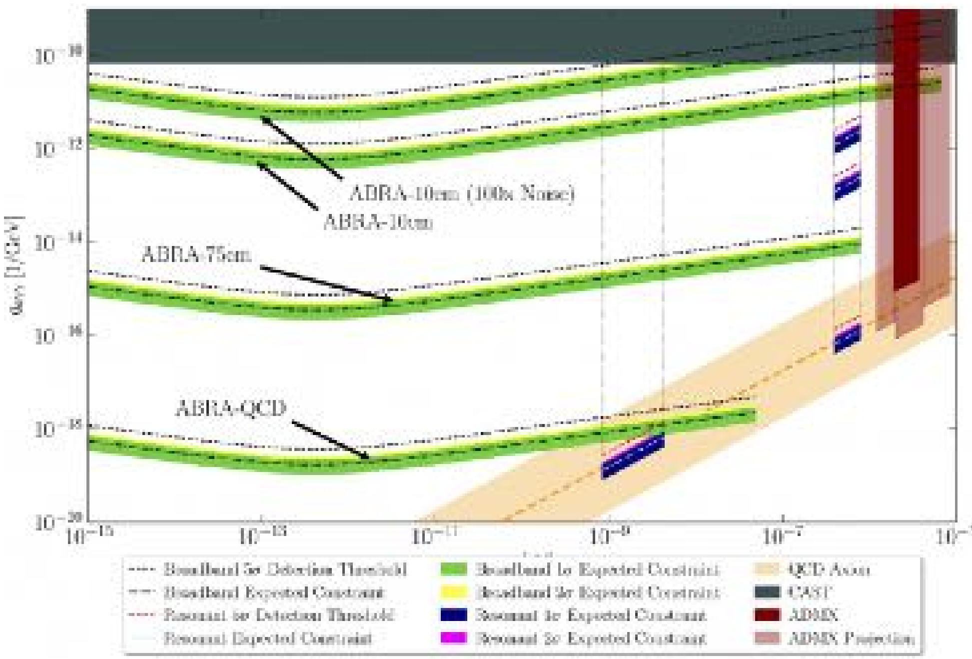

Higher Frequency Electromagnetic Resonant Detection

1
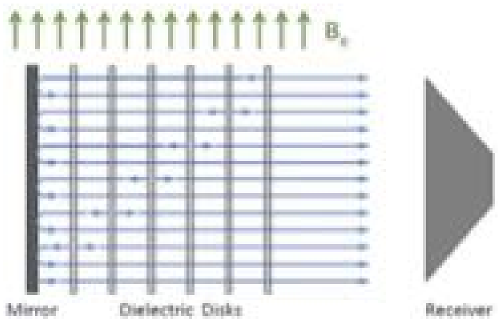

2
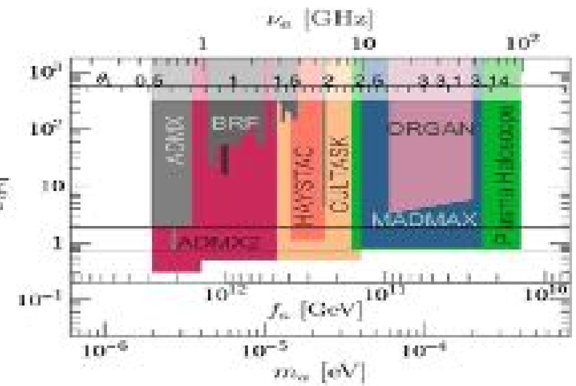

3
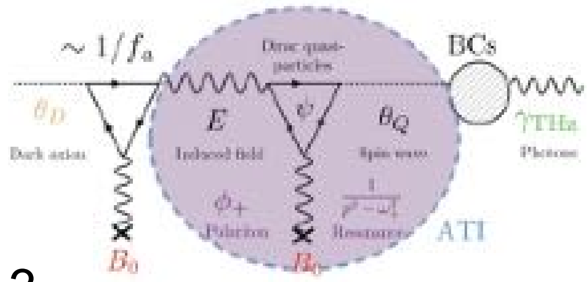

- 1 **Dielectric Haloscope**: discontinuity of E-field leads to coherent emission of photons from each surface, up to 50 GHz. [A.Caldwell et al 17']

- **2.Plasma Haloscope**: using tunable cryogenic plasma to match axion mass, up to 100 GHz. [M.Lawson et al 19']

- **3.Topological Insulator**: quasiparticle in it mixing with E field becomes polariton whose frequency can be tuned by magnetic field, up to THz. [D.J.E.Marsh et al 19']

Birefringent effect

Axion induced birefringent effect

$$\Box A_\pm = \pm 2 i g_{a\gamma} [\partial_z a \dot{A}_\pm - \dot{a} \partial_z A_\pm],$$

$$\omega_\pm \approx k \pm \tfrac{1}{2} g \left(\frac{\partial \varphi}{\partial t} + \nabla \varphi \cdot \frac{\boldsymbol{k}}{k} \right)$$

different phase velocities for +/- helicities

For linearly polarized photons

$$\begin{aligned} \Delta\Theta &= g_{a\gamma} \Delta a(t_{\rm obs}, \mathbf{x}_{\rm obs}; t_{\rm emit}, \mathbf{x}_{\rm emit}) \\ &= g_{a\gamma} \int_{\rm emit}^{\rm obs} ds\ n^\mu\ \partial_\mu a \\ &= g_{a\gamma} [a(t_{\rm obs}, \mathbf{x}_{\rm obs}) - a(t_{\rm emit}, \mathbf{x}_{\rm emit})], \end{aligned}$$

Measure the change of the position angle:

Requires polarimetric measurements

GW Interferometers and Birefringent Cavity

- Interferometer: using vertically polarized laser and measuring the horizontal component, resonant when baseline matches λ_c. [DeRocco, Hook 18']

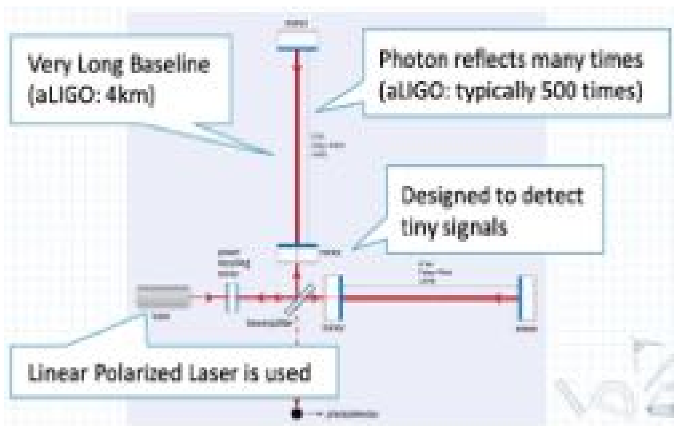

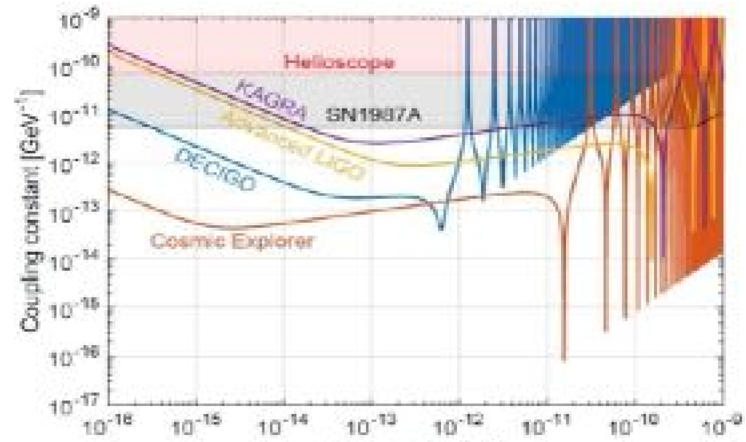

- Birefringent cavity: using mirror to accumulate the axion induced sideband. [Liu, Elwood et al 18']

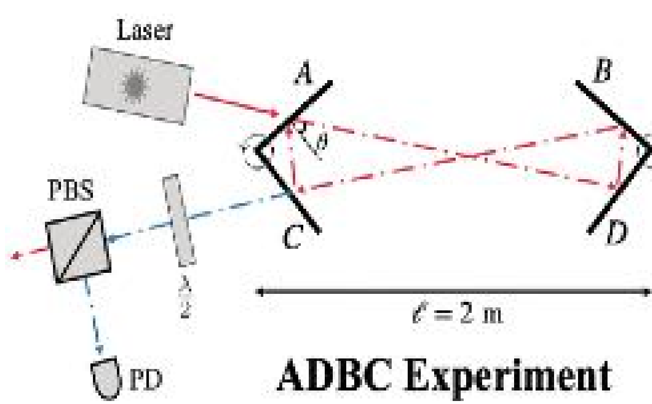

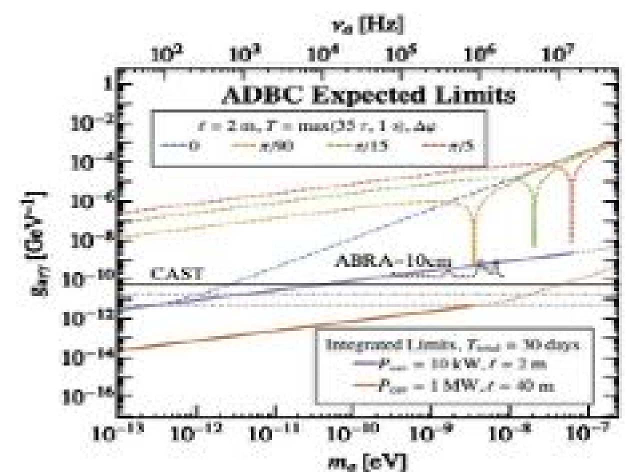

Light Shining Through Walls [Redondo, Ringwald 10']

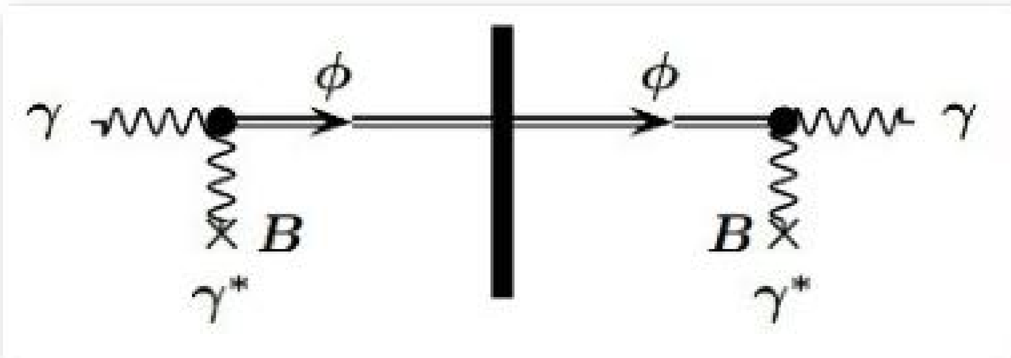

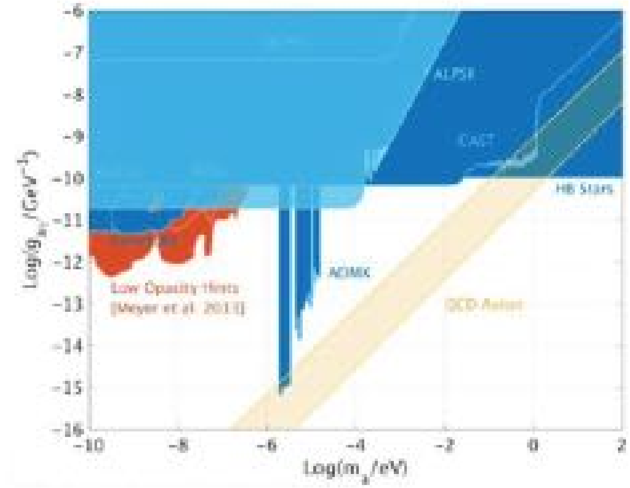

- Photons **convert into axions in B field, pass through a wall and convert back into photons.**

- Both optical and SRF cavity [Janish et al 19'].

- Not dependent on if axion is the major dark matter.

Nuclear Magnetic Resonance [Budker, Graham et al 13']

- **CASPEr Electric**: axion gluon coupling leads to oscillating EDM.
- **CASPEr-Wind:** axion nucleons coupling ~ **$\nabla a \cdot \sigma_N$ leads to precession of the spin, proportional to axion DM velocity (wind).**

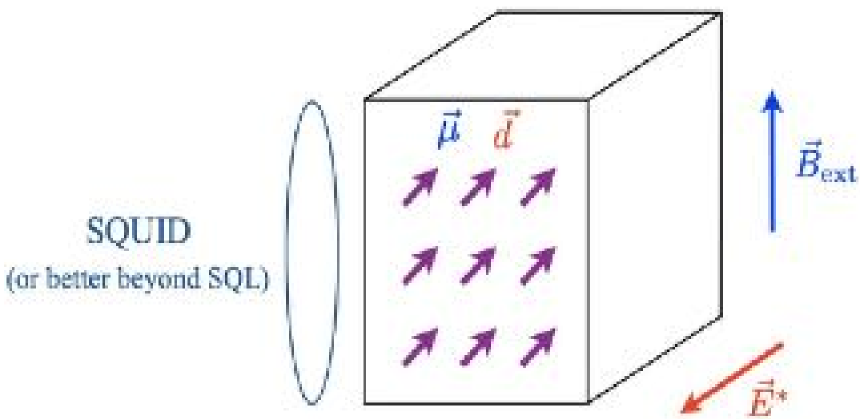

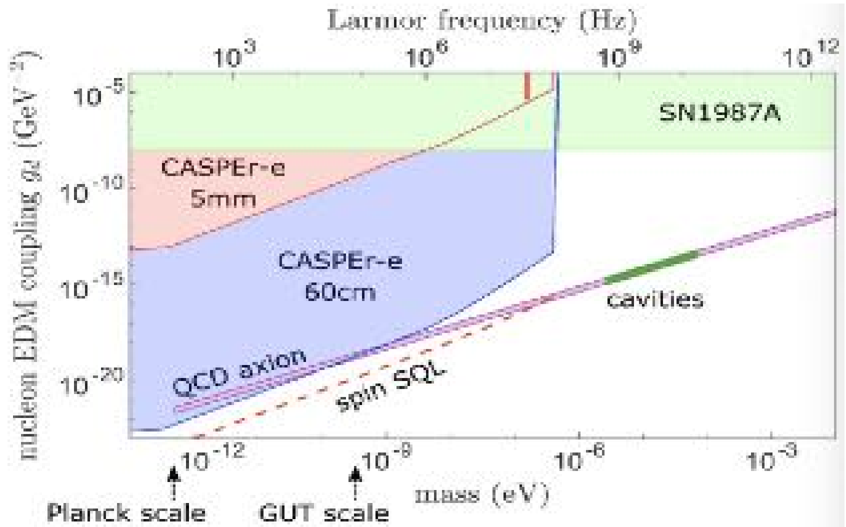

Larmor frequency $2\,\mu B_{ext} = m_a$ leads to NMR-like resonant enhancement.

Axion-Induced Fifth Force [Moody, Wilczek, 84']

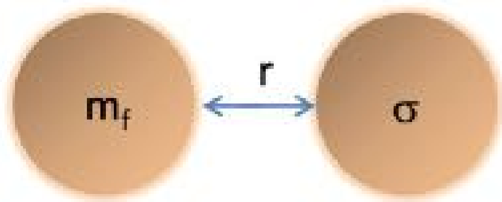

Monopole-Dipole axion exchange

Axion-mediated **monopole-dipole interaction** between nucleons:

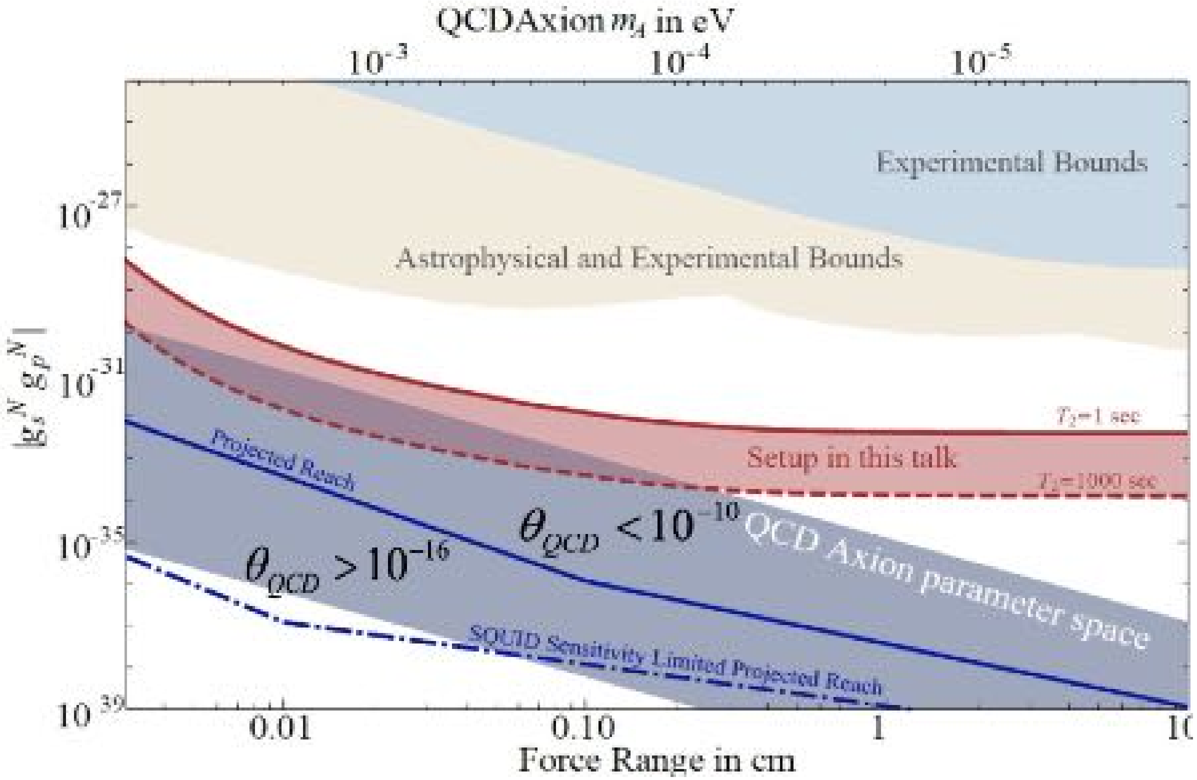

[ARIADNE 14']

SRF with AC B field

Signal Mode: $\mathbf{E_1}$

Source: **a**
(almost monochromatic)

$$\sum_n \left(\partial_t^2 + \frac{\omega_n}{Q_n}\partial_t + \omega_n^2 \right) \mathbf{E}_n = g_{a\gamma\gamma}\partial_t(\mathbf{B}\partial_t a)$$

Pump Mode: $\mathbf{B_0}$

Static $\mathbf{B_0}$:

$$\omega_1 \simeq m_a \qquad \partial_t(\mathbf{B}) \simeq 0$$

$$\mathbf{E}_1 \sim \frac{m_a g_{a\gamma\gamma}\sqrt{\rho_{\rm DM}}\mathbf{B}}{m_a^2 - \omega_1^2 + i\frac{m_a\omega}{Q_1}}$$

Oscillating $\mathbf{B_0}$:

$$\omega_1 \simeq \omega_0 + m_a \qquad \partial_t(\mathbf{B}) \simeq i\omega_0\mathbf{B}$$

$$\mathbf{E}_1 \sim \frac{\omega_0 g_{a\gamma\gamma}\sqrt{\rho_{\rm DM}}\mathbf{B}}{(\omega_0 + m_a)^2 - \omega_1^2 + i\frac{(\omega_0+m_a)\omega}{Q_1}}$$

Signal enhancement at low frequency $m_a << \omega_0$

A.Berlin, R.T. D'Agnolo, et al, JHEP07(2020)no.07, 088.

SRF with AC B field

Signal Mode: $\mathbf{E}_1$

Source: **a**
(almost monochromatic)

$$\sum_n \left(\partial_t^2 + \frac{\omega_n}{Q_n}\partial_t + \omega_n^2 \right) \mathbf{E}_n = g_{a\gamma\gamma}\partial_t(\mathbf{B}\partial_t a)$$

Pump Mode: $\mathbf{B}_0$

Oscillating $\mathbf{B}_0$:

$$\omega_1 \simeq \omega_0 + m_a \qquad \partial_t(\mathbf{B}) \simeq i\omega_0 \mathbf{B}$$

Scanning the axion mass by tuning the differences between two quasi-degenerate modes

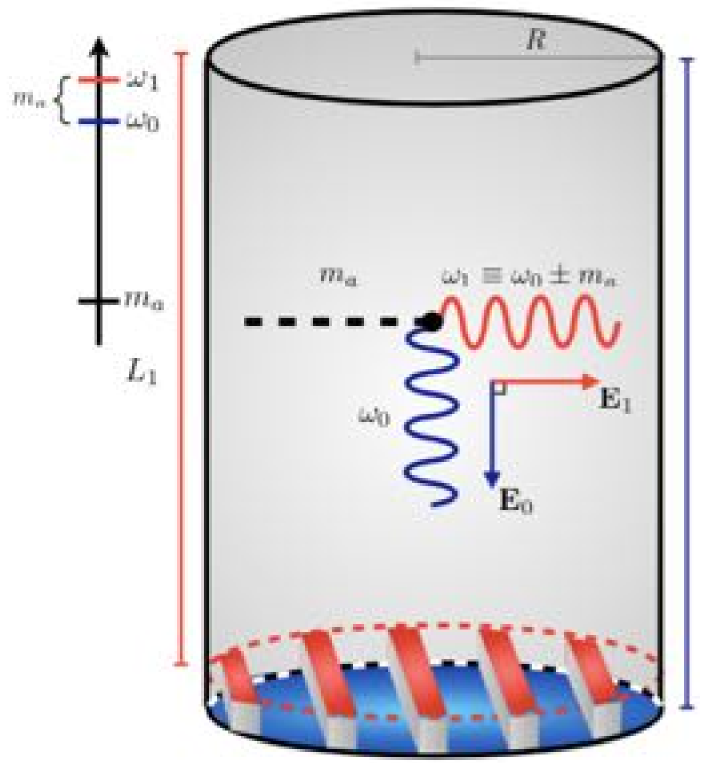

A.Berlin, R.T. D'Agnolo, et al, JHEP07(2020)no.07, 088.

SRF with AC B field

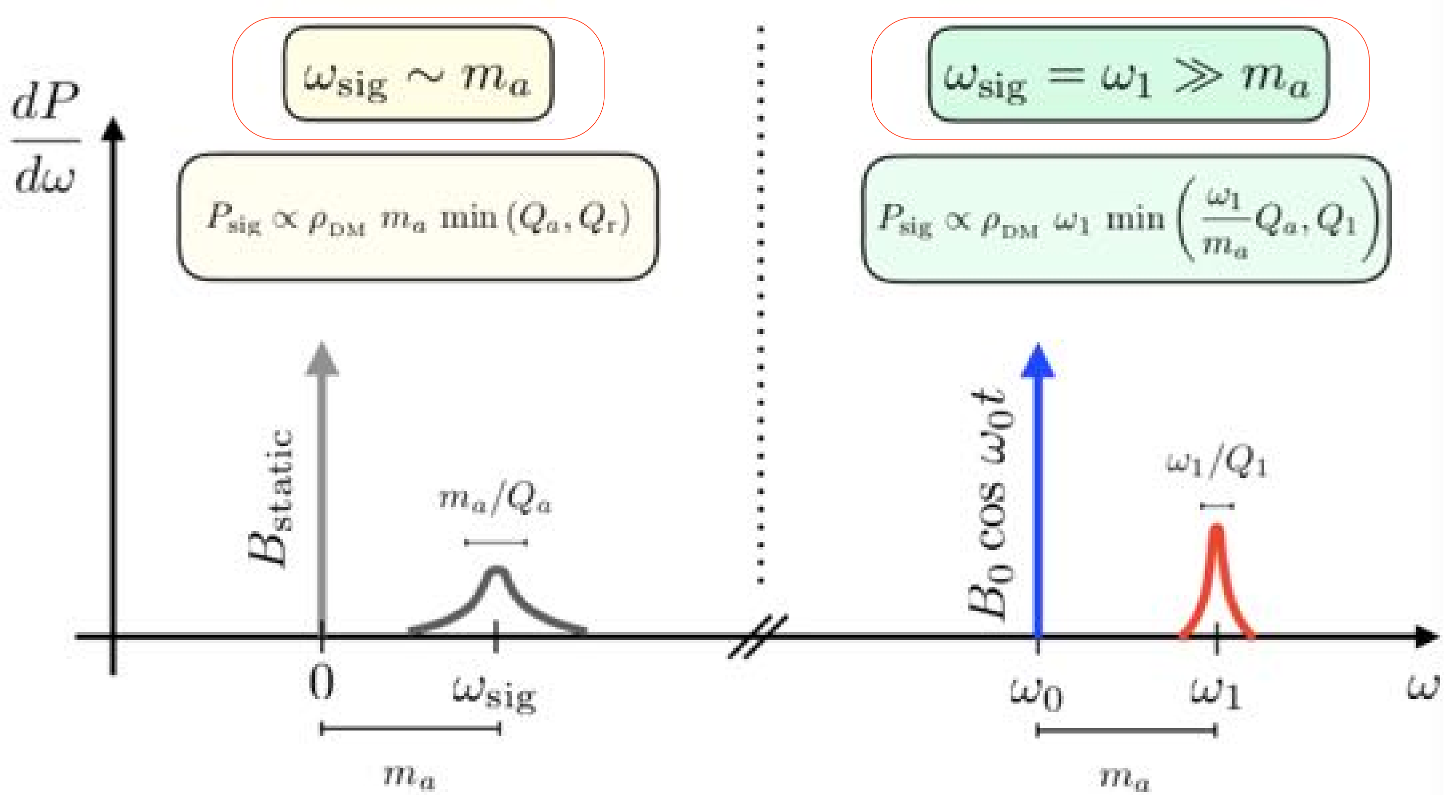

Main differences: signal power

$$P_{\rm sig}^{(\rm r)} \sim \frac{\mathcal{E}_a^2}{R} \min\left(1, \frac{\tau_a}{\tau_{\rm r}}\right) \sim \omega_{\rm sig}^2\, B_a^2 V \min(Q_{\rm r}/\omega_{\rm sig}, Q_a/m_a)$$

A.Berlin, R.T. D'Agnolo, et al, JHEP07(2020)no.07, 088.

Main noise for SRF haloscope

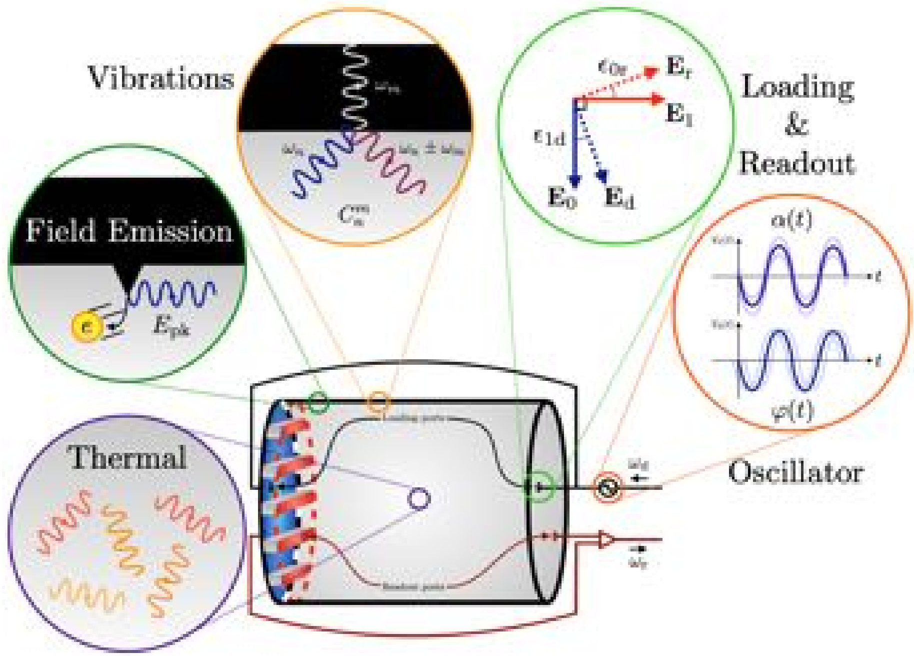

Traditional noise: thermal and readout;

Transition from pumping mode due to geometric fluctuation:
phase noise, mechanical oscillation noise; (well-studied by pioneer work on ultra-high frequency gravitational wave detection. [Class.Quant.Grav. 20 (2003) 3505-3522, gr-qc/ 0502054])

Axion Dark Matter Detection Using SRF

Hard to scan for a broad mass window in traditional cavity!

$\omega_1 \simeq m_a \qquad \partial_t(\mathbf{B}) \simeq 0$

narrow mass window due to size of the cavity

$\omega_1 \simeq \omega_0 + m_a \qquad \partial_t(\mathbf{B}) \simeq i\omega_0 \mathbf{B}$

The AC magnetic field inside the SRF and two nearly degenerate modes enable the scan of axion mass from the frequency splitting.

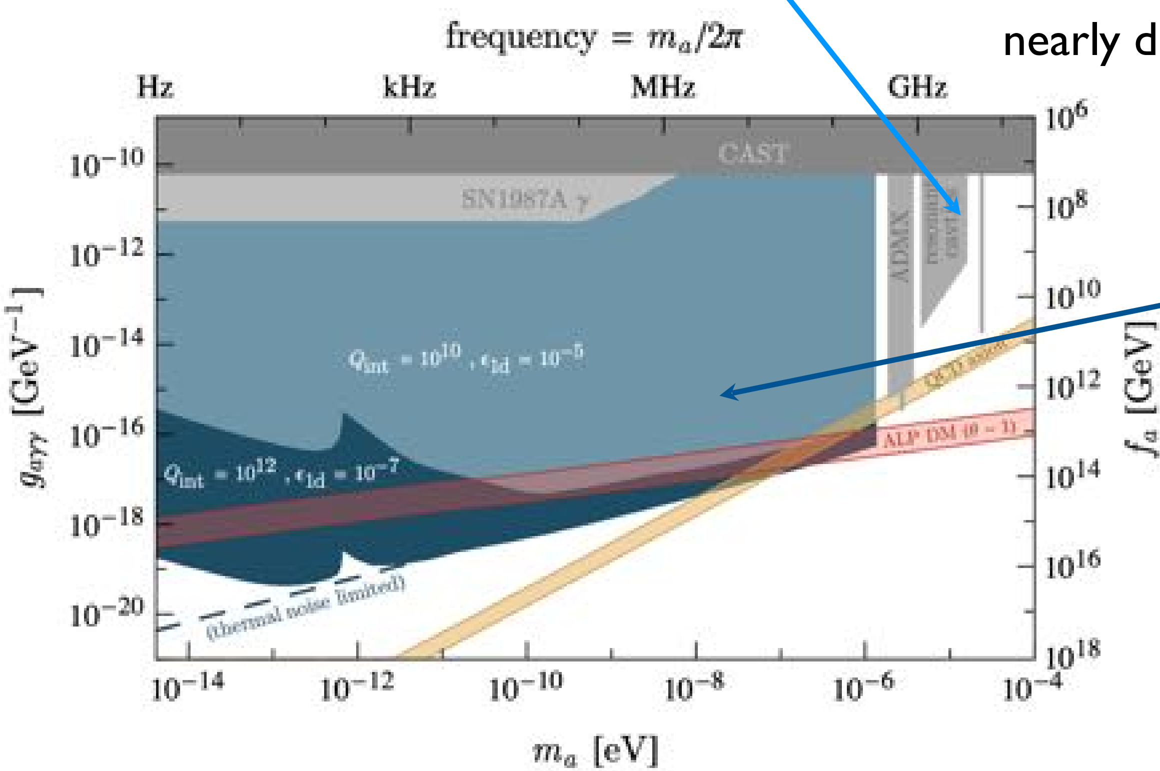

Much broader detection mass window at lower frequency.

Only gray region is excluded. Large unexplored parameter space!

A.Berlin, R.T. D'Agnolo, et al, JHEP07(2020)no.07, 088.

Axion Dark Matter Detection Using SRF

The high Q-factor will improve the sensitivity of the detection.

- Traditional resonant cavity: Q < 10^6.
- Higher Q on the detection does not have significant effect.

Strong DC background magnetic field
can destroy superconductivity.

- New detection method: using AC magnetic field in the SRF.

AC background magnetic field.

Background frequency is much higher than the axion mass

The high Q value of SRF cavity can be fully exploited, and the detection sensitivity is greatly enhanced.

Broadband case

For ultra-light axion, $\omega_1 = \omega_0 + m_a \simeq \omega_0$

Two degenerate and transverse modes can reach the ultra-light region!

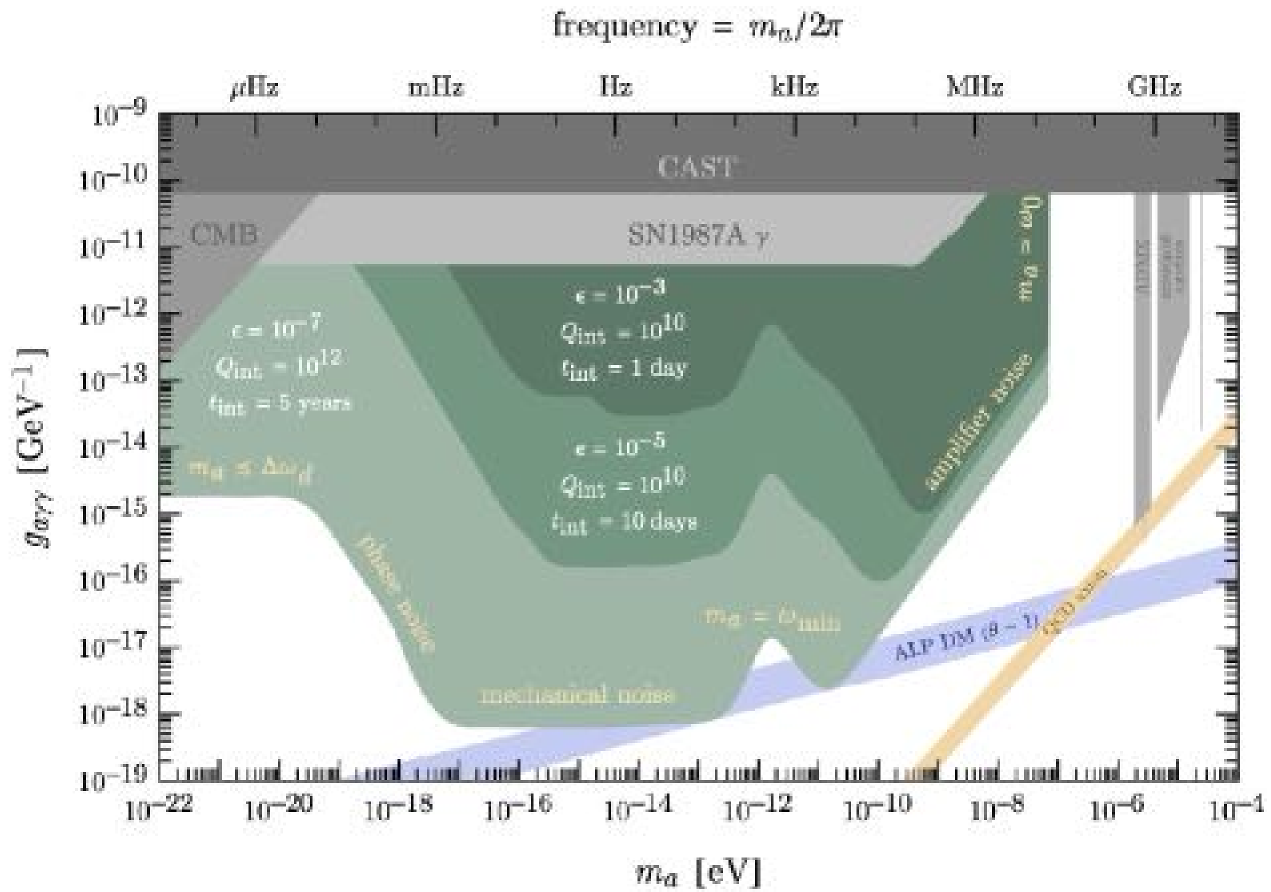

A.Berlin, R.T. D'Agnolo, et al, [arXiv:2007.15656 [hep-ph]].

ULDM: Quantum Detection Schemes

Traditional resonant cavity detection suffers that DM mass must match the cavity's resonant frequency, depending on the cavity size.

$\omega_1 \simeq m_a \qquad \partial_t(\mathbf{B}) \simeq 0$

$\omega_1 \simeq \omega_0 + m_a \qquad \partial_t(\mathbf{B}) \simeq i\omega_0 \mathbf{B}$

Cavities cannot be very large or very small, leading to a narrow detection range.

The alternating magnetic field in a superconducting cavity means DM mass depends on the frequency difference.

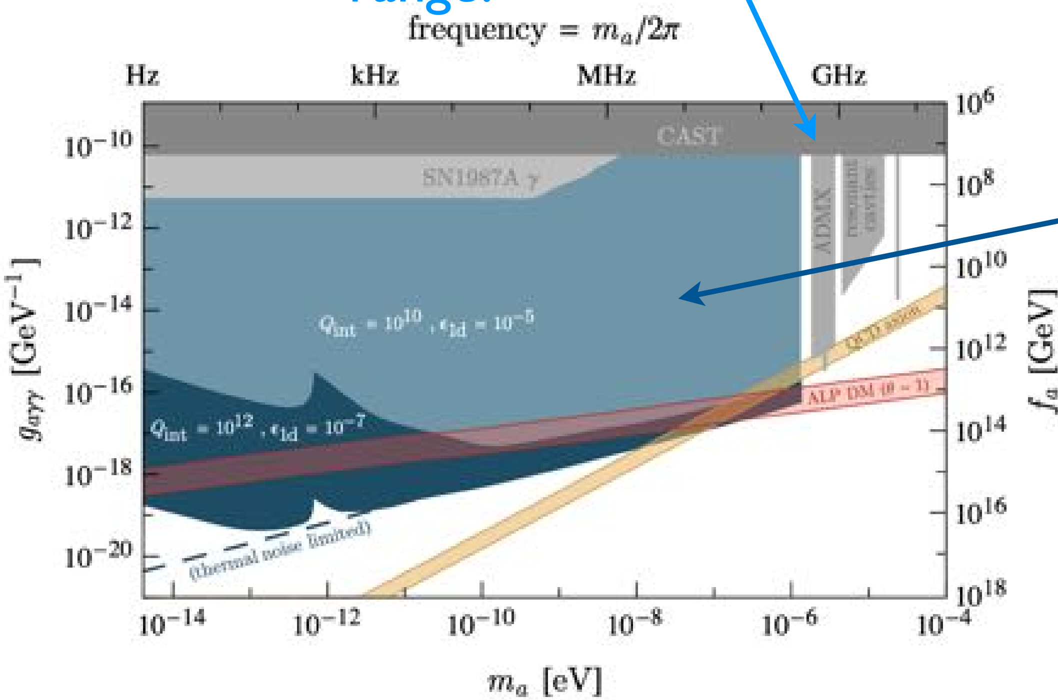

With the quasi-degenerate energy levels superconducting cavity, the DM mass range is much broader in the lighter region.

The gray area represents the already detected regions, with nearly no current detection!

Quantum Detection of ULDM

Quantum detection of ultralight DM also faces quantum limit. New design schemes will surpass these quantum limits, improving sensitivity by 2 orders of magnitude.

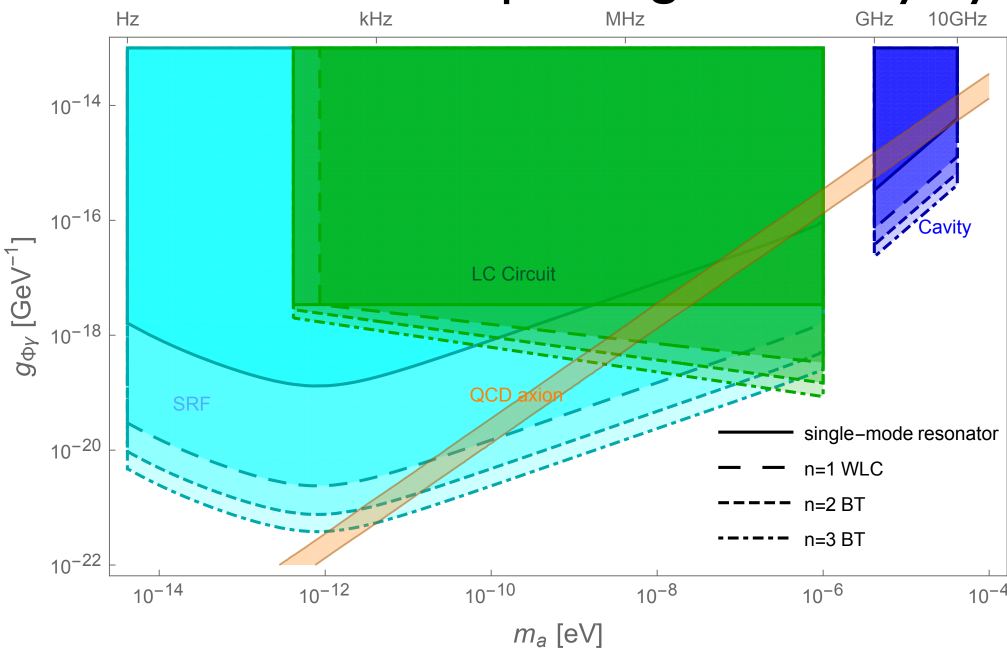

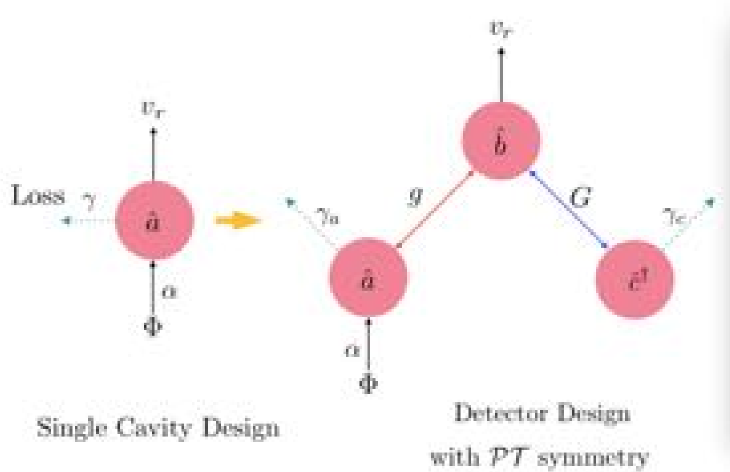

Y-f. Chen, M-y. Jiang, J. Shu., Y-t. Yang, arxiv: 2103.12085

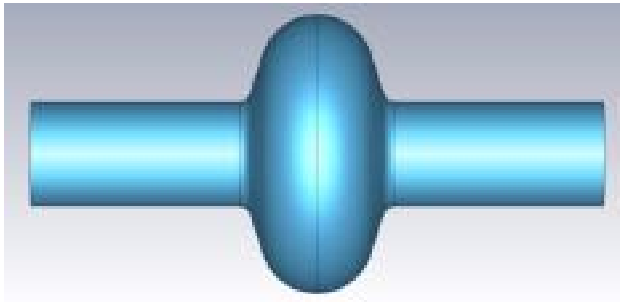

In collaboration with the Heavy Ion Institute at Peking University, we are conducting tests to validate ultralight DM detection technology around 200 MHz frequency.

Clever test of wave-like DM

QCD axion motivated by the Strong-CP Problem:
Why is the neutron electric dipole moment so small?

Norman Ramsey
Nobel Prize 1989.
Neutrino oscillation expts are "Ramsey interferometers"

Naive estimate gives
nEDM ≈ 10^{-16} e-cm

spin

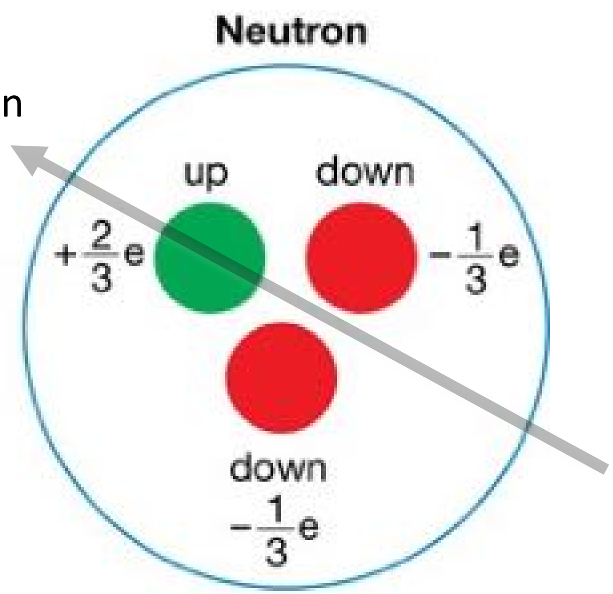

10^{-15} m

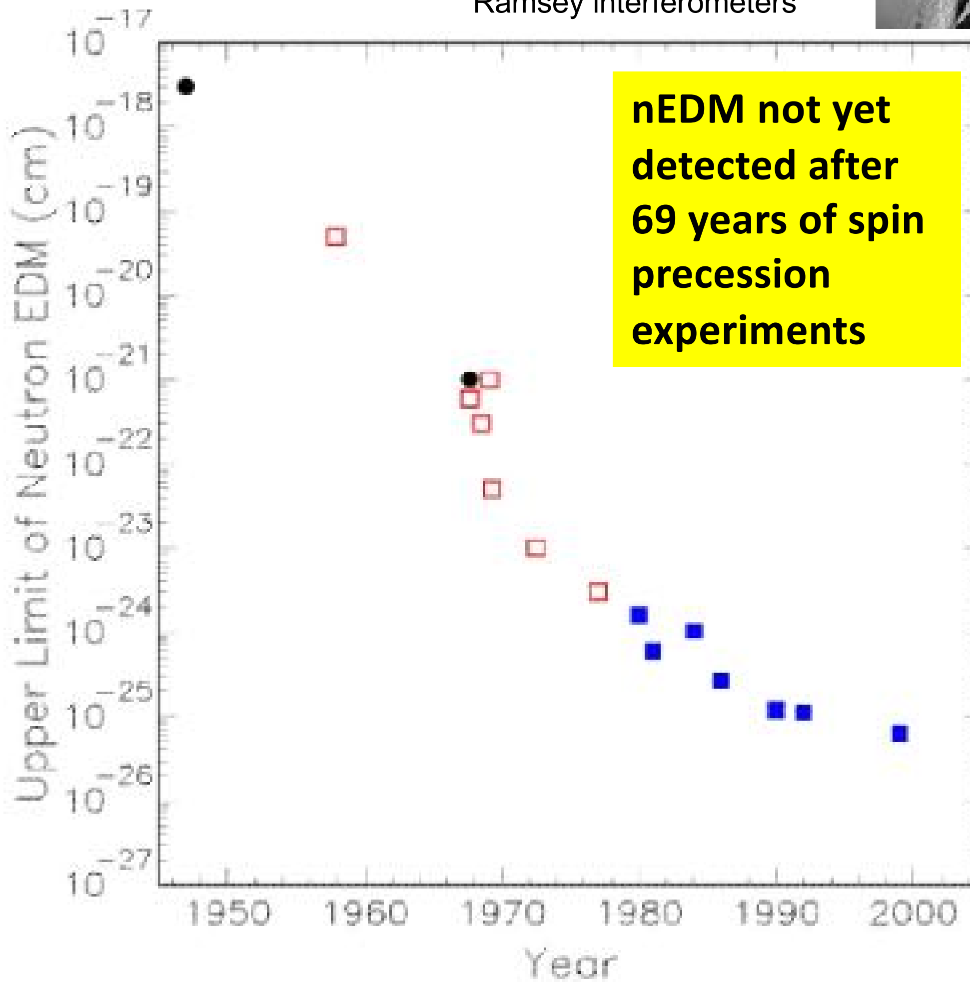

nEDM not yet detected after 69 years of spin precession experiments

Aaron S. Chou, QSFP lecture 2021

The CP Problem of Strong Interactions

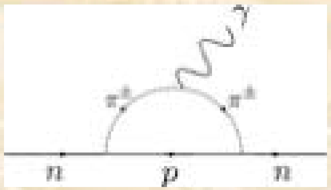

Characterizes degenerate QCD ground state (Θ vacuum)

Phase of Quark Mass Matrix

Standard QCD Lagrangian contains a CP violating term

$$L_{CP} = -\frac{\alpha_s}{8\pi}\underbrace{(\Theta - \arg\det M_q)}_{0\le\overline{\Theta}\le 2\pi}\,\mathrm{Tr}\,\tilde{G}_{\mu\nu}G^{\mu\nu}$$

Induces a neutron electric dipole moment (EDM) much in excess of experimental limits

$$d_n \approx \overline{\Theta}\,10^{-16}\,e\,\mathrm{cm} \approx \frac{\overline{\Theta}}{10^2}\mu_n < 3\times 10^{-26}\,e\,\mathrm{cm}$$

$\overline{\Theta} \lesssim 10^{-10}$ **Why so small?**

Slide from G. Raffelt

The 1977 Peccei-Quinn solution to the strong-CP problem

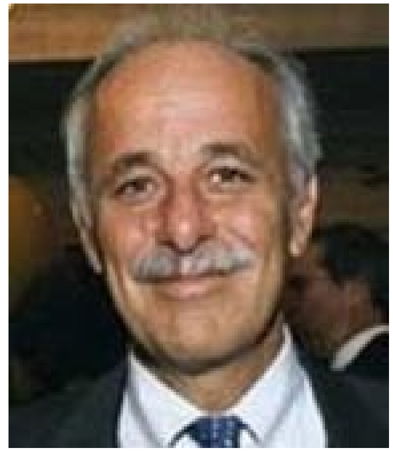

Dirac Medal (2000)

- Promote theta to become a new **dynamical** scalar field which has a two-gluon coupling. (dynamical = can vary in space and time)

- Think like an electrical engineer: Use this field in a cosmological feedback loop to dynamically zero out any pre-existing CP-violating phase angles.

Natural potential energy function

$$V(A) = -f_a^2 A^2 + \frac{\lambda}{4!} A^4 + \left(\frac{g^2}{32\pi^2} \arg(A) - \frac{\alpha_s}{8\pi} \left(\theta_{QCD} + \theta_{quark} \right) \right) \langle G\tilde{G} \rangle$$

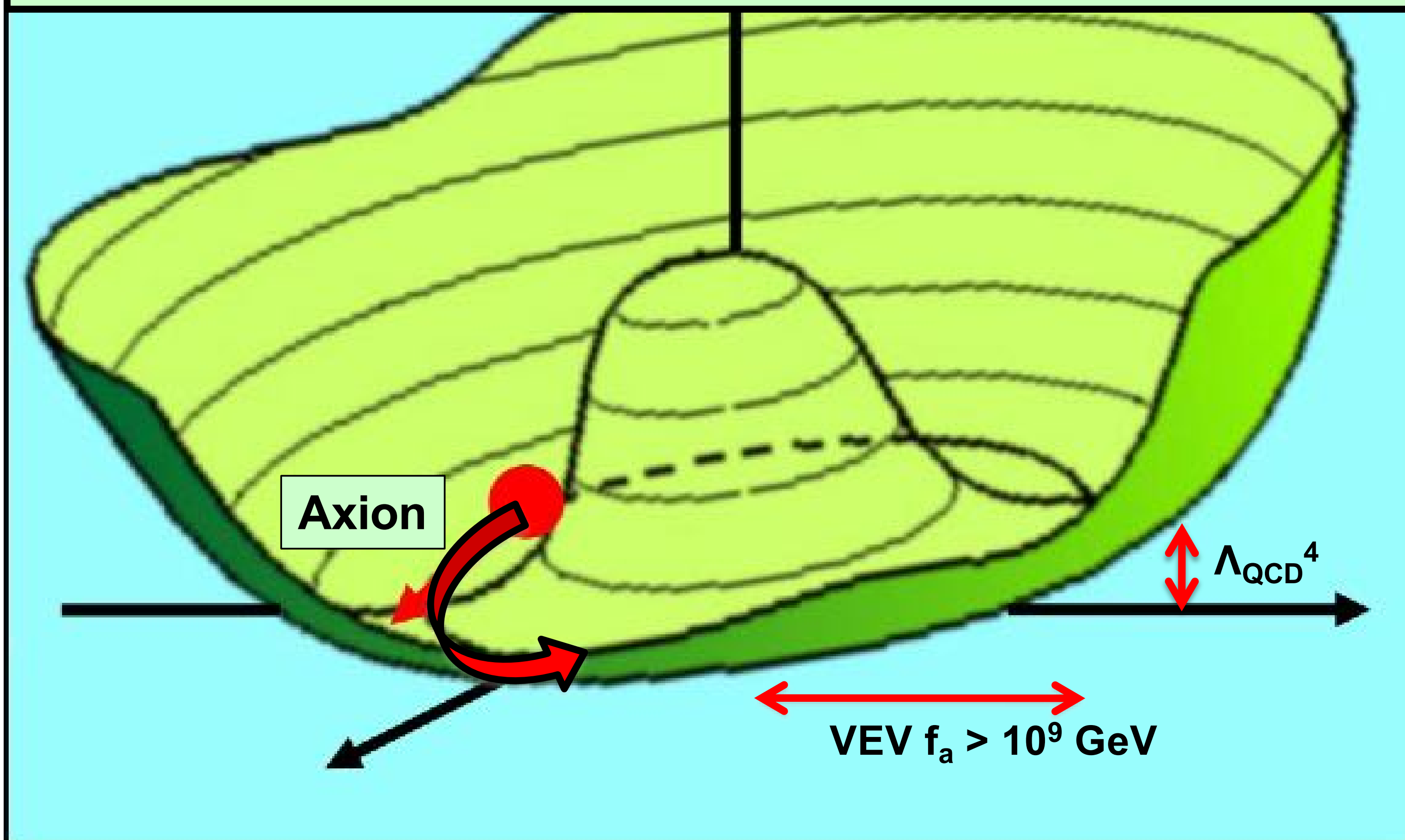

Natural potential energy function

$$V(A) = -f_a^2 A^2 + \frac{\lambda}{4!} A^4 + \left(\frac{g^2}{32\pi^2} \arg(A) - \frac{\alpha_s}{8\pi} \left(\theta_{QCD} + \theta_{quark} \right) \right) \langle G\tilde{G} \rangle$$

The axion field zeroes out any other CP-violating phases from the strong or electroweak quark sector.

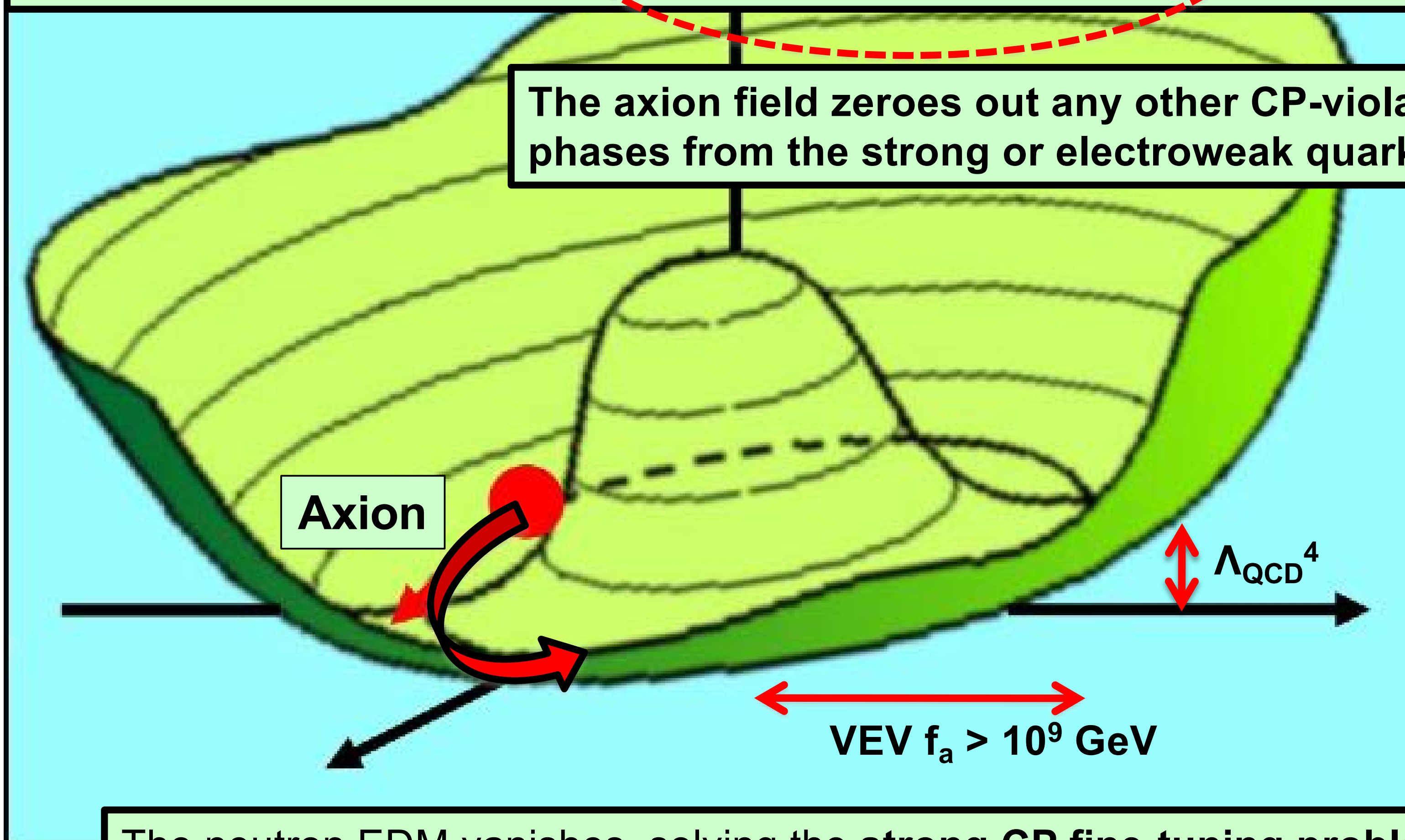

The neutron EDM vanishes, solving the **strong CP fine-tuning problem**.

Axion mass = harmonic oscillator frequency

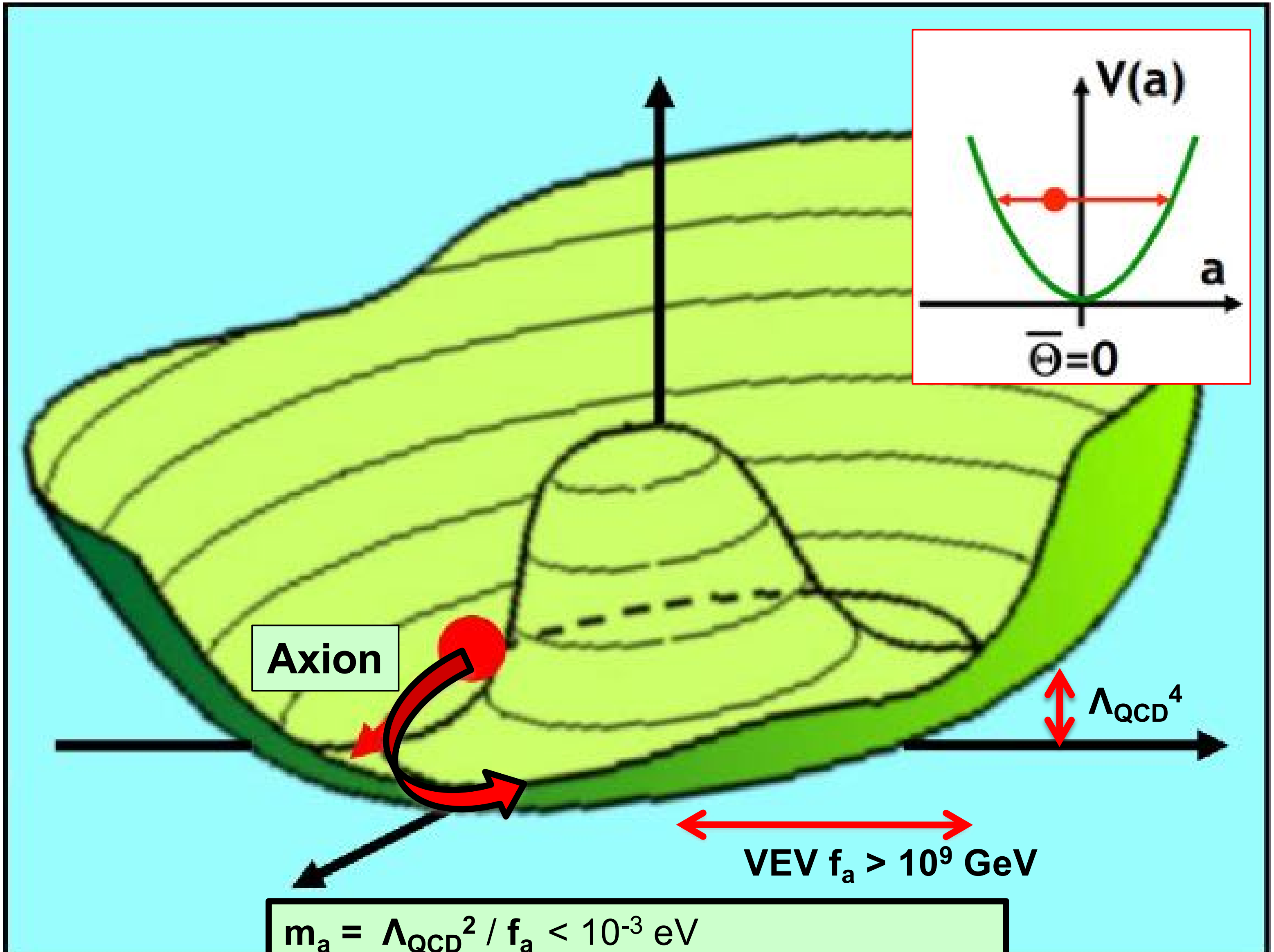

$m_a = \Lambda_{QCD}^2 / f_a < 10^{-3}$ eV
Single parameter model for axions

The initial potential energy density is released as ultracold dark matter

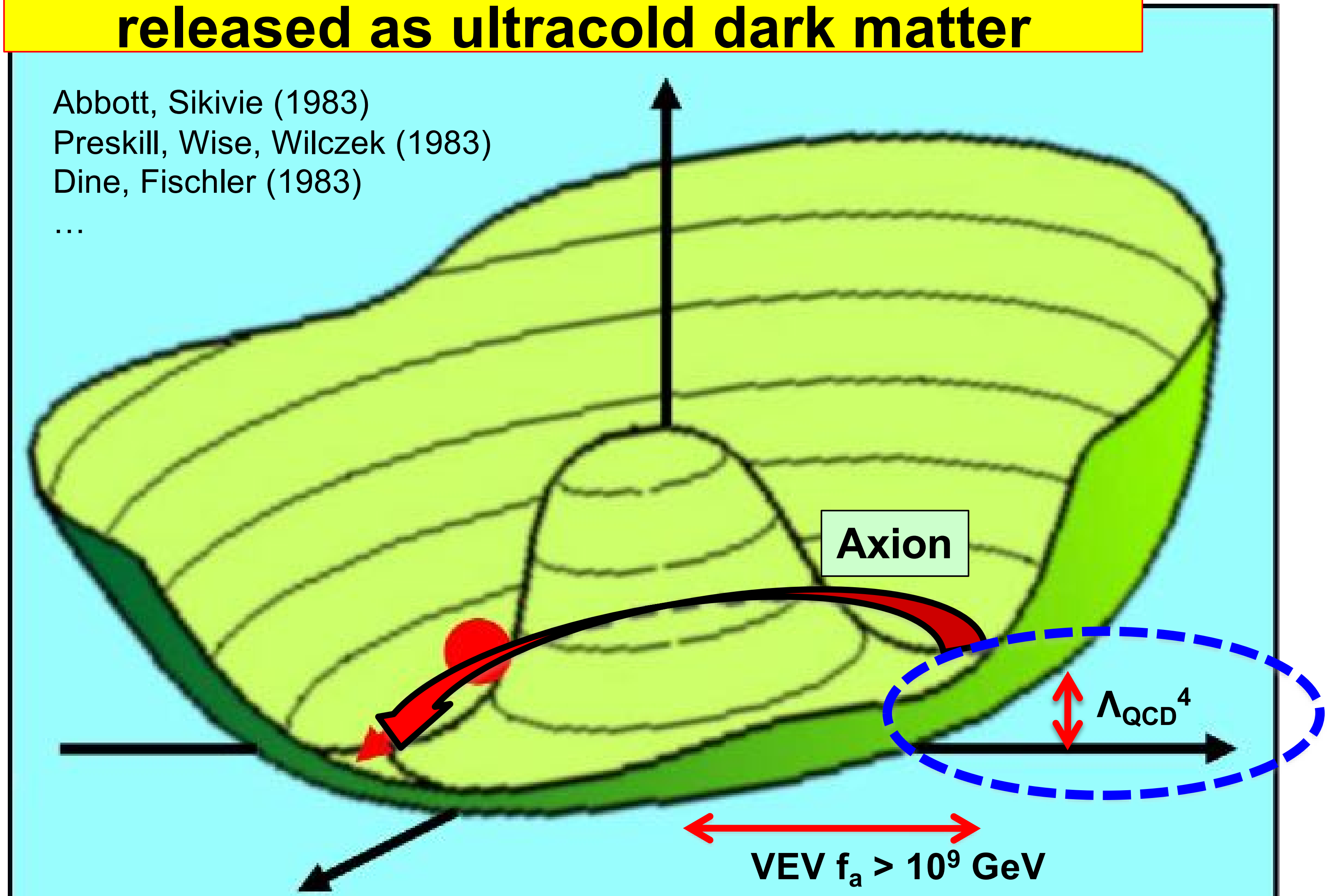

The initial azimuthal angle $\boldsymbol{\theta_0}$, determines the available potential energy to be released. $\mathbf{O(1)\times\Lambda_{QCD}{}^4}$ of potential energy density is converted into **dark matter**.

Axion dark matter = waves of oscillating θ_{CP}

Locally coherent oscillation of the QCD θ angle about its CP-conserving minimum:

$$\theta(x,t) = \theta_{\max} e^{i(kx - m_a t)}$$

where $$\theta_{\max} = \sqrt{\frac{2\rho_a}{\Lambda_{\rm QCD}^4}} \approx 3.7 \times 10^{-19} \text{radians}$$

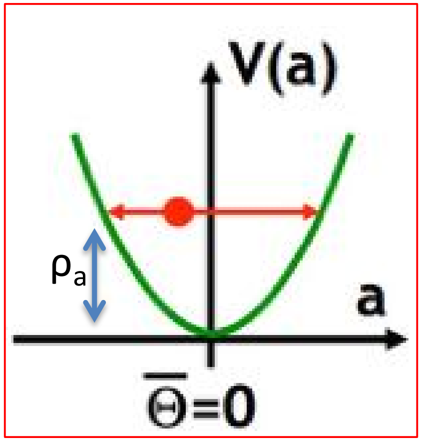

DM oscillations partially undo the Peccei-Quinn mechanism by enabling the coherent field to climb out of the potential minimum. **Signal strength depends only on local dark matter density, and is independent of DM mass and phase transition scale f_a**

Phenomenology based on a classically oscillating CP-violating angle which:

- **Rotates B-fields into E-fields**
- **Creates AC nucleon EDMs**
- **Creates AC torques on fermion spins**

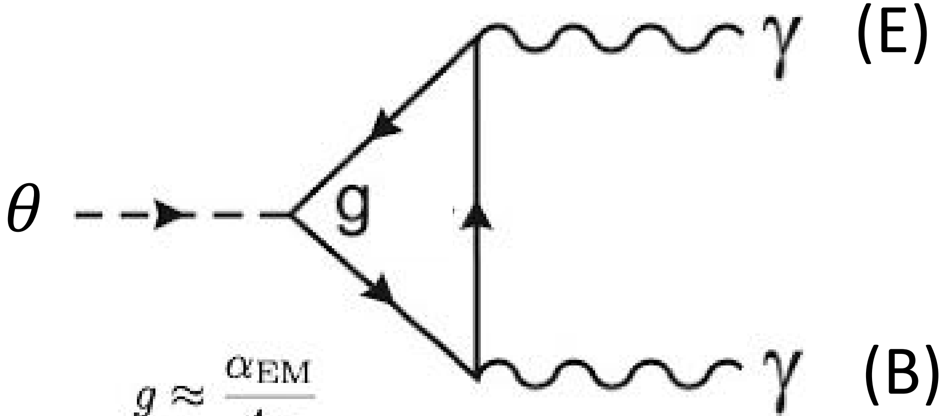

$$g \approx \frac{\alpha_{\rm EM}}{4\pi}$$

Bucket of dark matter is dumped into the red-shifting photon bath at time $1/H \approx 1/m_a$

Non-DM density redshifting away →

Global warming

For a bucket filled to the level **$\langle \sin^2 \theta_0 \rangle \times \chi$** of fish,
dumping it too late creates an improper balance of fish/water.

If you are going to procrastinate and dump it late, you better not have too many fish in that bucket since there is not a lot of water left!

→ **Small m_a requires small $\langle \sin^2 \theta_0 \rangle$ to avoid overproducing dark matter.**

Fullness of bucket depends on whether the axion phase transition happens before or after cosmic inflation

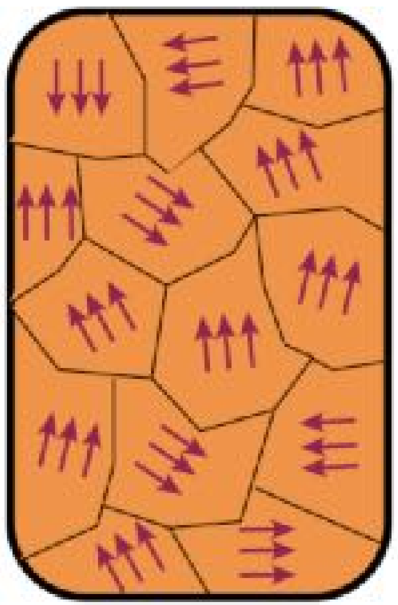

Ferromagnetic spin domains

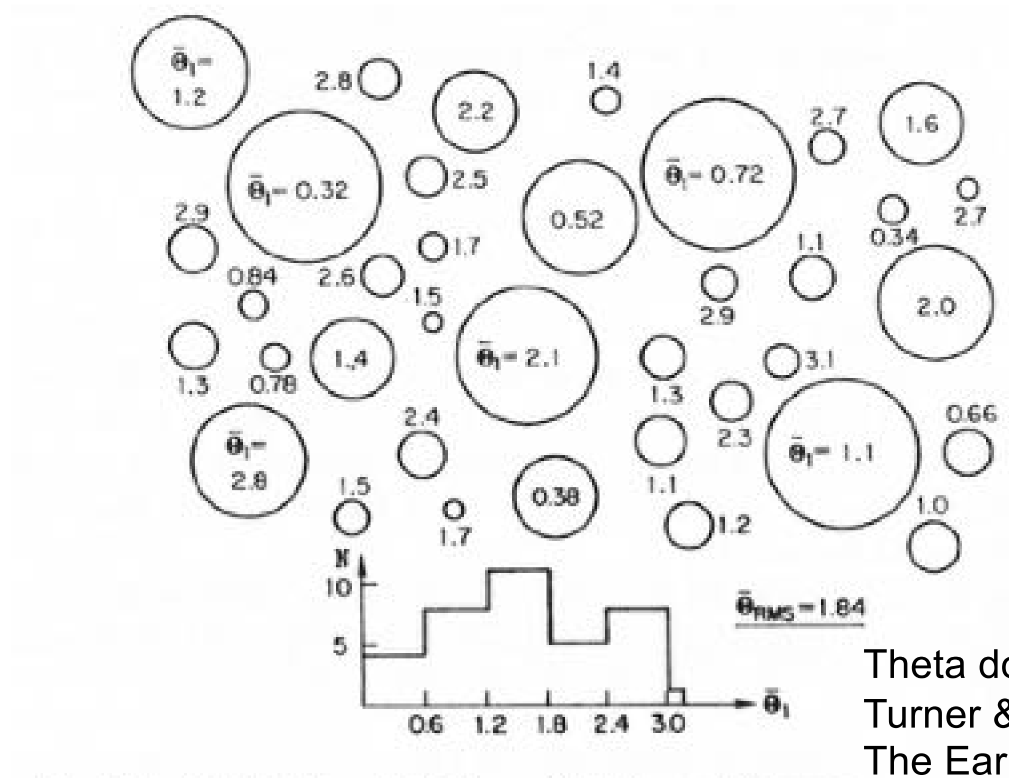

Fig. 10.9: Distribution of $|\bar{\Theta}_1|$ in an inflationary Universe.

Theta domains,
Turner & Kolb
The Early Universe

- If axion phase transition occurs **pre-inflation**, bubbles are inflated, and we live in a single bubble which by chance can have $\theta<1$.
- If axion phase transition occurs **post-inflation**, many bubbles are contained within our horizon, and so we get average value $\langle\sin^2\theta\rangle \times \Lambda_{QCD}^4$ of dark matter.

New lattice result gives dividing line at $m_a \approx 50$ μeV between pre- vs post-inflationary axion phase transition

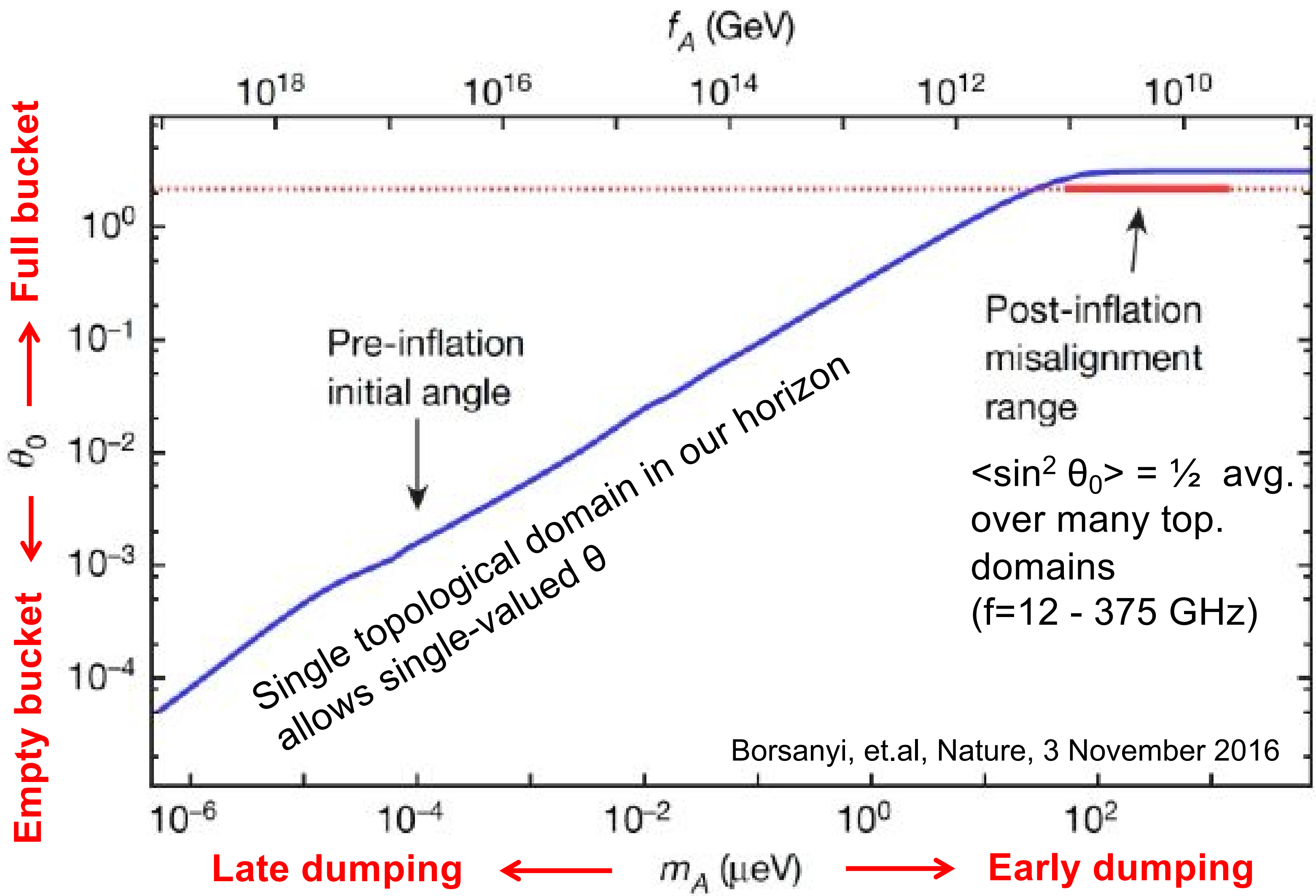

The classic axion window

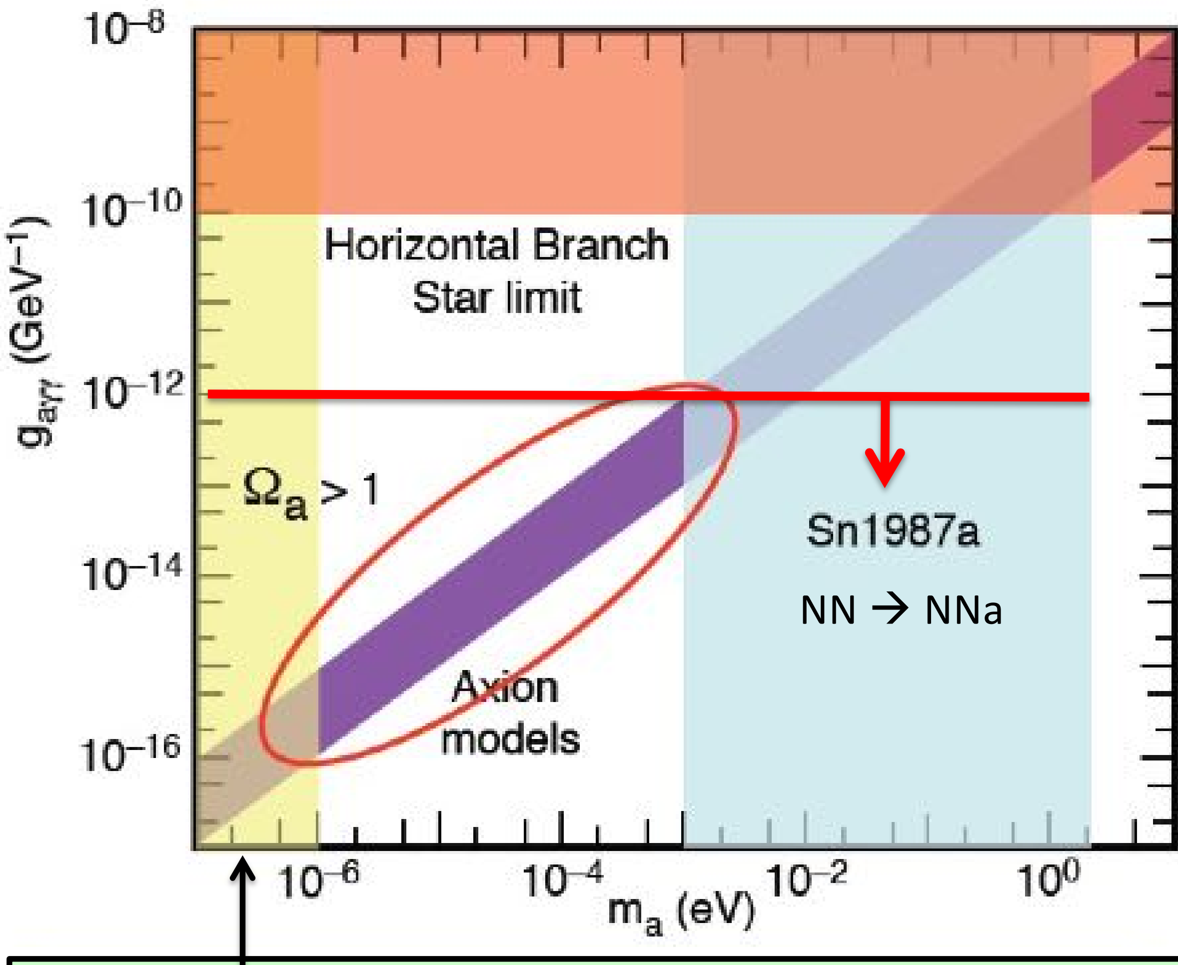

$$\Omega_a \approx \left(\frac{6\,\mu\mathrm{eV}}{m_a}\right)^{\frac{7}{6}}$$

or even more due to cosmic string decay.

PQ model + local energy conservation **guarantees** the existence
of dark matter axions in the last place we haven't looked!

Disfavored by "naturalness." Requires small initial θ to avoid DM overproduction.

Low mass dark matter generically takes the form of classical bosonic sine waves

Fermions: 1 DM particle per mode volume ($\lambda_{deBroglie}$)^3

For **mass < 70 eV**, Pauli exclusion principle causes dark matter clumps to swell up to be larger than the size of the smallest dwarf galaxies. (Randall, Scholtz, Unwin 2017)

→ If lower mass, dark matter must be coherent bosonic sine waves with **macroscopic mode occupation number >>1**

Not billiard balls.

Need coherent wave detector.

Ultracold low mass dark = classical wave

Described by a **Glauber** coherent state with properties similar to a modern laser.

Huge number density 10^{14}/cc,
Linewidth $\approx$ kHz

$$a \approx \frac{\sqrt{2\rho_a}}{m_a} e^{i(\vec{k}\cdot\vec{x} - m_a t + \phi)}$$

$$|\vec{A}| \approx \frac{\sqrt{Z_0 P_{\text{laser}}/\text{Area}}}{\omega} e^{i(\vec{k}\cdot\vec{x} - \omega t + \phi)}$$

e.g. 10^{-5} eV = GHz dark matter

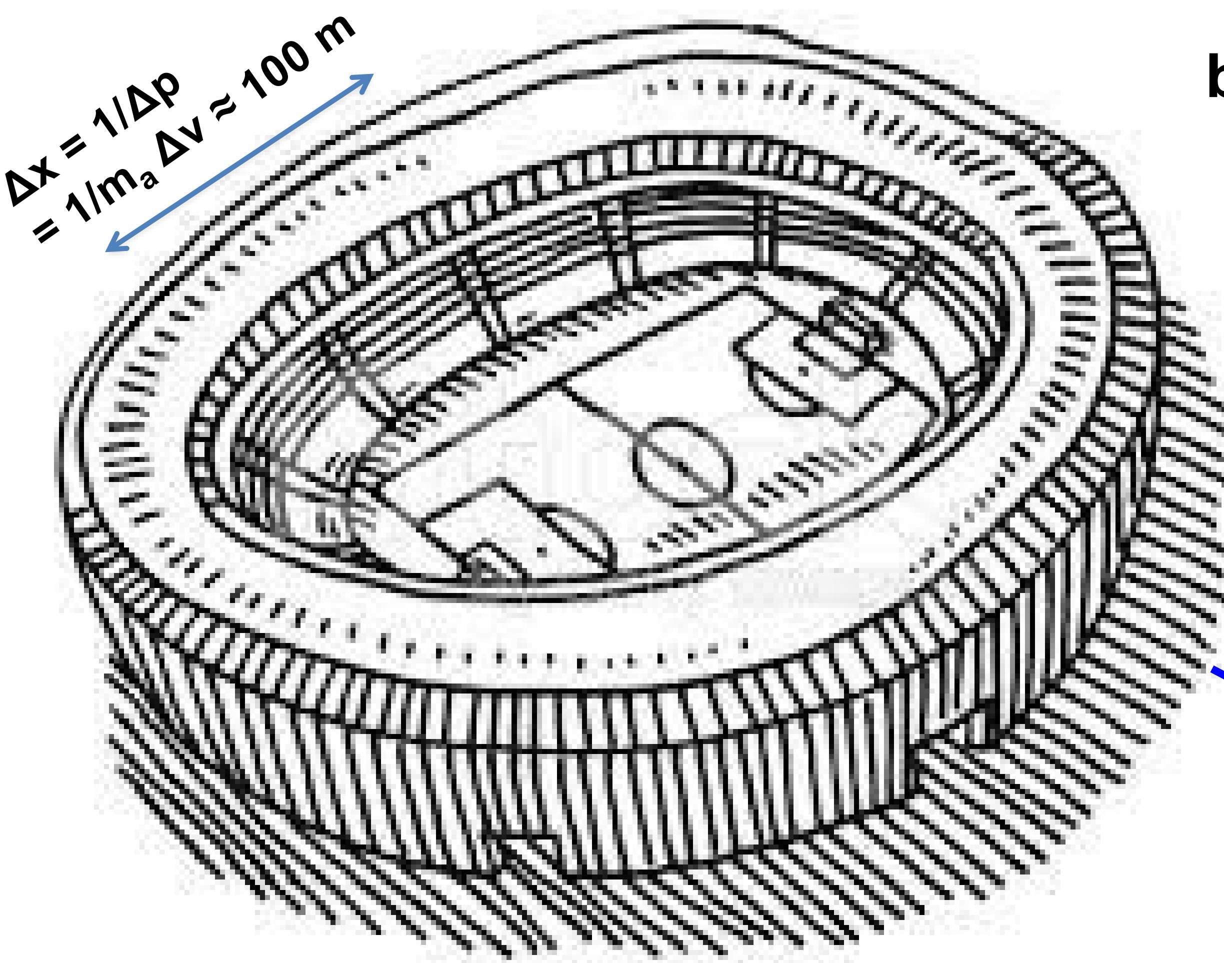

Non-relativistic bosonic DM is like a slow CW laser with $f = m_a/2\pi$

$v \approx \Delta v \approx 300$ km/s (galactic escape velocity)

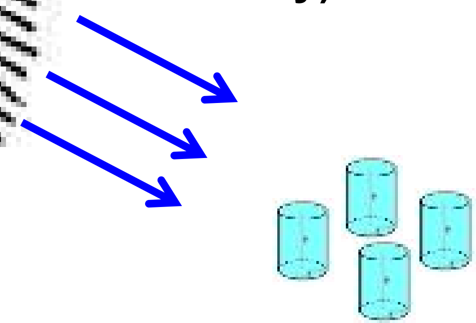

Football stadium-sized regions of coherently oscillating **classical sine waves** slowly drifting through detectors. Mean DM occupation number **$N > 10^{22}$ per mode.**

Accumulate oscillatory signals in various kinds of laboratory oscillators which are weakly coupled to the DM wave

Axion energy is kinetically broadened by virial velocity

Non-relativistic DM:
$v \sim \Delta v \sim 10^{-3}$ c
(galactic escape velocity)

Kinetic energy = $\frac{1}{2} m_a v^2$
$\Delta E = m_a v \Delta v$
$E_{rest} = m_a c^2$

$\Delta E/E = v \Delta v / c^2 \sim 10^{-6}$

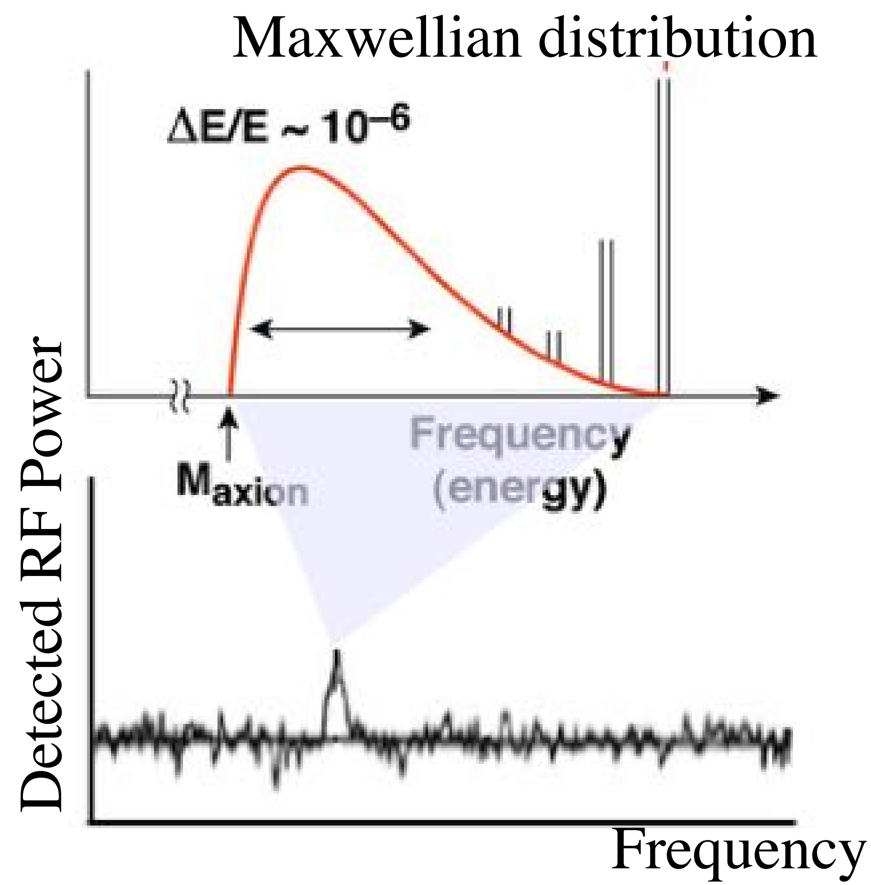

Very narrowband line, but can reconfirm signal in minutes once found.

Most of search time spent slowly stepping through frequency space, one frequency tuning at a time.

Signal strength is independent of m_a, f_a

Locally coherent oscillation of the QCD θ angle about its CP-conserving minimum:

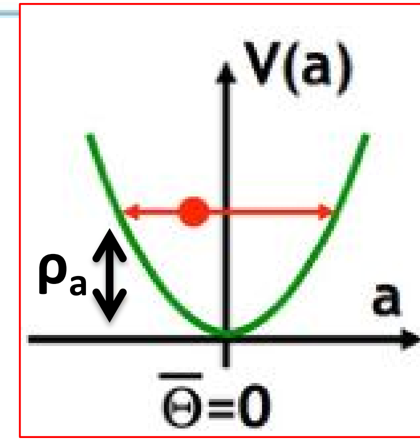

$$\theta(x,t) = \theta_{\max} e^{i(kx - m_a t)}$$

where $$\theta_{\max} = \sqrt{\frac{2\rho_a}{\Lambda_{QCD}^4}} \approx 3.7 \times 10^{-19} \text{radians}$$

DM oscillations partially undo the Peccei-Quinn mechanism by enabling the coherent field to climb out of the potential minimum.

Wave amplitude and hence signal strength depends only on local dark matter density ρ_a !

Experimental goal:
Determine frequency of the signal and hence the axion mass

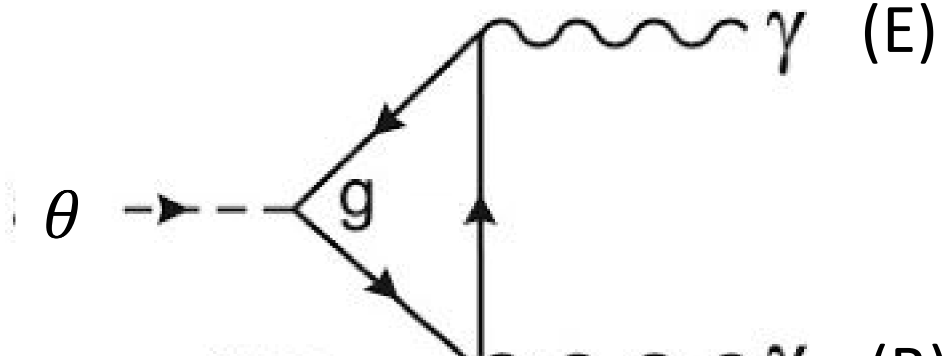

$$g \approx \frac{\alpha_{EM}}{4\pi}$$

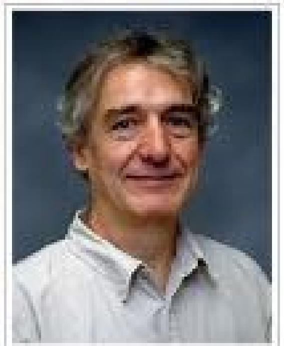

The Dark Matter Haloscope:
Classical axion wave drives RF cavity mode

Pierre Sikivie,
Sakurai Prize 2019

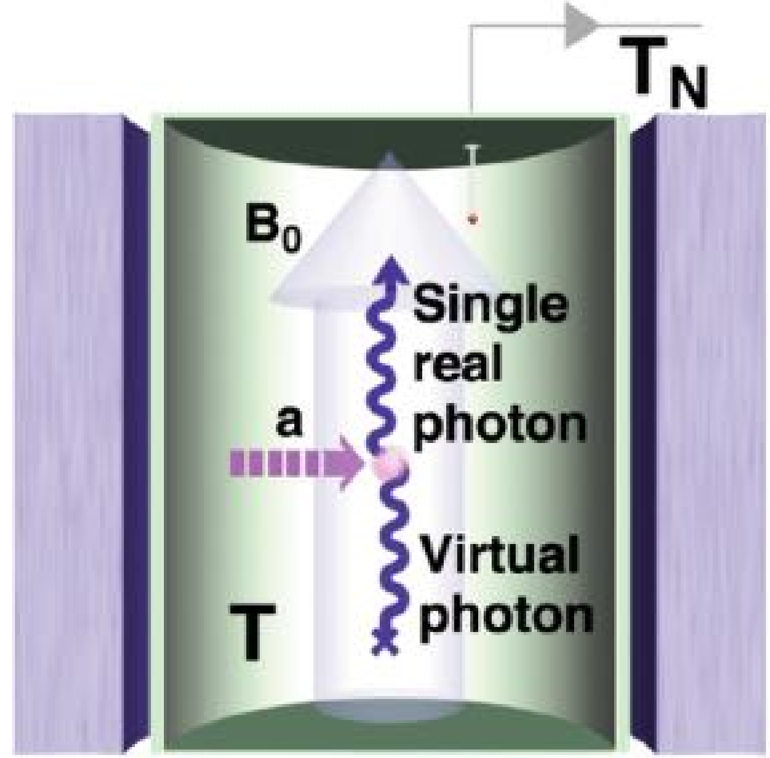

- In a constant background B_0 field, the oscillating axion field acts as an exotic, space-filling current source

$$\vec{J}_a(t) = -g\theta \vec{B}_0 m_a e^{i m_a t}$$

which drives E&M via Faraday's law:

$$\vec{\nabla} \times \vec{H}_r - \frac{d\vec{D}_r}{dt} = \vec{J}_a$$

- Periodic cavity boundary conditions extend the coherent interaction time **(cavity size ≈ 1/m_a)** → the exotic current excites standing-wave RF fields.

A spatially-uniform cavity mode can **optimally** extract power from the dark matter wave

$$P_a(t) = \int \vec{J}_a(t) \cdot \vec{E}_r(t)\, dV$$

Axions vs WIMPs:

Resonant scattering requires size of scattering target = 1/(momentum transfer)

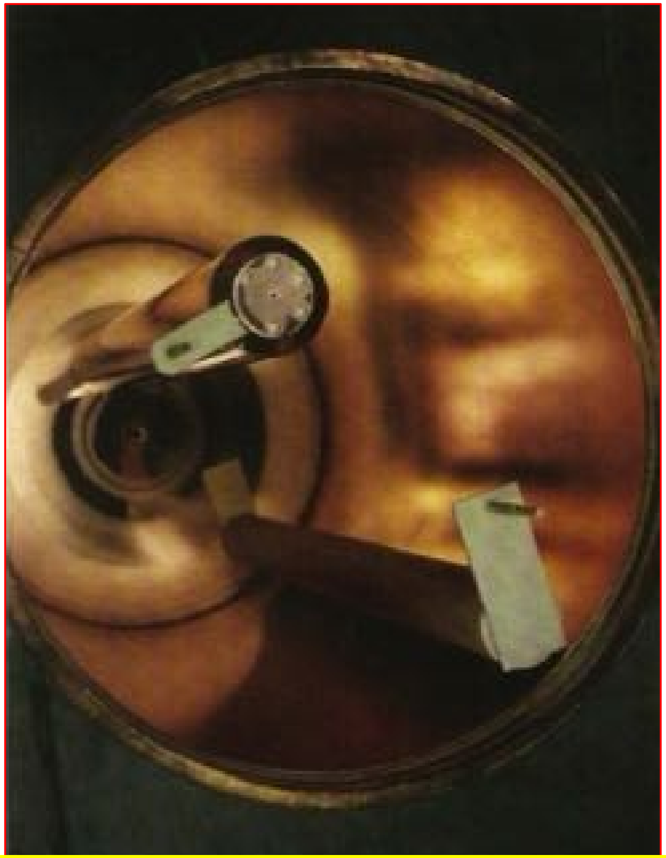

4 μeV mass axions scatter on 50cm size microwave cavities

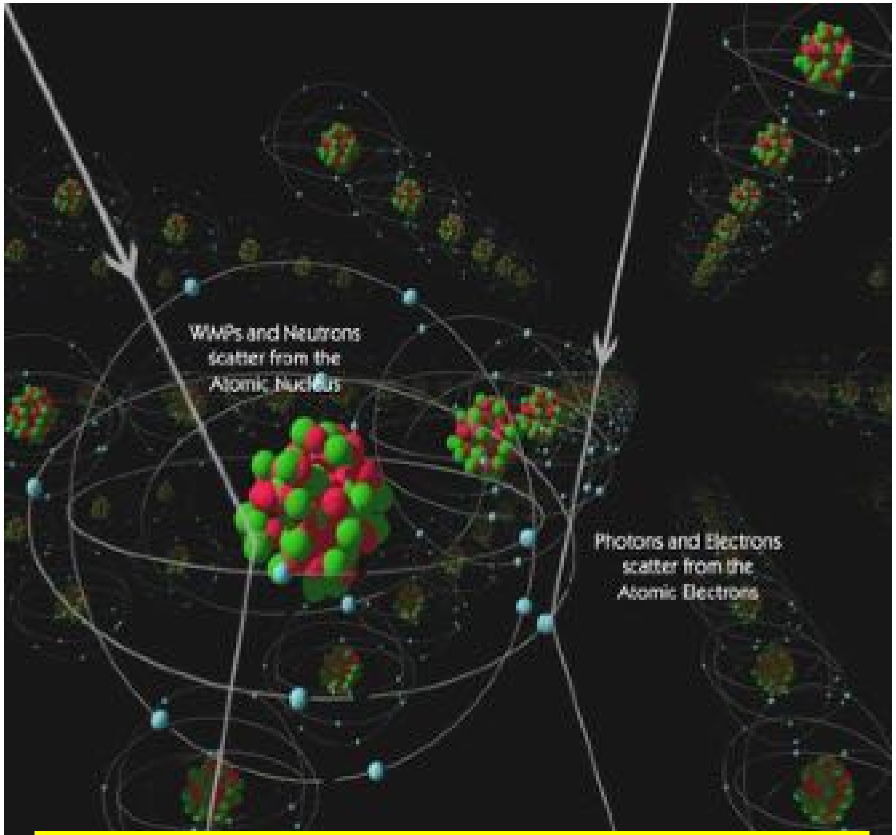

WIMPS scatter on 10 Fermi size atoms

Match size of antenna to wavelength of signal

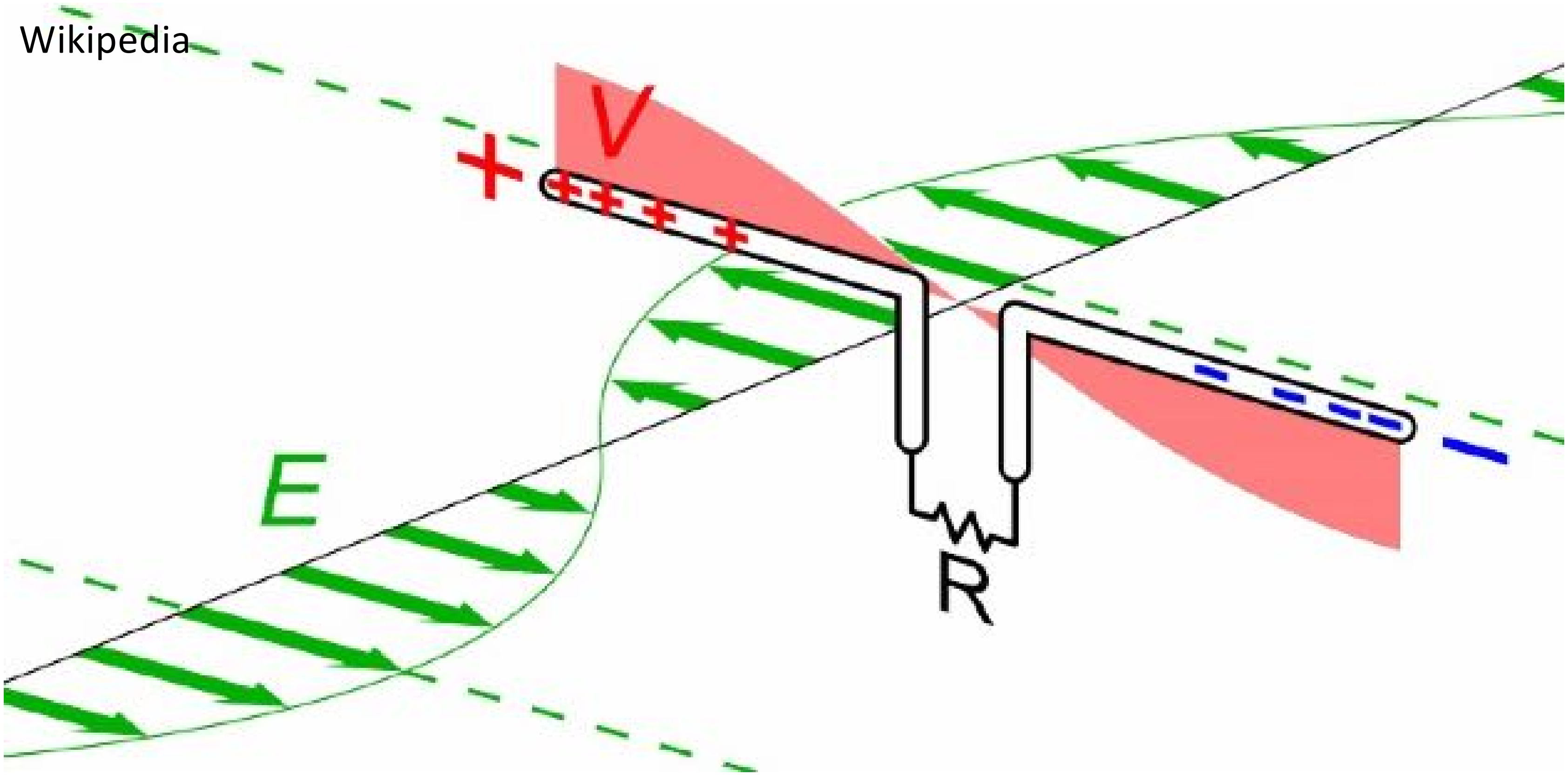

Wave mechanics: scattering matrix element is proportional to spatial Fourier transform of the scattering potential, with respect to the momentum transfer

Spectral analysis of output voltage time series

Discrete Fourier transform

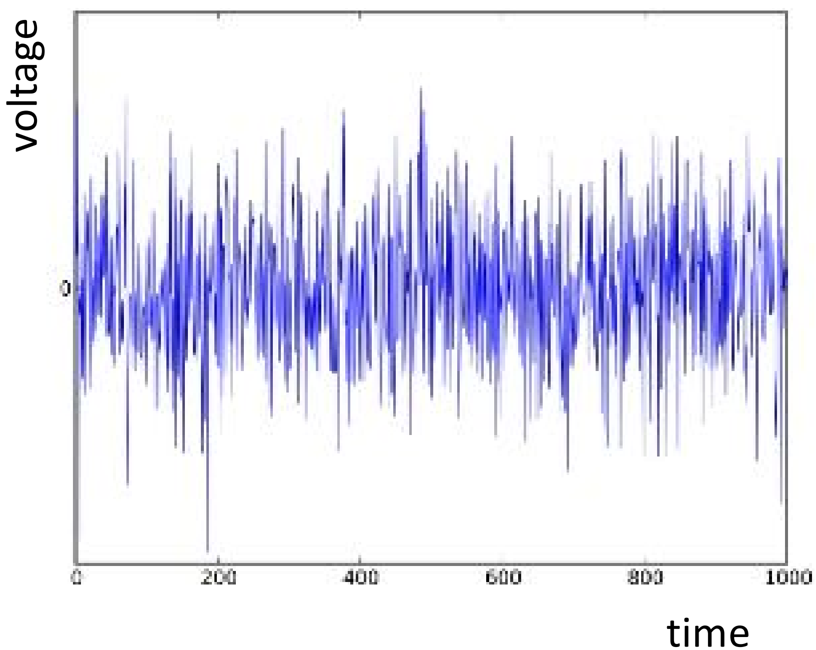

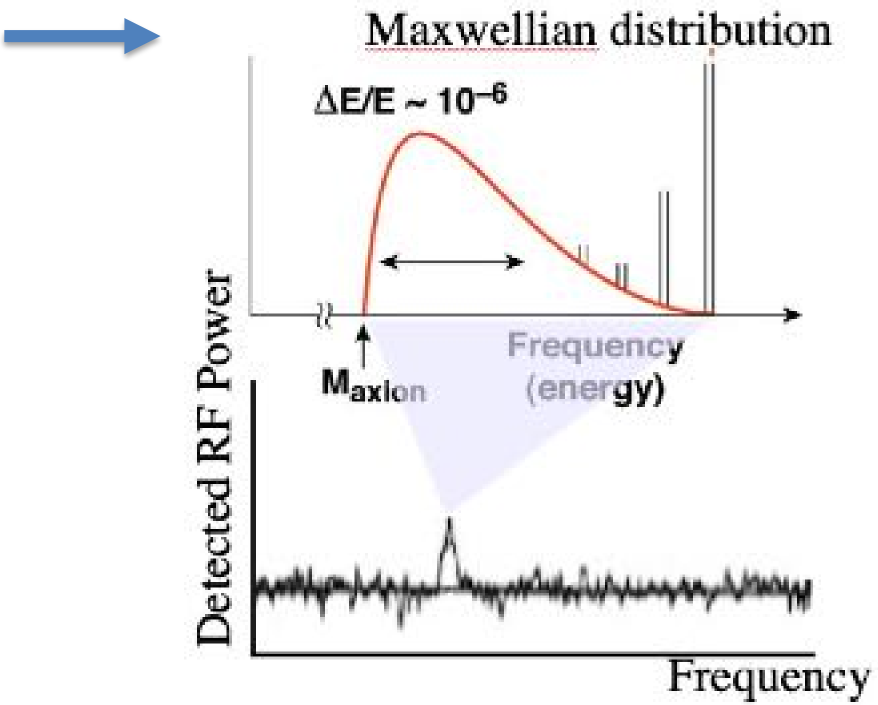

Digitization rate f_{dig} gives maximum resolvable “Nyquist” frequency $f_{dig}/2$.
Duration Δt of acquired time series gives frequency resolution $\Delta f = 1/2\Delta t$.

Dark matter signal = excess above white noise backgrounds.

2017: 30-year axion R&D program culminates in first sensitivity to DFSZ axions

PRL 120, 151301 (2018)

ADMX at U.Washington,
FNAL = DOE lead lab

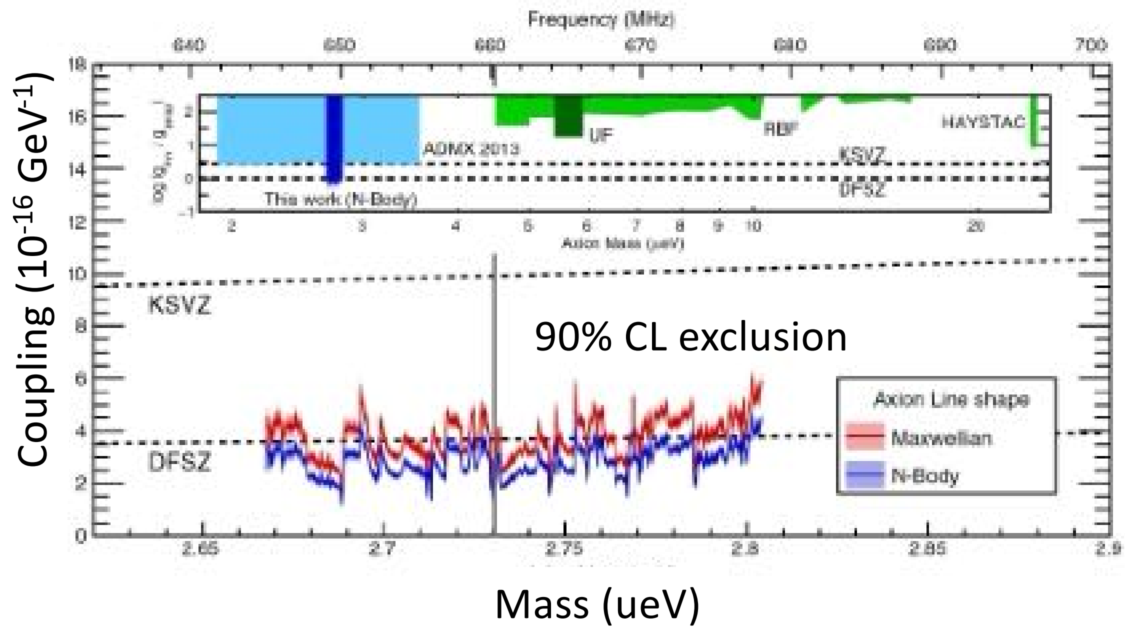

Operate an ultrasensitive radio in a cold, RF-shielded box to tune in to the axion broadcast.

Look for "spontaneous" emission from local axion dark matter into the empty cavity mode.

Signal power level = 10^{-23} W
Need 15 minutes integration per radio tuning to beat thermal noise power at 500 mK.

How a theorist sees a spherical cow

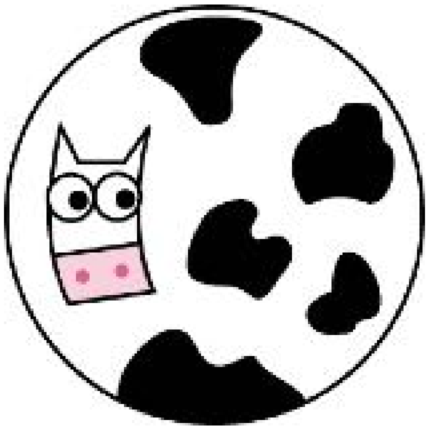

How an experimentalist sees a spherical cow

Bose-Einstein occupancy of photon modes on a 1-dim transmission line, + zero point fluctuations:

$$n(\omega) = \frac{1}{2}\coth\frac{\hbar\omega}{2kT} = \frac{1}{e^{\hbar\omega/kT}-1} + \frac{1}{2}$$

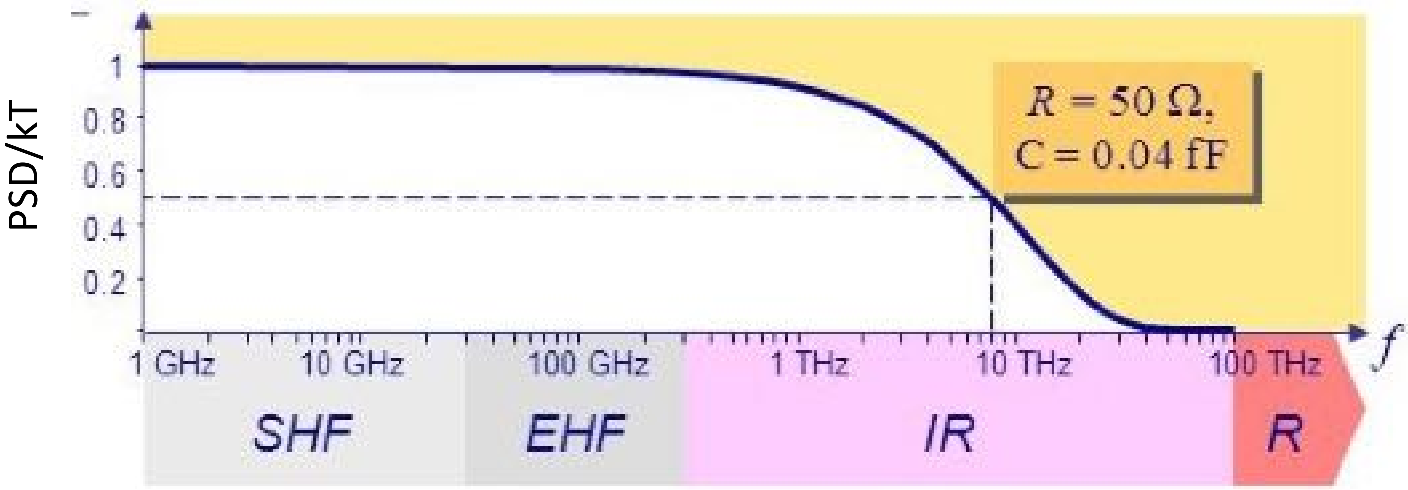

Energy/mode = kT (½ kT for each quadrature).
Modes of linewidth Δf are defined by the integration time Δt = 1/(2 Δf) required to resolve these modes.
→ **Thermal noise power emitted from each mode P = kT Δf.**

Detect small signal excesses by averaging away the noise over many power spectrum measurements

10^{-3} (for ADMX)

$$SNR = \frac{P_{\text{signal}}}{\sqrt{2}kT\Delta f}\sqrt{2\Delta f t}$$

Require >10^6 averages!

Each measurement takes 10^{-3} s to resolve a kHz-wide bin.
→ 10^6 measurements takes 10^3 s = 15 minutes.

Aaron S. Chou, QSFP lecture 2021

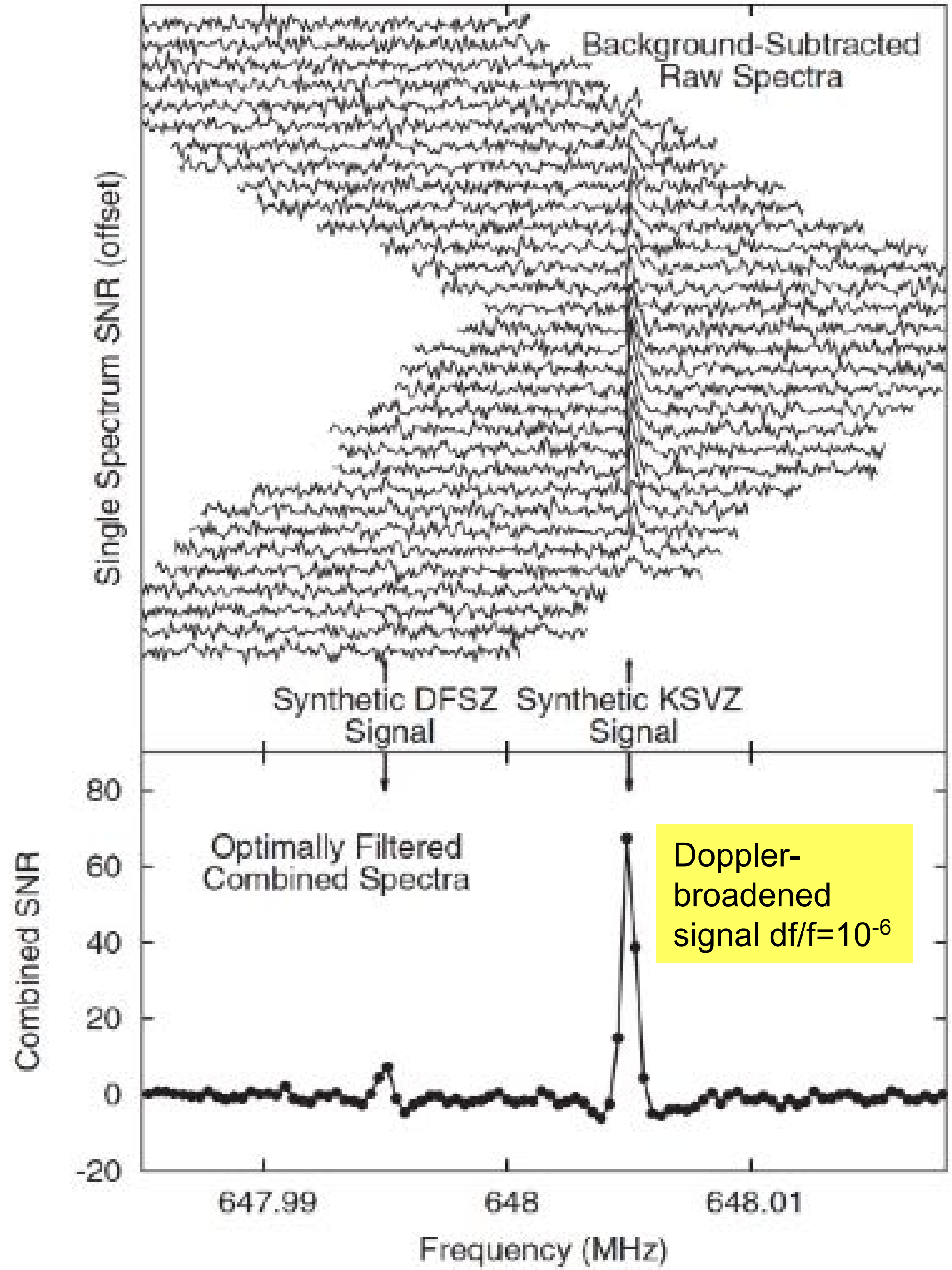

Targeting higher axion masses predicted in cosmological scenarios with *high energy scale* cosmic inflation

These simple inflation models also produce detectable primordial B-mode polarization patterns in the cosmic microwave background – science target for CMB-S4.

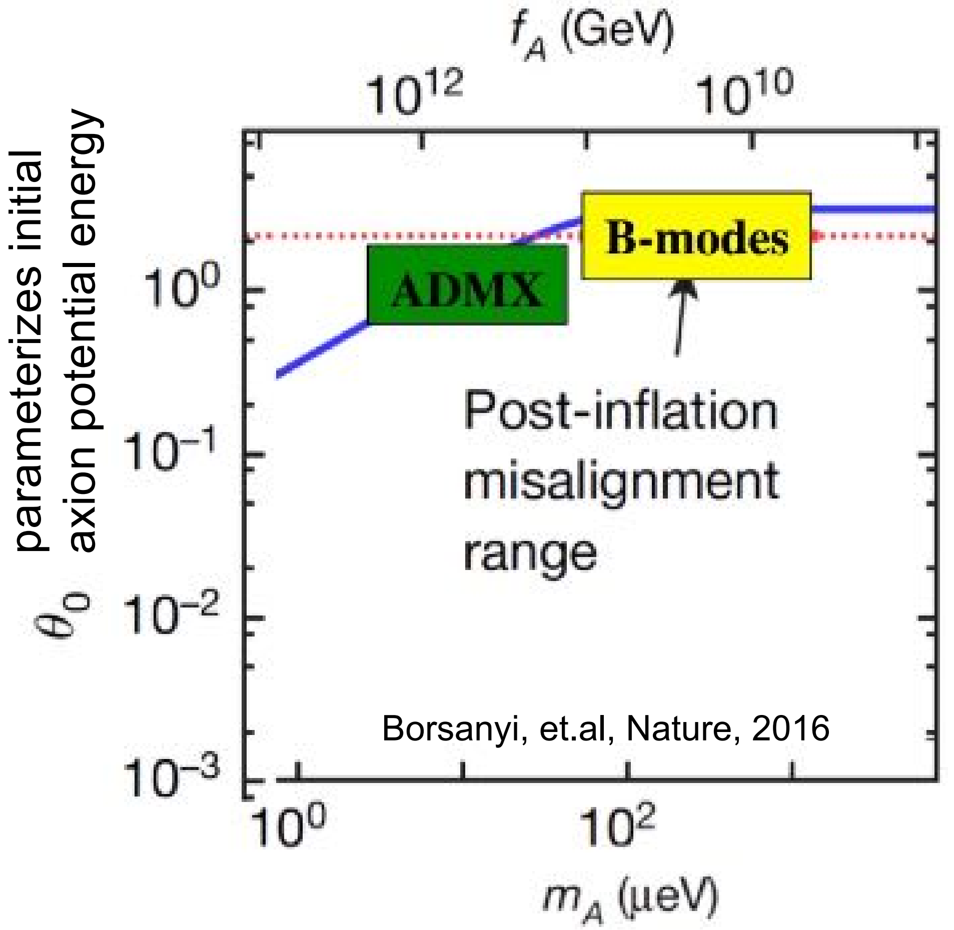

Higher axion mass allows early release of QCD vacuum energy. Avoids overproduction of dark matter.

What prevents us from immediately going to higher frequencies?

The predicted axion DM signal/noise ratio plummets as the axion mass increases → SQL readout is not scalable.

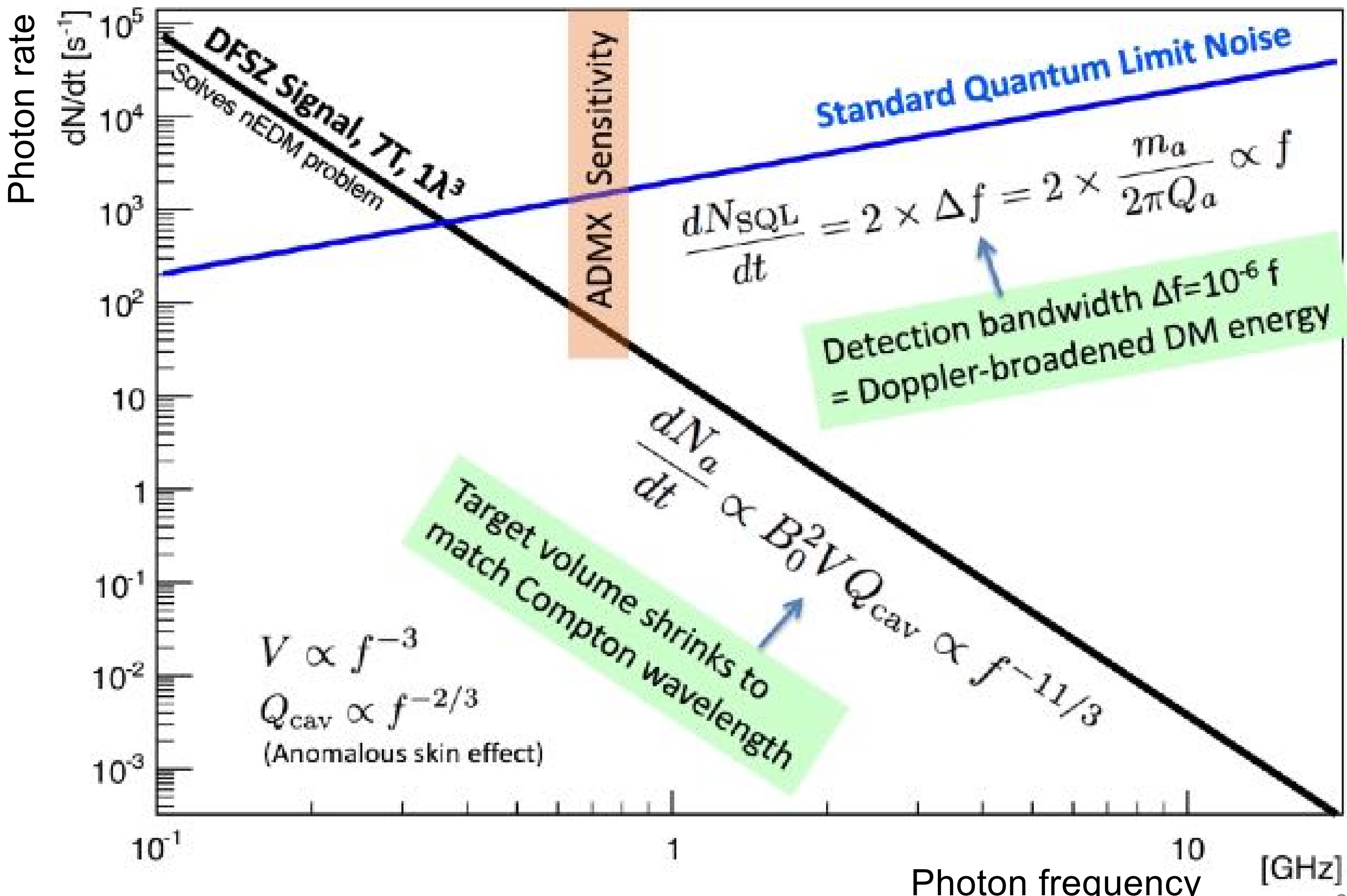

Summary of lecture 1:
Axion dark matter forms a slow classical wave

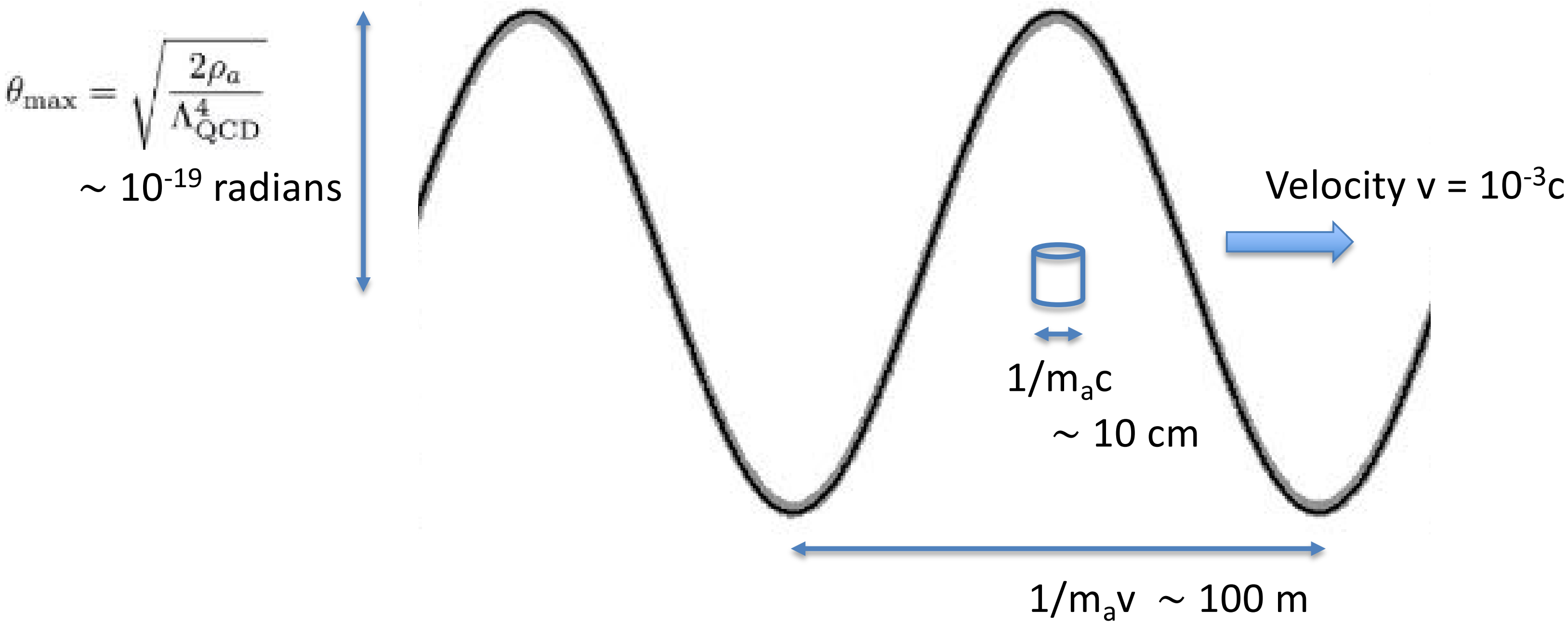

Mode volume V = $(1/m_a v)^3$
Occupation number N = $(\rho_a/m_a)V = \rho_a/m_a^4 v^3 \sim 10^{23}$

Both axion and photon waves oscillate in time at the same frequency m_a

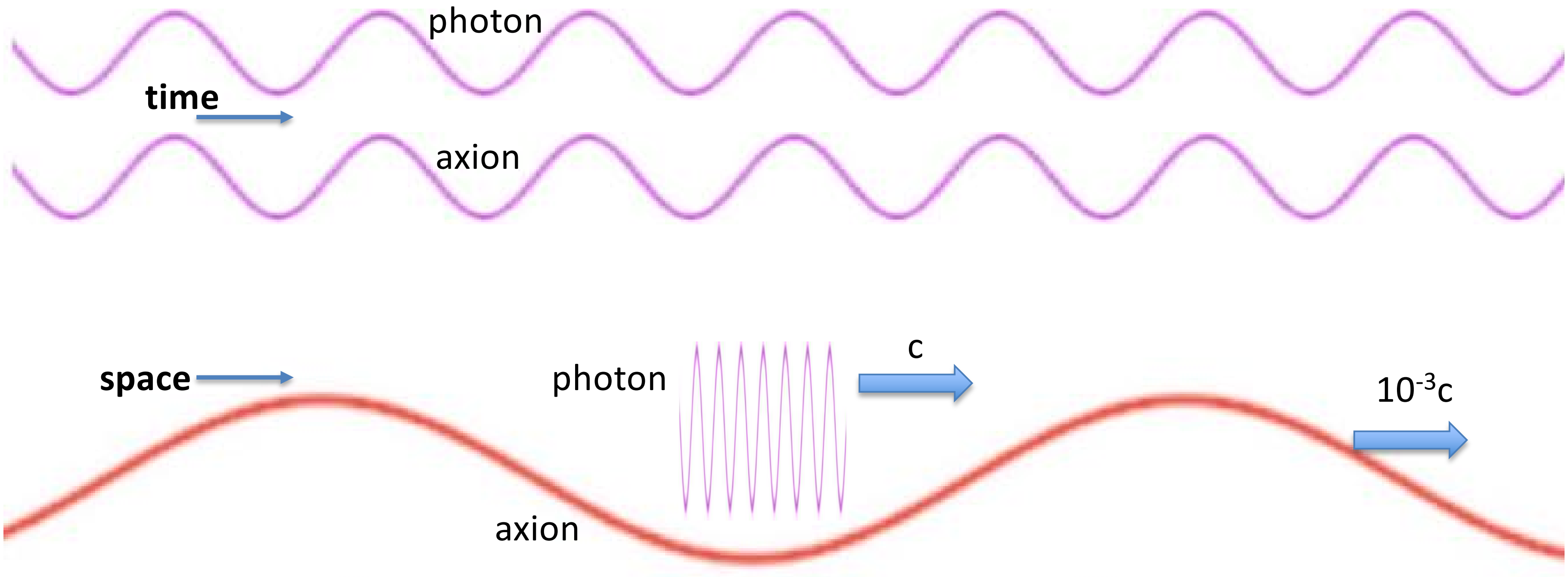

In space, the axion wave is 1000x longer and 1000x slower,
so it can coherently drive the same photon wave through $Q_a=10^6$ temporal oscillations.

In real life, the cavity has losses and so the photon might not live as long as 10^6 oscillations.

Usually $Q_c < Q_a$

Periodic boundary conditions keep the photon wave in phase with the 10^6 axion oscillations

- In a constant background B_0 field, the oscillating axion field acts as an exotic, space-filling current source

$$\vec{J}_a(t) = -g\theta \vec{B}_0 m_a e^{i m_a t}$$

which drives E&M via Faraday's law:

$$\vec{\nabla} \times \vec{H}_r - \frac{d\vec{D}_r}{dt} = \vec{J}_a$$

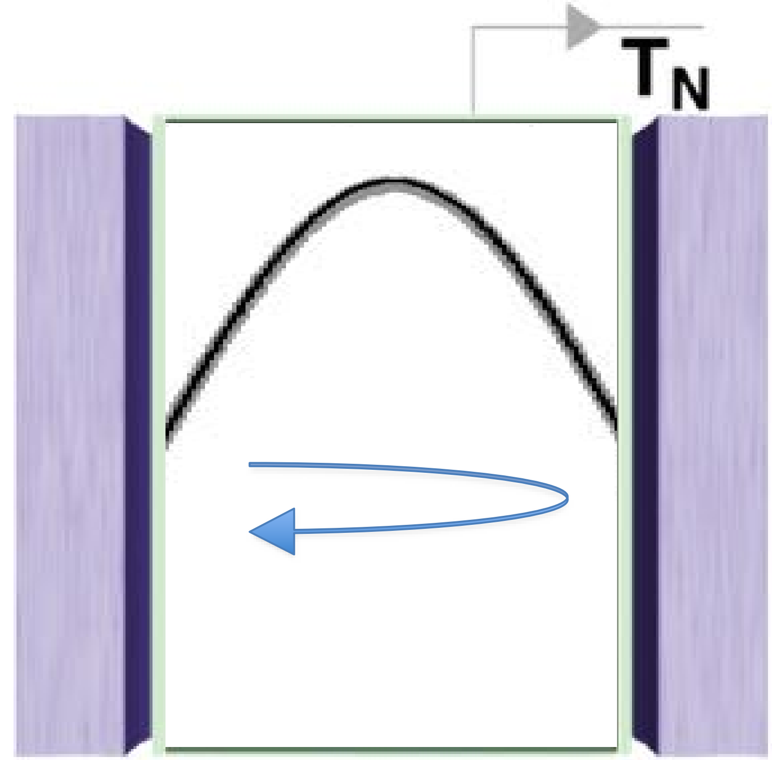

D = gθB for one oscillation…
D = gθBQ for Q coherent oscillations

Stored energy $U = D^2 V/\varepsilon$, cavity lifetime $\tau = Q/m_a$,
Signal power $P = U/\tau \sim (g\theta B)^2 V m_a Q/\varepsilon$

ε = permittivity

Energy transfer between axion and photon

Weak coupling -- takes many swings to fully transfer the wave amplitude.
In real life, Q = number of useful swings is limited by coherence time.

A classical sine wave is described by a rotating phasor:

The energy oscillates between potential energy and kinetic energy, as parameterized by the **position X** and **momentum P**.

$$H = \frac{p^2}{2m} + \frac{1}{2} m\omega^2 x^2$$

$$= \hbar\omega(a^\dagger a + 1/2)$$

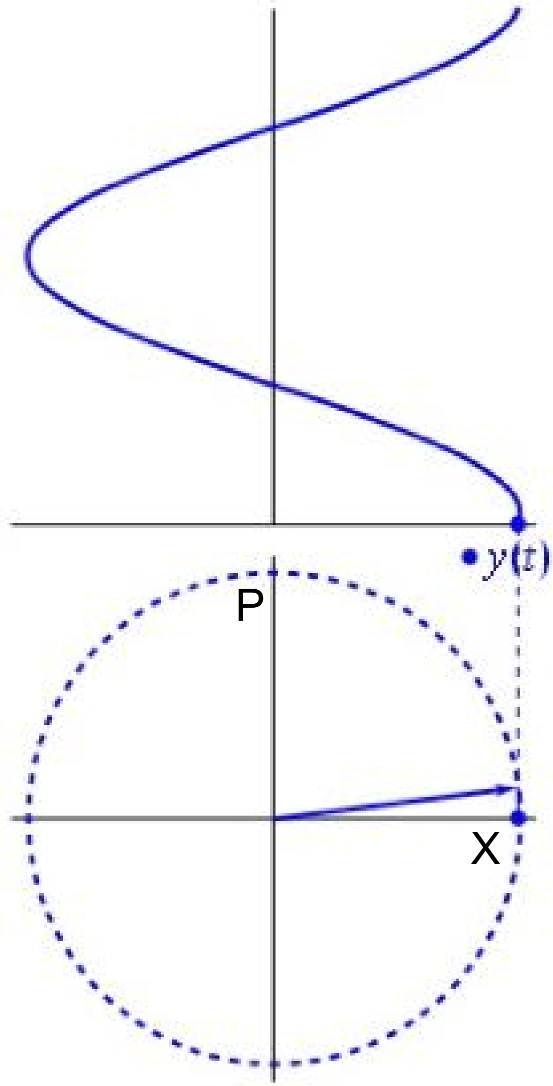

For photons, “X” and “P” are the cosine and sine quadratures of the electric field oscillation.

2nd quantization: [X,P]=i even for internal field quadratures (since these can drive mechanical oscillators.)

Heisenberg uncertainty principle
= quantization of (internal) phase space area

Wigner pseudo-probability distributions for the endpoint of the phasor:

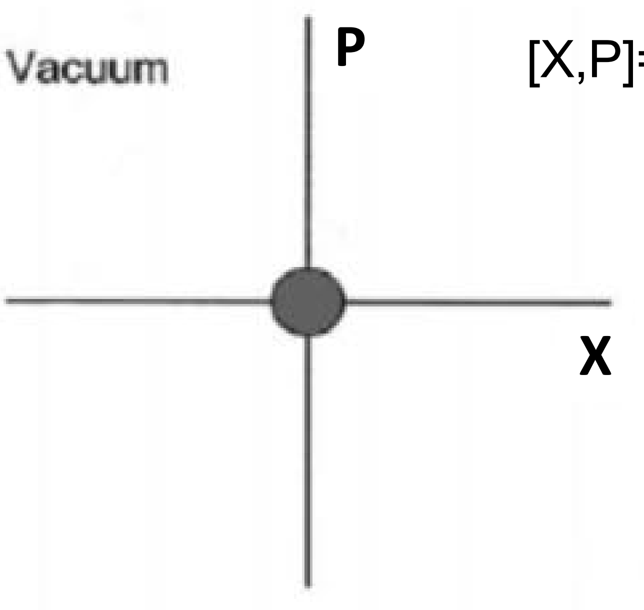

$[X,P]=i$ so $\Delta X \cdot \Delta P = ½$

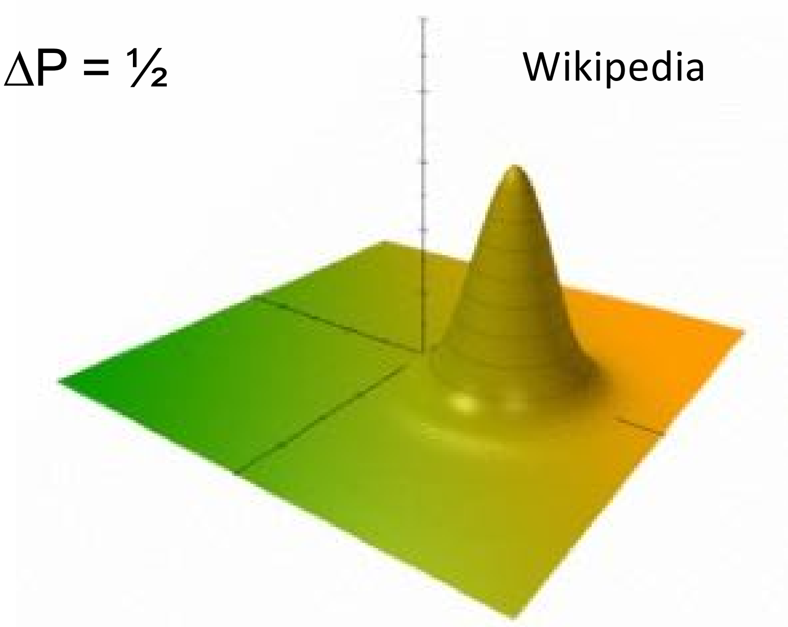

Wikipedia

The vacuum state of the oscillator is a zero length phasor which still exhibits **zero-point noise**.

Sine wave with quantum uncertainty included. The Gaussian width in the radial direction manifests as Poisson **shot noise.**

In polar coordinates, Heisenberg becomes number-phase uncertainty: $\Delta N \times \Delta \varphi \geq ½$

Classical pendulum system: $|\alpha = 3\rangle \otimes |\alpha = 0\rangle$

Time evolution of Wigner distributions in X-P "phasor" space.
Each gaussian blob of phase space area satisfies $\Delta X \cdot \Delta P = \frac{1}{2}$

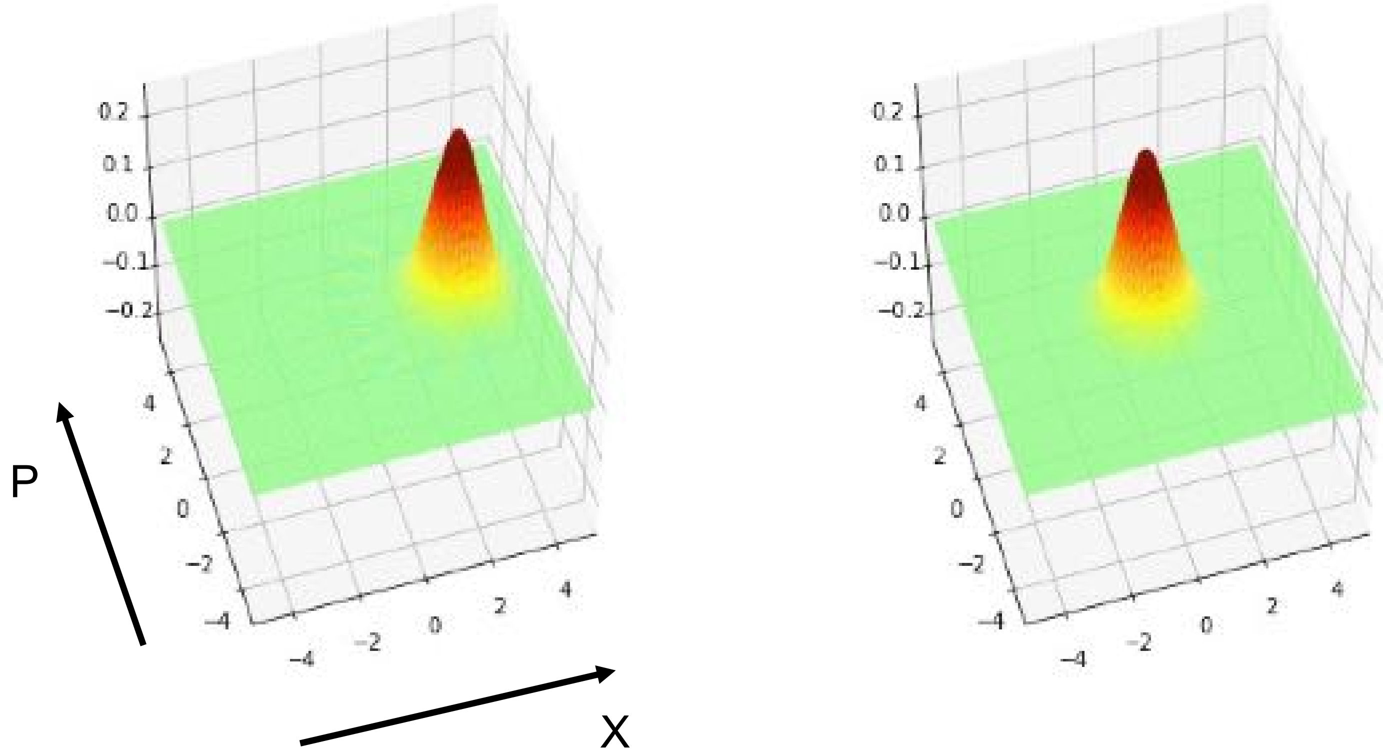

The two pendula swap their coherent states.

Simulated with QuTIP

Classically-driven quantum harmonic oscillator

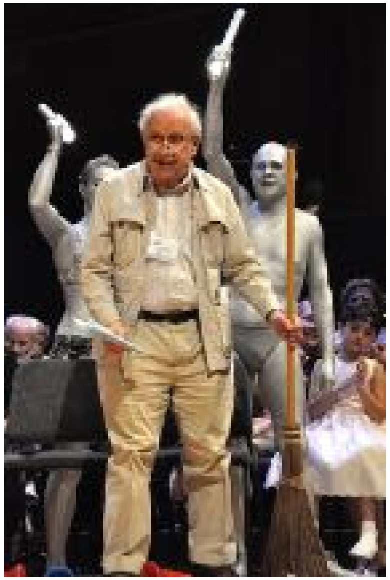

Roy Glauber
Nobel Prize
2005,
“Keeper of the
Broom”

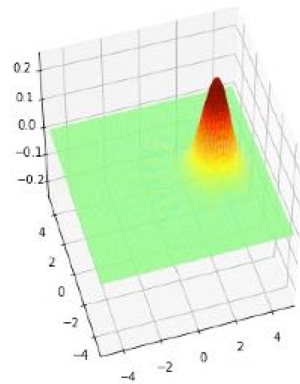

Osc1 is classical sine wave

$f(t) = f_0 e^{-i\omega t}$

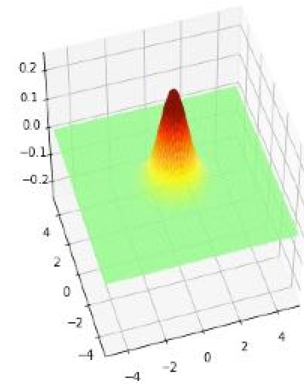

Osc2 is 2nd quantized

$a + a^\dagger$

$$\hat{H} = \hbar\omega\left(a^\dagger a + \frac{1}{2}\right) + i\hbar\left(f(t)a^\dagger - f^*(t)a\right)$$

$$U_{\mathrm{I}}(t) = \exp\left[(f_0 a^\dagger - f_0^* a)t\right]$$

Time evolution operator

$$|\psi(t)\rangle_{\mathrm{I}} = \exp[(f_0 a^\dagger - f_0^* a)t]|0\rangle = e^{-|f_0|^2 t^2/2} e^{f_0 a^\dagger t}|0\rangle$$

$\equiv D(f_0 t)|0\rangle$ **Displacement operator**

$\equiv |\alpha = f_0 t\rangle$ **Coherent state:** quantum description of a classical sine wave with amplitude $\alpha = \sqrt{\langle n \rangle}$

The Glauber displacement operator and coherent states

$$p = i\frac{d}{dx}$$ Generates translations in position

$$x = i\frac{d}{dp}$$ Generates translations in momentum

$$a^\dagger = x + ip$$
$$a = x - ip$$
Generate translations in an arbitrary direction in x-p phase space

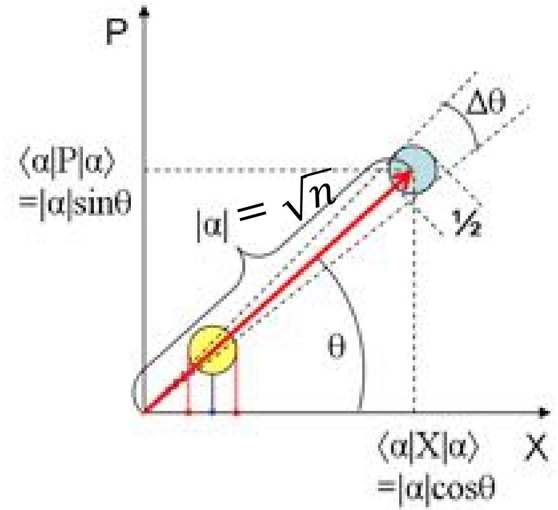

Exponentiate differential operator to get finite translation α in complex plane: $$\hat{D}(\alpha) = \exp\left(\alpha\hat{a}^\dagger - \alpha^*\hat{a}\right)$$

Phasor of amplitude α is generated as: $D(\alpha)\,|0\rangle = |\alpha\rangle$ Classical sine wave

This is an eigenstate of the annihilation operator: $a\,|\alpha\rangle = \alpha\,|\alpha\rangle$ Prove this!

Classical sine waves have intrinsic Poisson noise

Coherent states are eigenstates of the annihilation operator: $a\,|\alpha\rangle = \alpha\,|\alpha\rangle$

They form a Poisson distribution in the number state basis:

$$|\alpha\rangle = e^{-\frac{|\alpha|^2}{2}} e^{\alpha \hat{a}^\dagger} |0\rangle = e^{-\frac{|\alpha|^2}{2}} \sum_{n=0}^{\infty} \frac{\alpha^n}{\sqrt{n!}} |n\rangle$$

$$P(n) = |\langle n|\alpha\rangle|^2 = e^{-\langle n\rangle} \frac{\langle n\rangle^n}{n!}$$

$$\langle n\rangle = \langle \hat{a}^\dagger \hat{a}\rangle = |\alpha|^2$$

$$(\Delta n)^2 = \mathrm{Var}\left(\hat{a}^\dagger \hat{a}\right) = |\alpha|^2$$

Like the zero-point fluctuations, the Poisson shot noise in classical wave intensity is a consequence of the Heisenberg uncertainty principle.

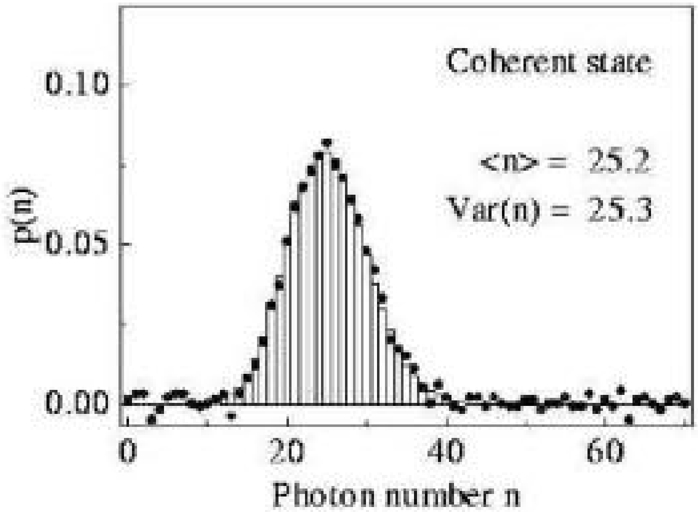

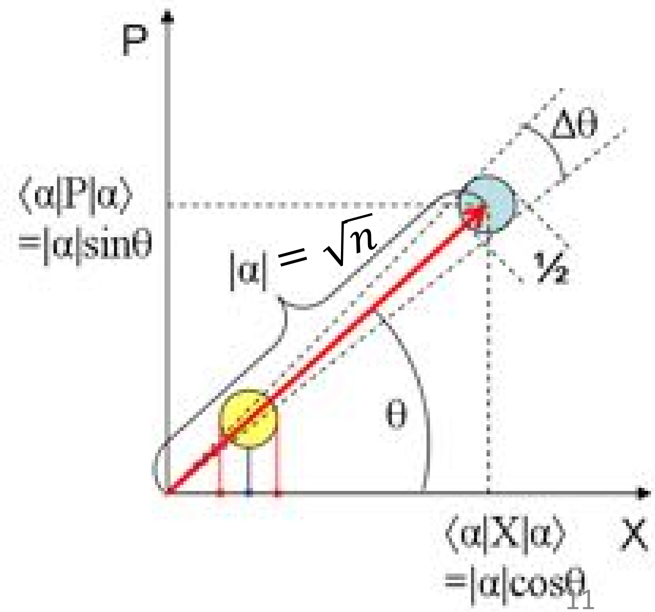

Only a small amplitude displacement of the photon field can be accumulated over the cavity or axion coherence time

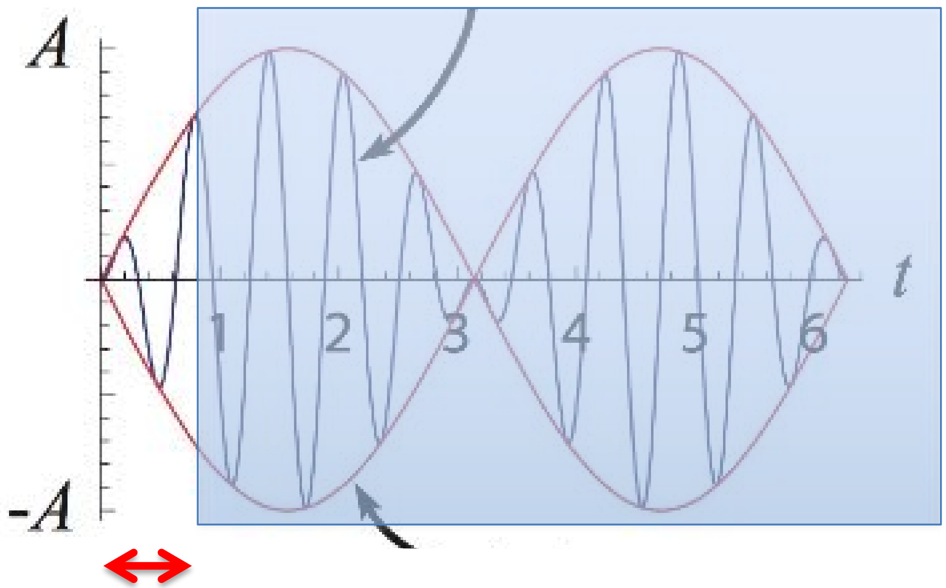

$t_{cav} = 1/df_{cav} = Q_{cav}/f$

Beat period = 1/(Interaction Energy)

>> cavity coherence time

The signal will be tiny!

Need 10^5 seconds to completely convert the axion wave into a photon wave. But only have 10^{-4} s of cavity time…

"Real world values"

$|\alpha\rangle = 10^{11}$

$\frac{\omega}{2\pi} = 10^{10}$ Hz

$\frac{2g}{2\pi} = 10^{-5}$ Hz (beat freq)

$t_{coherence} = 10^{-4}$ s

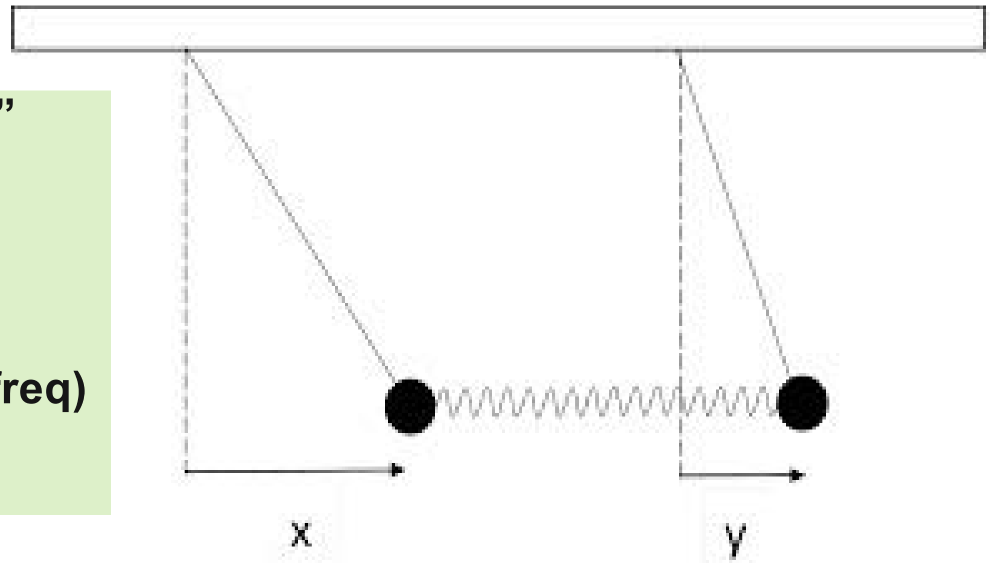

Axion = classical wave

$$\theta(t) = \sqrt{\frac{2\rho_a}{\Lambda_{QCD}^4}}\, e^{i m_a t}$$

$$H_I = \underbrace{igB\sqrt{\omega V}}_{\text{Beat frequency}}\,(\theta(t)a^\dagger - \theta(t)^* a)$$

Beat frequency (derive this!)

Due to limited coherence time << mixing period, the axion wave displaces the cavity vacuum state by an amount much smaller than the zero-point vacuum noise

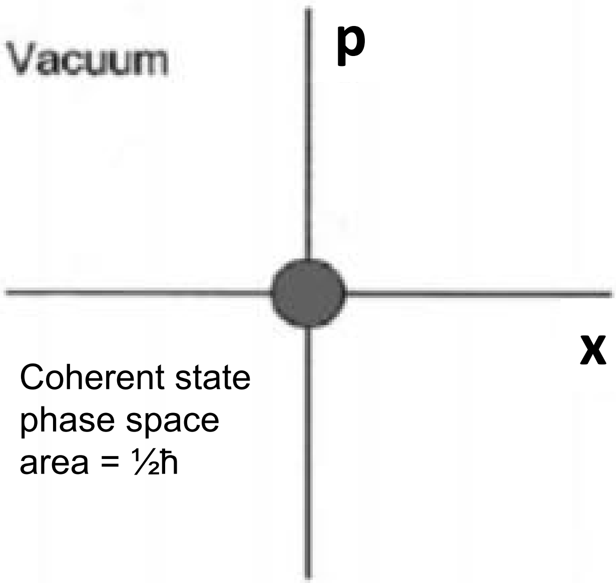

Axion-photon mixing induces tiny coherent state displacement $D(g\theta B_0 Q_{cav}/m_a^2)|0\rangle$

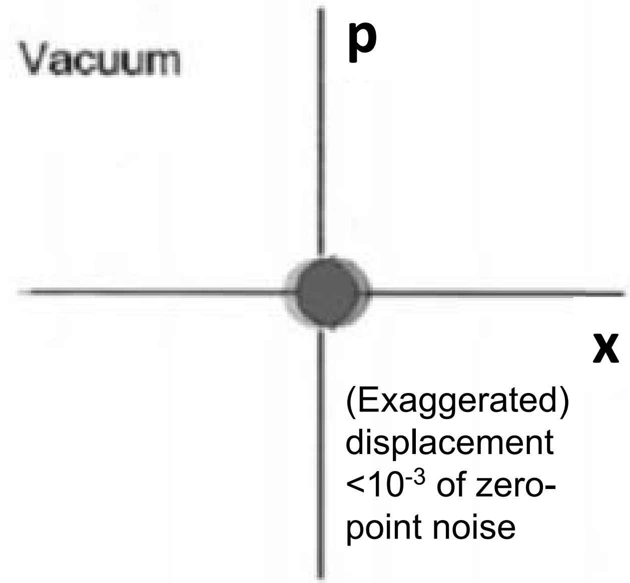

Standard quantum limit: As T→0, even the best phase-preserving amplifiers have an irreducible zero-point noise floor of +/-1 photon/mode (Carlton Caves, 1982)

Simultaneous measurement of non-commuting observables N and φ incurs the Heisenberg uncertainty principle $\Delta N \times \Delta\varphi \geq ½$. The blob is effectively the probe resolution.

Need millions of power spectrum measurements to average away the zero-point noise.

The predicted axion DM signal/noise ratio plummets as the axion mass increases → SQL readout is not scalable.

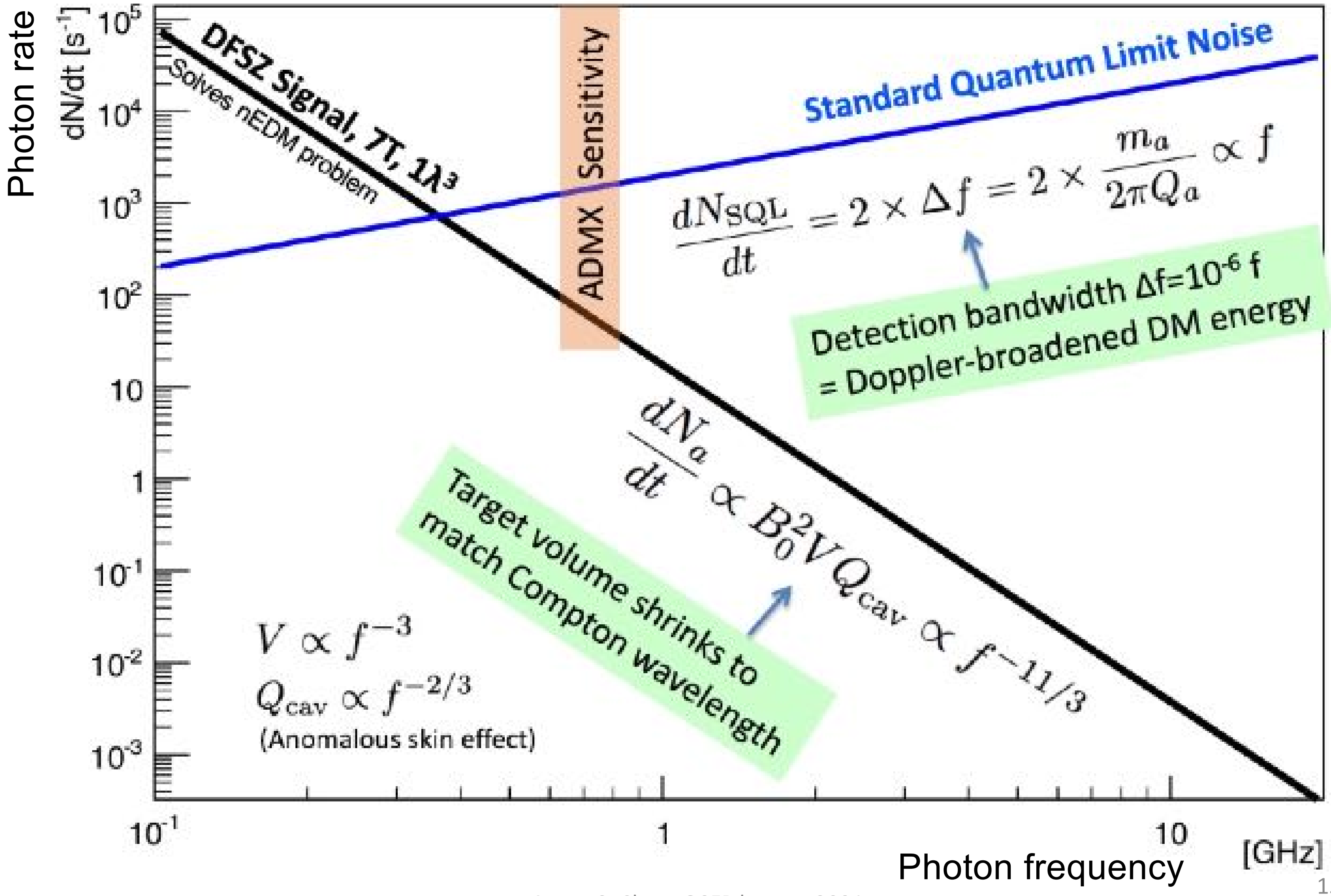

Amplifiers = scattering process via nonlinear 4-*wave mixing*

Ex. Josephson Traveling Wave Parametric Amplifier uses Josephson waveguide

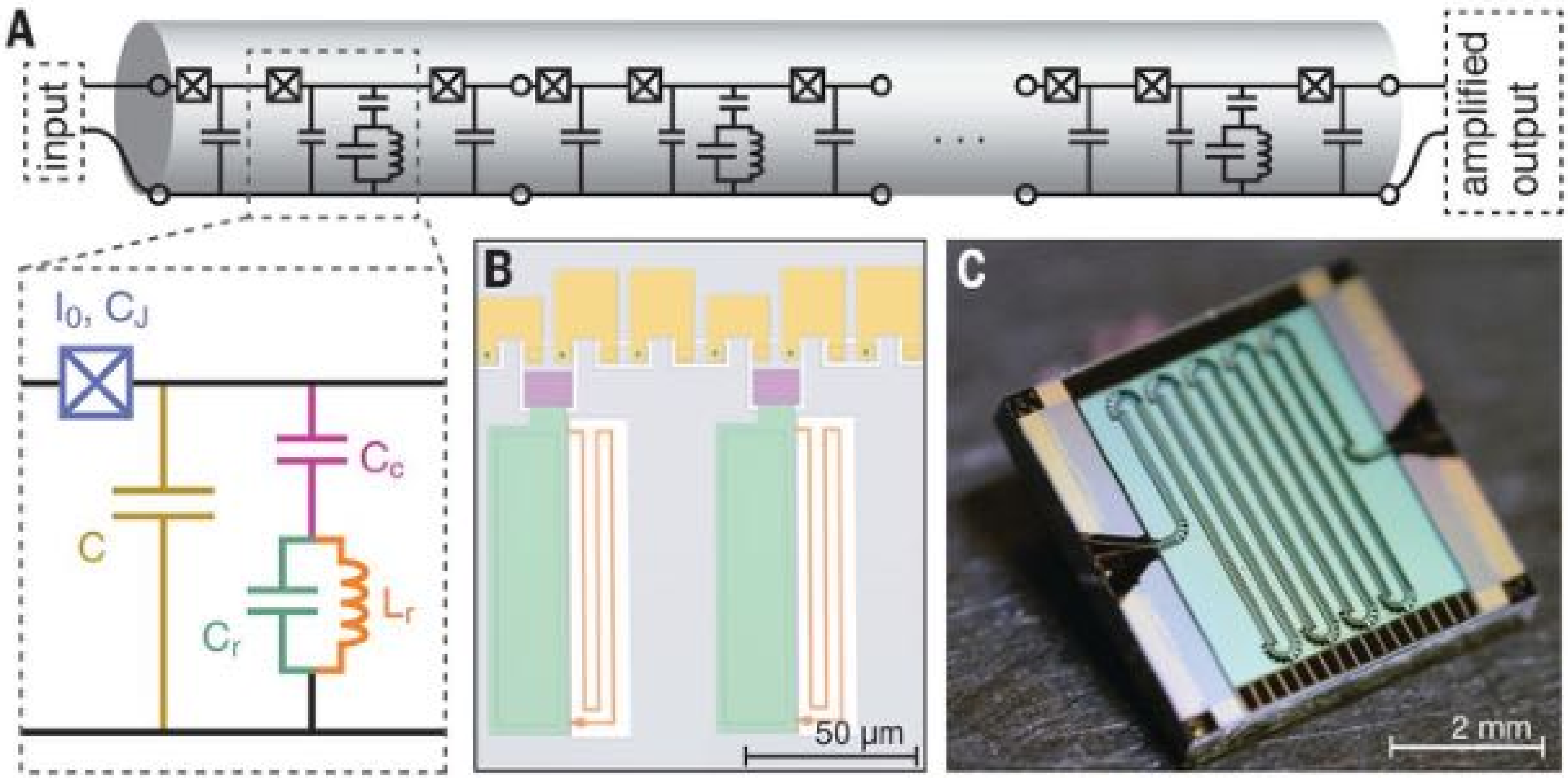

Parametric amplification:
Kicking at twice the swing frequency **amplifies** the in-phase quadrature but ***deamplifies*** the 90-degree phase quadrature

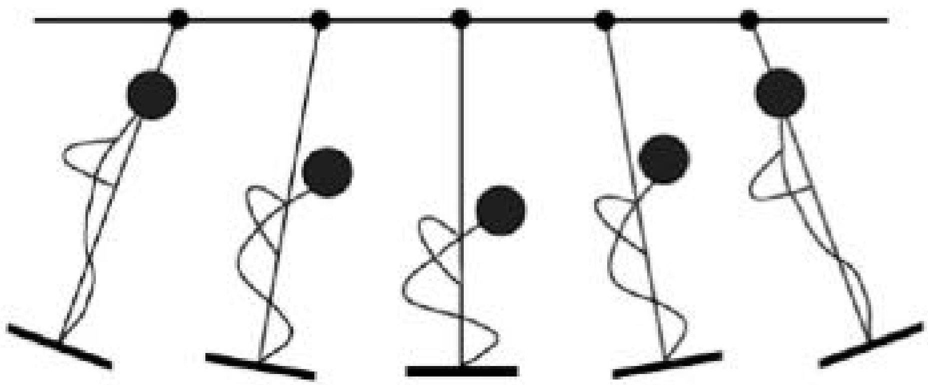

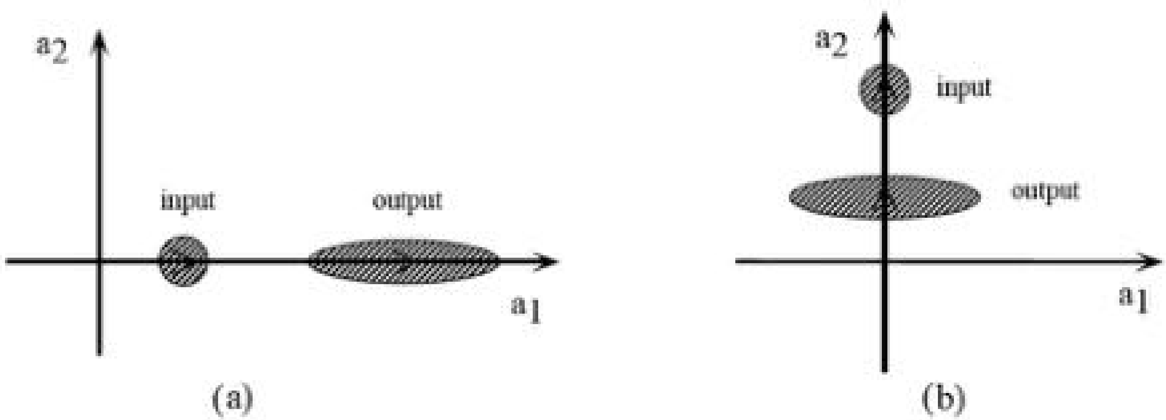

For signal frequencies offset from the pump frequency, amplifiers mix signal and idler waves and amplify both

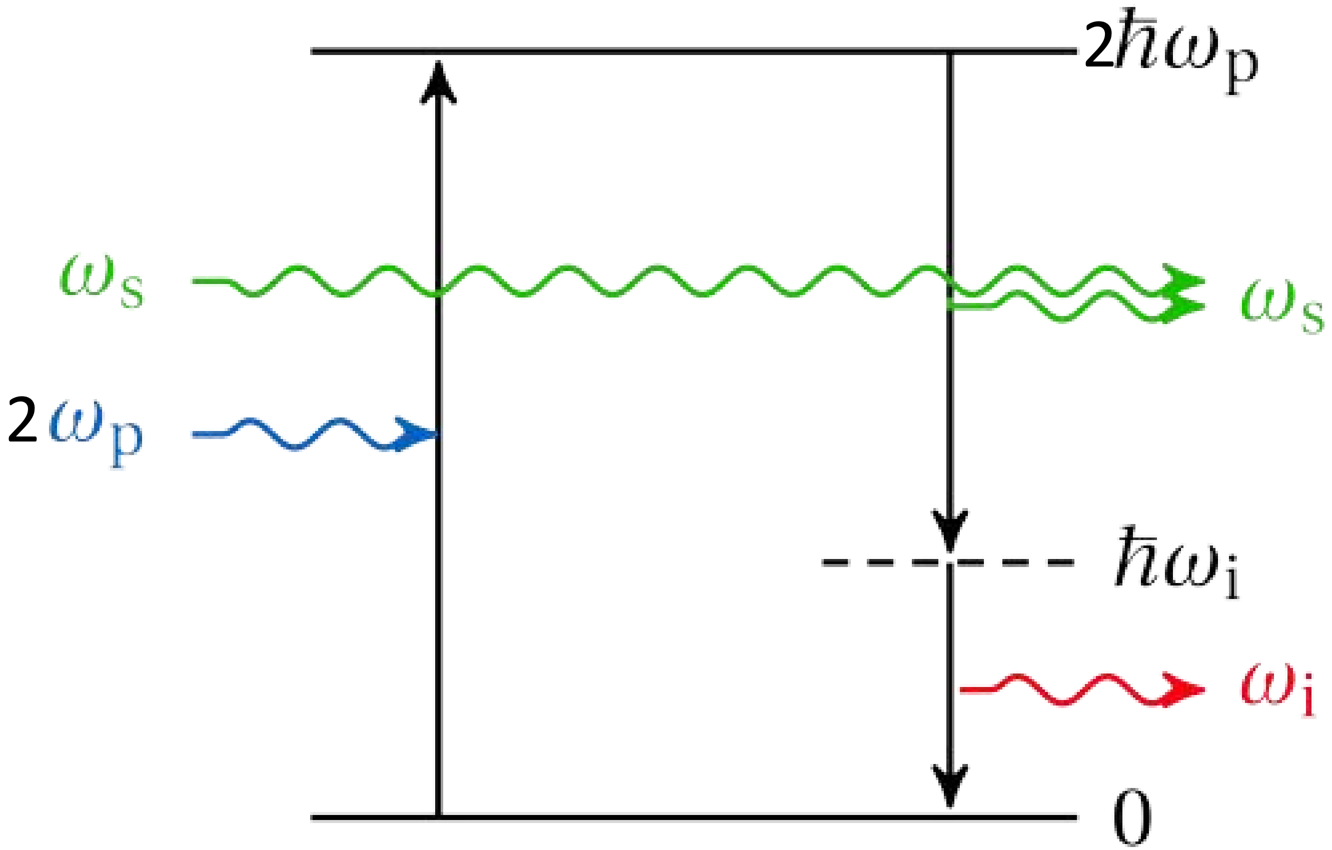

Signal + Idler

In-phase combination of signal and idler is amplified

Out-of-phase combination of signal and idler is deamplified

By superposition of above, signal in only 1 sideband generates output at both sidebands

Noise at all frequencies is amplified and doubled as it is mirrored across all sideband pairs.

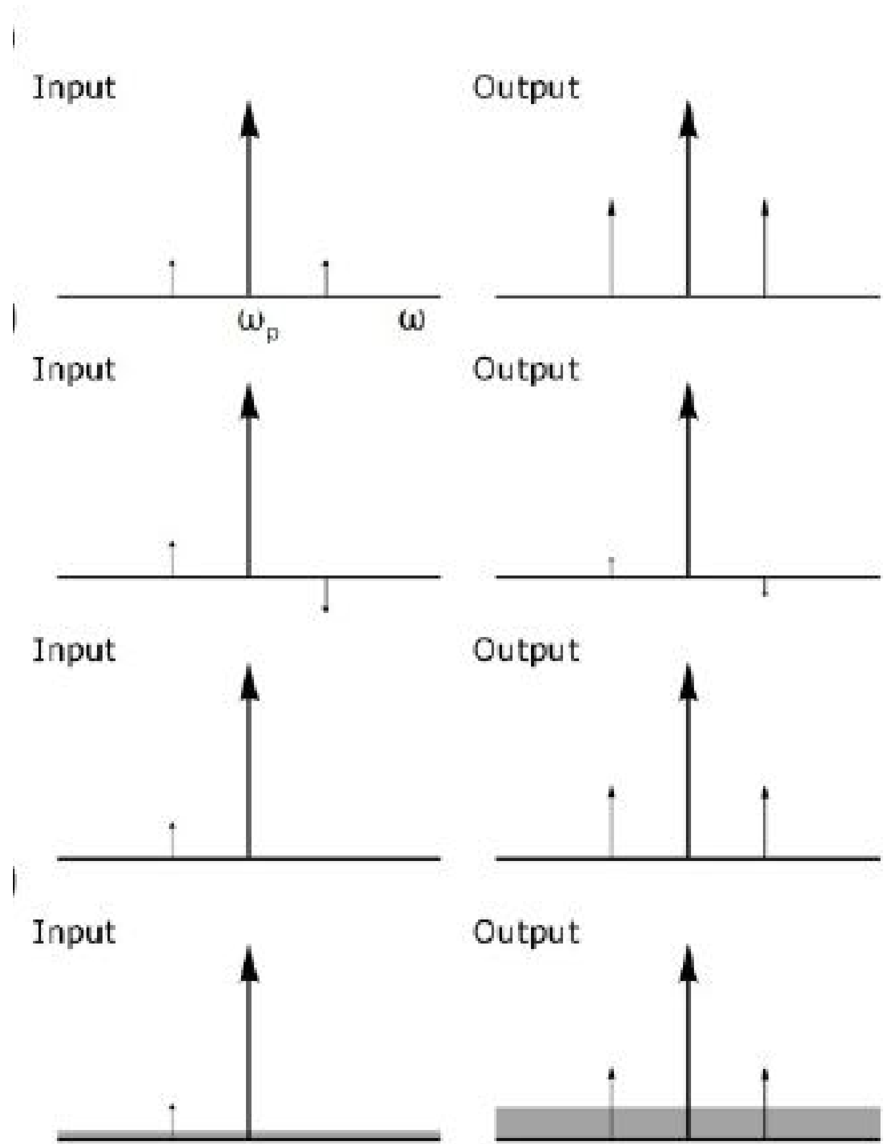

Ben Brubaker thesis

When signal and idler frequencies coincide → noiseless single quadrature amplification → squeezed states.

Inject squeezed vacuum state into the open port of the cavity.

HAYSTAC Collaboration, Nature 590 (2021)

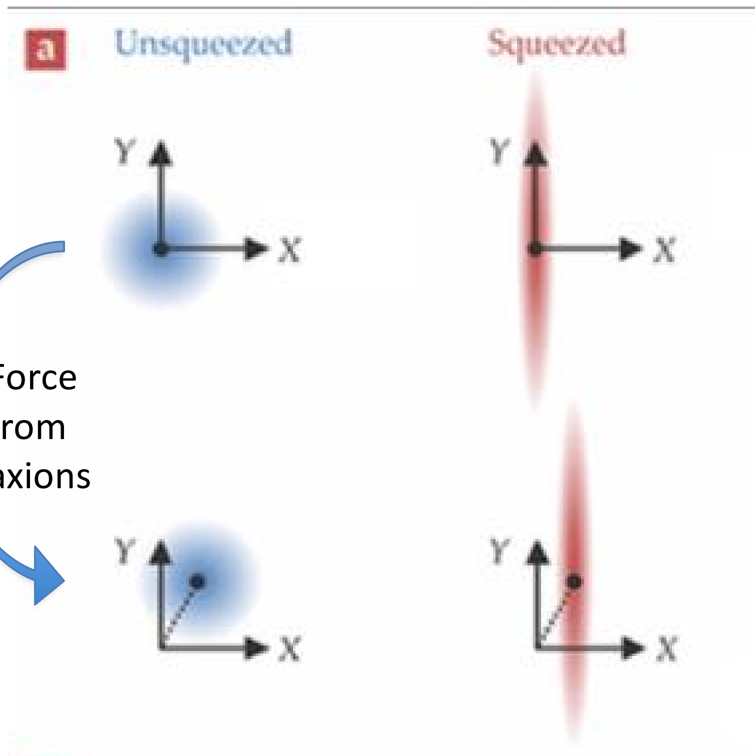

Force from axions

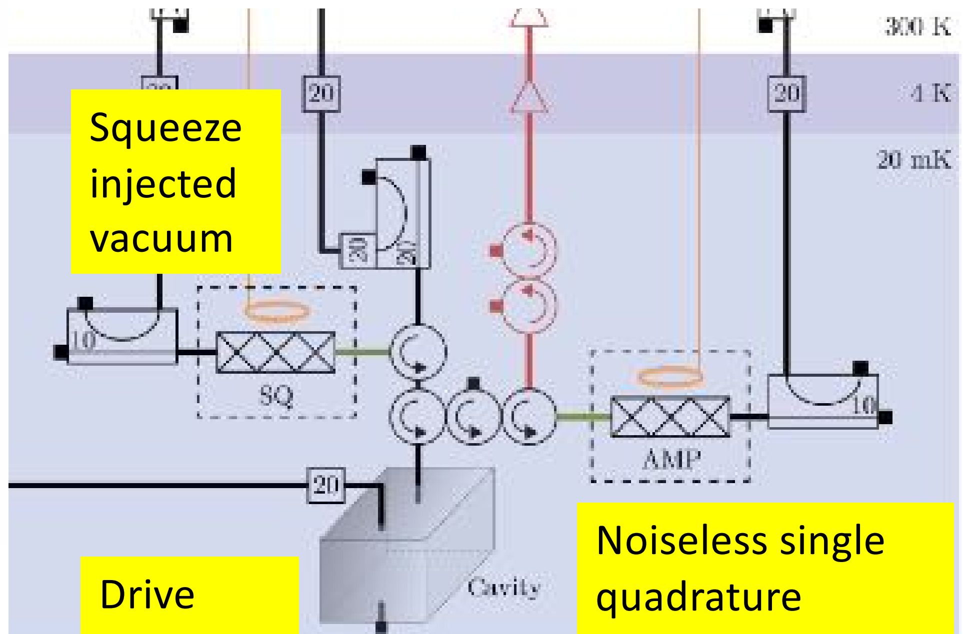

Squeeze injected vacuum

Drive with dark matter

Noiseless single quadrature amplification in orthogonal phase space direction

Again, think of the phase space distribution of the probe as its resolution function.

When squeezing the amplifier noise, the effective filter bandwidth of the cavity can be increased to many linewidths while maintaining constant Signal/(Cavity Noise) ratio

Cavity filters both signal and its own noise by the same Lorentzian transfer function.

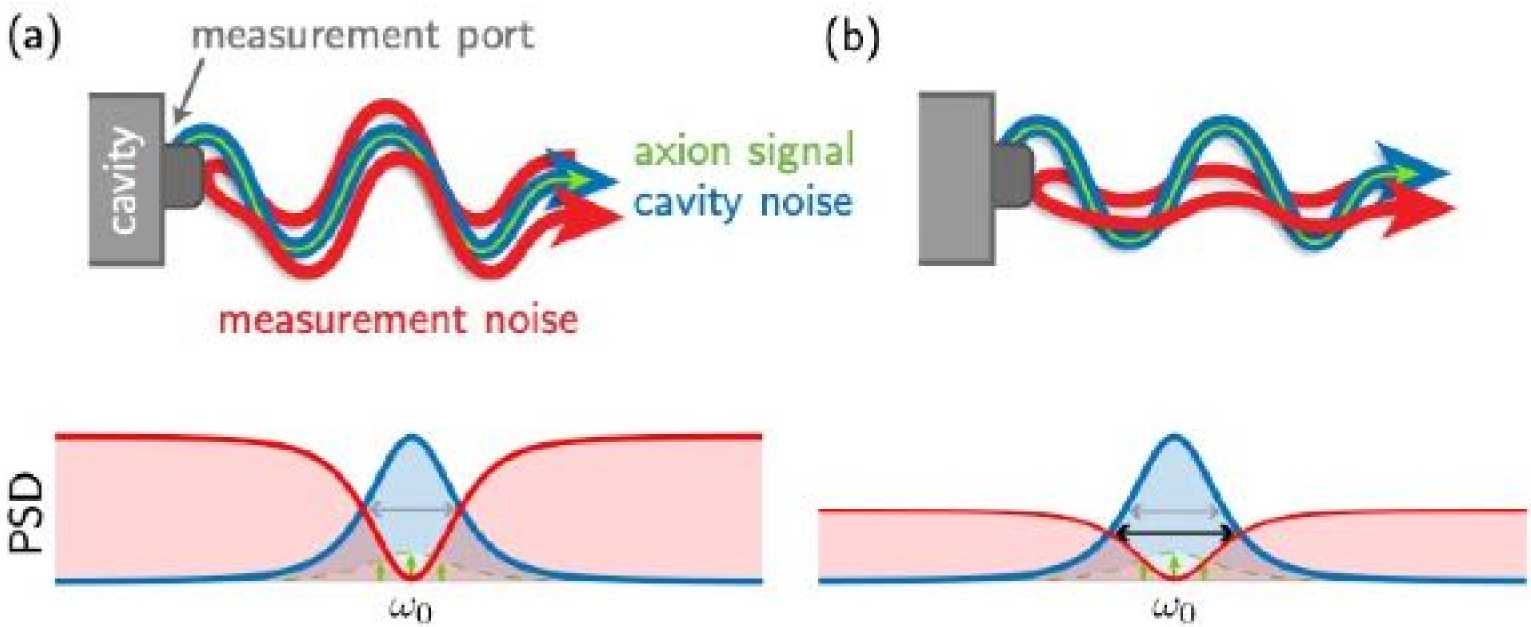

Figure from K.Wurtz, et.al, arXiv:2107.04147

Speeds up the radio scan rate since more frequencies can be simultaneously checked.

To further reduce readout noise, use photon counting to measure displacement using the Fock basis, i.e. number eigenstates

Previously we measured *both amplitude and phase*, but this is dumb since the axion phase is randomized every coherence time. Useless information obtained at high cost!

Phase space area of each annulus is still ½ħ but is squeezed in radial (amplitude) direction. Phase of photon state is randomized.

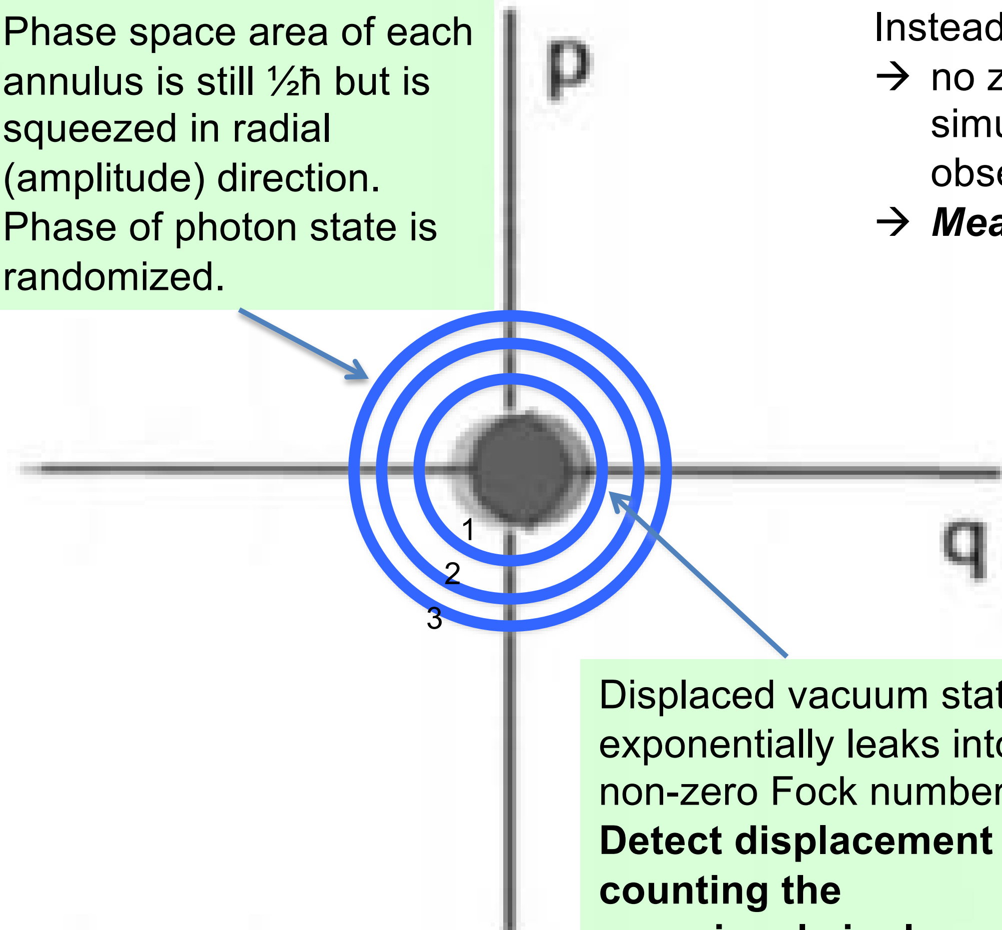

Displaced vacuum state exponentially leaks into non-zero Fock number. **Detect displacement by counting the occasional single photon.**

Instead, measure only displacement amplitude

→ no zero-point noise since we are not simultaneously measuring non-commuting observables

→ ***Measurement noise can be arbitrarily low***

Quantum non-demolition “off-shell” sensors transduce photon occupation numbers into atomic frequency shifts

Index of refraction diagrams:

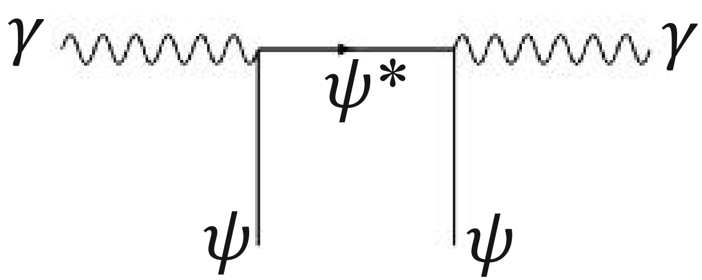

Photons slow down when passing through a dielectric medium

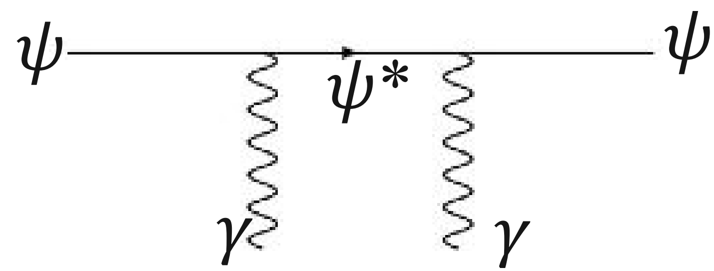

Atomic clocks slow down when interacting with a bath of background photons

The photon occupation number of the cavity mode is encoded as a frequency shift of the probe atom.

Being far off-resonance of ψ^* results in **no net absorption** of photons.

Quantum non-demolition: indirectly measure the same photon many times (via atom’s frequency shift) to achieve higher measurement fidelity.

Cavity QED:
Use 2-level atom to measure cavity photon population

Linear cavity
Bosonic oscillator,
Number operator = $a^\dagger a$

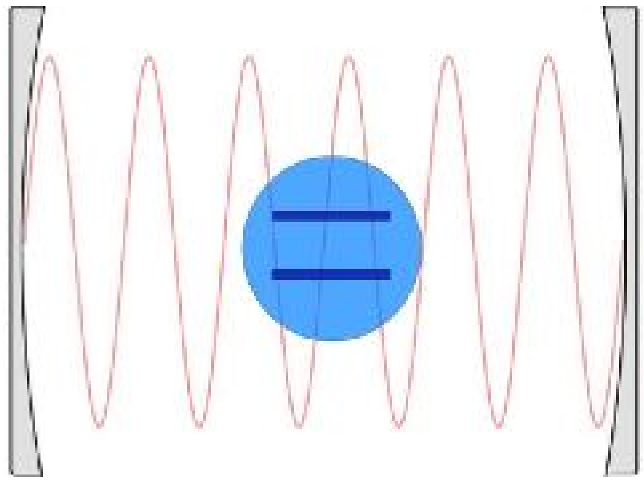

2-level "atom"
Fermionic oscillator,
Number operator = σ_z

The 1st order non-linearity in (number operator)^2 in the undiagonalized Hamiltonian is:

$$H \approx \hbar\omega_r\left(a^\dagger a + 1/2\right) + \frac{\hbar}{2}\left(\omega_a + \frac{2g^2}{\Delta}a^\dagger a + \frac{g^2}{\Delta}\right)\sigma_z$$

$g \approx \vec{d}\cdot\vec{E}_0 \approx d\sqrt{\omega/V}$

$\Delta = \omega_r - \omega_a$

The atom frequency depends on the cavity resonator's occupation number!
Frequency shift of $2\chi = 2g^2/\Delta$ per photon in the cavity mode.
This product of number operators commutes with H and allows QND measurement.

Quantum non-demolition measurements using atoms

Electric field of even a single trapped photon can "stretch" the atom and change its frequency. Just like tightening a violin string.

Serge Haroche 2012 Nobel prize: Measure the same photon with 100's of atoms using Ramsey phase-shift interferometry

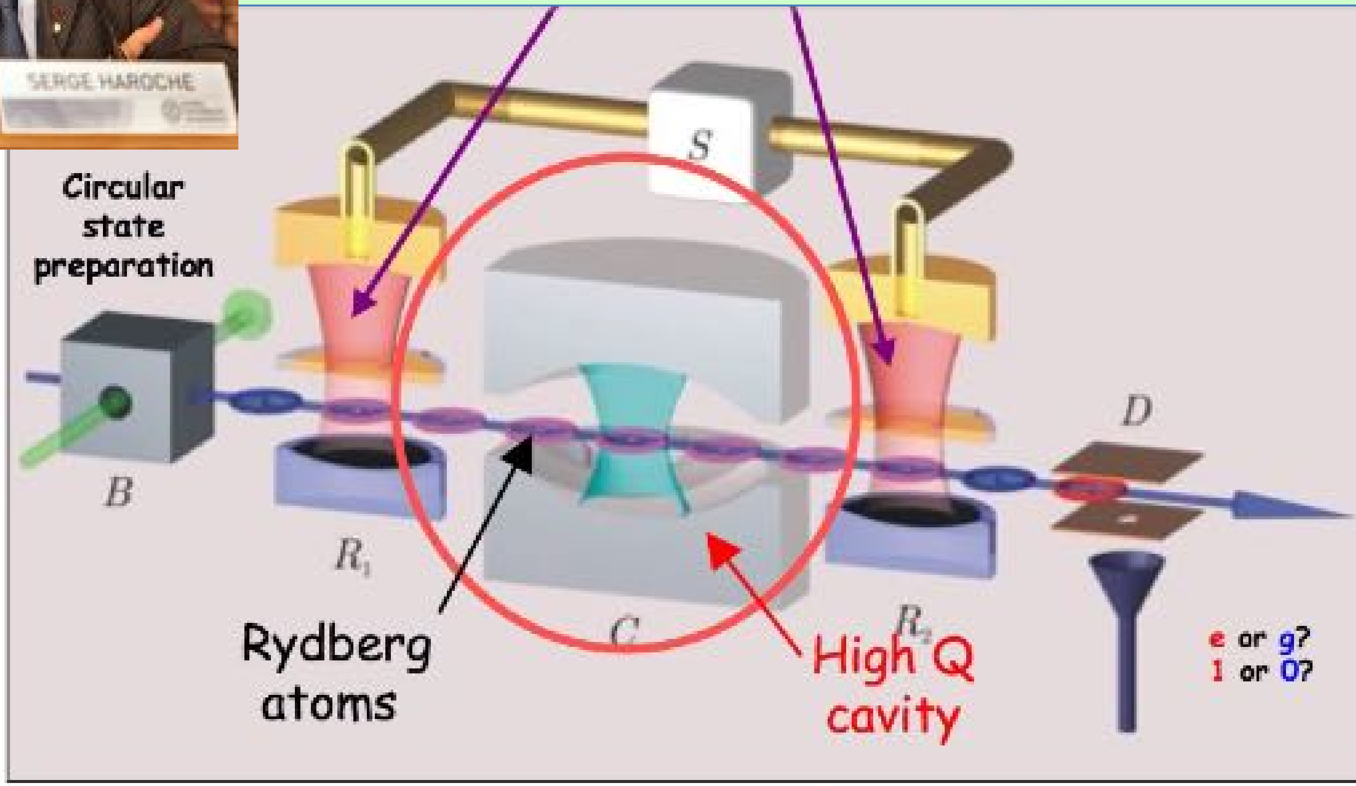

An atomic clock delayed by photons trapped inside

Quantum computing terminology: controlled phase (parity) gate

Any anharmonic oscillator exhibits 2-level system behavior and acts as a fermionic artificial atom

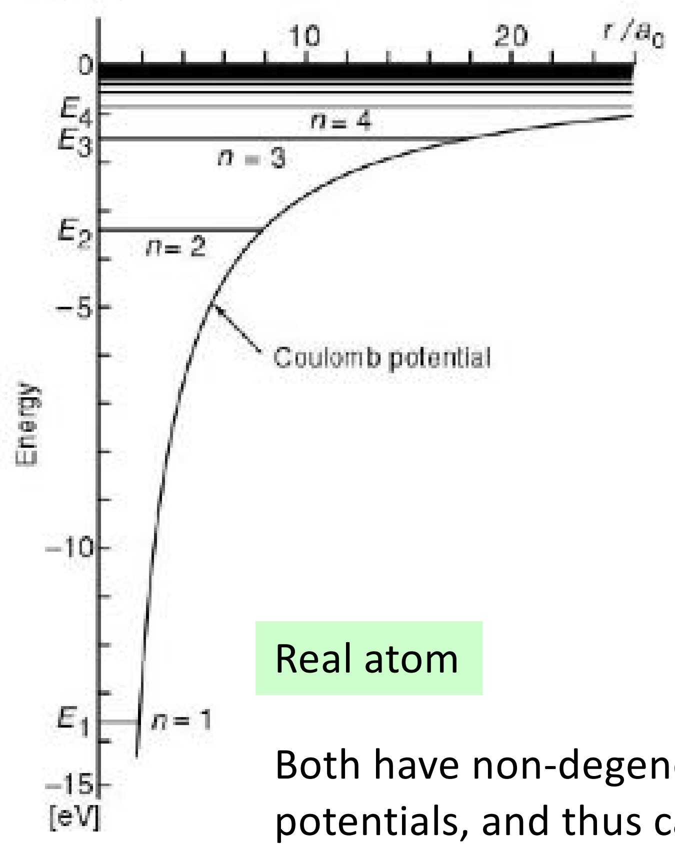

Real atom

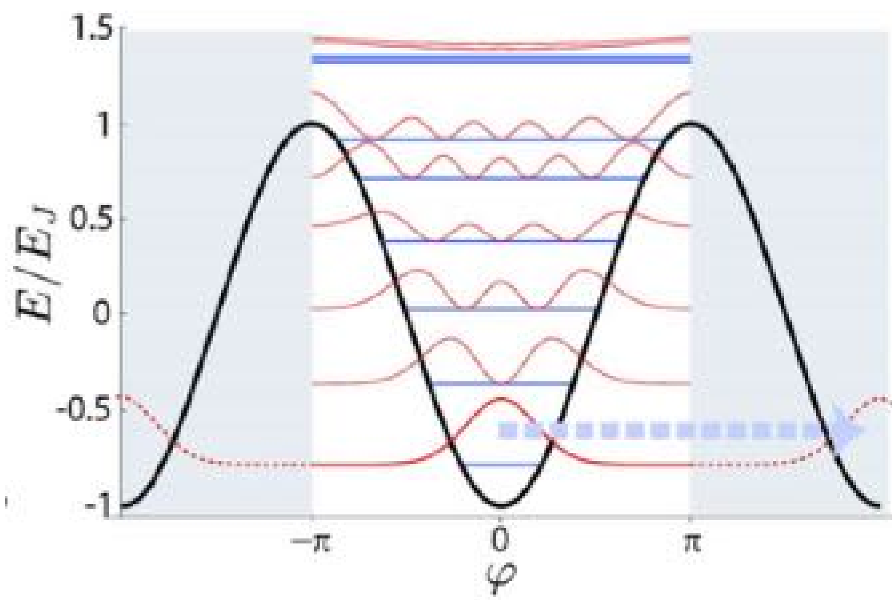

Artificial atom (Josephson junction oscillator)

Both have non-degenerate energy level spacings due to the nonlinear potentials, and thus can act as fermionic 2-level systems.

Jostling of the nonlinear oscillator due to electric fields from background photon fields result in frequency shifts as the restoring force changes for larger amplitude motion

→ Lamb shift from zero-point fluctuations

→ **quantized AC Stark shift from finite background photon occupation number**

Use artificial atoms made of superconducting "transmon" qubits to nondestructively sense photons

A.S. Chou, Dave Schuster, Akash Dixit, Ankur Agrawal, …

$$H \approx \hbar\omega_r a^\dagger a + \frac{\hbar}{2}(\omega_a' + 2\chi a^\dagger a)\sigma_z$$

Funded by

HEISING-SIMONS FOUNDATION

DOE QuantISED

Fermilab LDRD

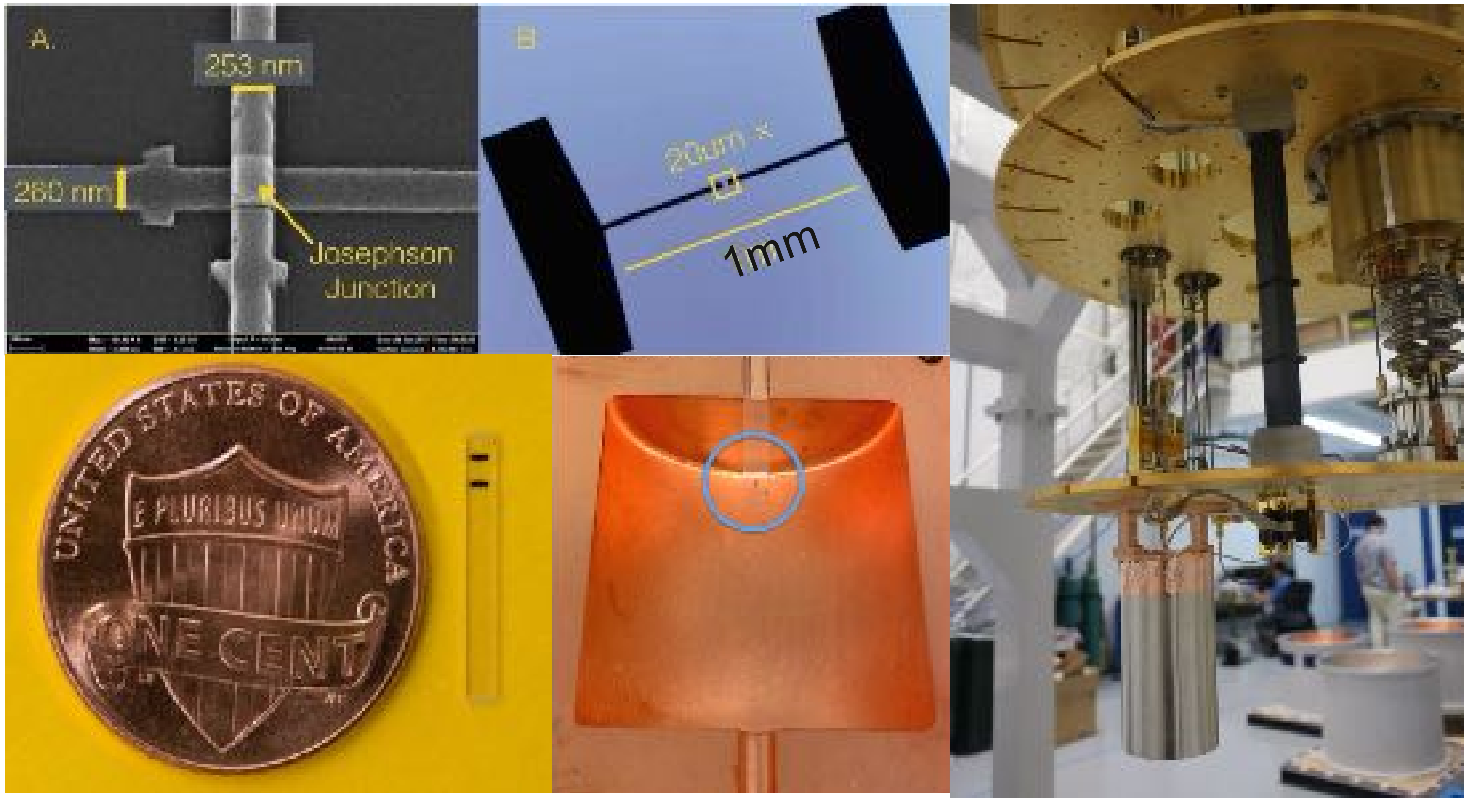

The electric field of individual photons exercises the nonlinear inductance of the Josephson junction. **Photon number is transduced into frequency shifts of the $|g\rangle \rightarrow |e\rangle$ transition.** Same as Lamb shift, but for finite photon number.

Single photon resolution:

Measure qubit $|g\rangle \rightarrow |e\rangle$ transition frequencies while weakly driving the primary cavity mode into a Glauber state with <n>=1

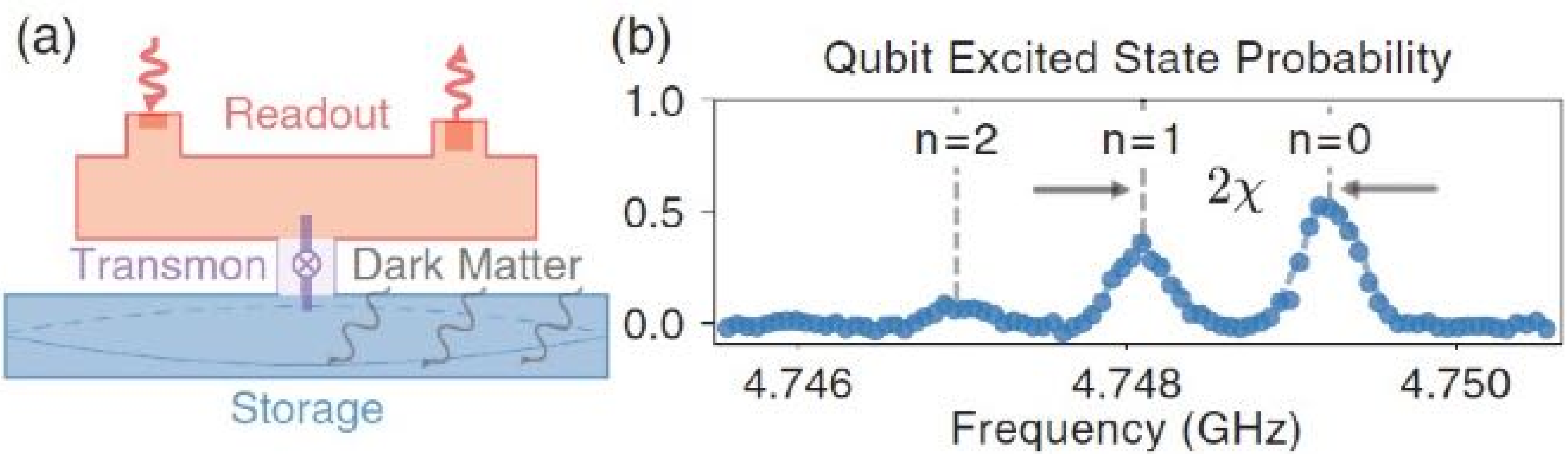

After displacing cavity with a sinusoidal drive, the measured qubit spectrum exhibits a distribution of resonances which are in 1-1 correspondence with the Poisson distribution of the cavity's coherent state.

Non-destructively count photons by measuring the qubit's quantized frequency shift.

Perform Ramsey interferometry with the oscillating qubit "clock" to measure cavity photon number parity

Just like asking in an oscillation experiment, do the neutrinos see "matter effects" or not?
If there is a photon, the clock runs slow. If no photon, the clock runs fast.

Bloch sphere:
Map qubit states to spin ±1/2

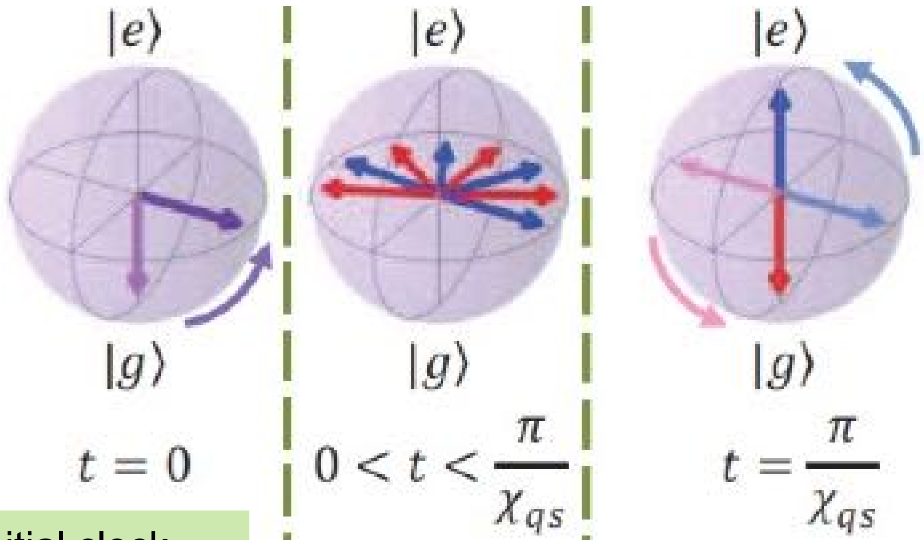

Prepare initial clock state with $\pi/2$ pulse to give $|g\rangle + |e\rangle$ state

Evolve system to accumulate π phase difference over Stark period

Analyze with final $\pi/2$ pulse to map:
Even N → $|g\rangle$
Odd N → $|e\rangle$

The qubit's "spin" flips only if a cavity photon is present.

Measure final qubit state $|g\rangle$ *or* $|e\rangle$ via freq. shift of an auxiliary cavity mode.

Aaron S. Chou, QSFP lecture 2021

Cavity QED again:
Use another cavity mode to measure atom's final state

Linear cavity
Bosonic oscillator,
Number operator = $a^\dagger a$

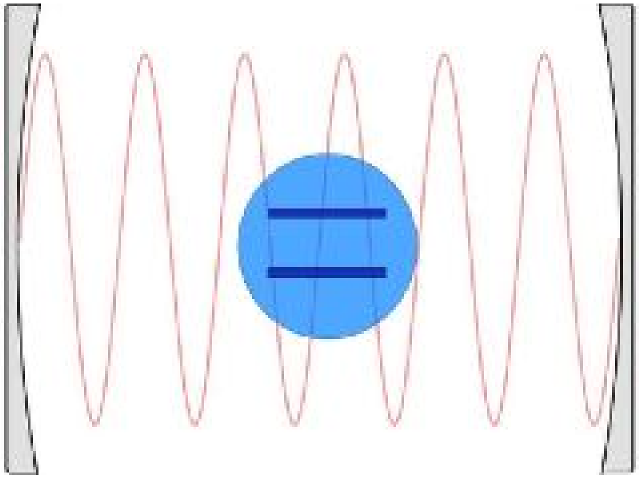

2-level "atom"
Fermionic oscillator,
Number operator = σ_z

$$H \approx \hbar\omega_r\left(a^\dagger a + 1/2\right) + \frac{\hbar}{2}\left(\omega_a + \frac{2g^2}{\Delta}a^\dagger a + \frac{g^2}{\Delta}\right)\sigma_z$$

$g \approx \vec{d}\cdot\vec{E}_0 \approx d\sqrt{\omega/V}$

$\Delta = \omega_r - \omega_a$

Rewrite as:

$$H \approx \hbar\left(\omega_r + \frac{g^2}{\Delta}\sigma_z\right)\left(a^\dagger a + 1/2\right) + \frac{\hbar}{2}\left(\omega_a + \frac{g^2}{\Delta}\right)\sigma_z$$

The cavity mode's frequency also depends on the atom's occupation number (0 or 1)!
Measure cavity's frequency shift with many probe photons without disturbing the atom.

Signature of a single signal photon is many sequential successful qubit "spin-flips" from $|g\rangle \leftrightarrow |e\rangle$

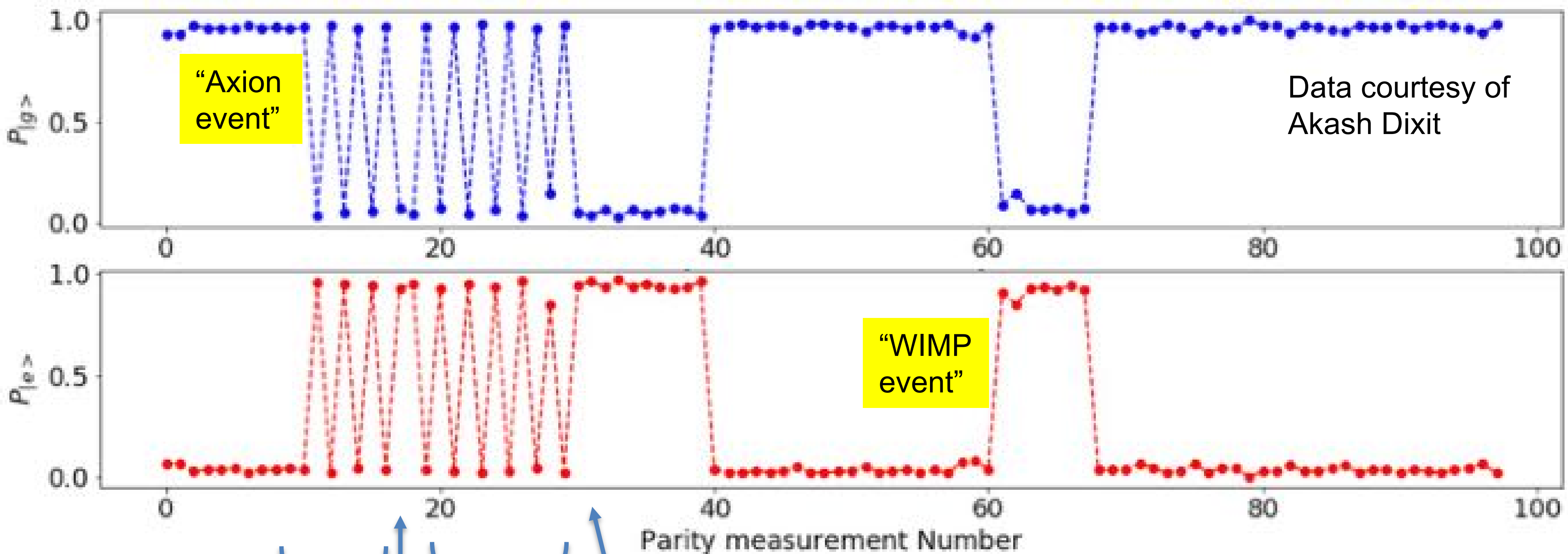

Single photon injected, repeated successful qubit spin flips

Failed spin-flip = readout error

More successful readouts

Photon decays, qubit stuck in $|e\rangle$ state

Qubit decays

Many failed spin-flips indicate that no photon is present.

Qubit spontaneously excited and then decays. Does not mimic photon event since subsequent spin-flip attempts fail.

Trigger on photons by placing threshold on MCMC probability ratio Prob(γ)/Prob(no γ) for observed spin-flip sequence

Akash V. Dixit, et.al, Phys.Rev.Lett. 126, 141302 (2021)

Background = few 10^{-3} of leakage photons per measurement.

Compare to amplifier readout which gives +/- 1 photon of zero-point variance per measurement.

Noise equivalent of 15.7 dB of squeezing!

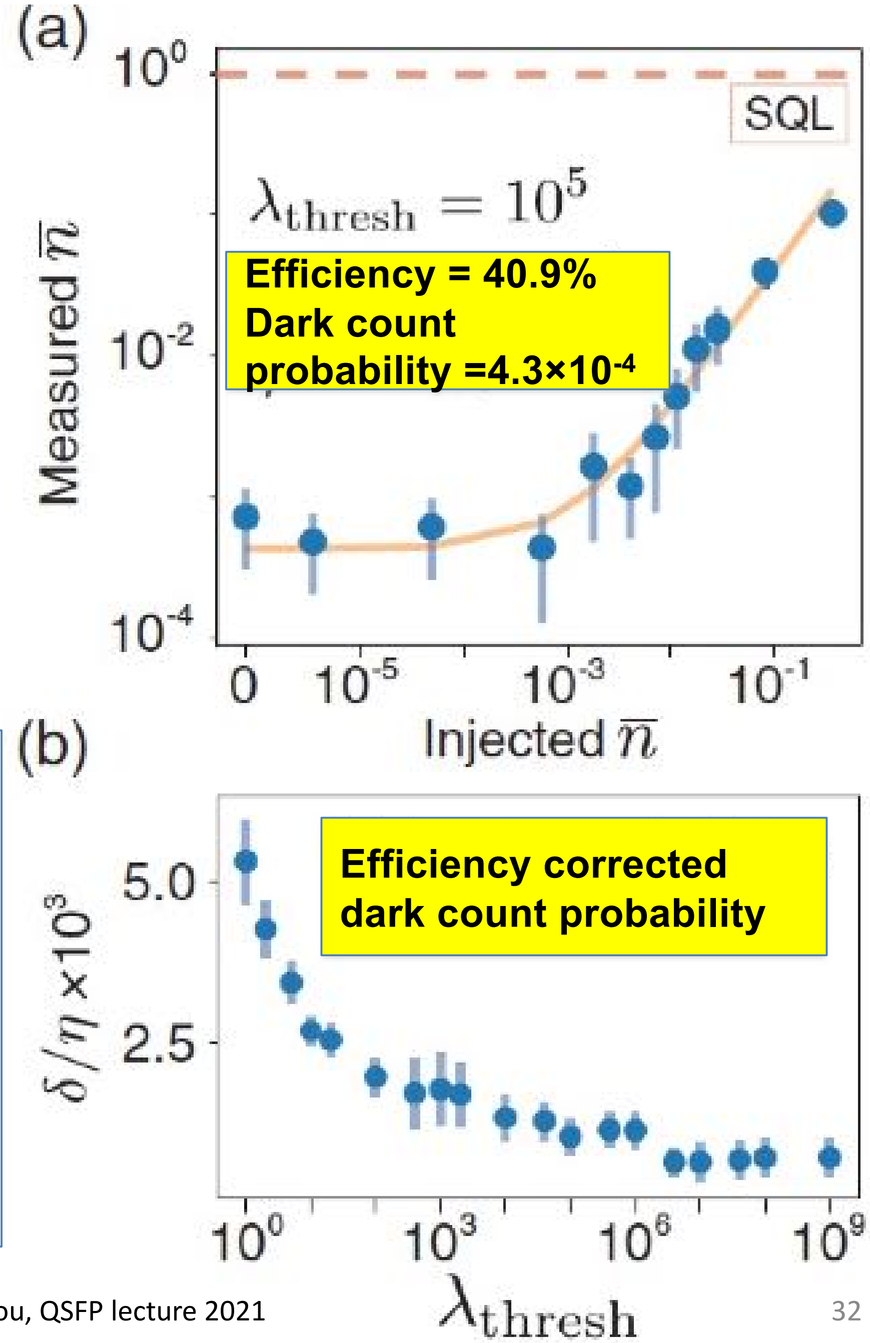

Photon counting device

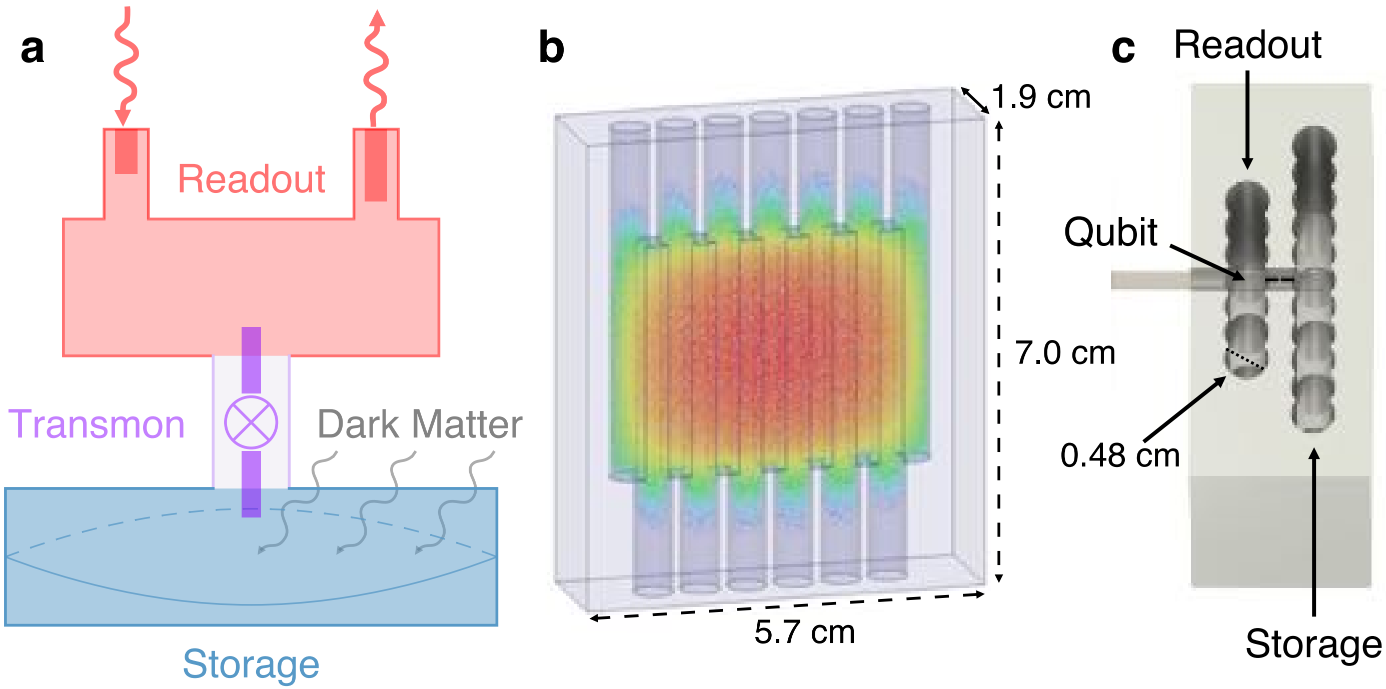

Storage	6.011 GHz
Readout	8.052 GHz
Qubit	4.749 GHz

$$\mathcal{H} = \omega_c a^\dagger a + \frac{1}{2}\omega_q \sigma_z + 2\chi a^\dagger a \frac{1}{2}\sigma_z$$

Building a microwave cavity

$$\mathcal{H} = \omega_c a^\dagger a + \frac{1}{2}\omega_q \sigma_z + 2\chi a^\dagger a \frac{1}{2}\sigma_z$$

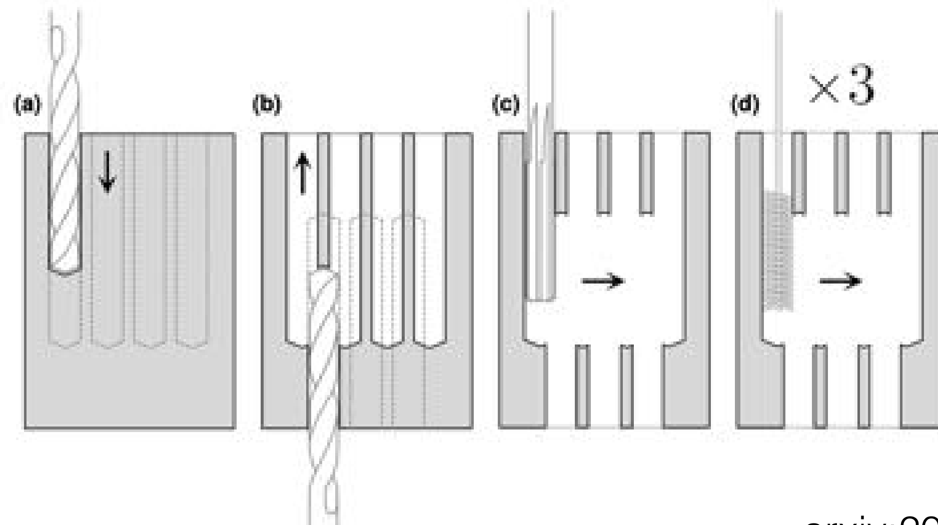

arxiv:2010.16382

Building a superconducting qubit

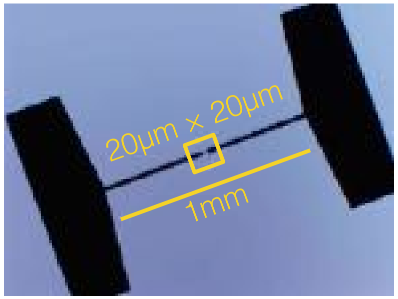

$$\mathcal{H} = \omega_c a^\dagger a + \frac{1}{2}\omega_q \sigma_z + 2\chi a^\dagger a \frac{1}{2}\sigma_z$$

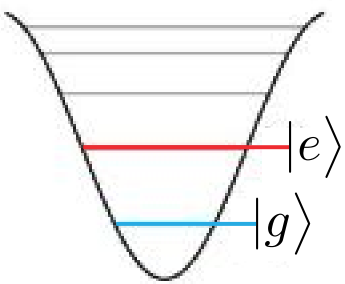

Harmonic Oscillator (LC) +
nonlinearity (Josephson Junction)

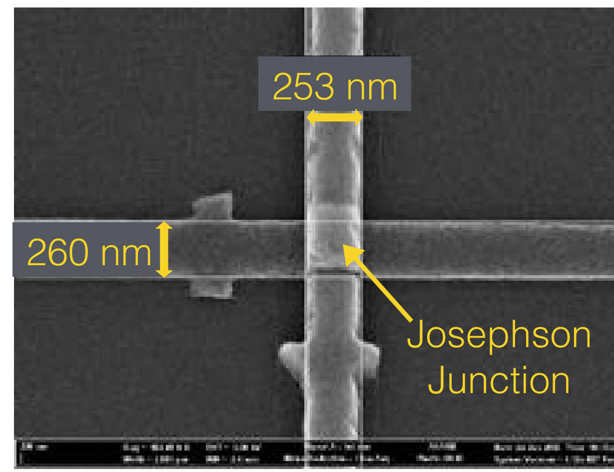

Engineering the qubit-cavity interaction

$$\mathcal{H} = \omega_c a^\dagger a + \frac{1}{2}\omega_q \sigma_z + 2\chi a^\dagger a \frac{1}{2}\sigma_z$$

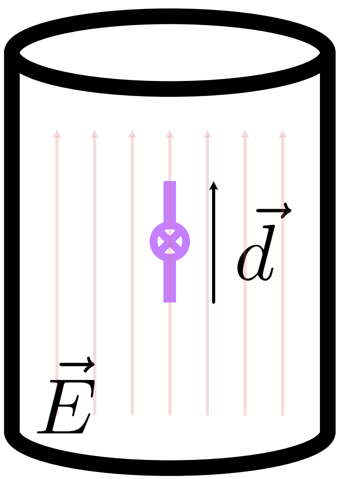

$$\begin{aligned}\mathcal{H}_{int} &= \vec{d}\cdot\vec{E} \\ &= g(\sigma_+ + \sigma_-)(a + a^\dagger) \\ &\sim 2\chi a^\dagger a \frac{1}{2}\sigma_z\end{aligned}$$

Δ qubit-cavity detuning

α qubit anharmonicity

$$\chi = \frac{g^2}{\Delta(\Delta+\alpha)}\alpha$$

Exercises

- Calculate order of magnitude of g
- Compare to an atom from nature
- Derive dispersive interaction from Jaynes-Cummings hamiltonian

Operate device in very cold environment

Device cooled to 8mK

Why so cold?

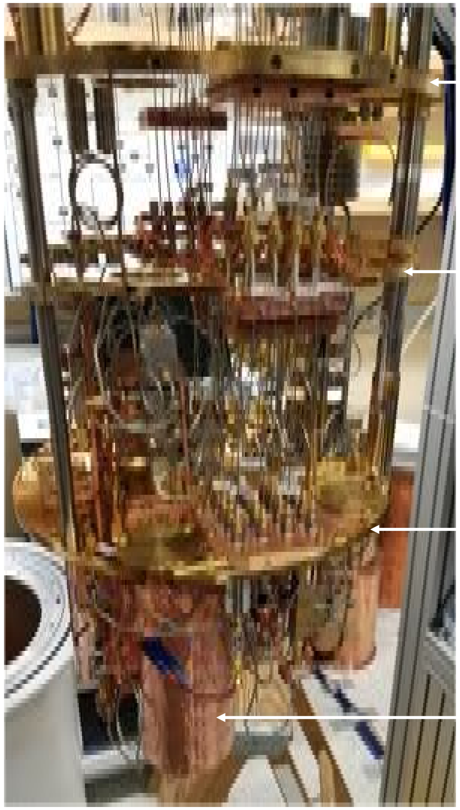

Cavity occupation imprinted on qubit transition frequency

$$\mathcal{H} = \omega_c a^\dagger a + \frac{1}{2}(\omega_q + 2\chi a^\dagger a)\sigma_z$$

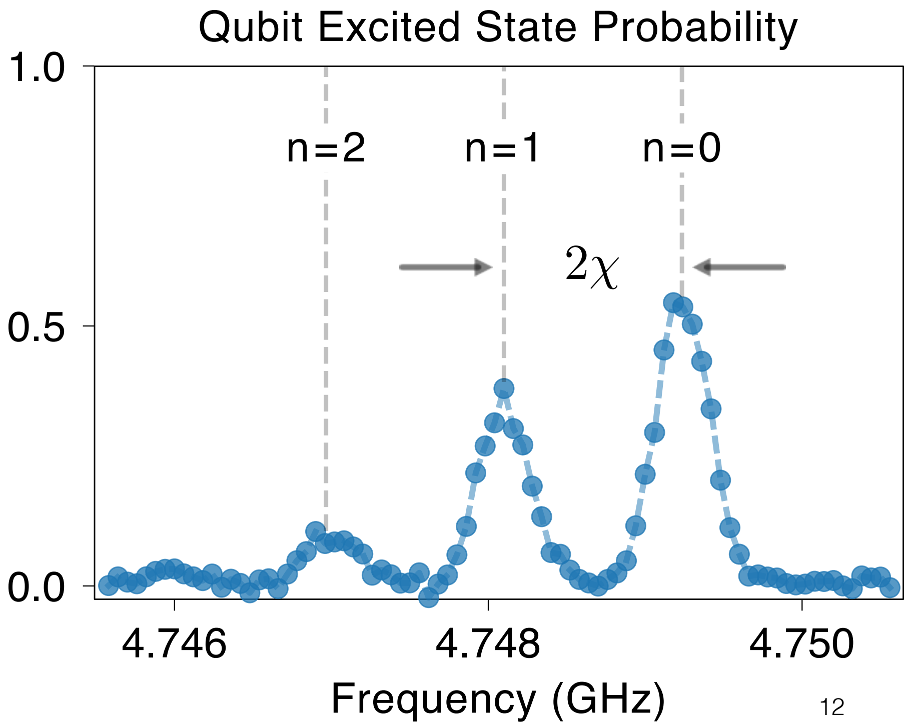

Qubit transition frequency is photon number dependent

Perform Ramsey type measurement on qubit frequency to infer cavity photon number

Electric analogue of Larmor precession

$$\mathcal{H} = \mu \cdot B$$
$$\mathcal{H} = \Omega \sigma_z$$

Ω depends on gyromagnetic ratio, mass, charge

$$\mathcal{H} = d \cdot E$$
$$\mathcal{H} = 2\chi a^\dagger a \frac{1}{2} \sigma_z$$

2χ depends on qubit-cavity coupling, detuning, anharmonicity

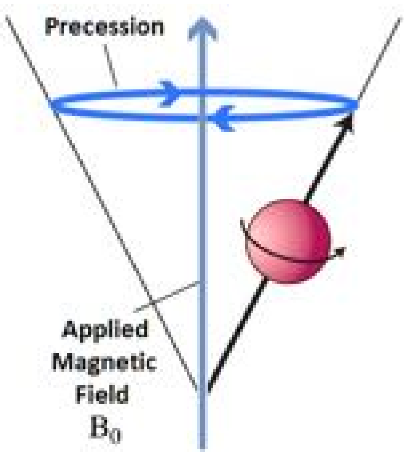

Qubit state precession rate is proportional to number of photons in cavity

Parity measurement maps cavity state onto qubit

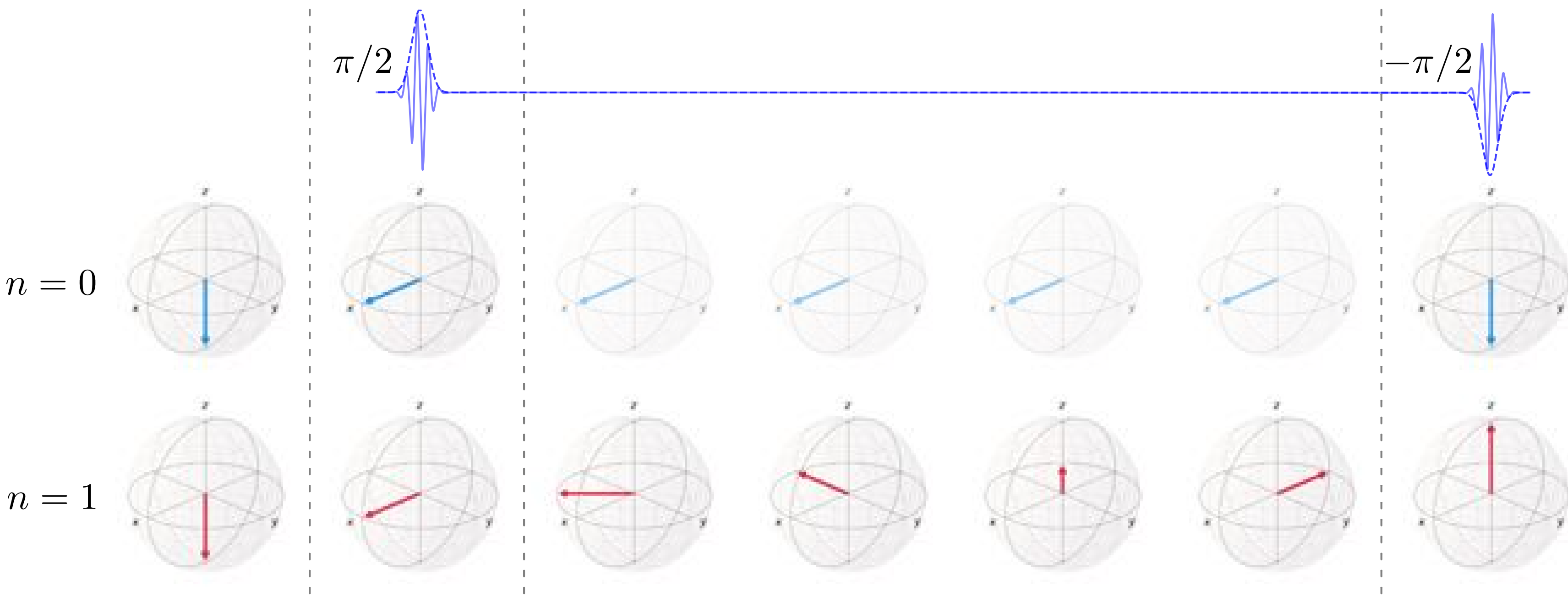

No zero-point noise → no noise floor

If leaks can be sealed and qubit-error-induced dark counts are under control, then a background-free experiment is possible.

Assumes axion detection bandwidth Δf ~ MHz

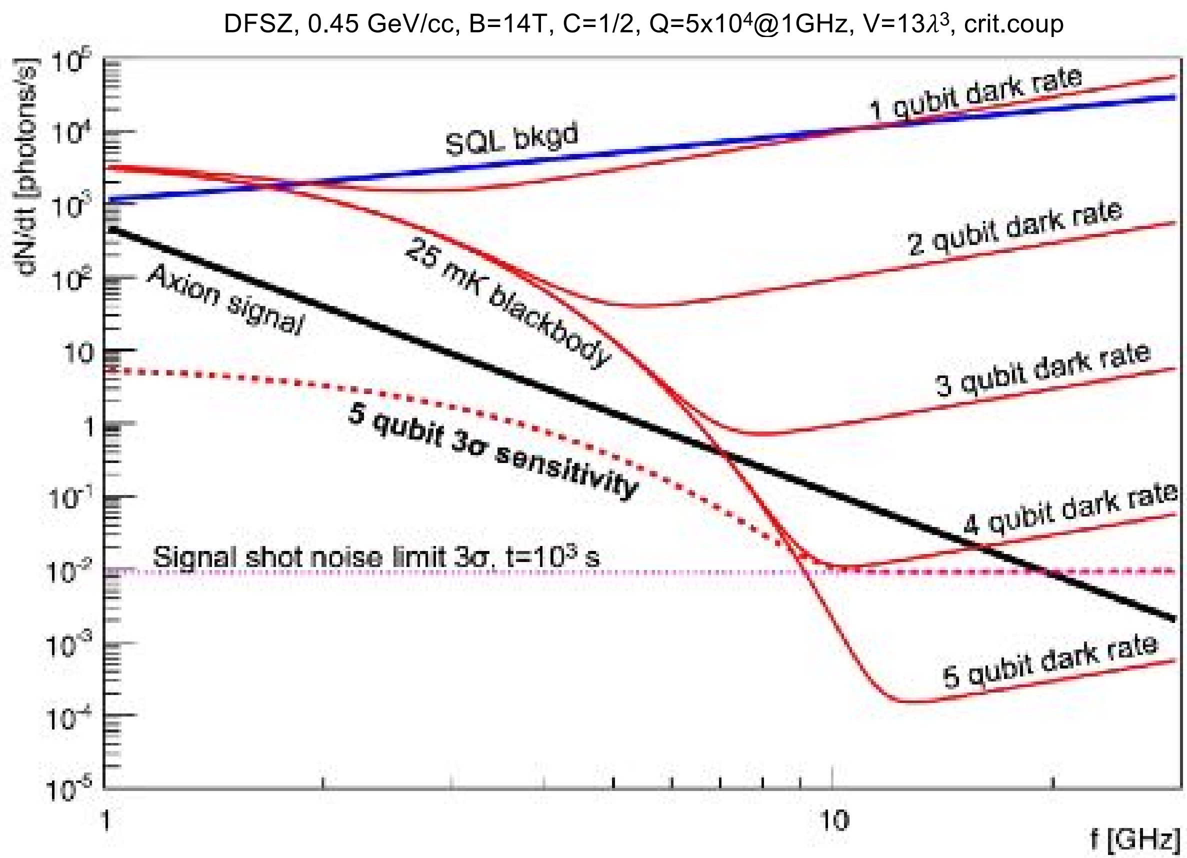

Good qubit single measurement error probability $p=10^{-2}$

With N QND measurements, **dark rate = $(10^{-2})^N \Delta f$**

Sensitivity limited only by signal photon shot noise.

Serge Haroche used majority vote out of 8 atoms → Nobel prize 2012.
Here we assume unanimous vote amongst 5 qubit measurements to potentially **reduce dark rates by 10 orders of magnitude.**

Lecture 2 review:

Transfer of energy from the axion DM to the RF cavity is the same as that of a system of two pendula coupled by a weak spring

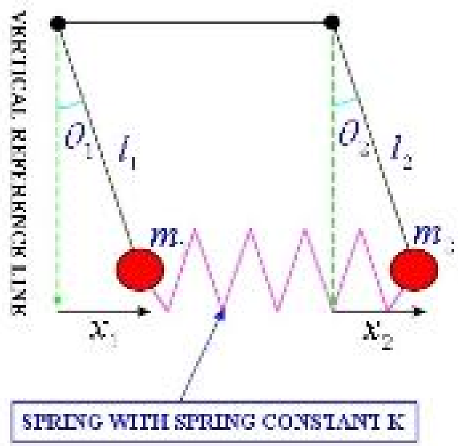

Axions

Standing wave photons

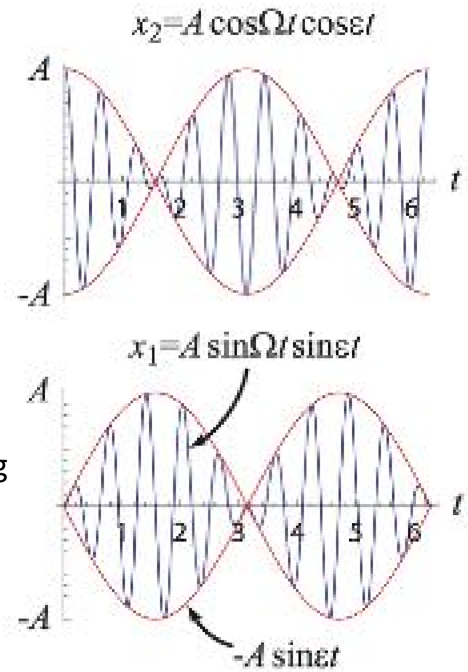

$$H = \begin{pmatrix} \omega_1 & g \\ g & \omega_2 \end{pmatrix}$$

Mixing angle=45° on resonance when w1=w2:

Mixing frequency = energy "g" stored in spring.
In the limit of infinite coherence time, **all** of the dark matter would be converted into photons. In finite coherence time, only get a few signal photons.

Lecture 2 review:

Creation/annihilation operators are just translation operators in phase space

$$p = i\frac{d}{dx}$$ Generates translations in position

$$x = i\frac{d}{dp}$$ Generates translations in momentum

$$a^\dagger = x + ip$$
$$a = x - ip$$
Generate translations in an arbitrary direction in x-p phase space

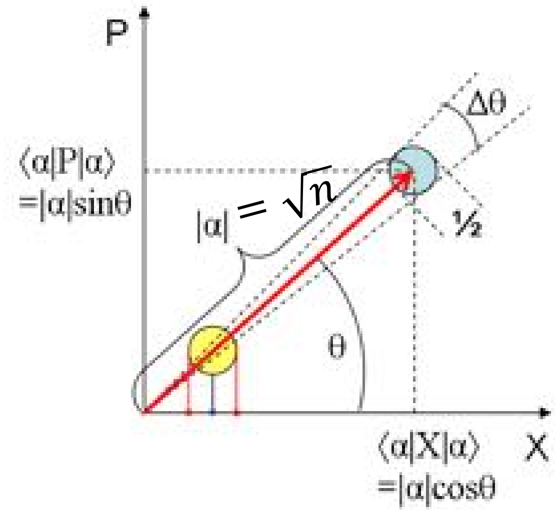

Exponentiate differential operator to get finite translation α in complex plane: $$\hat{D}(\alpha) = \exp\left(\alpha\hat{a}^\dagger - \alpha^*\hat{a}\right)$$

Phasor of amplitude α is generated as: $$D(\alpha)\,|0\rangle = |\alpha\rangle$$

"Coherent state" describing a classical sine wave

Classical sine waves have intrinsic Poisson noise

Coherent states form a Poisson distribution in the number state basis:

$$|\alpha\rangle = e^{-\frac{|\alpha|^2}{2}} e^{\alpha \hat{a}^\dagger} |0\rangle = e^{-\frac{|\alpha|^2}{2}} \sum_{n=0}^{\infty} \frac{\alpha^n}{\sqrt{n!}} |n\rangle$$

$$P(n) = |\langle n|\alpha\rangle|^2 = e^{-\langle n\rangle} \frac{\langle n\rangle^n}{n!}$$

$$\langle n\rangle = \langle \hat{a}^\dagger \hat{a}\rangle = |\alpha|^2$$

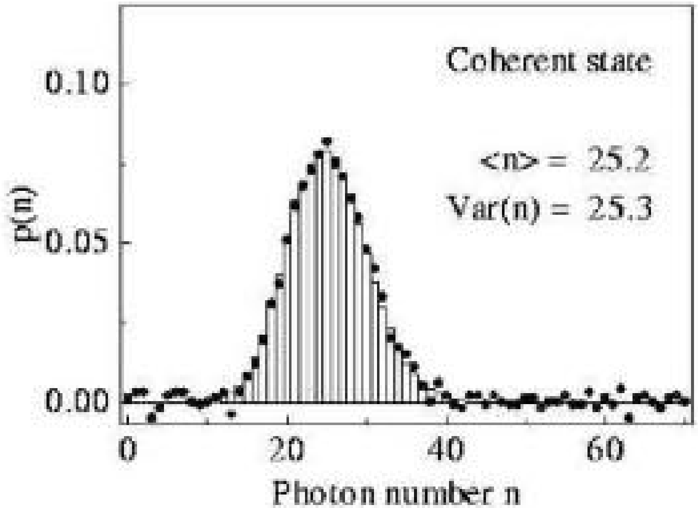

Like the zero-point fluctuations, the Poisson shot noise in classical wave intensity is a consequence of the Heisenberg uncertainty principle.

Lecture 2 review:

The resolution of a probe to displacement signals is given by its phase space distribution

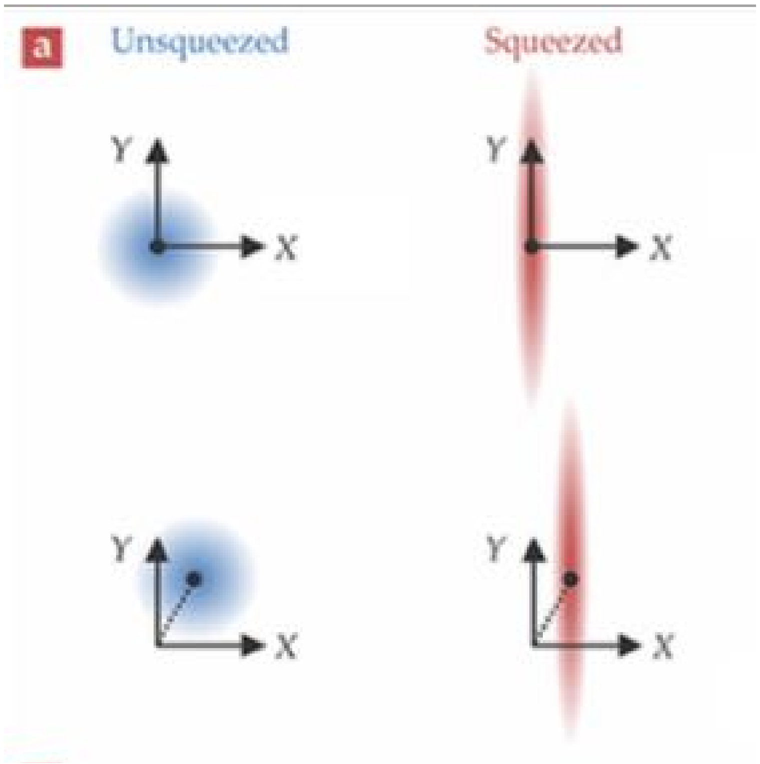

Lecture 2 review:

The displaced vacuum state is usually measured using a quantum-limited amplifier whose phase-space resolution function satisfies the standard quantum limit

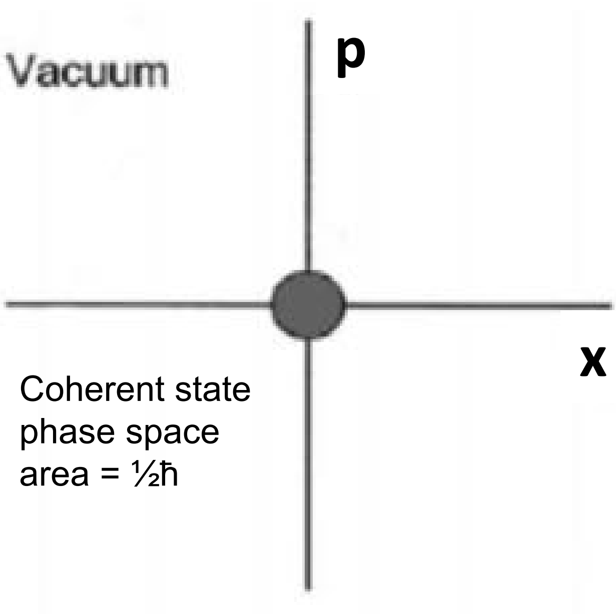

Axion-photon mixing induces tiny coherent state displacement $D(g\theta B_0 Q_{cav}/m_a^2)|0\rangle$

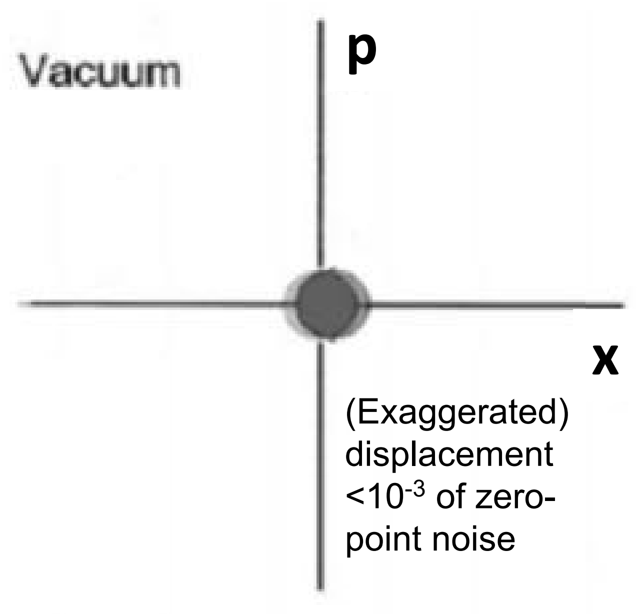

Blob represents variance from:

- ½ photon from the zero-point noise of the signal oscillator
- ½ photon from the zero-point noise of the idler mode required by the amplifier to conserve energy when converting pump quanta into signal quanta.

More stupid qubit tricks:
Stimulated emission of photons from DM axions

Start the photon wave swinging so it can more easily accept energy from the axions.

Good!

Waiting…

Oops, wrong phase

Power = $\overrightarrow{Force} \cdot \overrightarrow{velocity}$

Phase offset determines the direction of energy flow.

But the axion wave is a coherent state of unknown phase which changes every millisecond… How do we prepare the cavity oscillator???

A sinusoidally swinging oscillator actually has exactly the same resolution as the vacuum state

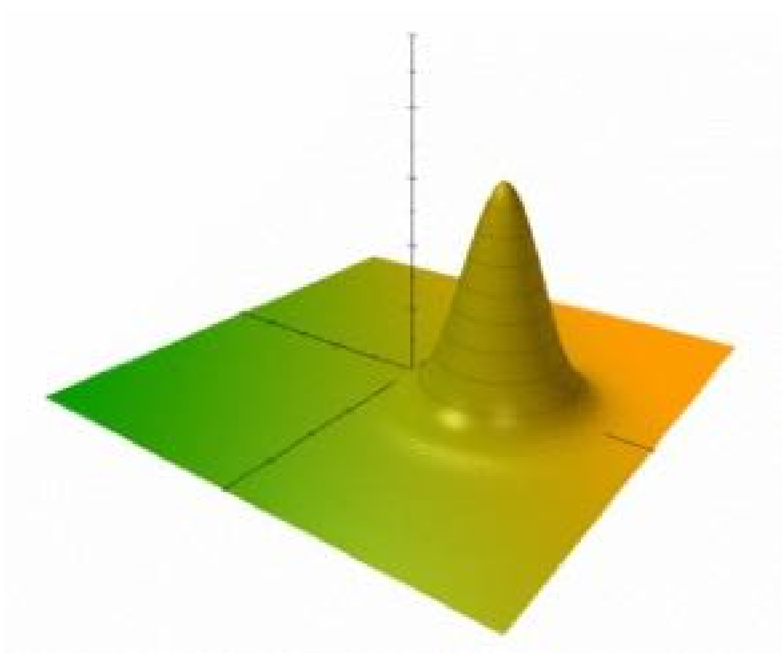

Resolution is just the size of the Gaussian blob in phase space.

Displacements from forces just act linearly on this phase space distribution:

$$\hat{D}(\alpha)\hat{D}(\beta) = e^{(\alpha\beta^* - \alpha^*\beta)/2}\hat{D}(\alpha+\beta)$$

It doesn’t matter whether you prepared the state at finite amplitude β or if you started with β=0. The resolution on α is the same.

Annuli corresponding to integer occupation number become more closely spaced for larger n

$$\langle n \rangle = \langle \hat{a}^\dagger \hat{a} \rangle = |\alpha|^2$$

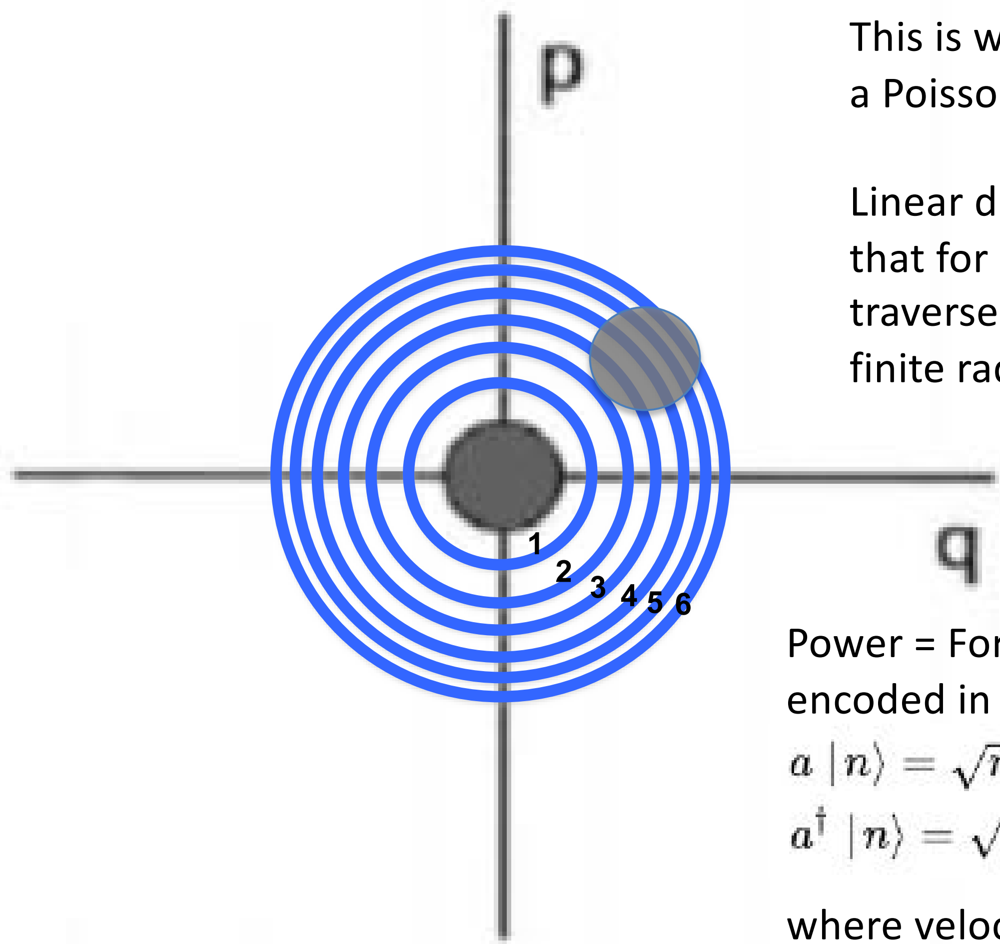

This is why a displaced Gaussian blob produces a Poisson distribution.

Linear displacement already encodes the fact that for a displacement D(α), more annuli are traversed if the starting point is already at finite radius β

Power = Force x velocity is also already encoded in the operator normalizations:

$$a\,|n\rangle = \sqrt{n}\,|n-1\rangle$$

$$a^\dagger\,|n\rangle = \sqrt{n+1}\,|n+1\rangle$$

where velocity is proportional to wave amplitude

The actual Fock states are Laguerre-Gauss functions

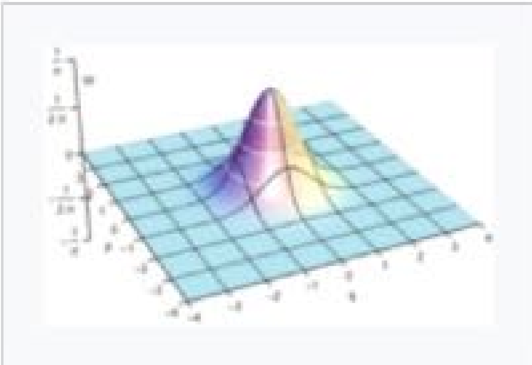

Wigner function of $|0\rangle$

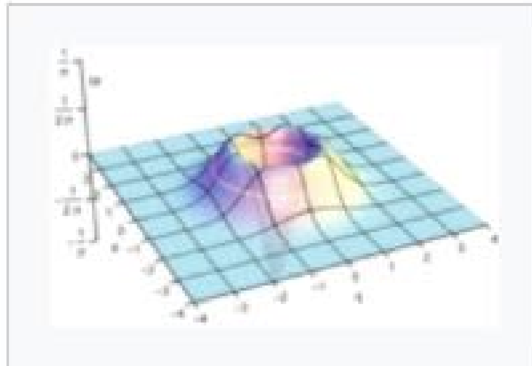

Wigner function of $|1\rangle$

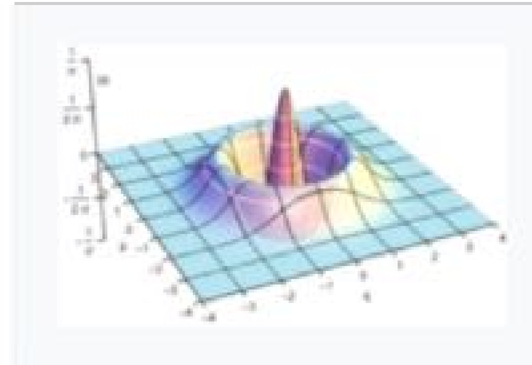

Wigner function of $|2\rangle$

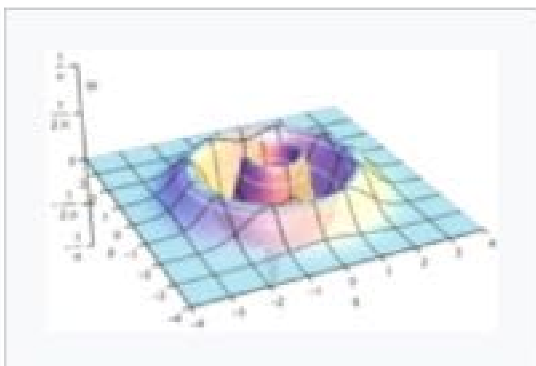

Wigner function of $|3\rangle$

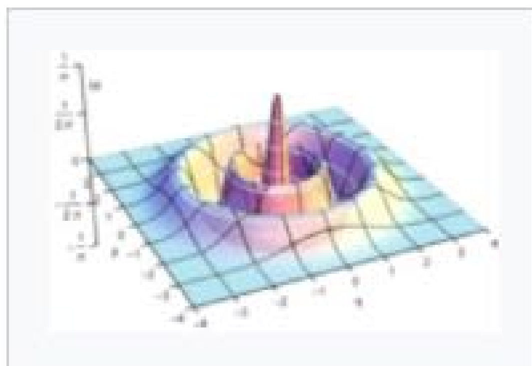

Wigner function of $|4\rangle$

Wikipedia

Just like Hermite-Gauss eigenfunctions, but in cylindrical coordinates. The Hamiltonian can be viewed as a 2-dim harmonic potential with linear restoring force for excursions in x or p.

$$H = \frac{p^2}{2m} + \frac{1}{2} m\omega^2 x^2$$

Wait! Wouldn't a Fock state be perfect for measurements of tiny displacements where the phase is unknown?

The Fock state is symmetric in phase angle
→ **responds equally well to pushes at any time.**
It also has definite occupation number N
→ **no Poisson noise!**

$H_I = g(a^\dagger b + a b^\dagger)$ → $\langle \alpha, N+1 | H_I | \alpha, N \rangle = g\alpha\sqrt{N+1}$

Konrad Lehnert
(Colorado)

N=1 Fock state $\Delta N \times \Delta\varphi = ½$

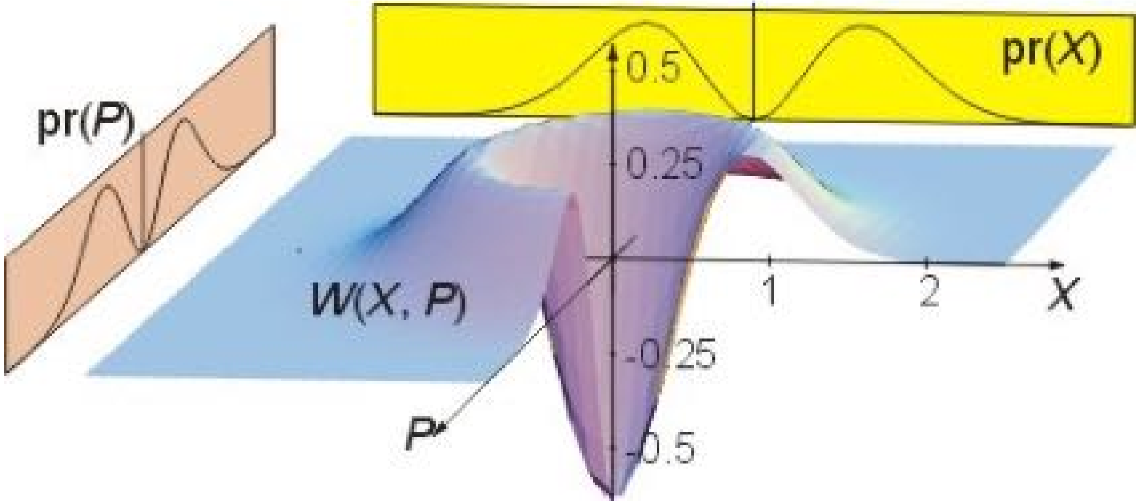

A Fock state is a superposition of an oscillator in all possible phases of its sinusoidal motion

Mixing between a coherent state and a Fock state

The axion wave is a sine wave described by a Glauber coherent state

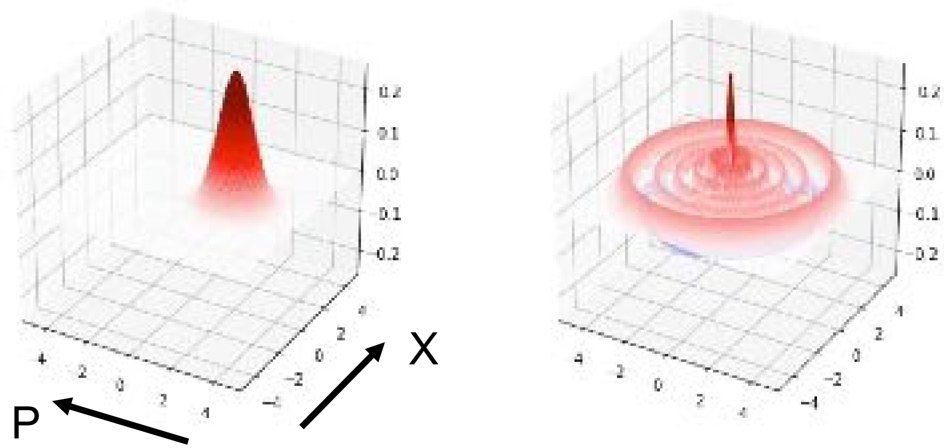

The cavity photon mode has been prepared as a N=10 Fock state

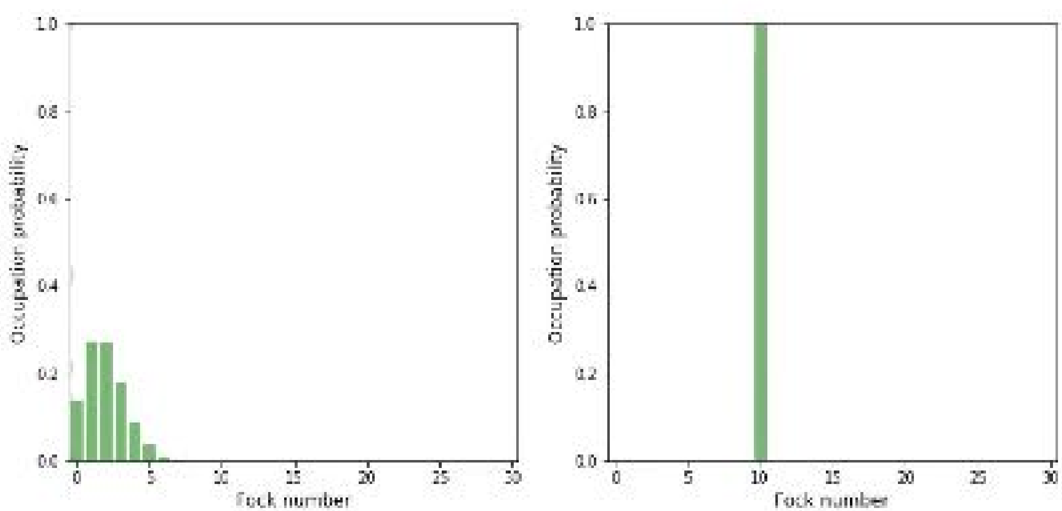

QuTiP simulation

For finite coherence time << mixing time, the transfer of quanta from axions to photons is enhanced by a factor (N+1)

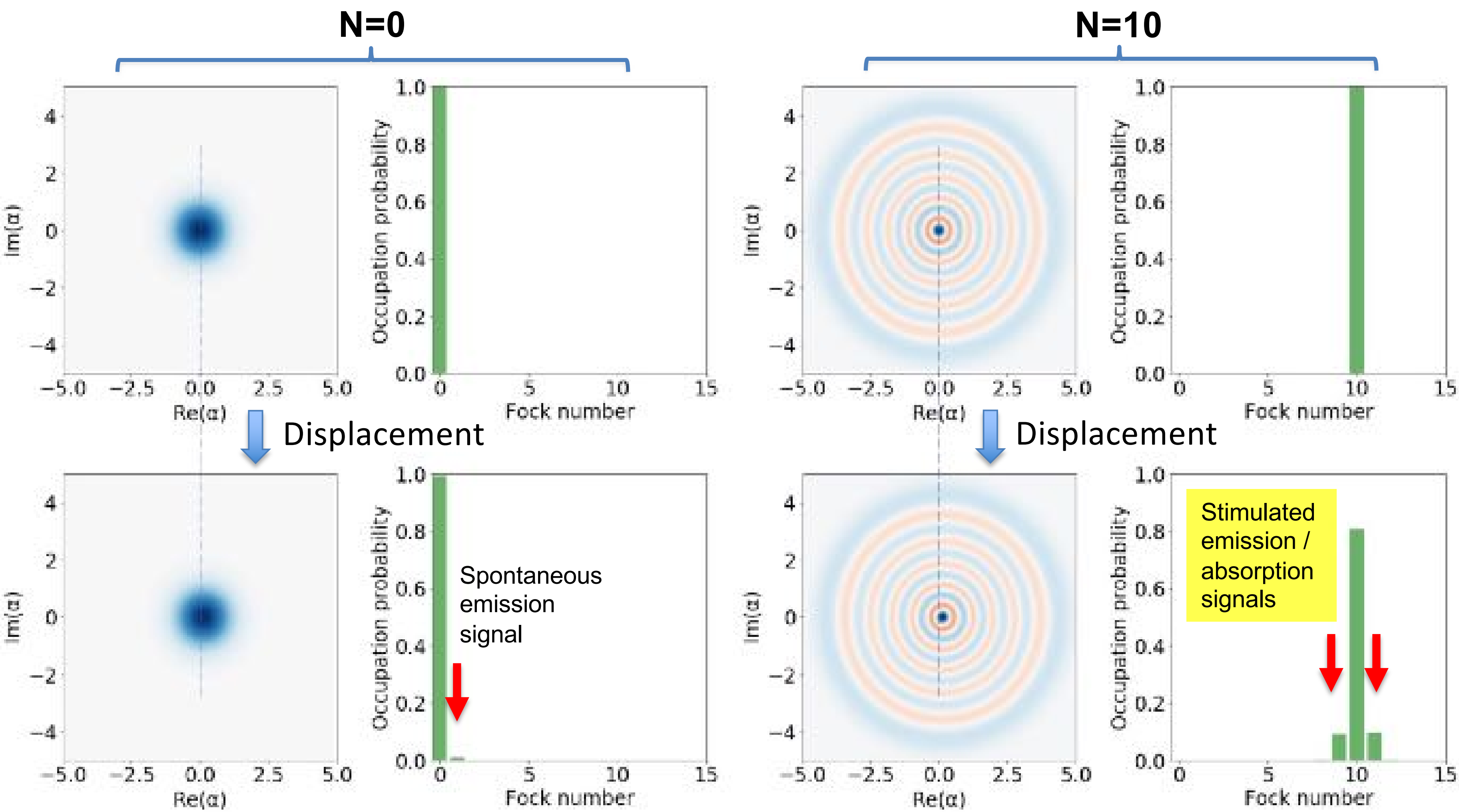

QuTiP simulation

Universal, optimal control is used to initialize a cavity photon mode to an arbitrary initial quantum state

Example: Preparation of photon Fock state $|n=6\rangle$

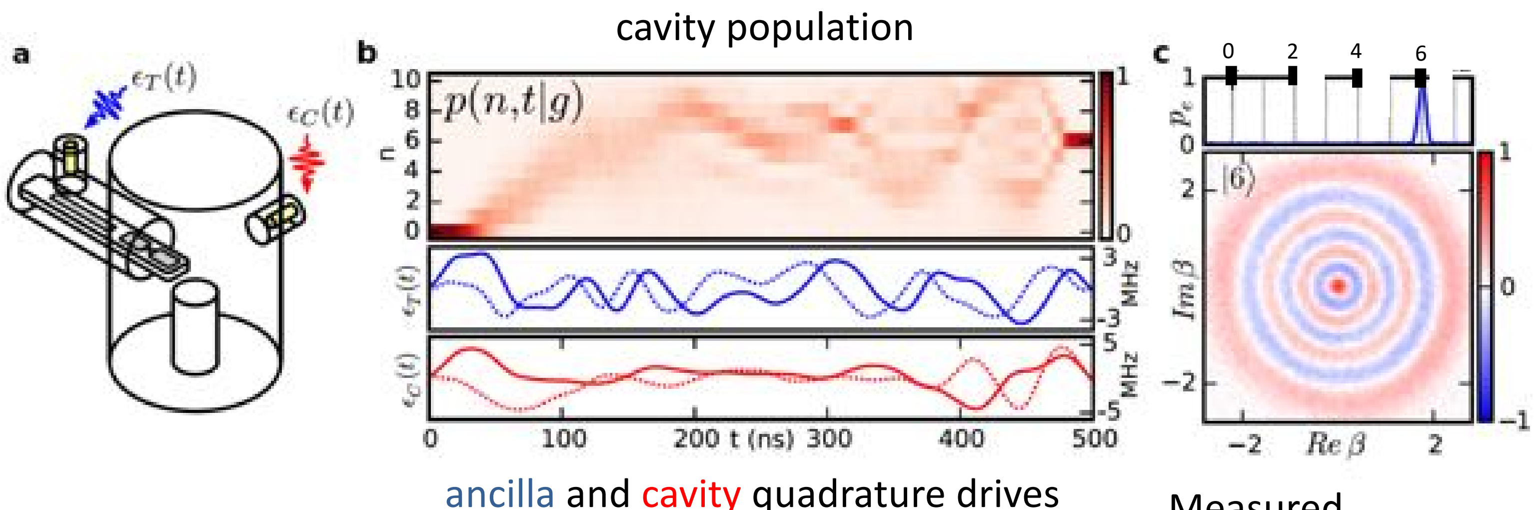

Heeres et al. *Nature Communications* 8, 94 (2017)

Requires nonlinear oscillator (qubit) to enable this nonlinear transformation.

Sequence of waveforms determined by computer. No known general recipe.
Used in quantum computing to load arbitrary initial states into the qRAM.

Using Q=10^8 cavities, stimulated emission boosts axion signal by factors up to 100.

Not only increases SNR at lower masses, but also extends range to higher masses!

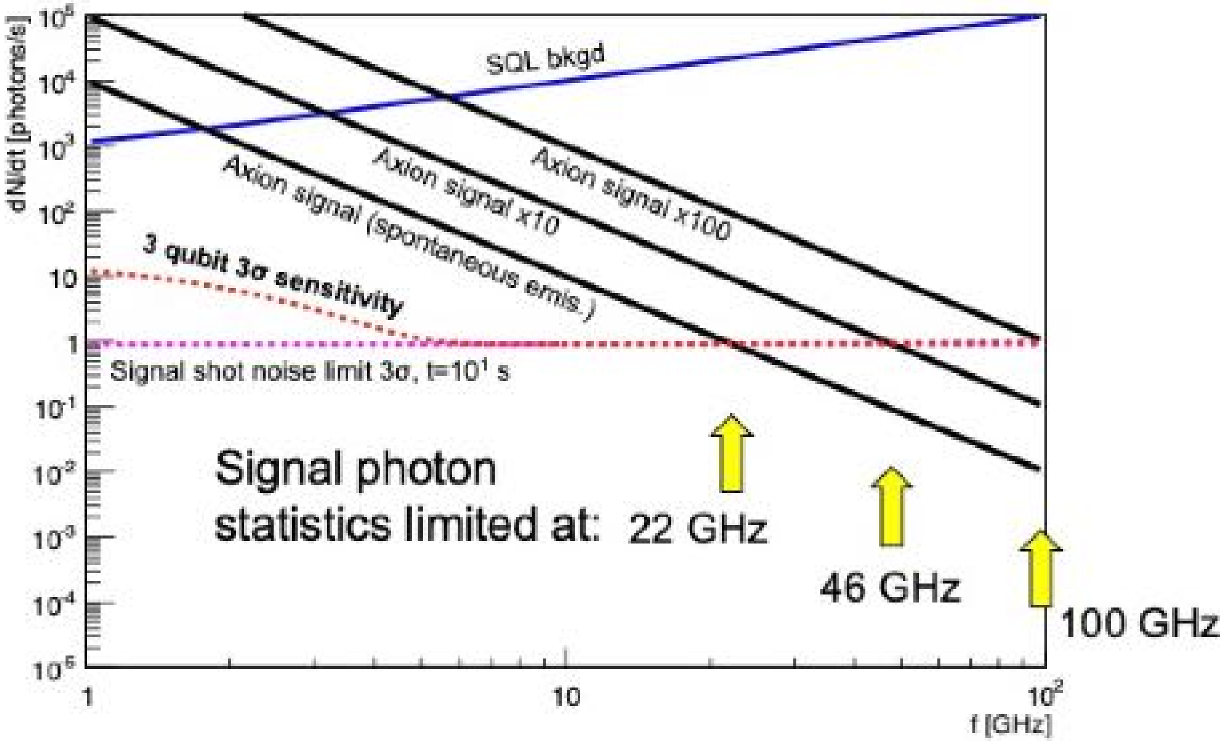

Only works up to around 30 GHz where we get too close to the Josephson plasma frequency where resistive heating in the junction is enough to break Cooper pairs

So what do we do for even higher frequencies?

Figure adapted from DOE "Small Dark Matter" BRN Study, 2018

Atom interferometry (MAGIS)

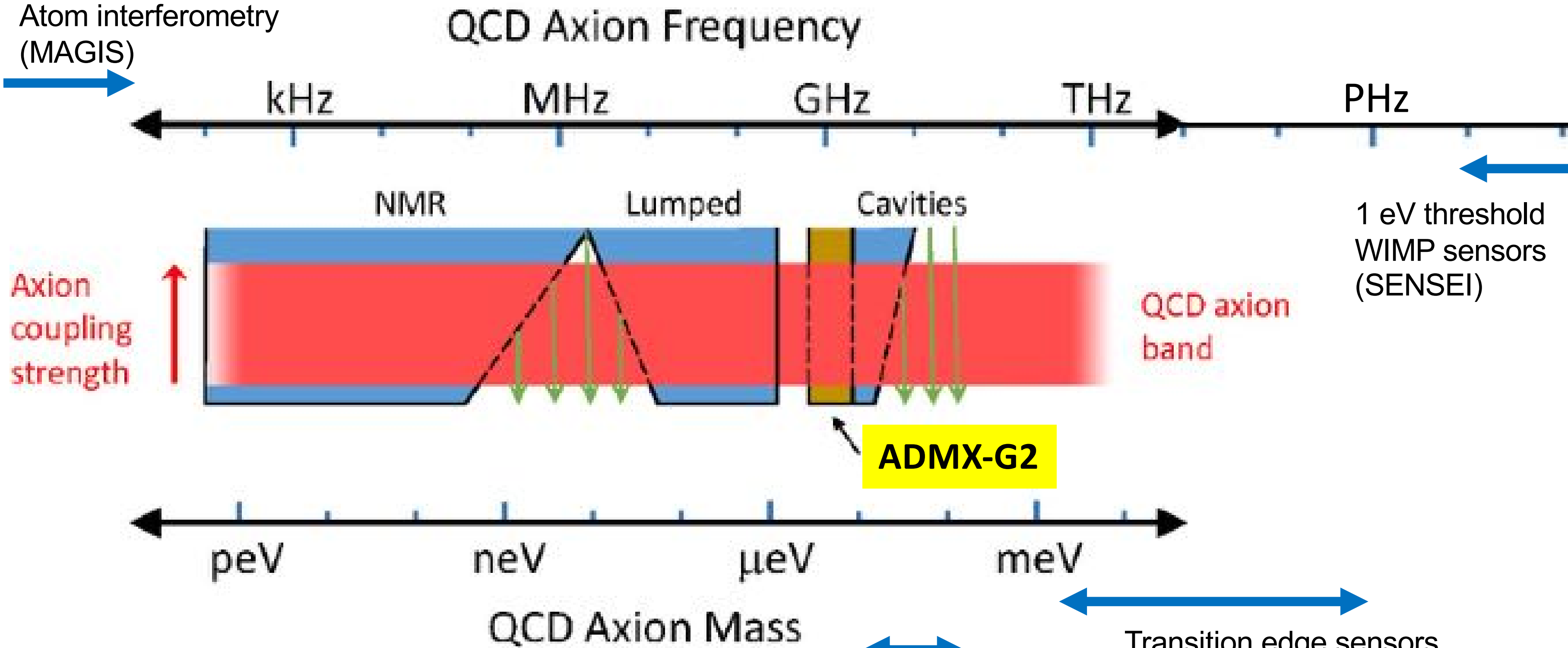

1 eV threshold WIMP sensors (SENSEI)

Squeezed photon states,
Quantum nondemolition with aluminum qubits

Transition edge sensors,
Superconducting nanowire,
Quantum capacitance det.
MKID microcalorimeters

Noiseless photon upconvertors,
spin-squeezing

High-Tc qubits/amps
Rydberg atoms
Josephson PMTs

Actually, only the cavity volume within one Compton wavelength from the wall matters

Nothing can possibly happen in the empty space far from a cavity wall since empty space is translation symmetric. The extra interior wiggles in the higher frequency mode all cancel each other out in this semi-classical power calculation:

$$P_a(t) = \int \vec{J}_a(t) \cdot \vec{E}_r(t)\, dV$$

J is spatially uniform on laboratory scales and points in the direction of the applied B field

The direction of E oscillates up/down

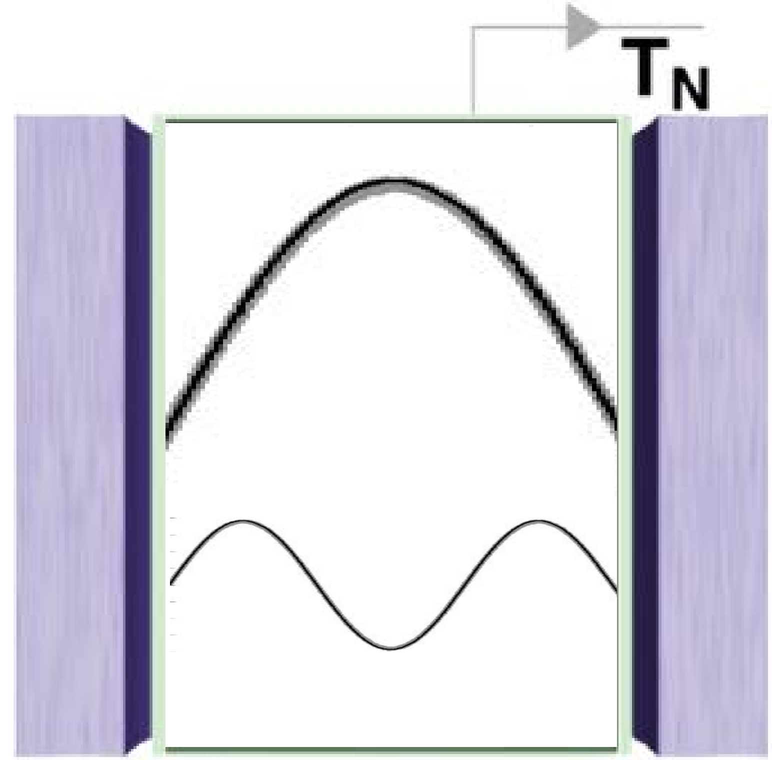

The interior region integrates to zero

One can instead use a huge dish antenna whose area contains many wavelength-squared pixels

D. Horns, et.al, JCAP 1304, 016 (2013)

This is like having an array of N cavities, where each cavity only gets 1 bounce.

Axion emits transition radiation upon impedance mismatch.

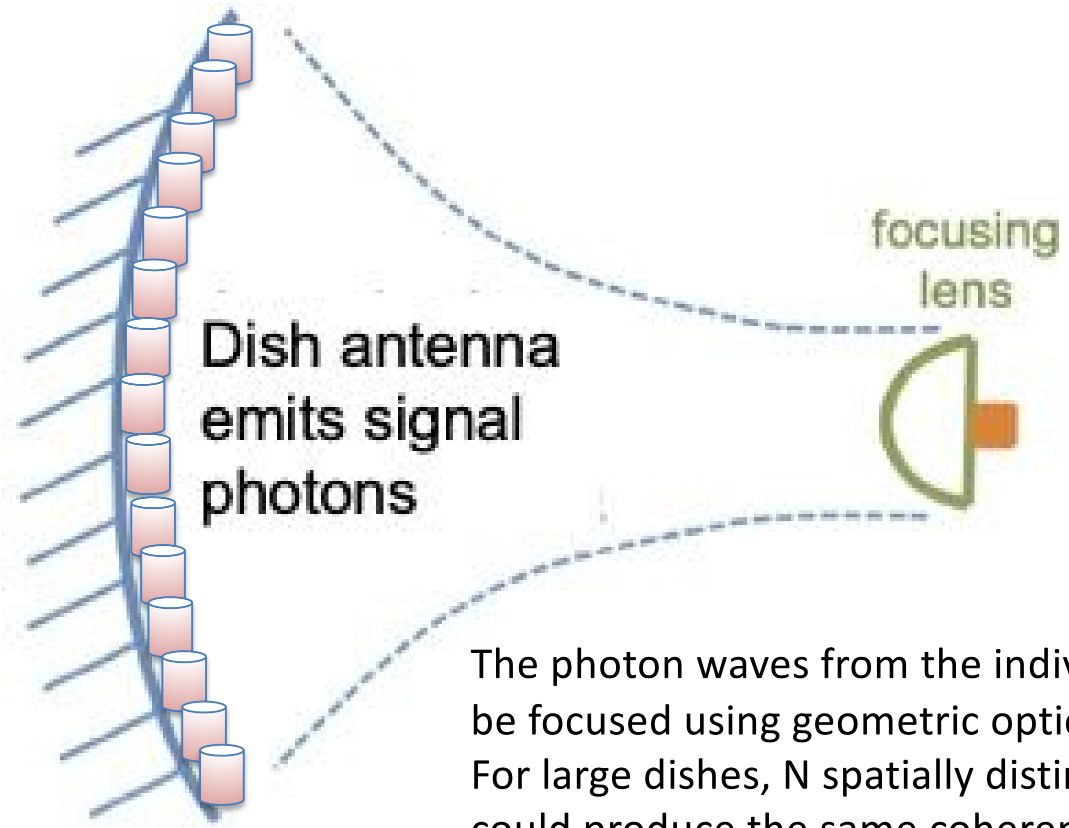

The photon waves from the individual pixels can be focused using geometric optics.
For large dishes, N spatially distinct emitters could produce the same coherent sum as that of Q bounces inside a resonant cavity.

Since the axion can convert into photons when encountering any interface which breaks translation symmetry, we can also use many dielectric plates

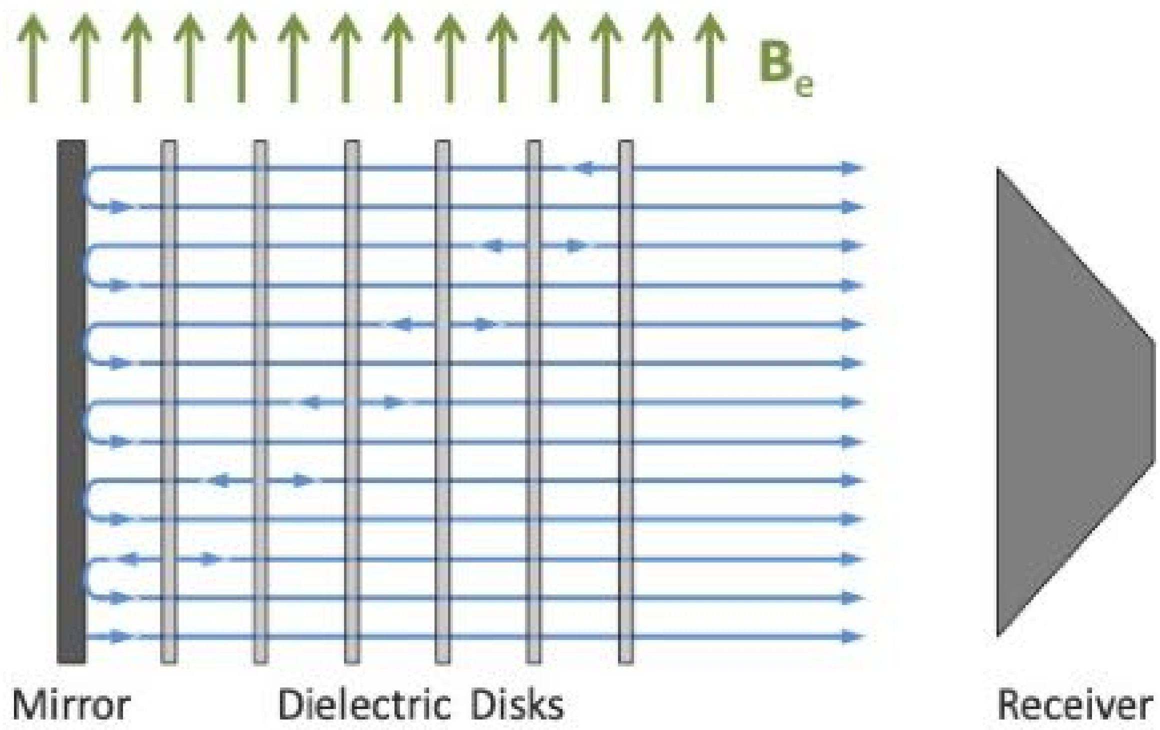

MADMAX idea,
A. Caldwell, et.al, Phys. Rev. Lett. 118, 091801 (2017)

However, for achievable magnetic fields, the photon signal rate is low

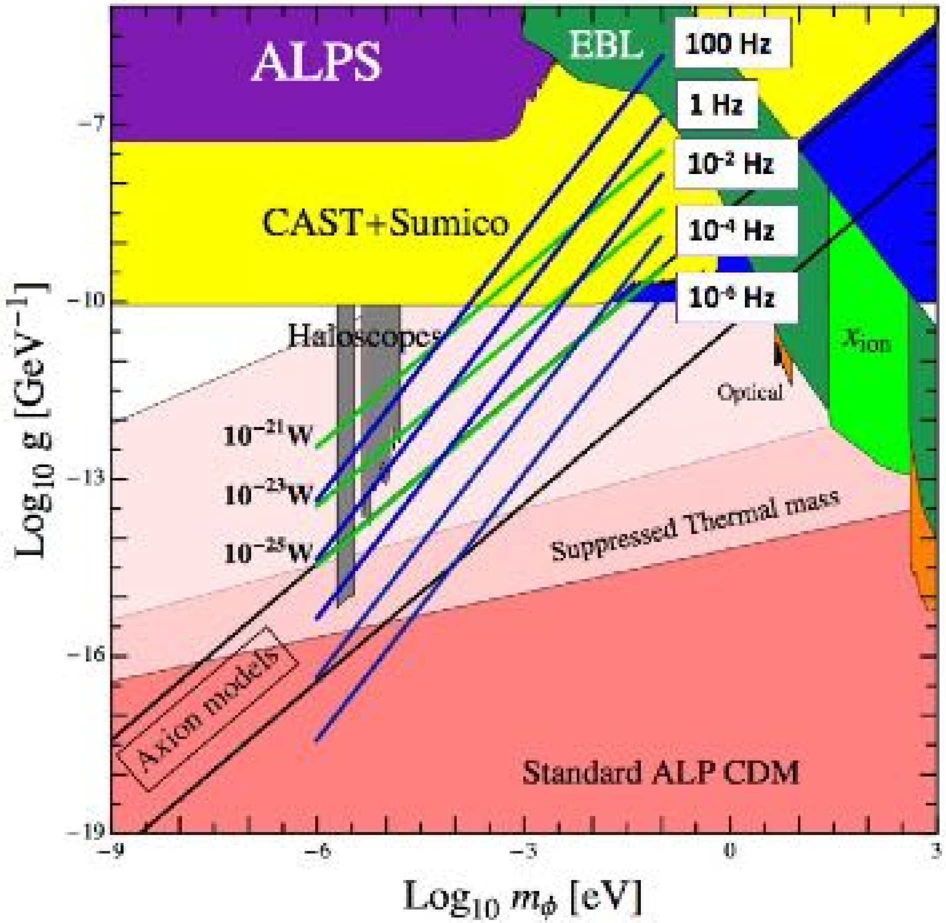

Figure adapted from Horns et.al (2012)

These will be long duration experiments, and we do not yet have the single photon detection technology with sufficiently low dark rates.

Cavity detectors (e.g. ADMX)

1 eV threshold particle detectors (e.g. SENSEI)

Need better sensors

Superconducting nanowire single photon detector

Create a large pixel with a meandering SC wire. Apply a current bias. Heating due to absorbing a photon will cause the wire to quench and become resistive, triggering a large voltage response.

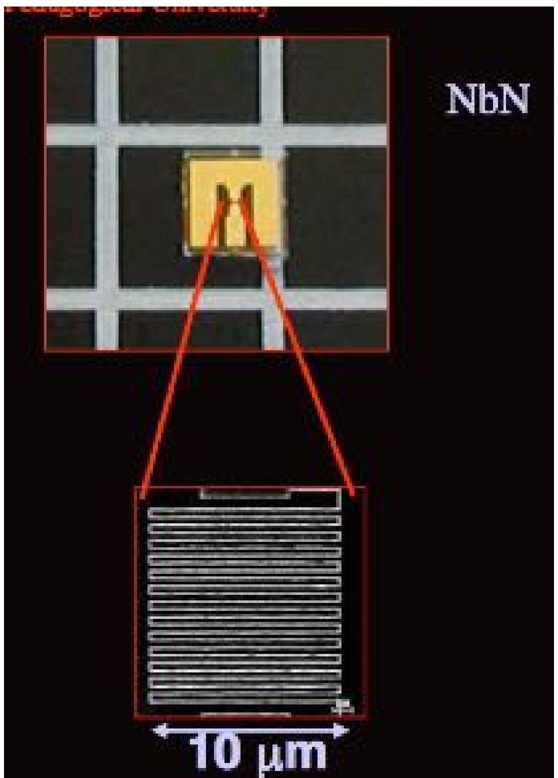

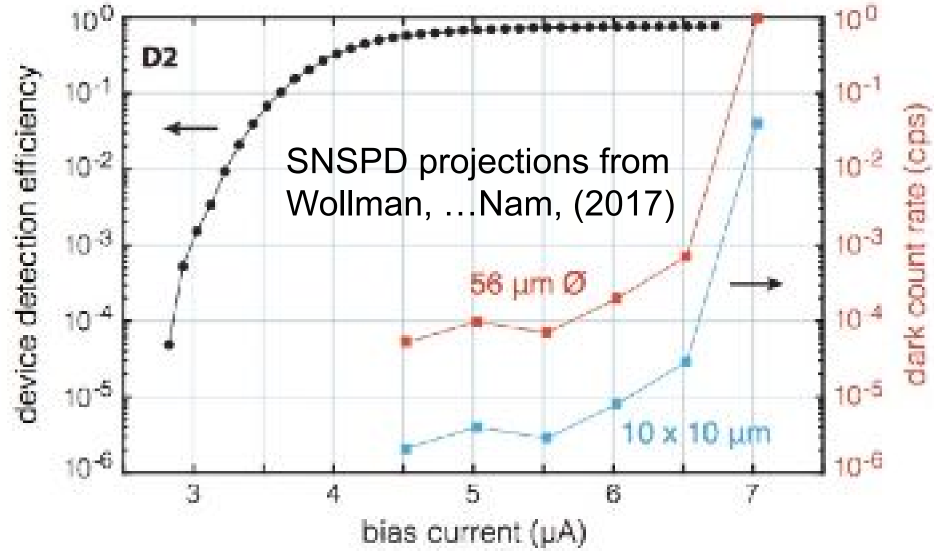

- Deployed in Lamppost hidden photon search.
- **Dark rates <10^{-5} Hz already achieved for NIR photons.**
- Seem to work okay when placed parallel to high magnetic fields. (B. Lawrie, et. al, unpublished)
- Need to reduce threshold to detect FIR photons for axion dark matter.

Quantum Capacitance Detector

Senses single photons which break even a single Cooper pair.

Based on the Cooper pair box, a.k.a. a charge qubit.

The effective capacitance of this Josephson oscillator has a large discrete change depending on whether the superconducting island has an even or odd number of charges on it.

5x5 pixel array from Jet Propulsion Lab

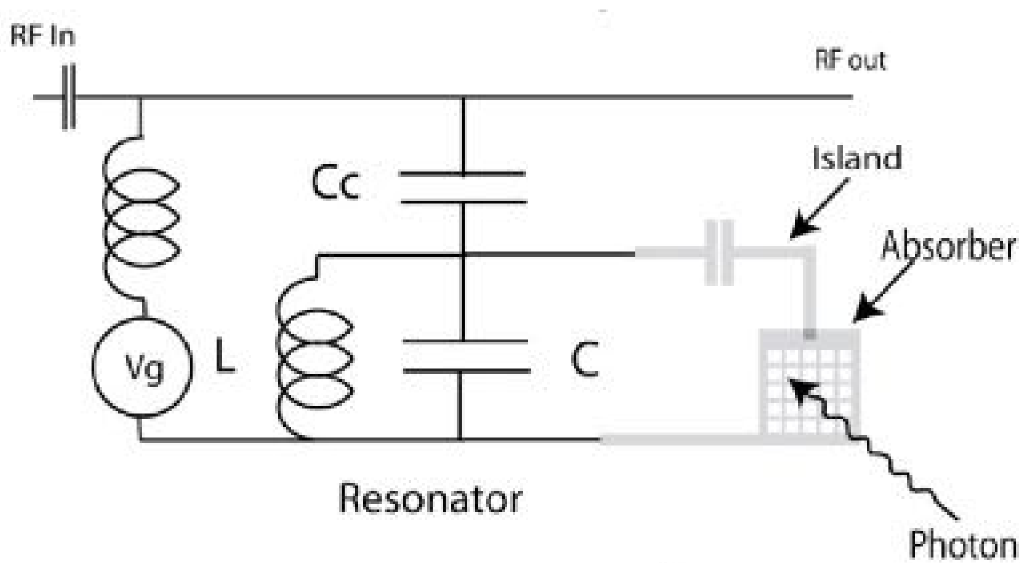

Connect the qubit in parallel to a regular LC oscillator and the resonant frequency of the combined circuit will have a large discrete shift when a photon is absorbed, creating excess charged quasiparticles

QCD detects single THz frequency photons

Lowest noise-equivalent power 10^{-21} W/rtHz of any FIR photon detector

P.M. Echternach, et.al, Nature Astronomy 2, 90-97 (2018)

However, the corresponding 100 Hz background rate is still too high for the axion dark matter detector

What could be causing these dark counts?

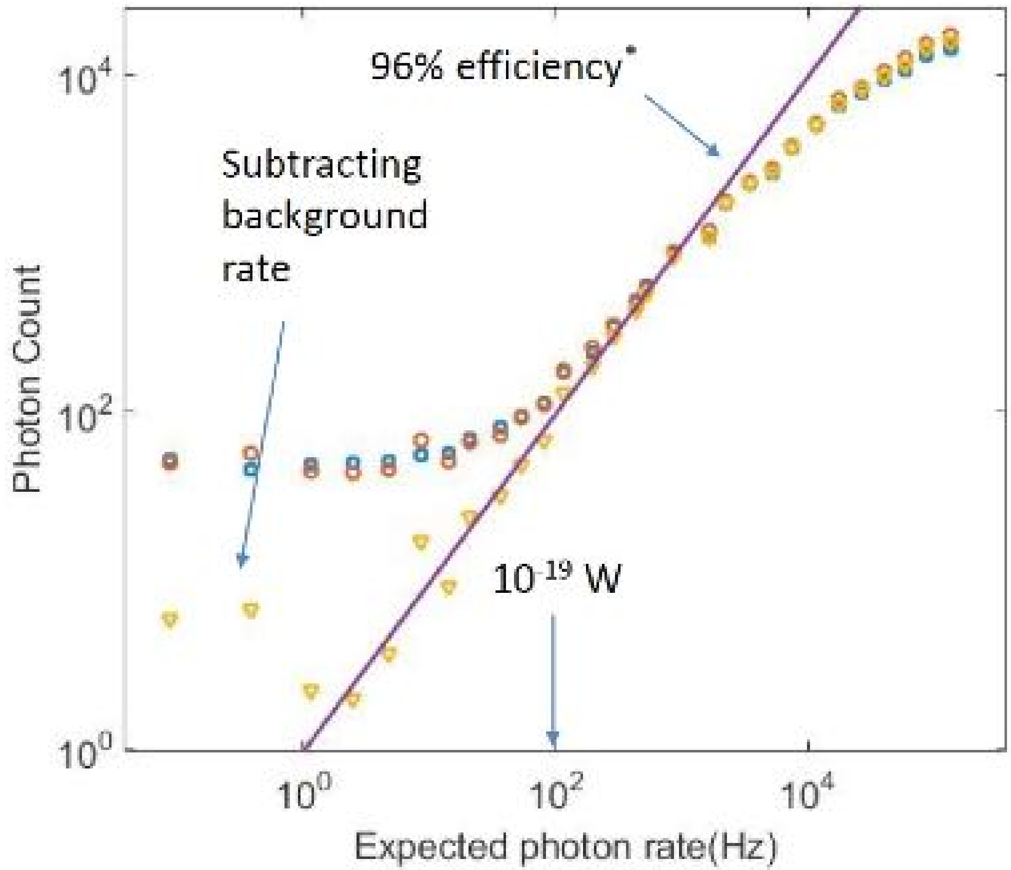

from blackbody source

Dark counts probably not cosmic rays – observed 10^{-2} Hz rate in qubit CPU's is too low

Resolving catastrophic error bursts from cosmic rays in large arrays of superconducting qubits

Matt McEwen,[1,2] Lara Faoro,[3] Kunal Arya,[2] Andrew Dunsworth,[2] Trent Huang,[2] Seon Kim,[2] Brian

M. McEwen, et.al, arXiv:2104.05219

Google Sycamore chip already functions as a phonon detector with 100% chip-wide failure in response to ionizing radiation events which can be localized in both space and time

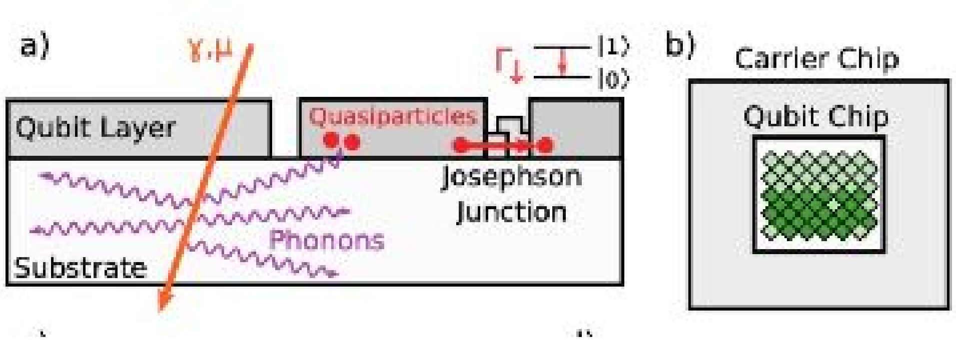

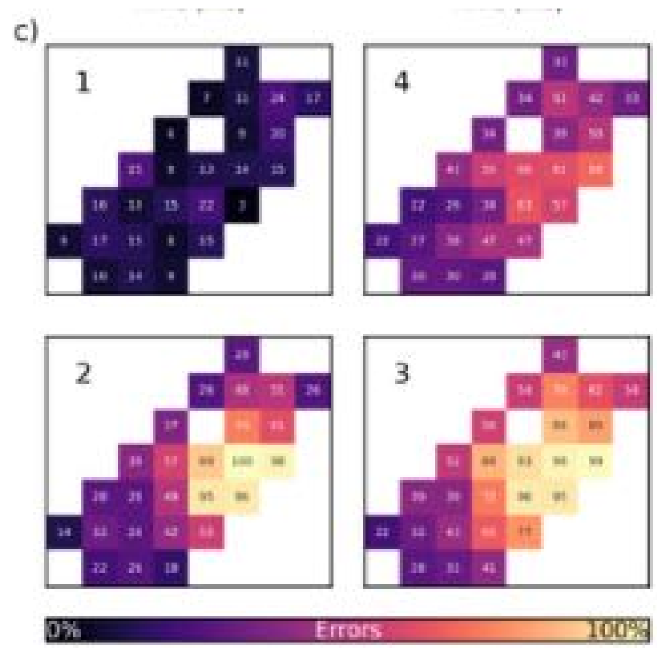

Figure 3. **Localization and spread of error.** (a-b) Time-

Eventually axion experiments will have to move underground just like WIMP experiments, but cosmic rays are not currently the dominant background.

Superconducting devices all suffer from mysterious non-equilibrium quasiparticle population

These now appear to be created in discrete, time-resolved events.

E.T. Mannila, et.al, arXiv:2102.00484 *(2021)*

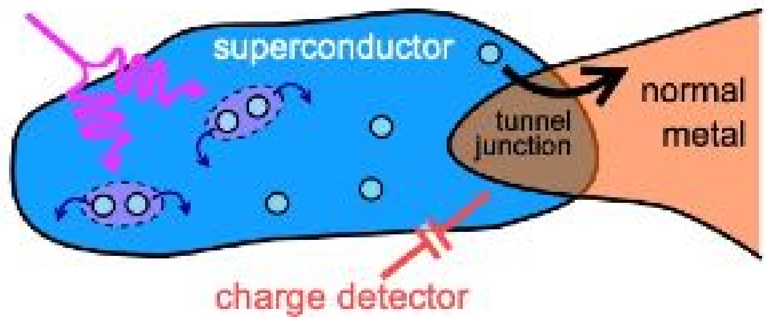

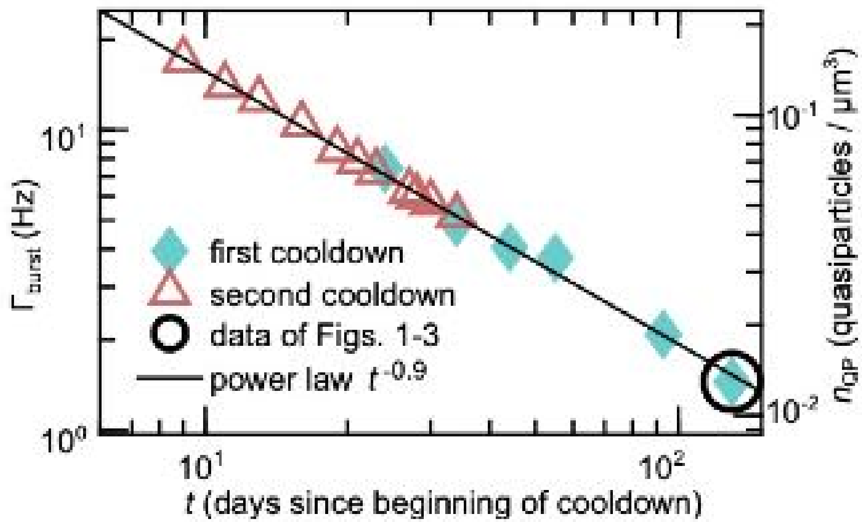

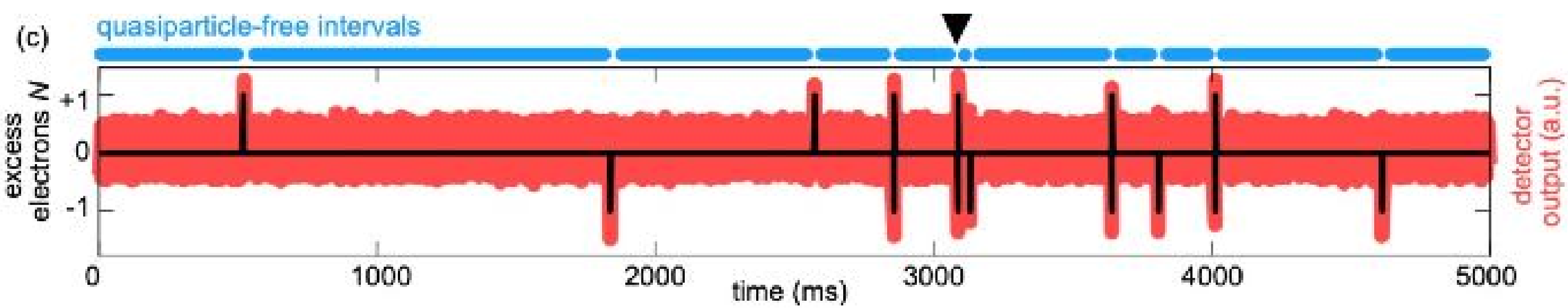

Origins of events still a 20-year-old mystery….

Study guide

- Low mass dark matter form classical bosonic wave which can drive quantum oscillators
- The signal wavefunction is squared in offline analysis to compare the signal variance to the noise variance
- Measurement of non-commuting observables incurs the penalty of zero-point noise, which can be squeezed
- Forces induce displacements in phase space
- “a” stands for “amplitude” in polar phase space coordinates, not “annihilation”
- The resolution of a probe is determined by its phase space distribution
- Better to measuring only a single observable – wave amplitude
- Quantum non-demolition measurements can drastically reduce noise
- Fock states are the ideal basis to measure amplitude displacements in arbitrary directions
- The signal from wave dark matter is secretly transition radiation on interfaces with mismatched electromagnetic response
- Large area reflector dishes can focus signals onto single photon detectors
- Existing detectors have demonstrated single photon sensitivity but dark rates are too high. Some clues coming from the quantum computing community.

Summary and Outlooks

Summary

- Astronomers discovered the "dark matter problem" nearly a century ago, but what DM is remains an unsolved mystery.

- Exploring the physical nature of DM is a long and challenging journey.

- Discovering the existence or non-existence of DM would both be a significant breakthrough, likely triggering a new revolution in physics (fundamental science).

Thanks!

Modern astronomy plays an increasingly prominent role in science

Since 1936, 28 people in the field of astrophysics have won the Nobel Prize in Physics 13 times in 17 categories

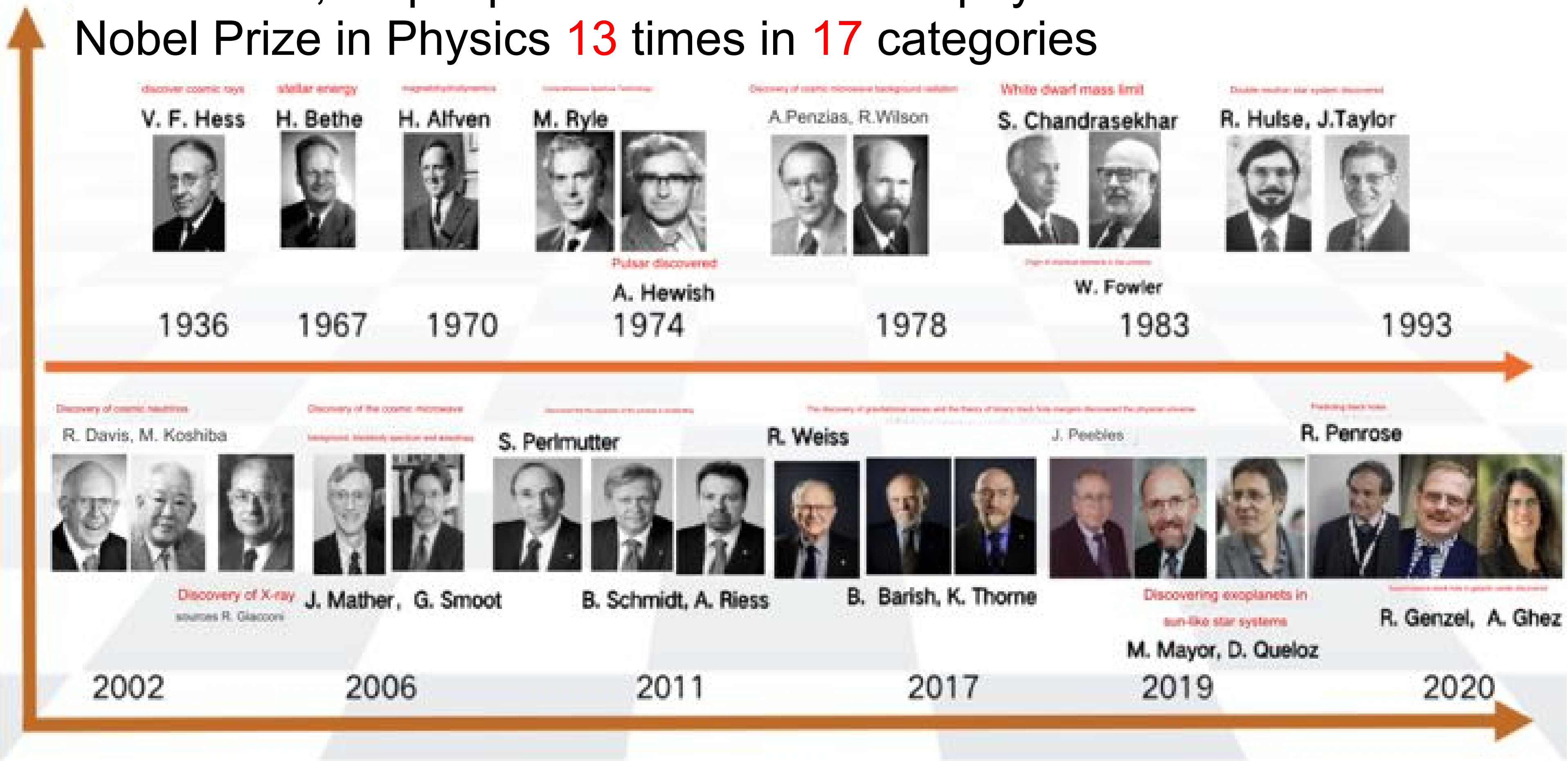

Backup slice

Observable

- The observable is the anomalous residue in the pulse arrival time:

$$R(t) \equiv \int_0^t dt' \left(\frac{\nu_0 - \nu(t')}{\nu_0}\right) \qquad \langle R^2(t)\rangle = \frac{1}{T}\int_0^T R^2(t)dt\ ,$$

- pulse frequencies redshift $z \equiv \dfrac{\nu_0 - \nu(t)}{\nu_0}$
- In GR, the metric perturbation only has two polarization modes: $h_+, h_\times$ and we can express $h_{\mu\nu} = \sum_{A=+,\times} e^{A}_{\mu\nu} h_A$. For each mode, we define a <u>receiving function</u> to denote the influence on the redshift:

$$\tilde{z}(f,\hat{\Omega}) = \left(e^{-i2\pi f L(1+\hat{\Omega}\cdot\hat{p})} - 1\right)\sum_A h_A(f,\hat{\Omega})F^A(\hat{\Omega}) \qquad F^A(\hat{\Omega}) \equiv e^A_{ij}(\hat{\Omega})\frac{1}{2}\frac{\hat{p}^i\hat{p}^j}{1+\hat{\Omega}\cdot\hat{p}}.$$

Correlation function

- One can separate the two-point correlation function in power spectrum $\Omega_{\rm gw}$ and the overlap reduction function $\Gamma(|f|)$ assuming the isotropic SGWB

$$\langle \tilde{z}_1^*(f)\tilde{z}_2(f')\rangle = \frac{3H_0^2}{32\pi^3}\frac{1}{\beta}\delta(f-f')|f|^{-3}\Omega_{\rm gw}(|f|)\Gamma(|f|),$$

- Overlap reduction function:

$$\Gamma(|f|) = \beta \sum_A \int_{S^2} d\hat{\Omega} \left(e^{i2\pi f L_1(1+\hat{\Omega}\cdot\hat{p}_1)} - 1\right) \times \left(e^{-i2\pi f L_2(1+\hat{\Omega}\cdot\hat{p}_2)} - 1\right) F_1^A(\hat{\Omega})F_2^A(\hat{\Omega}),$$

- Exponential factor!

Hellings-Downs curve

- Overlap reduction function:

$$\Gamma(|f|) = \beta \sum_A \int_{S^2} d\hat{\Omega} \left(e^{i2\pi f L_1(1+\hat{\Omega}\cdot\hat{p}_1)} - 1\right) \times$$
$$\times \left(e^{-i2\pi f L_2(1+\hat{\Omega}\cdot\hat{p}_2)} - 1\right) F_1^A(\hat{\Omega}) F_2^A(\hat{\Omega}),$$

- Hellings-Downs curve:

$$\Gamma_0 \equiv \frac{3}{4\pi}\sum_A \int_{S^2} d\hat{\Omega}\, F_1^A(\hat{\Omega}) F_2^A(\hat{\Omega})$$
$$= 3\left\{\frac{1}{3} + \frac{1-\cos\xi}{2}\left[\ln\left(\frac{1-\cos\xi}{2}\right) - \frac{1}{6}\right]\right\},$$